

Thermal Comfort Conditions Near Highly Glazed Façades:

An Experimental and Simulation Study

Mark Bessoudo

A Thesis in the Department of

Building, Civil, and Environmental Engineering

Presented in Partial Fulfillment of the Requirements for the Degree of Master  
of Applied Science (Building Engineering) at Concordia University

Montreal, Quebec, Canada

February 2008

© Mark Bessoudo, 2008



Library and  
Archives Canada

Bibliothèque et  
Archives Canada

Published Heritage  
Branch

Direction du  
Patrimoine de l'édition

395 Wellington Street  
Ottawa ON K1A 0N4  
Canada

395, rue Wellington  
Ottawa ON K1A 0N4  
Canada

*Your file    Votre référence*  
*ISBN: 978-0-494-40863-6*  
*Our file    Notre référence*  
*ISBN: 978-0-494-40863-6*

**NOTICE:**

The author has granted a non-exclusive license allowing Library and Archives Canada to reproduce, publish, archive, preserve, conserve, communicate to the public by telecommunication or on the Internet, loan, distribute and sell theses worldwide, for commercial or non-commercial purposes, in microform, paper, electronic and/or any other formats.

The author retains copyright ownership and moral rights in this thesis. Neither the thesis nor substantial extracts from it may be printed or otherwise reproduced without the author's permission.

**AVIS:**

L'auteur a accordé une licence non exclusive permettant à la Bibliothèque et Archives Canada de reproduire, publier, archiver, sauvegarder, conserver, transmettre au public par télécommunication ou par l'Internet, prêter, distribuer et vendre des thèses partout dans le monde, à des fins commerciales ou autres, sur support microforme, papier, électronique et/ou autres formats.

L'auteur conserve la propriété du droit d'auteur et des droits moraux qui protègent cette thèse. Ni la thèse ni des extraits substantiels de celle-ci ne doivent être imprimés ou autrement reproduits sans son autorisation.

---

In compliance with the Canadian Privacy Act some supporting forms may have been removed from this thesis.

Conformément à la loi canadienne sur la protection de la vie privée, quelques formulaires secondaires ont été enlevés de cette thèse.

While these forms may be included in the document page count, their removal does not represent any loss of content from the thesis.

Bien que ces formulaires aient inclus dans la pagination, il n'y aura aucun contenu manquant.

■ ■ ■  
**Canada**

## ABSTRACT

### Thermal Comfort Conditions near Glass Façades: An Experimental and Simulation Study

Mark Bessoudo

There is a current trend of designing new commercial buildings with large glazed façade areas. Maintaining comfort in the perimeter zones of these buildings is difficult due to their exposure to solar radiation and cold outdoor air temperature. Designing these buildings with high-performance fenestration systems, however, can improve energy performance, provide a high-quality thermal and visual environment, and reduce thermal loads.

This study presents an experimental and simulation study of thermal comfort conditions of a perimeter zone office with a glass façade and solar shading device. The study investigates the impact of climate, glazing type, and shading device properties on thermal comfort conditions. The objective of this study is to determine the façade properties that will provide a comfortable indoor environment without the need for secondary perimeter heating.

Experimental measurements were taken in an office equipped with two different shading devices: venetian blind and roller shade. The thermal environment was measured with thermocouples, an indoor climate analyzer, and thermal comfort meter.

For the simulation study, a one-dimensional transient thermal simulation model of a typical glazed perimeter zone office and a transient two-node thermal comfort model were developed. The impact of solar radiation and shading device properties on thermal comfort was also quantified. Simulation results were compared with experimental measurements.

The impact of diffuser location for primary heating supply on indoor airflow and comfort is also investigated using computational fluid dynamics software and it is shown that good comfort is achieved without the presence of perimeter heating.

## ACKNOWLEDGMENTS

I would like to express my gratitude to my supervisor Dr. A. K. Athienitis for his continuous encouragement, support, and patience during my graduate studies.

I am also indebted to Dr. A. Tzempelikos for his assistance, support, and advice.

A special thanks to Dr. R. Zmeureanu for his helpful advice.

Many thanks go to my friends and colleagues in the Solar Lab for their friendship and support.

I would also like to thank my mom, dad, and sister for their unwavering support and encouragement throughout my studies. I am forever grateful.

Financial support of this work was provided by NSERC through the Solar Buildings Research Network.

*To my parents*

## TABLE OF CONTENTS

<b>LIST OF FIGURES .....</b>	<b>x</b>
<b>LIST OF TABLES .....</b>	<b>xvi</b>
<b>NOMENCLATURE.....</b>	<b>xvii</b>
<b>1 INTRODUCTION .....</b>	<b>1</b>
1.1 Context.....	1
1.2 Background .....	2
1.3 Motivation .....	4
1.4 Objectives.....	5
1.5 Thesis layout.....	6
<b>2 LITERATURE REVIEW.....</b>	<b>8</b>
2.1 Thermal comfort .....	8
2.1.1 The indoor thermal environment .....	9
2.1.2 Human thermoregulation.....	12
2.1.3 Prediction of thermal comfort.....	14
2.1.3.1 Steady-state thermal environments .....	14
2.1.3.2 Transient thermal environments.....	17
2.1.4 Conditions for thermal comfort.....	20
2.1.4.1 The comfort zone.....	20
2.1.4.2 Local discomfort.....	22
2.1.4.3 Adaptive approach.....	26
2.2 Fenestration systems and perimeter zones.....	28
2.2.1 Windows and glazing.....	29
2.2.2 Shading devices.....	32
2.2.3 Mechanical systems.....	35
2.2.4 Perimeter zones and thermal comfort.....	38
2.3 Summary .....	47

<b>3</b>	<b>EXPERIMENTAL STUDY AND RESULTS</b> .....	<b>48</b>
3.1	Experimental perimeter zone.....	49
3.2	Data acquisition system, sensors, and measurements.....	52
3.3	Experimental results.....	55
3.3.1	Clear winter day.....	55
3.3.2	Cloudy winter day.....	59
3.4	Summary.....	63
<b>4</b>	<b>NUMERICAL SIMULATION STUDY</b> .....	<b>65</b>
4.1	Description of thermal simulation model.....	65
4.1.1	Typical meteorological year weather data.....	66
4.1.2	Solar radiation model.....	66
4.1.3	Geometry of perimeter zone office.....	70
4.1.4	Solar radiation transmission through glazing.....	71
4.1.5	Building thermal simulation model.....	74
4.1.6	Indoor thermal environment.....	79
4.2	Comparison of thermal simulation model and measurements.....	81
4.2.1	Clear winter day: no shading.....	82
4.2.2	Clear winter day: roller shade.....	84
4.2.3	Cloudy winter day: no shading.....	88
4.3	Description of thermal comfort model.....	90
4.4	Comparison of thermal comfort model with measurements.....	97
4.5	Parameters and assumptions.....	99
4.6	Results of simulation study.....	106
4.6.1	Clear winter day.....	106
4.6.2	Cloudy winter day.....	119
4.7	Further investigation using CFD.....	124
4.7.1	Description of CFD model.....	125
4.7.2	Results of CFD investigation.....	128
<b>5</b>	<b>CONCLUSIONS AND RECOMMENDATIONS</b> .....	<b>135</b>

5.1	Conclusions .....	135
5.2	Recommendations for future work .....	138
<b>REFERENCES .....</b>		<b>140</b>
<b>APPENDIX A: Perez irradiance model.....</b>		<b>147</b>
<b>APPENDIX B: Room geometry and view factors .....</b>		<b>154</b>
<b>APPENDIX C: Building thermal simulation model .....</b>		<b>166</b>
<b>APPENDIX D: Indoor thermal environment and thermal comfort model.....</b>		<b>206</b>

## LIST OF FIGURES

Figure 2.1: Mean value of angle factors between seated person and horizontal or vertical rectangle (ASHRAE Handbook of Fundamentals, 2005).....	11
Figure 2.2: Thermal interaction between the human body and surrounding environment (ASHRAE Handbook of Fundamentals, 2005).....	13
Figure 2.3: Relationship between the Predicted Percentage of Dissatisfied (PPD) and Predicted Mean Vote (PMV) (ASHRAE Handbook of Fundamentals, 2005).....	17
Figure 2.4: Representation of the concentric skin and core compartments in the two-node thermal comfort model.....	19
Figure 2.5: The indoor comfort zone (ASHRAE Standard 55 - 2004).....	21
Figure 2.6: Angle factors between a small plane element and surrounding surfaces (ASHRAE Handbook of Fundamentals, 2005).....	23
Figure 2.7: Percentage of people dissatisfied for different surfaces (ASHRAE Handbook of Fundamentals, 2005).....	24
Figure 2.8: Percentage of people dissatisfied at different air temperatures as a function of mean air velocity (ASHRAE Handbook of Fundamentals, 2005).....	26
Figure 2.9: The components of heat transfer through glazing (left) and a simplified view of the components of solar heat gain (Carmody et al., 2004).....	31
Figure 2.10: Shortwave (solar) and longwave energy spectrum. Area 1 represents idealized transmittance for low solar heat gain glazing; Area 2 represents idealized transmittance for high solar heat gain glazing (Carmody et al., 2004).....	32
Figure 2.11: The perimeter and interior zones of a building (Carmody et al., 2004).....	35
Figure 2.12: Cross section of perimeter zone office with typical HVAC configuration: overhead supply air (primary heating) and perimeter baseboard unit beneath glazing (secondary heating)	37
Figure 2.13: Sources of thermal discomfort in glazed perimeter zones (Carmody et al., 2004).....	38
Figure 2.14: Notation pertinent to calculating the effective radiation area (left) and a chart for determining the projected area factors for a seated person (right) (Rizzo et al., 1991).....	43

Figure 3.1: The EV Building at Concordia University in Montreal where the experimental measurements were completed (KPMB Architects, 2006). The image on the right shows one of the experimental sections with a dividing curtain.....	50
Figure 3.2: Schematic of experimental section used for measurements (not to scale).....	51
Figure 3.3: Schematic of the six sections of the experimental façade (interior view). The roller shade is used for section 4; the venetian blinds are used for section 5.....	51
Figure 3.4: Instruments for measuring indoor environmental parameters: (a) air velocity; (b) shielded air temperature; (c) humidity; (d) plane radiant temperature. (Parsons, 2003) .....	53
Figure 3.5: Temperature and total incident solar radiation measurements on clear day with no shading .....	55
Figure 3.6: Temperature and total incident solar radiation measurements on a clear day with roller shade .....	56
Figure 3.7: Temperature and total incident solar radiation measurements on a clear day with venetian blind (tilt = 0°) .....	57
Figure 3.8: Temperature and total incident solar radiation measurements on a clear day with venetian blind (tilt = 45°) .....	58
Figure 3.9: Temperature and total incident solar radiation measurements on a clear day with venetian blind (tilt = 90°) .....	59
Figure 3.10: Temperature and total incident solar radiation measurements on cloudy day with no shading device.....	61
Figure 3.11: Temperature and total incident solar radiation measurements on a cloudy day with venetian blind (tilt = 0°).....	61
Figure 3.12: Temperature and total incident solar radiation measurements on a cloudy day with venetian blind (tilt = 45°).....	62
Figure 3.13: Temperature and total incident solar radiation measurements on a cloudy day with venetian blind (tilt = 90°).....	62
Figure 4.1: Solar angles for vertical and horizontal surfaces (ASHRAE Handbook of Fundamentals, 2005).....	67
Figure 4.2: Direct radiation, ground reflected radiation, and different components of diffuse radiation (Fieber, 2005) .....	69
Figure 4.3: Graphical representation of view factors for radiation heat transfer calculation (ASHRAE Handbook of Fundamentals, 2005).....	71
Figure 4.4: Thermal network diagram of perimeter zone office.....	75

Figure 4.5: Operative temperature: verification of simulation model with measured values for a clear winter day with no shade .....	82
Figure 4.6: Room air temperature: verification of simulation model with measured values for a clear winter day with no shade .....	83
Figure 4.7: Interior glass surface temperature: verification of simulation model with measured values for a clear winter day with no shade.....	84
Figure 4.8: Operative temperature: verification of simulation model with measured values for a clear winter day with roller shade.....	85
Figure 4.9: Room air temperature: verification of simulation model with measured values for a clear winter day with roller shade.....	85
Figure 4.10: Interior glass surface temperature: verification of simulation model with measured values for a clear winter day with roller shade.....	86
Figure 4.11: Roller shade: verification of simulation model with measured values for a clear winter day with roller shade .....	87
Figure 4.12: Radiant temperature asymmetry: verification of simulation model and measured values for a clear winter day with roller shade.....	87
Figure 4.13: Operative temperature: verification of simulation model with measured values for a cloudy winter day with no shade.....	88
Figure 4.14: Room air temperature: verification of simulation model with measured values for a cloudy winter day with no shade.....	89
Figure 4.15: Glass temperature: verification of simulation model with measured values for a cloudy winter day with no shade.....	89
Figure 4.16: Comparison of skin temperature values for thermal comfort simulation model vs. Grivel experimental data .....	98
Figure 4.17: Comparison of thermal discomfort index for thermal comfort simulation model vs. Gagge computer model.....	99
Figure 4.18: Climatic data for representative days used in simulation .....	100
Figure 4.19: Schematic of typical office used for simulations (not to scale) ..	101
Figure 4.20: Effective solar transmittance of glazing as function of incidence angle .....	102
Figure 4.21: Absorptance of glazing as function of incidence angle .....	102
Figure 4.22: MRT due to surrounding surfaces only and MRT due to surrounding surfaces and solar radiation with an unshaded double-glazed window on a clear winter day .....	107

Figure 4.23: Effect of glazing type on interior window surface temperature on a clear winter day .....	108
Figure 4.24: Effect of glazing type on mean radiant temperature for a clear winter day with no shading .....	109
Figure 4.25: Effect of glazing type on room air temperature for a clear winter day with no shading.....	109
Figure 4.26: Effect of glazing type on operative temperature for a clear winter day with no shading.....	110
Figure 4.27: Effect of glazing type on radiant temperature asymmetry for a clear winter day with no shading .....	110
Figure 4.28: Effect of glazing type on thermal discomfort for a clear winter day with no shading.....	111
Figure 4.29: Effect of shade absorptance on shade temperature with glazing 2 (double-glazed, low-e) for a clear winter day .....	112
Figure 4.30: Effect of shade absorptance on maximum shade temperature for a clear winter day .....	112
Figure 4.31: Effect of shade absorptance on maximum mean radiant temperature for a clear winter day .....	113
Figure 4.32: Effect of shade absorptance on maximum room air temperature for a clear winter day .....	114
Figure 4.33: Effect of shade absorptance on maximum operative temperature for a clear winter day .....	114
Figure 4.34: Effect of shade absorptance on maximum radiant temperature asymmetry for a clear winter day .....	115
Figure 4.35: RTA as a function of distance from façade for three different shade absorptances using glazing 1.....	116
Figure 4.36: RTA as a function of distance from façade for three different shade absorptances using glazing 2.....	116
Figure 4.37: RTA as a function of distance from façade for three different shade absorptances using glazing 3.....	117
Figure 4.38: Effect of shade absorptance on maximum thermal discomfort for a clear winter day .....	117
Figure 4.39: Effect of shade absorptance on number of hours per day in discomfort zone for a clear winter day.....	118
Figure 4.40: Effect of shade absorptance on daily total heating demand for a clear winter day .....	119

Figure 4.41: Minimum window surface temperature (glazing or shade): Effect of glazing type for a cloudy winter day.....	120
Figure 4.42: Minimum mean radiant temperature: Effect of glazing type for a cloudy winter day .....	121
Figure 4.43: Minimum operative temperature: Effect of glazing type for a cloudy winter day .....	121
Figure 4.44: Minimum thermal discomfort rating: Effect of glazing type for a cloudy winter day .....	122
Figure 4.45: Daily heating demand: Effect of glazing type for a cloudy winter day .....	122
Figure 4.46: RTA as a function of distance from façade for glazing 1 with and without shading.....	123
Figure 4.47: RTA as a function of distance from façade for glazing 2 with and without shading.....	123
Figure 4.48: RTA as a function of distance from façade for glazing 3 with and without shading.....	124
Figure 4.49: Model of perimeter zone office used for Airpak simulation (left); representation of mesh (right).....	127
Figure 4.50: Variation in air speed at three different heights with diffuser 0.7 m from window ( $T_{\text{supply}} = 30\text{ }^{\circ}\text{C}$ ; $v_{\text{supply}} = 1.5\text{ m/s}$ ).....	129
Figure 4.51: Variation in air speed at three different heights with diffuser 1.1 m from window ( $T_{\text{supply}} = 30\text{ }^{\circ}\text{C}$ ; $v_{\text{supply}} = 1.5\text{ m/s}$ ).....	129
Figure 4.52: Variation in air speed at three different heights with diffuser 1.5 m from window ( $T_{\text{supply}} = 30\text{ }^{\circ}\text{C}$ ; $v_{\text{supply}} = 1.5\text{ m/s}$ ).....	130
Figure 4.53: Cross sectional contour plot of air speed with diffuser 0.7 m from window .....	130
Figure 4.54: Cross sectional contour plot of air speed with diffuser 1.1 m from window .....	131
Figure 4.55: Cross sectional contour plot of air speed with difusser 1.5 m from window .....	131
Figure 4.56: Cross sectional contour plot of operative temperature with diffuser 0.7 m from window.....	132
Figure 4.57: Cross sectional contour plot of operative temperature with diffuser 1.1 m from window.....	133
Figure 4.58: Cross sectional contour plot of operative temperature with diffuser 1.5 m from window.....	133



## LIST OF TABLES

Table 4.1: Climatic data for representative days used in simulations.....	100
Table 4.2: Properties of the three different glazing types used for parametric analysis (ASHRAE Handbook of Fundamentals, 2005).....	103
Table 4.3: Thermal properties of building materials used for simulation.....	104
Table 4.4: Parameters of indoor environmental conditions and occupant properties used for the thermal comfort simulation.....	106

## NOMENCLATURE

<b>a</b>	horizon brightness coefficient
<b>A<sub>D</sub></b>	DuBois surface area of body, m <sup>2</sup>
<b>A<sub>cg</sub></b>	area of center of glass, m <sup>2</sup>
<b>A<sub>eg</sub></b>	area of edge of glass, m <sup>2</sup>
<b>A<sub>f</sub></b>	area of frame, m <sup>2</sup>
<b>b</b>	horizon brightness coefficient
<b>c<sub>p</sub></b>	specific heat, J/kg·K
<b>c<sub>p,b</sub></b>	specific heat capacity of body, J/kg·K
<b>C</b>	thermal capacitance
<b>C<sub>res</sub></b>	rate of convective heat loss from respiration, W/m <sup>2</sup>
<b>DISC</b>	index of thermal discomfort
<b>DR</b>	draft risk, %
<b>E</b>	rate of heat released from body via evaporation, W/m <sup>2</sup>
<b>E<sub>dif</sub></b>	heat transfer by evaporation of moisture through the skin, W/m <sup>2</sup>
<b>E<sub>max</sub></b>	maximum rate of evaporative heat loss, W/m <sup>2</sup>
<b>E<sub>sk</sub></b>	rate of evaporative heat loss from skin, W/m <sup>2</sup>
<b>E<sub>res</sub></b>	rate of evaporative heat loss from respiration, W/m <sup>2</sup>
<b>E<sub>rsw</sub></b>	rate of regulatory sweating, W/m <sup>2</sup>
<b>E<sub>rsw,req</sub></b>	sweat rate required for comfort, W/m <sup>2</sup>
<b>F<sub>1</sub></b>	circumsolar brightening coefficient
<b>F<sub>2</sub></b>	horizon brightening coefficient
<b>F<sub>p-i</sub></b>	angle factor between person and surface i
<b>F<sub>ij</sub></b>	angle (view) factor from surface i to surface j
<b>f<sub>cl</sub></b>	clothing area factor
<b>f<sub>p</sub></b>	projected area factor
<b>h<sub>e</sub></b>	evaporative heat transfer coefficient, W/m <sup>2</sup> ·kPa
<b>h<sub>i</sub></b>	interior convective heat transfer coefficient, W/m <sup>2</sup> ·°C
<b>h<sub>n</sub></b>	natural convection heat transfer coefficient, W/m <sup>2</sup> ·°C

<b><math>h_o</math></b>	exterior convective heat transfer coefficient, $W/m^2 \cdot ^\circ C$
<b><math>h_r</math></b>	heat transfer coefficient, radiation, $W/m^2 \cdot ^\circ C$
<b><math>h_c</math></b>	heat transfer coefficient, convection, $W/m^2 \cdot ^\circ C$
<b><math>i_m</math></b>	clothing moisture permeability
<b><math>I</math></b>	total incident solar radiation, $W/m^2$
<b><math>I_b</math></b>	incident beam solar radiation, $W/m^2$
<b><math>I_{bh}</math></b>	beam horizontal irradiance, $W/m^2$
<b><math>I_{bn}</math></b>	direct normal solar radiation, $W/m^2$
<b><math>I_{cl}</math></b>	thermal insulation of clothing, clo
<b><math>I_d</math></b>	total hemispherical diffuse solar radiation, $W/m^2$
<b><math>I_{dg}</math></b>	ground reflected diffuse irradiance, $W/m^2$
<b><math>I_{dh}</math></b>	sky diffuse horizontal irradiance, $W/m^2$
<b><math>k</math></b>	thermal conductivity, $W/^\circ C$
<b><math>K</math></b>	heat released from body via conduction, $W/m^2$
<b><math>L</math></b>	length, m; thermal load on body, $W/m^2$
<b><math>m</math></b>	body mass, kg
<b><math>M</math></b>	metabolic rate of body, $W/m^2$
<b>MRT</b>	mean radiant temperature
<b><math>n</math></b>	Julian day number
<b>Nu</b>	Nusselt number
<b><math>P_a</math></b>	partial pressure of water vapour, kPa
<b>PMV</b>	Predicted Mean Vote
<b>PPD</b>	Predicted Percentage Dissatisfied, %
<b><math>P_{sk}</math></b>	saturated water vapour pressure on skin surface, kPa
<b><math>q</math></b>	heat source, W
<b><math>q_{sk}</math></b>	total rate of heat loss from skin, $W/m^2$
<b><math>q_{res}</math></b>	total rate of heat loss through respiration, $W/m^2$
<b><math>Q</math></b>	instantaneous heat flow, W
<b><math>Q_{crsk}</math></b>	heat transfer from core to skin, $W/m^2$
<b><math>R</math></b>	thermal resistance, $m^2 \cdot ^\circ K/W$
<b>Ra</b>	Rayleigh number

<b>RTA</b>	radiant temperature asymmetry, °C
<b>S</b>	heat storage in body, W/m <sup>2</sup>
<b>S<sub>sk</sub></b>	rate of heat storage in skin compartment, W/m <sup>2</sup>
<b>S<sub>cr</sub></b>	rate of heat storage in core compartment, W/m <sup>2</sup>
<b>SKBF</b>	rate of blood flow from core to skin, kg/hr·m <sup>2</sup>
<b>t</b>	time, s
<b>t<sub>sk,req</sub></b>	skin temperature required for comfort, °C
<b>T<sub>a</sub></b>	room air temperature, °C
<b>T<sub>b</sub></b>	mean body temperature, °C
<b>T<sub>b,c</sub></b>	mean body temperature (cold set point), °C
<b>T<sub>b,h</sub></b>	mean body temperature (hot set point), °C
<b>T<sub>c</sub></b>	comfort temperature, °C
<b>T<sub>i</sub></b>	temperature of surface i, °C
<b>T<sub>cl</sub></b>	temperature of clothing, °C
<b>T<sub>cr</sub></b>	temperature of core compartment, °C
<b>T<sub>op</sub></b>	operative temperature, °C
<b>T<sub>o</sub></b>	outdoor air temperature, °C
<b>T<sub>sk</sub></b>	temperature of skin compartment, °C
<b>TSENS</b>	thermal sensation
<b>Tu</b>	turbulence, %
<b>U</b>	overall heat transfer coefficient, W/m <sup>2</sup> ·K
<b>U<sub>cg</sub></b>	overall heat transfer coefficient for center of glass, W/m <sup>2</sup> ·K
<b>U<sub>eg</sub></b>	overall heat transfer coefficient for edge of glass, W/m <sup>2</sup> ·K
<b>U<sub>f</sub></b>	overall heat transfer coefficient for frame, W/m <sup>2</sup> ·K
<b>U<sub>o</sub></b>	overall heat transfer coefficient of fenestration system, W/m <sup>2</sup> ·K
<b>v<sub>o</sub></b>	outdoor wind speed, m/s
<b>V<sub>sd</sub></b>	standard deviation of instantaneous air velocities
<b>V</b>	mean velocity, m/s
<b>Vol</b>	volume, m <sup>3</sup>
<b>w</b>	skin wettedness
<b>W</b>	mechanical work of body, W/m <sup>2</sup>

<b>WWR</b>	window-to-wall ratio
$\alpha_s$	solar altitude
$\alpha_{sk}$	fraction of body mass concentrated in skin compartment
$\alpha_{cl,d}$	clothing absorptance for diffuse solar radiation
$\alpha_{cl,b}$	clothing absorptance for beam solar radiation
$\varepsilon$	emissivity
$\varepsilon_s$	emissivity of person
$\Psi$	surface azimuth angle
$\beta$	surface tilt angle
$\sigma$	Stefan-Boltzmann constant
$\rho_g$	ground reflectance (albedo)
$\rho$	density, kg/m <sup>3</sup>
$\theta$	solar incidence angle
$\phi$	solar azimuth angle

# 1 INTRODUCTION

## 1.1 Context

The operation of buildings, including heating, cooling, and lighting, accounts for roughly 50 per cent of Canada's electricity use and almost 30 per cent of its energy consumption and greenhouse gas emissions (Ayoub et al., 2000). This figure could be reduced significantly if buildings were designed to take advantage of the surrounding climate. An obstacle to implementing energy-conscious principles into building design, however, is the division of building systems into different components that are handled separately, often with conflicting interests. Therefore, in order to attain true energy-efficient buildings, there is a need for a whole-system view of the building: its structure, subsystems, and the way they interact with each other, the natural environment, and its occupants.

Energy-related issues of buildings are only secondary factors; the primary objective of buildings is to provide shelter, space, and comfort for the people that live, work, and interact in them. Therefore, the primary objective should not be neglected in the building design in order to attain energy-efficiency.

## 1.2 Background

It can be said that the “success” of a building depends on whether a comfortable indoor environment is achieved. Achieving an acceptable indoor environment, however, is one of the biggest challenges with respect to energy use. There are several parameters that define the indoor environment including indoor air quality, visual comfort, and thermal comfort; each has an impact on occupant health and productivity, and, therefore, the total economic value of the building (Poirazis, 2005).

Thermal comfort is often listed by occupants as one of the most important requirements for any building. In surveys of user satisfaction in buildings with passive solar features, it was found that having the “right temperature” was one of the most important considerations (Nicol, 1993). Additionally, it was determined that air freshness was an important requirement. Even the subjective feeling of air freshness was found to be closely linked to the air temperature. Therefore, two important requirements of user satisfaction with the indoor environment are closely related to temperature.

Creating a comfortable indoor environment is also important because occupants will react to any perceived discomfort by taking actions to restore their comfort. Sometimes these actions will come with an energy cost; for example, using a shading device and turning on lights is a costly way to eliminate glare and overheating due to the presence of solar radiation. Similarly, opening a

window in the winter due to overheating is also a costly way to alleviate discomfort. Therefore, it is important to recognize that a 'low energy' standard that increases occupant discomfort may be no more sustainable than one that encourages energy use (Nicol, 2003).

The building envelope is the most critical element of a building and can influence every other component of the building. A poorly designed envelope leads to higher energy consumption (for space heating, cooling, and lighting) and poor comfort conditions in perimeter zones. A well-designed, high-performance envelope, on the other hand, can improve building energy performance, provide a higher quality thermal and visual environment, and reduce peak thermal loads in perimeter zones.

Windows are one of the most significant components of the building envelope, and therefore of the entire building. Although windows have always been used as architectural components for providing outdoor view and natural light, it has only been in recent years that the benefits of windows and their effect on the satisfaction, health, and productivity of the building occupants have been recognized (Carmody et al., 2004). This is reflected in the current trend of designing commercial buildings with glass façades. In addition to these more immediate human-related needs, there is also an urgent need for significant improvements in building energy performance.

This growing recognition of the benefits related to the improvement of both the human-related and energy performance aspects of buildings is evident in the recent popularity of green building rating systems and certification programs such as LEED (Leadership in Energy and Environmental Design). These rating systems require high-quality design in order to deliver superior daylight, views, comfort, ventilation, and energy performance – all of which are directly related to fenestration systems (U.S. Green Building Council, 2007). In addition, sustainable building design requires consideration of passive and active solar energy systems; good performance of these systems cannot be achieved unless the integration of solar technologies is considered from the early design stage. The systems' performance is directly related with the location, form, and orientation of the building, and, thus, affects the quality of the indoor environment.

### **1.3 Motivation**

There is a current trend of designing commercial buildings with glass façades. The reasons for this trend range from providing an expression of transparency between the client and public to providing conditions that maximize daylighting and views to aesthetics. In reality, however, these intentions often clash with occupant behaviour. This is because the building, as a system, is not always designed with occupant comfort in mind.

Although there exist a variety of models that can be used to predict human thermal comfort, with varying complexity, many are not sufficient to predict comfort based on the environmental conditions experienced in highly-glazed perimeter zones. For example, most comfort models used in engineering design assume steady-state thermal conditions, which is in contrast with the transient thermal conditions often associated with highly-glazed perimeter zones. In addition, the most common method to calculate mean radiant temperature considers interior surface temperatures without considering high-intensity sources such as solar radiation.

Therefore, there exists an opportunity to develop a thermal comfort model that takes into account the impact of solar radiation in order to investigate comfort conditions in highly-glazed perimeter zones. The model will investigate how the design of façades, including glazing and shading devices, affects thermal comfort; this knowledge can then be used to determine design alternatives such as incorporating high-performance glazing and shading in order to eliminate the need to use secondary perimeter heating.

#### **1.4 Objectives**

The objectives of this thesis are to:

1. Develop a one-dimensional transient thermal simulation model of a glazed perimeter zone office environment which incorporates a transient two-node thermal comfort model
2. Include the effect of solar radiation incident upon a person into the thermal comfort model
3. Analyze the effect of glazing type and shading properties on the indoor thermal environment and thermal comfort conditions under various climatic conditions
4. Determine which façade configurations provide thermal comfort conditions without the need for a secondary (perimeter) heating system

## **1.5 Thesis layout**

Chapter 2 provides a literature review of thermal comfort, human thermoregulation, and fenestration systems. Chapter 3 presents the methods and results of experimental measurements taken in an experimental perimeter zone office. Chapter 4 presents an overview of the numerical simulation study detailing the modeling methods used, its verification with experimental measurements, and results of a parametric analysis using the numerical simulation model. Chapter 5 provides a summary of the study with conclusions and recommendations for possible extensions of future work.



## 2 LITERATURE REVIEW

This chapter presents an overview of the major concepts related to thermal comfort, fenestration systems, and perimeter zones and the interactions between them. A literature review of the previous experimental and simulation work completed on these subjects is also presented.

### 2.1 Thermal comfort

The principle purpose of heating, ventilation, and air-conditioning (HVAC) is to provide conditions for human thermal comfort (ASHRAE Handbook of Fundamentals, 2005). ASHRAE Standard 55 (2004) defines thermal comfort as *“that state of mind which expresses satisfaction with the thermal environment”*. Although this broad definition has been subject to deep inquiry and philosophical debate (Cabanac, 1996), it nevertheless emphasizes that the judgement of comfort is a cognitive process that is influenced by a combination of physical, psychological, and physiological factors. In general, comfort is attained when body temperature is held within a narrow range, skin moisture is low, and the physiological effort of regulation is minimized (ASHRAE Handbook of Fundamentals, 2005).

### 2.1.1 The indoor thermal environment

From earlier research (Fanger, 1973; McIntyre, 1980; Gagge et al., 1986), it is known that thermal comfort is affected by the thermal interaction between the body and surrounding environment. There are six primary factors that affect this thermal interaction:

- Air temperature
- Mean radiant temperature (MRT)
- Air speed
- Humidity
- Metabolic rate
- Clothing insulation

The first four factors define the conditions of the surrounding environment while the latter two represent “personal” variables that can vary between people exposed to the same environmental conditions.

#### Mean Radiant Temperature

The mean radiant temperature is defined in ASHRAE Standard 55 (2004) as “*the uniform surface temperature of an imaginary black enclosure in which an occupant would exchange the same amount of radiant heat as in the actual non-uniform space*”. It is an important parameter affecting thermal comfort and also one of the most difficult parameters to analyze. The MRT ( $T_{mrt}$ ) can be calculated with knowledge of the absolute temperature of the surrounding surfaces ( $T_i$ ) and the angle factors between the person and the surrounding surfaces ( $F_{p-i}$ ):

$$T_{mrt}^4 = \sum T_i^4 F_{p-i} \quad (2.1)$$

The angle factors between the person and the surfaces depend on the posture, position and orientation of the person relative to each surface. Generally, the angle factors are difficult to determine since the geometry of a person is complex; however, practical estimates can be made for simplified analysis with the aid of graphs (Figure 2.1). A simplified algorithm to calculate these view factors has been developed by Cannistraro et al. (1992) and was found to give an error of less than 1% when compared to the graphs. The algorithm is able to calculate the view factors based on the original criteria of posture, position, and orientation of the person. More complex algorithms to calculate the view factors of individual body parts to surrounding surfaces have also been developed, such as the model developed by Zhang et al. (2004) which divides the surface of the human body into more than five thousand nodes.

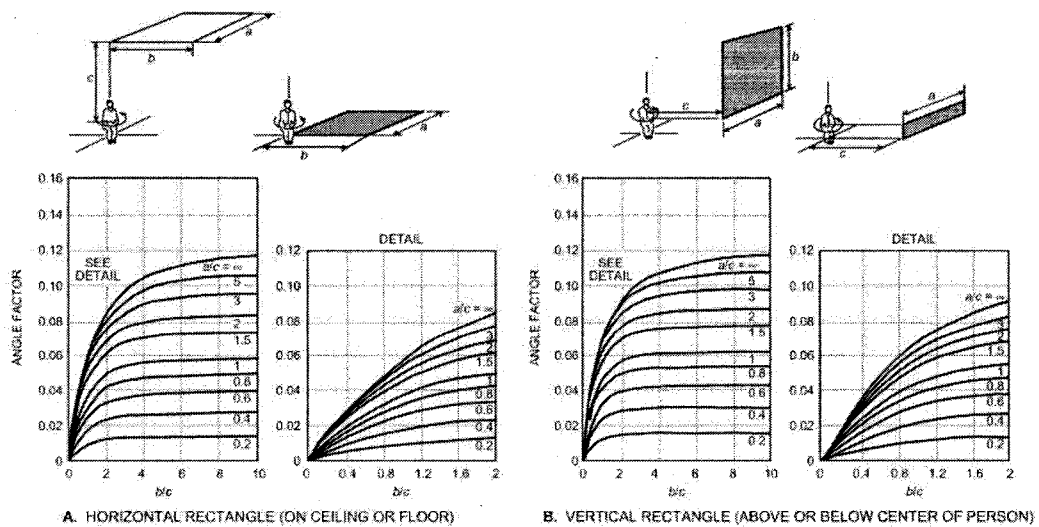


*Figure 2.1: Mean value of angle factors between seated person and horizontal or vertical rectangle (ASHRAE Handbook of Fundamentals, 2005)*

## **Humidity**

Humidity affects the heat loss by evaporation, which is important at high temperatures and high metabolism, and can have a large impact on the perception of thermal comfort. In an office space, relative humidity usually varies between 30% and 60%.

## **Air Speed**

Air speed and turbulence intensity affect the convective heat loss from the body. A study of air speeds over the whole body in neutral environments found that air speeds up to 0.25 m/s had no significant effect on thermal acceptability (ASHRAE Handbook of Fundamentals, 2005).

## **Clothing Insulation**

Clothing provides thermal insulation and its quantity is measured in units of clo, where 1 clo is equivalent to 0.155 m<sup>2</sup>K/W. Since people normally adapt their clothing to suit the climate, typical values of clothing insulation are 0.5 clo in the summer and 0.9 clo in the winter. Tables of the thermal insulation values of various clothing ensembles can be found in ASHRAE Handbook of Fundamentals (2005).

### 2.1.2 Human thermoregulation

In order to quantify how the environment influences thermal comfort, it is important to first understand the principles of human physiology and thermoregulation.

The human body produces heat primarily by metabolism, exchanges heat with the environment via radiation, convection, and conduction, and loses heat by evaporation of body fluids (Figure 2.2). The metabolic heat generated by a resting adult is about 100 W. Since this heat is dissipated to the external environment mainly through the skin, metabolic activity is usually defined in terms of heat production per unit area of skin. For an average resting person this is about 58.2 W/m<sup>2</sup>, or 1 met.

The human heat balance equation describes how the body maintains an internal body temperature close to 37 °C and skin temperature between 33 °C and 34 °C. The metabolic rate of the body ( $M$ ) provides energy to the body needed to do mechanical work ( $W$ ), with the remainder released as heat ( $M-W$ ). Heat is transferred from the body via conduction ( $K$ ), convection ( $C$ ), radiation ( $R$ ), and evaporation ( $E$ ). The heat production that is not transferred from the body provides a rate of heat storage ( $S$ ). Therefore, the conceptual heat balance equation is (Parsons, 2003):

$$M - W = E + R + C + K + S \quad (2.2)$$

Or more specifically:

$$\begin{aligned}
 M - W &= q_{sk} + q_{res} + S \\
 &= (C + R + E_{sk}) + (C_{res} + E_{res}) + (S_{sk} + S_{cr})
 \end{aligned}
 \tag{2.3}$$

where:

$q_{sk}$  = total rate of heat loss from skin, W/m<sup>2</sup>

$q_{res}$  = total rate of heat loss through respiration, W/m<sup>2</sup>

$E_{sk}$  = total rate of evaporative heat loss from skin, W/m<sup>2</sup>

$C_{res}$  = rate of convective heat loss from respiration, W/m<sup>2</sup>

$E_{res}$  = rate of evaporative heat loss from respiration, W/m<sup>2</sup>

$S_{sk}$  = rate of heat storage in skin compartment, W/m<sup>2</sup>

$S_{cr}$  = rate of heat storage in core compartment, W/m<sup>2</sup>

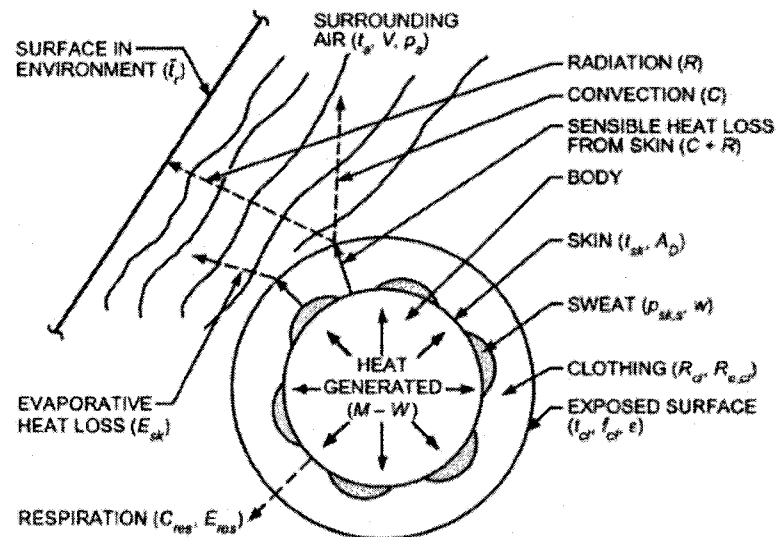


Figure 2.2: Thermal interaction between the human body and surrounding environment (ASHRAE Handbook of Fundamentals, 2005)

The controlled variable for thermoregulation is a combined value of internal (core) temperatures and skin temperature. The thermoregulatory system is influenced by internal and external thermal disturbances. Thermoreceptors

located in the skin detect external thermal disturbances and enable the thermoregulatory system to act before the disturbances reach the body core. In addition to responding to temperature, thermoreceptors also respond to the rate of temperature change (Hensen, 1990).

The central control system of human thermoregulation, located in the brain, is the hypothalamus. In order to control various physiological processes of the body for regulation of body temperature, the hypothalamus is responsible for autonomic regulation such as heat production (shivering), internal thermal resistance (control of skin blood flow), external thermal resistance (control of respiratory dry heat loss), and water secretion and evaporation (sweating and respiratory evaporative heat loss). These control behaviours are primarily proportional to deviations from skin and core set point temperatures with some integral and derivative response aspects involved (ASHRAE Handbook of Fundamentals, 2005).

### **2.1.3 Prediction of thermal comfort**

#### ***2.1.3.1 Steady-state thermal environments***

The most significant contribution to research in thermal comfort for practical application to the built environment was delivered by Fanger in his landmark publication *Thermal Comfort* (1973). Fanger outlines the conditions necessary for thermal comfort and the methods and principles necessary to evaluate thermal

environments. These methods and principles are now the most influential and widely-used throughout the world. The reason for this success is due to the practical method with which conditions for “average thermal comfort” could be predicted. Fanger defines three conditions for a person to be in thermal comfort:

1. The body is in heat balance (i.e. no thermal storage;  $S = 0$ );
2. The sweat rate is within comfort limits; and
3. The mean skin temperature is within comfort limits.

The objective of Fanger’s work was to develop a comfort equation that required as inputs only the six basic parameters, based on the three conditions above. The heat balance equation was therefore reduced to:

$$\begin{aligned}
 M - W = 3.96 \times 10^{-8} f_{cl} \left[ (T_{cl} + 273)^4 - (T_{mrt} + 273)^4 \right] + f_{cl} h_c (T_{cl} - T_a) \\
 + 3.05 \left[ 5.73 - 0.007(M - W) - P_a \right] + 0.42 \left[ (M - W) - 58.12 \right] \\
 + 0.0173M(5.87 - P_a) + 0.0014M(34 - T_a)
 \end{aligned} \tag{2.4}$$

where:

$$\begin{aligned}
 T_{cl} = 35.7 - 0.0275(M - W) - 0.155I_{cl}[(M - W) - 0.007(M - W) - P_a] \\
 - 0.42[(M - W) - 58.15] - 0.0173M(5.87 - P_a) - 0.0014M(34 - T_a)
 \end{aligned} \tag{2.5}$$

where:

$f_{cl}$  = clothing area factor

$T_{cl}$  = temperature of clothing, °C

$h_c$  = convective heat transfer coefficient, W/m<sup>2</sup>

$T_a$  = room air temperature, °C

$P_a$  = partial pressure of water vapour, kPa

An index was created that correlates this heat balance equation with the mean response of thermal sensation of a large group of people. This index, the Predicted Mean Vote (PMV), is based on a seven-point scale of thermal sensation:

- +3 hot
- +2 warm
- +1 slightly warm
- 0 neutral
- 1 slightly cool
- 2 cool
- 3 cold

The PMV is calculated by:

$$PMV = [0.303 \exp(-0.036M) + 0.028]L \quad (2.6)$$

where  $L$  is the thermal load on the body, defined as “*the difference between internal heat production and heat loss to the actual environment for a person hypothetically kept at comfort values of the mean skin temperature and sweat secretion at the actual activity level*” (ASHRAE Handbook of Fundamentals, 2005). It is essentially the difference between the left and right sides of the heat balance equation. In comfort conditions the thermal load will be zero (i.e.  $PMV = 0$ ). Therefore, for deviations from comfort condition, the thermal sensation experienced will be a function of the thermal load and activity level.

With the PMV value known, it is possible to estimate the percentage of people who would be dissatisfied with the given environmental conditions. This

index, called Predicted Percentage Dissatisfied (PPD), is a function of the PMV index:

$$PPD = 100 - 95 \exp[-(0.03353PMV^4 + 0.2179PMV^2)] \quad (2.7)$$

An acceptable thermal environment for general comfort is within the range of -0.5 to +0.5, corresponding to a PPD < 10%. It can be seen from Figure 2.3 that even at thermal neutrality ( $L = 0$ ,  $PMV = 0$ ), 5% of the people are expected to be dissatisfied. The PMV-PPD model is widely used for practical application and is accepted for design and field assessment of comfort conditions.

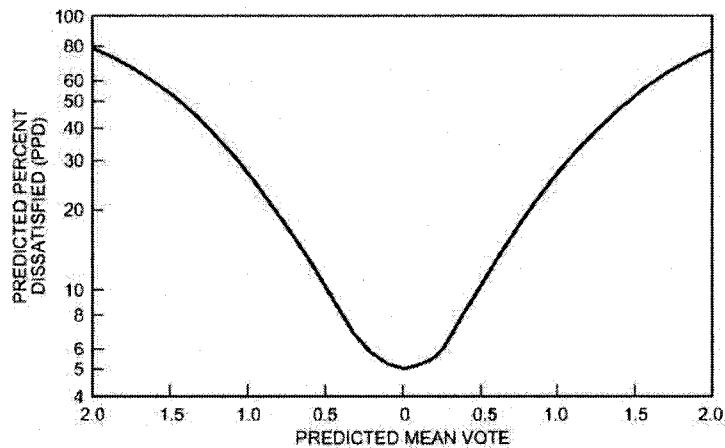


Figure 2.3: Relationship between the Predicted Percentage of Dissatisfied (PPD) and Predicted Mean Vote (PMV) (ASHRAE Handbook of Fundamentals, 2005)

### 2.1.3.2 Transient thermal environments

Because of the thermal interaction between the HVAC system, climate, building mass, and occupancy, pure steady-state conditions rarely exist in practice. This is even more evident in the perimeter zones of buildings where interaction between

the indoor and outdoor environments are more pronounced. Since the PMV-PPD model is valid only in predicting steady-state conditions, a transient comfort model is needed in order to predict physiological responses under transient conditions. Several transient comfort models exist, ranging from the more complex 65-node thermoregulation model (Tanabe et al. 2002) to the simpler two-node model (Gagge et al., 1970).

The two-node model considers the body as two concentric thermal compartments: skin and core (Figure 2.4). The temperature of each compartment is assumed to be uniform. Metabolic heat is generated within the core and dissipated via conduction (through a massless conductor to the skin), and convection (by way of blood circulation and respiration). The skin compartment loses heat to the environment via convection, radiation, evaporation of sweat, and diffusion of water vapour (Figure 2.2). The rate of change of temperature in each compartment is a function of its heat storage and heat capacity of the body:

$$\frac{dT_{cr}}{dt} = \frac{S_{cr} \cdot A_D}{(1 - \alpha_{sk}) \cdot m \cdot c_{p,b}} \quad (2.8)$$

$$\frac{dT_{sk}}{dt} = \frac{S_{sk} \cdot A_D}{\alpha_{sk} \cdot m \cdot c_{p,b}} \quad (2.9)$$

where:

$\alpha_{sk}$  = fraction of body mass concentrated in skin compartment

$m$  = body mass, kg

$c_{p,b}$  = specific heat capacity of body, J/kg · K

$A_D$  = DuBois surface area,  $m^2$

$T_{cr}$  = temperature of core compartment,  $^{\circ}C$

$T_{sk}$  = temperature of skin compartment,  $^{\circ}C$

$t$  = time, s

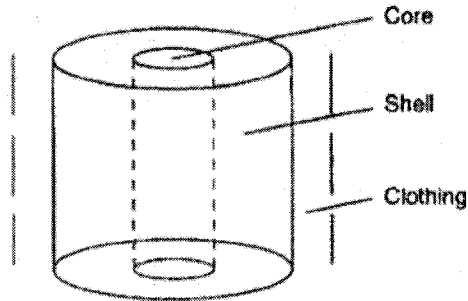


Figure 2.4: Representation of the concentric skin and core compartments in the two-node thermal comfort model

The heat storage in each compartment can be expressed as:

$$S_{cr} = M - W - (C_{res} - E_{res}) - Q_{crsk} \quad (2.10)$$

$$S_{sk} = Q_{crsk} - (C + R + E_{sk}) \quad (2.11)$$

where  $Q_{crsk}$  [ $W/m^2$ ] is the heat transfer from the core to the skin by convection through blood circulation and by conduction through the body tissue.

Thermoregulatory control processes (rate of blood flow, sweating and shivering) are governed by temperature signals from the skin and core. These signals are assumed to be proportional to the difference between actual temperature and corresponding set-point temperature for neutral condition (Zmeureanu and Doramajian, 1992).

By determining the values of skin temperature, core temperature, and skin wettedness, the two-node model uses empirical expressions to predict thermal sensation (TSENS) and thermal discomfort (DISC). Both of these indices are based on 11-point scales, with positive values representing the warm side of the neutral sensation and the negative values representing the cold side. TSENS is based on the same scale as the PMV index, but with extra values of  $\pm 4$  and  $\pm 5$  indicating very hot/cold and intolerably hot/cold, respectively.

## 2.1.4 Conditions for thermal comfort

### 2.1.4.1 *The comfort zone*

Since neither MRT nor dry-bulb temperature alone are good thermal comfort indicators, Fanger (1967) suggested using the operative temperature ( $T_{op}$ ) as an indicator. The operative temperature is defined as “*the uniform temperature of an imaginary black enclosure in which an occupant would exchange the same amount of heat by radiation plus convection as in the actual non-uniform environment*” and can be calculated as the average of the MRT and air temperature weighted by their respective heat transfer coefficients:

$$T_{op} = \frac{h_r T_r + h_c T_a}{h_r + h_c} \quad (2.12)$$

ASHRAE Standard 55 (2004) specifies conditions (operative temperature and humidity) where 80% of sedentary or slightly active people will find the

thermal environment acceptable ( $PPD \leq 20\%$ ) (Figure 2.5). Since people typically change their clothing for different seasons, ASHRAE Standard 55 (2004) specifies summer and winter comfort zones differentiating between clothing insulation levels of 0.5 and 0.9 clo, respectively. Within the comfort zones, a typical person wearing the prescribed clothing insulation levels would have a thermal sensation at or near neutrality ( $-0.5 \leq PMV \leq +0.5$ ). The comfort zones are also only valid for primarily sedentary activity ( $1.0 \text{ met} \leq M \leq 1.3 \text{ met}$ ) in low velocity environments ( $v \leq 0.2 \text{ m/s}$ ).

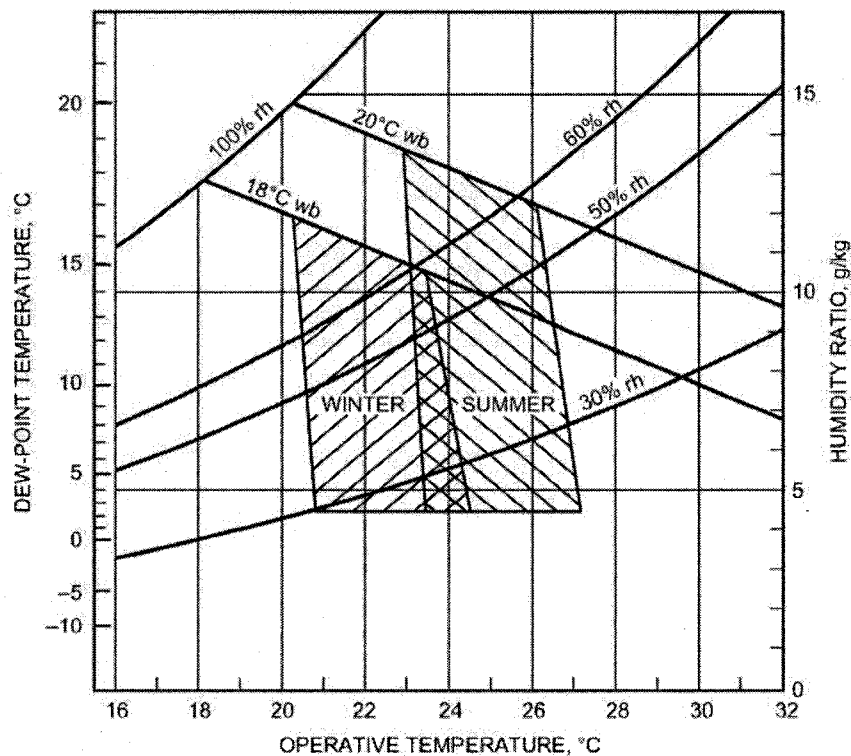


Figure 2.5: The indoor comfort zone (ASHRAE Standard 55 - 2004)

It should be noted that although ASHRAE Standard 55 (2004) states that environmental conditions should be kept within the comfort zone, it also allows for the operative temperature to temporarily deviate from the limits of the

comfort zone. Temperature drifts or ramps are allowed, for example, given that the operative temperature does not change more than 1.1 °C during a 15-minute period or 2.2 °C during a one-hour period. Based on these criteria, Zmeureanu and Doramajian (1992) were able to demonstrate that energy savings could be obtained in office buildings in the summer if the indoor air temperature was allowed to drift in the afternoon, exceeding the upper limit of the comfort zone.

#### ***2.1.4.2 Local discomfort***

Although a person may feel thermally neutral as a whole, there may be instances when they still feel uncomfortable due to one or more body parts being too warm or too cold. These non-uniformities may be due to a cold window, a hot surface, a draft, or a temporal variation of these. The comfort zones of ASHRAE Standard 55 (2004) specify a thermal acceptability level of 90% if the environment is thermally uniform, but since the Standard's objective is to specify conditions for 80% acceptability, it is permitted to decrease acceptability by 10% due to local non-uniformities.

#### **Radiant Temperature Asymmetry**

A non-uniform thermal environment will give rise to radiant temperature asymmetry (RTA). It is defined as the difference between the plane radiant temperatures of two opposite sides of a small plane element, where the plane radiant temperature quantifies the thermal radiation in one direction. The angle

factors between a small plane element and surrounding surfaces can be determined from Figure 2.6. ASHRAE Standard 55 (2004) recommends that RTA due to a warm wall should not exceed 23 °C and 10 °C for a cool wall. Figure 2.7 shows the predicted percentage of dissatisfied occupants as a function of RTA due to a cool or warm wall or ceiling.

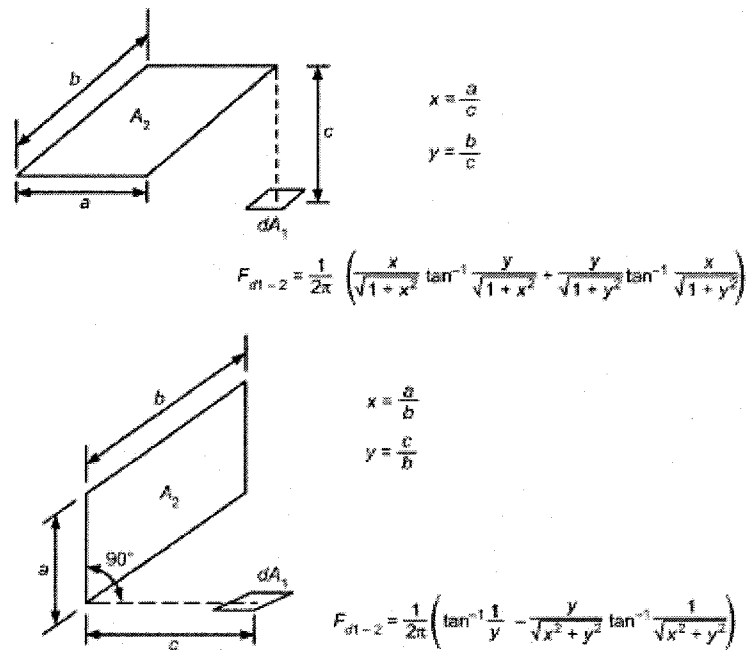


Figure 2.6: Angle factors between a small plane element and surrounding surfaces (ASHRAE Handbook of Fundamentals, 2005)

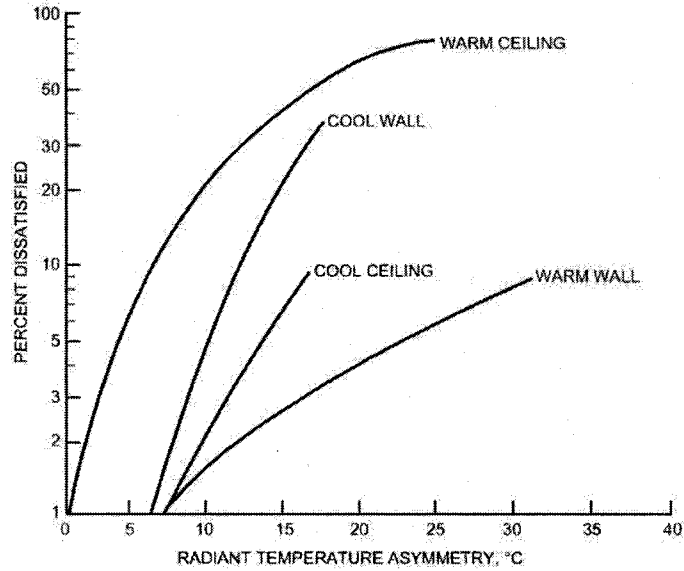


Figure 2.7: Percentage of people dissatisfied for different surfaces (ASHRAE Handbook of Fundamentals, 2005)

## Draft

Draft is an undesired local cooling of the body caused by the movement of surrounding air and has been identified as one of the most influential factors of discomfort in offices (ASHRAE Handbook of Fundamentals, 2005). People often compensate for draft by raising air temperature or stopping ventilation systems. The sensation of draft depends on air speed and temperature, turbulence intensity, activity, and clothing.

Turbulence intensity ( $Tu$ ) represents the degree of fluctuation in velocity and is a function of the standard deviation of the instantaneous velocities,  $V_{sd}$ , and mean velocity,  $V$ :

$$Tu = 100 \frac{V_{sd}}{V} \quad (2.13)$$

Air speed and turbulence intensity affect the convective heat loss from the body. A study of air speeds over the whole body in neutral environments found that air speeds up to 0.25 m/s had no significant effect on thermal acceptability. However, air temperature has a significant influence on the percentage of dissatisfied due to mean air speed (Figure 2.8) (ASHRAE Handbook of Fundamentals, 2005).

It has been found that there is a much higher percentage of people dissatisfied for situations with fluctuating velocity than of constant velocity (Huizenga et al., 2006). Fanger et al. (1988) investigated the effect of turbulence intensity on sensation of draft and developed an equation to predict the percentage of people dissatisfied due to draft risk (*DR*):

$$DR = (34 - T_a)(V - 0.05)^{0.62}(0.37V \cdot Tu + 3.14) \quad (2.14)$$

ASHRAE Standard 55 (2004) states that the maximum draft risk for maintaining comfort is 20%.

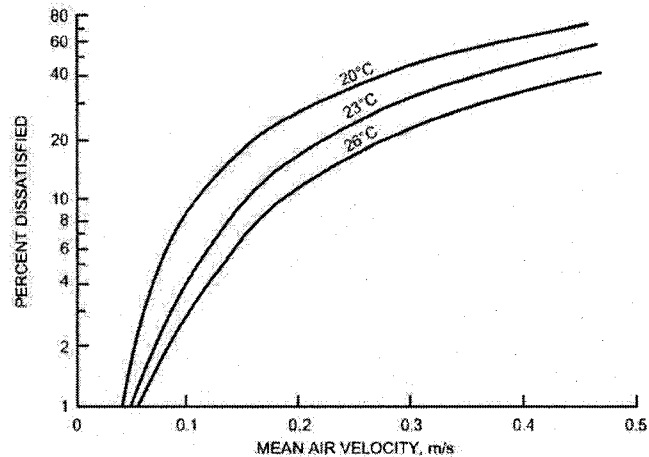


Figure 2.8: Percentage of people dissatisfied at different air temperatures as a function of mean air velocity (ASHRAE Handbook of Fundamentals, 2005)

### 2.1.4.3 Adaptive approach

The adaptive approach to thermal comfort is not related to thermoregulatory modeling. Rather, it is based on the observation that there is a range of actions, or “adaptive opportunities” that a person can perform in order to achieve thermal comfort. Adaptive opportunities, which include the ability of an occupant to open a window, draw a blind, use a fan, or change clothing, increase the “forgiveness” of the building (i.e. occupants will overlook shortcomings in the thermal environment more readily) and will therefore have a beneficial effect on occupant’s perception of comfort. The adaptive approach is best expressed with the adaptive principle: *“if a change occurs such as to produce discomfort, people react in ways which tend to restore their comfort”* (Nicol and Humphreys, 2002).

Nicol and Humphreys also state that the adaptive approach is dependent on many factors (climate, HVAC systems, and time) and context dependent (i.e.

solar shading on an appropriate façade). Adaptive thermal comfort is a function of the possibilities for change as well as the actual temperatures achieved. For example, in situations where there are no possibilities for changing clothing or air movement, the comfort zone may have a range as narrow as  $\pm 2$  °C, whereas situations where adaptive opportunities are available and appropriate, the comfort zone may be considerably wider.

Standards based on the adaptive approach are used to define good practice as opposed to standardizing a methodology. However, based on data collected from a wide range of buildings, climates, and cultures, it was deduced that the relationship between comfort temperature ( $T_c$ ) and monthly mean outdoor air temperature ( $T_o$ ) for free-running buildings is remarkably stable (Nicol and Humphreys, 2002):

$$T_c = 24.2 + 0.43(T_o - 22) \exp \left[ - \left( \frac{T_o - 22}{24\sqrt{2}} \right)^2 \right] \quad (2.15)$$

In the case of mechanically cooled buildings, the relationship becomes more complex and less stable. The indoor comfort temperature of these buildings will naturally change with the seasons as people adjust their clothing to the weather. Therefore, the idea of an “adaptive algorithm” to define a variable indoor temperature in terms of the running mean outdoor air temperature (or even solar air temperature) is attractive. The comfort zones defined in ASHRAE Standard 55 (2004) already present a form of such an algorithm since it describes different

indoor ranges of operative temperatures and simply named “winter” and “summer”. These seasonal temperature ranges are based on crude assumptions about the seasonal change in clothing insulation and metabolic rate. The adaptive algorithm, on the other hand, does not rely on these vague descriptions. Rather, it relates the comfort temperature directly to the running mean of the outdoor air temperature. It is even suggested that such a method does not increase occupant discomfort, yet significantly reduces energy consumption of the cooling system compared to a method using a constant indoor set point.

## **2.2 Fenestration systems and perimeter zones**

Fenestration is a term that refers to windows, skylights, and door systems within a building. Fenestration system components of windows include glazing, framing, and shading devices (interior, exterior, integral). The principle energy concern of fenestration systems is their ability to control heat gains losses. They affect building energy use through four basic mechanisms: heat transfer (conduction, convection, radiation), solar heat gain, air leakage, and daylighting. Therefore, fenestration systems play a significant role in the heating, cooling, and lighting loads of perimeter zones. The recognition of the benefits that can be attained by providing occupants with better access to daylight, views, and fresh air is leading to buildings that are thinner in profile with more perimeter and fewer core zones (Carmody et al., 2004).

### 2.2.1 Windows and glazing

The primary energy concern of windows is their ability to control heat loss. Heat transfer through window systems is an interaction of all heat transfer mechanisms: conduction, convection, and radiation. The standard way to quantify this heat flow is with the U-value - an expression of the total heat transfer coefficient of the window system. For a single pane of glass, the U-value is:

$$U = \frac{1}{1/h_i + 1/h_o + l/k} \quad (2.16)$$

where  $h_i$  and  $h_o$  are the interior and exterior heat transfer coefficients (combined convection and radiation), respectively,  $l$  is the thickness of the glass, and  $k$  is the thermal conductivity of the glass.

The overall U-value of a fenestration system ( $U_o$ ) can be determined knowing the separate heat transfer contributions of the center-of-glass, edge-of-glass, and frame (subscripts  $cg$ ,  $eg$ , and  $f$ ) in the absence of solar radiation. The total U-value thus becomes a weighted average of these contributions (ASHRAE Handbook of Fundamentals, 2005):

$$U_o = \frac{U_{cg}A_{cg} + U_{eg}A_{eg} + U_fA_f}{A_o} \quad (2.17)$$

where  $A_o$  is the overall area of the fenestration system.

Another major energy-related characteristic of windows is their ability to control solar heat gain. When direct and diffuse solar radiation coming from the sun and sky is incident on a window, some is transmitted to the interior and some is absorbed in the glazing and readmitted to the interior (Figure 2.9). The solar heat gain coefficient (SHGC) is the fraction of incident solar radiation that actually gets transmitted to the interior as heat gain. It is a dimensionless number from 0 to 1.

Therefore, the basic equation for the instantaneous energy flow through a fenestration system,  $Q$ , is (ASHRAE Handbook of Fundamentals, 2005):

$$Q = U \cdot A \cdot (T_o - T_i) + SHGC \cdot A \cdot I \quad (2.18)$$

where:

$Q$  = instantaneous energy flow, W

$U$  = overall heat transfer coefficient, W/m<sup>2</sup>K

$T_o$  = exterior air temperature, °C

$T_i$  = interior air temperature, °C

$I$  = incident solar radiation, W/m<sup>2</sup>

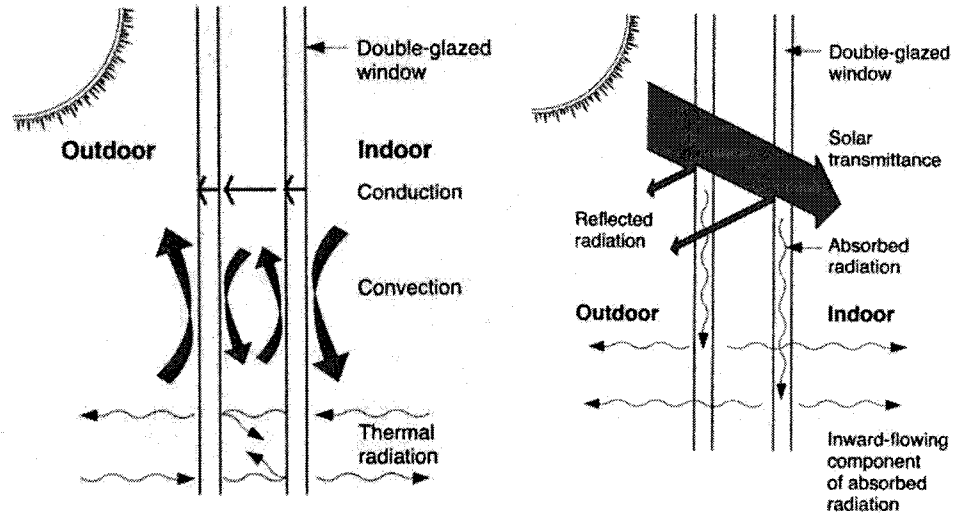


Figure 2.9: The components of heat transfer through glazing (left) and a simplified view of the components of solar heat gain (Carmody et al., 2004)

The glazing component of fenestration systems can be comprised of single or multiple layers, usually glass. The glass can be clear, tinted, and / or have coatings. Spectrally selective coatings, those that select specific portions of the energy spectrum to reflect or transmit, can be applied to windows and be designed to optimize energy flows for passive solar heating and daylighting (Figure 2.10). The emittance of glazing is also an important component for the overall heat transfer of a window. Reducing the emittance of a window can greatly improve its thermal performance. The most common type of coating is one that exhibits low-emissivity (low- $e$ ) over the longwavelength portion of the solar spectrum.

There are two types of low- $e$  coatings: low-solar-gain coatings and high-solar gain coatings. The low-solar-gain coatings are able to reduce solar heat gain by transmitting visible light but reflecting the infrared portion of the solar

spectrum. They are primarily used in hot climates. The high-solar-gain coatings are able to transmit visible light and infrared radiation while remaining highly reflective to the longwavelength infrared radiation emitted by the interior surfaces, thereby reflecting this radiation back into the indoor space. (Figure 2.10)

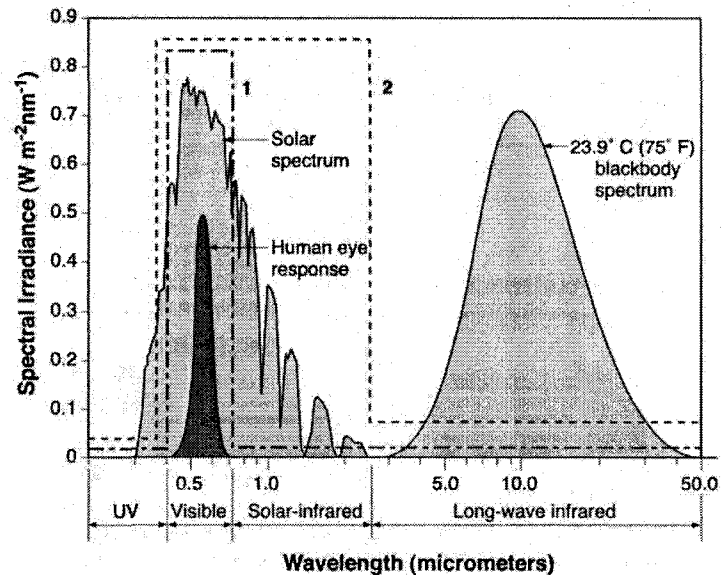


Figure 2.10: Shortwave (solar) and longwave energy spectrum. Area 1 represents idealized transmittance for low solar heat gain glazing; Area 2 represents idealized transmittance for high solar heat gain glazing (Carmody et al., 2004)

## 2.2.2 Shading devices

Solar control is important for preventing thermal (overheating) and visual (glare) discomfort. Shading devices are a necessity in office buildings, especially those with highly glazed façades. Shading devices must therefore be considered as a critical component of the fenestration system and its effect on the thermal and daylighting performance of perimeter zones must be carefully planned at the early design stage (Tzempelikos and Athienitis, 2007).

Shading devices can either be exterior to, interior to, or within the glazing system. Types include venetian blinds, roller shades, draperies, side fins, awnings, and overhangs. Exterior shading devices reduce solar heat gain more effectively than interior devices since a significant portion of solar radiation is rejected to the outdoor environment. However, exterior shading devices are not as versatile as interior shading devices since they must be robust enough to withstand the effects of the exterior environmental conditions.

Several studies have shown how the energy performance of a fenestration system is greatly affected by the presence of a shading device (Tzempelikos et al., 2007; Tzempelikos and Athienitis, 2007; Shahid and Naylor, 2005; Collins et al., 2002).

The thermal resistance of a window system with automated intermediate venetian blinds was measured experimentally by Tzempelikos and Athienitis (2003). The thermal resistance of the window system varied in the range of 0.52 - 0.78 m<sup>2</sup>K/W, depending on the blind tilt angle,  $\beta$ :

$$R(\beta) = \frac{0.068(\beta - 90^\circ)^2 + (-4)(\beta - 90^\circ) + 600}{1000} \quad (2.19)$$

Although the coefficients in this equation will change for different slat widths, slat distance, blind properties, and gap width, it was concluded that for this type of window system, the thermal resistance of the window is determined

by the blind tilt angle; the temperature difference between inside and outside had a small impact.

In another study examining the effects of louver angle ( $\varphi$ ) of an internal venetian blind on the thermal performance of a window, Shahid and Naylor (2005) demonstrated that the presence of a venetian blind significantly improves the energy performance of a single- and double-glazed window during ASHRAE summer design conditions. It achieves this by reducing the overall heat transfer rate through the window thereby reducing the thermal radiation from the interior glazing. It was determined that the blind had the greatest impact on energy performance of a window when the louvers were fully closed ( $\varphi = 90^\circ$ ), reducing the U-value of a single-glazed window by 22% when compared to a window with no blind. With the blind's louvers at a horizontal position ( $\varphi = 0^\circ$ ), the U-value could be reduced by 11%. Similarly, for a double-glazed window, the blinds in a fully closed position and horizontal position could reduce the window U-value by 18% and 10%, respectively. In addition, the study also quantified the effect that the blind has in shielding a nearby occupant from radiative heat flux. It was found that for a single-glazed window, the blind reduced the radiative heat transfer by 15% when  $\varphi = 0^\circ$  and 42% when  $\varphi = 90^\circ$ . For a double-glazed window, the blind reduced the radiative heat transfer by 12% and 37% for louver angles of  $0^\circ$  and  $90^\circ$ , respectively.

### 2.2.3 Mechanical systems

All commercial buildings are divided into thermal zones (Figure 2.11). These zones represent areas of the building that are served by different HVAC systems. A mechanical system zone may operate like a separate building in that it receives heating, cooling, and ventilation from either its own packaged unit or a central system as needed. A building is divided into zones because different spaces have different temperature and outdoor air requirements and therefore need separate control. Zones are also divided based on the orientation of perimeter zone's façade. For example, a north-facing perimeter zone may require heat in the winter while a south-facing perimeter zone within the same building may not due to passive solar gains. Perimeter zones, especially those with fenestration systems, are subject to the greatest fluctuation in thermal conditions due to its direct exposure to outdoor environmental conditions.

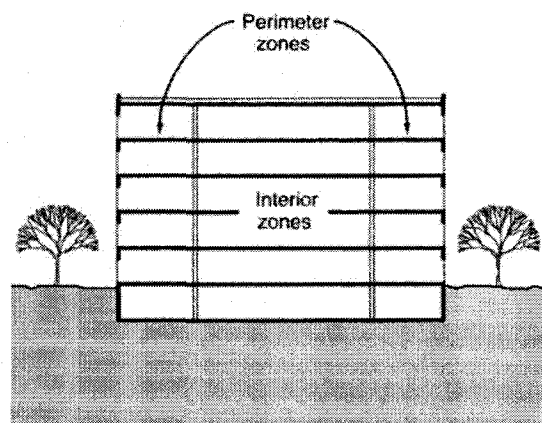


Figure 2.11: The perimeter and interior zones of a building (Carmody et al., 2004)

Traditionally, windows have affected the mechanical design of buildings by increasing the size of mechanical equipment needed for heating and cooling. While a majority of the buildings conditioning needs are delivered through forced-air HVAC systems, additional radiant and convective perimeter baseboard heating is often required near windows in order to mitigate downdraft (Figure 2.12).

With high-performance windows, heat loss and gain through the window is reduced significantly, lowering the peak heating and cooling loads, thereby reducing the size of the mechanical systems. Thus, they play an important role in reducing building energy consumption; a better understanding of how high-performance windows affect occupant comfort could accrue even greater savings. For example, as windows become more insulating, baseboard heaters can be replaced with slot diffusers delivering heated air from above the window. With highly insulating windows, a perimeter heating system may not be needed at all. A recent study found that when high-performance windows are used in houses, perimeter heating systems could be eliminated and energy savings of 10% - 15% could result from installing a simpler, less expensive duct system (Hawthorne and Reilly, 2000).

In another case study of façade and envelope design options for a large commercial building in Montreal, Tzempelikos et al. (2007) investigated the effect of window-to-wall ratio (WWR) and glazing type on thermal performance of a perimeter zone office (4m x 4m x 4.25m). After studying the thermal

performance of three glazing types, it was determined that a low- $e$  double glazing would need perimeter heating while a more insulated glazing ( $R=0.67\text{m}^2\text{K}/\text{W}$ ) would not ( $\text{WWR} = 0.6$ ).

A study by Tzempelikos and Athienitis (2007) showed the benefits of integrated daylighting, shading, and electric lighting control. It was demonstrated that optimum energy performance is only achieved if daylighting benefits due to reduced electric lighting operation exceed the increase in energy demand due to increased solar gains.

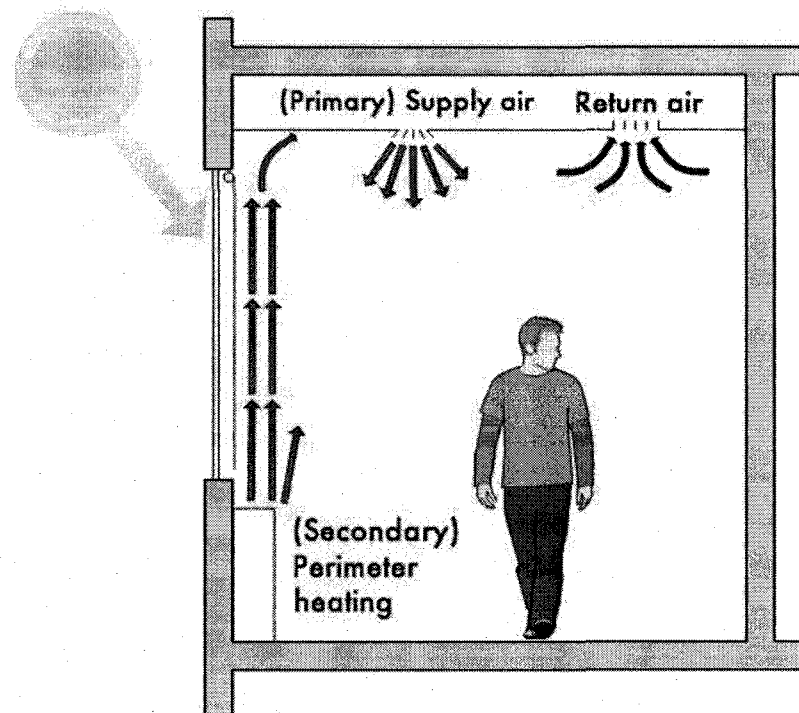


Figure 2.12: Cross section of perimeter zone office with typical HVAC configuration: overhead supply air (primary heating) and perimeter baseboard unit beneath glazing (secondary heating)

## 2.2.4 Perimeter zones and thermal comfort

The presence of fenestration systems adds complexity to the problem of human thermal comfort since fenestration components have different optical and thermal properties. For perimeter zones, it is important to take into account the effect that solar radiation has on the thermal environment since HVAC systems rarely achieve perfect control and, as a result, solar gain often raises the operative temperature of the perimeter zone.

Fenestration systems influence thermal comfort in three ways (Figure 2.13):

1. longwave radiation exchange between body and warm/cold interior window surface;
2. transmitted solar radiation; and
3. convective drafts induced by difference between interior window surface temperature and adjacent air temperature.

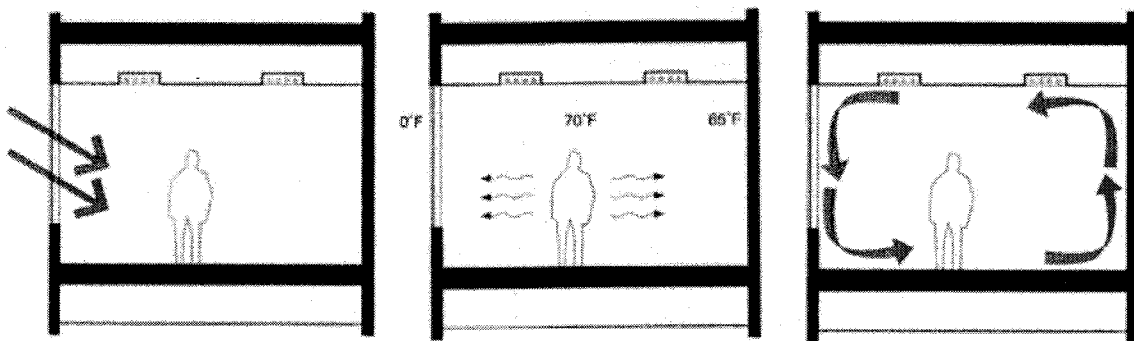


Figure 2.13: Sources of thermal discomfort in glazed perimeter zones (Carmody et al., 2004)

Thermal comfort is affected indirectly by the solar radiation absorbed in the fenestration system and interior surfaces, and directly by the transmitted solar radiation absorbed by the occupant.

Solar transmittance is the dominant factor with respect to the effect a particular glazing system will have on comfort. Simulations have shown that a double 3 mm low-*e* glass with solar transmittance of 0.53 can reduce discomfort by more than 50% when compared with a single 3 mm clear glass and solar transmittance of 0.83 (Lyons et al., 1999).

Carmody et al. (2004) carried out an extensive study into the effect of various façade designs of large commercial buildings on the indoor environmental and energy performance of perimeter zones. The performance of a typical perimeter zone office was analyzed (energy use, peak loads, daylighting, glare, thermal comfort) using different parameters (shading device, glazing properties, lighting control) for different climates. It was determined that for south-facing perimeter zones with large window area ( $WWR = 0.6$ ), interior shades improve thermal comfort for all window types except the double-glazed reflective window. For poor glazing, such as a double-glazed, clear window, overhangs and interior shades provided the biggest positive impact on comfort. For east- and west-facing perimeter zones with a large window area ( $WWR = 0.6$ ), interior shades improve comfort, however, only the interior shaded triple-glazed, low-*e* window attained the criteria of  $PPD \leq 20\%$ . Overall, it was found that shading is recommended for large window areas, for all window types.

Interior shades result in a significant improvement in energy use; even high-rise obstructions do not offset the need for shading.

A methodology to quantify the impact of fenestration systems on thermal comfort was developed by Chapman et al. (2003) using the radiant intensity method. This method considers discrete directions and nodes and calculates the radiant intensity at each point and direction within an enclosure. The enclosure space is divided into a three-dimensional space of finite control volumes. Four different cases were analyzed for rooms with and without fenestration systems and with and without a heating system. Comfort (defined as the operative temperature corresponding to a PPD of 10%) was quantified as a percentage of total floor space by plotting the PMV distribution across the room as contour plots. It was determined through this analysis that "whole-room" heating or cooling systems, such as forced air systems, do not impact the thermal comfort distribution created by the fenestration system. The "penetration depth" was introduced as a new metric for quantifying comfort, defined as the distance from the fenestration into the room, beyond which thermally comfortable conditions exist.

A study for the potential of electrochromic (EC) vacuum glazing (VG) to improve thermal comfort was completed by Fang et al. (2006). Using a finite volume model to analyze the heat transfer through an EC VG for ASTM standard winter boundary conditions, it was shown that when the EC layer faced the interior, glazing surface temperatures would be too high for occupant comfort;

therefore, it was recommended that the EC layer be facing the outdoor environment. With an indoor set-point temperature of 20°C and outdoor temperature of -20°C, it was shown that for incident solar radiation from 0 to 1000 W/m<sup>2</sup> interior surface temperature of the window increased from 13.4°C to 56.0°C. At an incident solar radiation level of 200 W/m<sup>2</sup>, the interior window surface begins to transfer heat to the interior. Based on these results, the authors concluded that their results suggest that EC VGs are comparable to a good triple-glazed window in terms of thermal performance.

Another emerging technology used to improve comfort in perimeter zones is electrically heated windows. When an electrical current is switched to a selective layer on a window pane, the entire glazing can be heated. This presents a unique opportunity for comfort conditioning in cold climates. When properly located, electrically heated zones of a window can avoid downdraft and asymmetric radiation caused by cold interior surfaces. Laboratory measurements conducted by Kurnitski et al. (2003) show that electrically heated windows are an efficient way for thermal conditioning when heated zones are properly dimensioned and proper surface temperatures are used.

### **Mean Radiant Temperature**

The method for calculating MRT as discussed in the previous section is valid when a person is exposed only to low-temperature surfaces emitting longwave radiation. If a person is situated near a window, however, the MRT is also

affected by the solar radiation hitting the body. Therefore, the previous equation is inadequate to accurately describe the MRT for a person situated near a window. A generalized algorithm to calculate the MRT of a person exposed to solar radiation has been developed by La Gennusa et al. (2005):

$$T_r^4 = \sum_i^N F_{p-i} T_i^4 + \frac{1}{\varepsilon_s \sigma} \left( \alpha_{irr,d} \sum_{j=1}^M F_{p-j} I_{d,j} + \alpha_{irr,b} f_p I_b \right) \quad (2.20)$$

where:

- $\varepsilon_s$  = emissivity of the person
- $\alpha_{irr,d}$  = absorptivity of person for diffuse solar radiation
- $\alpha_{irr,b}$  = absorptivity of person for beam solar radiation
- $F_{p-j}$  = view factor of the person to any non-opaque element of the building envelope
- $f_p$  = projected area factor

This equation takes into account the effect of three separate components on the MRT: low-temperature surfaces, absorbed diffuse solar radiation, and absorbed direct beam solar radiation. The amount of direct beam solar radiation striking the person is dependent on the solar geometry relative to the person, since the projection of the sun onto the person, or projected area factor, changes with the sun's altitude, azimuth, and person's orientation (Figure 2.14). Although the projected area factor for seated or standing persons can be determined manually from graphs (Figure 2.14), an algorithm to calculate it explicitly (discussed in detail in Chapter 4) was developed by Rizzo et al. (1991).

This method allows for the calculation of the MRT for the whole body, whereas more complex algorithms have been developed to model projected area factors for individual body segments for both direct and diffuse solar radiation using detailed three-dimensional geometry and numerical ray-tracing techniques (Kubaha et al., 2004).

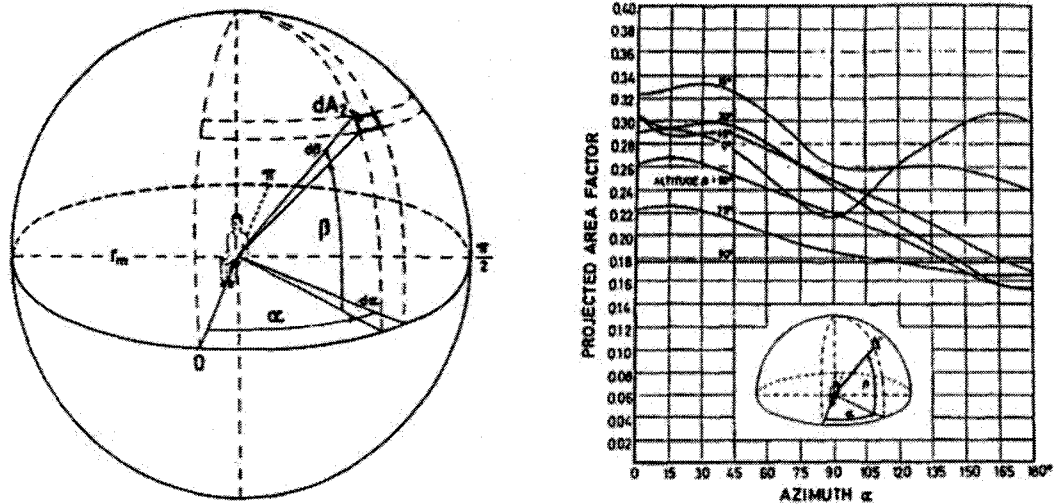


Figure 2.14: Notation pertinent to calculating the effective radiation area (left) and a chart for determining the projected area factors for a seated person (right) (Rizzo et al., 1991)

### Radiant Temperature Asymmetry

The most common sources of discomfort due to asymmetric thermal radiation in most buildings are cold, large windows or improperly installed radiant ceiling panels (ASHRAE Handbook of Fundamentals, 2005). There have been many studies that emphasize the effect of a warm or cold window on comfort (Zmeureanu et al., 2003; Lyons et al., 1999). In one study it was concluded that except in the case when the person is directly in the sun, longwave radiation

exchange with the window is the most significant factor affecting comfort (Lyons et al., 1999).

### **Draft**

A common source of draft is a cold interior surface of a window. Although warm windows can also induce air motion, because upward air movement is not near the occupied zone and since warm air temperature has little heat removal potential, it has little effect. Therefore, most studies of windows and their effect on draft and comfort are limited to cold windows (Ge and Fazio, 2004; Rueegg et al., 2001; Larsson et al., 2002; Heiselberg et al., 1994; Manz et al., 2004).

When a vertical surface has a temperature lower than that of the surrounding air, the air layer adjacent to the surface is cooled, and as a result of increased density, flows downwards. This air layer, called the natural convection boundary layer, increases in thickness from top to bottom. There are several parameters that influence the thermal behaviour of the downdraft, including the window height and width and temperature difference between the interior surface and the air.

A reduction of the cold natural convective flow can be obtained by increasing the surface temperature of the glass or by neutralizing the airflow. This can be accomplished with passive measures such as improving the thermal properties of the window (glazing layers, low-*e* layers, films, gas filling, etc.) or

using shading devices as radiant sources (to increase façade surface temperature) and disrupt the flow of the downdraft. Active measures include heating the surface with warm air from convectors, radiant heating, or electrically heated windows. Both are used with the aim to increase comfort, however the active measures increase energy consumption; even during periods when general room heating is not required, the active systems may be operating. Therefore, using the passive measures to reduce the risk of downdraft, active systems may not be needed, thereby providing an advantage with respect to energy savings in addition to thermal comfort.

Manz et al. (2004) conducted a study of thermal discomfort caused by downdraft due to cold vertical surfaces, which was completed using computational fluid dynamics (CFD). Simulating different wall surface temperatures (17.5, 15, and 10 °C) and internal heat loads (0 - 80 W/m<sup>2</sup>) in a 3 m x 3 m x 5 m room, it was found that draft risk caused more discomfort than reduced operative temperature or radiation asymmetry. Therefore, glazing with a low thermal transmittance not only reduces heat losses in the winter but also mitigate the possibility of downdraft due to cooler interior temperatures. A PPD of 20% due to draft was determined to be 1 m away from a 15 °C wall and 2 m away from a 10 °C wall.

The results of Larsson et al. (2002) show that the use of well-insulated windows not only reduces energy consumption but also considerably reduces air speeds and turbulent intensity. Measurements taken in a climate-control

chamber show that well-insulated triple-glazed window (krypton-filled, low-*e*,  $U = 1.0 \text{ W/m}^2\text{K}$ ) reduced the maximum speed of downdraft by 50%, reduced the turbulent intensity by 79%, and reduced temperature of the downdraft by  $2.2 \text{ }^\circ\text{C}$  when compared to a conventional triple-glazed window ( $U = 1.8 \text{ W/m}^2\text{K}$ ).

However, another study of discomfort due to drafts caused by glazing (Rueegg et al., 2001) concluded that the window frame, not the window glazing, was the critical element in reducing draft risk in the occupied zone. Based on experimental measurements, it was determined that neither active (perimeter heating) nor passive (sill openings) measures were needed to mitigate downdraft, but rather highly insulating glazing (triple-glazed,  $U = 0.55 \text{ W/m}^2\text{K}$ ) *and* frames (insulated profiles with  $U = 1.4 \text{ W/m}^2\text{K}$ ). The author also measured the velocity profile of a draft near a cold window and found that as the internal heat load increased, the boundary layer thickness increased but the peak velocity decreased. It was explained that plumes from the heat load spread at the ceiling and circulated downwards, mixing together with the draft layer, reducing the temperature of the layer thereby reducing the draft.

Structural components of façades that act as obstacles to the natural convection boundary layer can be used as a measure to mitigate downdraft. Heiselberg et al. (1995) showed that with turbulent flow and obstacles larger than the natural convection boundary layer thickness, the boundary layer could break down and reduce the downdraft from large glazed surfaces, thereby reducing the risk of thermal discomfort considerably.

## 2.3 Summary

Based on the literature review, it is evident that there is a need for further research into thermal comfort in perimeter zones. More specifically, there exists a need for further research into the following areas:

- Thermal comfort conditions near glazing in perimeter zones
- Impact of solar radiation and shading devices on thermal comfort
- Reduction or elimination of perimeter heating as a secondary heating system

### 3 EXPERIMENTAL STUDY AND RESULTS

As discussed in the literature review, thermal discomfort is often experienced in perimeter zones due to the impact of exterior climatic conditions and poor façade design. Therefore, an experimental study was undertaken to investigate the comfort conditions in a perimeter zone office with shading devices. A numerical model was developed and used for parametric analysis to predict the comfort conditions in a perimeter zone office and the results from the experimental study were used to verify the simulation results (Chapter 4).

This chapter presents the details of the experimental study of the indoor environment (air temperature, mean radiant temperature, radiant temperature asymmetry, and interior surface temperatures) and outdoor climatic conditions (air temperature and solar radiation) of an experimental façade section equipped with different shading devices in the perimeter zone of a highly glazed office building in Montreal. In order to determine the impact of solar radiation and shading devices on thermal comfort, the secondary perimeter heating system of the experimental façade section was turned off. An overview of the measurement methods and experimental setup is presented. Results are presented for clear and cloudy winter days.

### 3.1 Experimental perimeter zone

Experimental measurements were taken in the perimeter zone of the Solar and Lighting Laboratory at Concordia University in downtown Montreal (latitude 44°N, longitude 74°W) (Figure 3.1). The façade of the perimeter zone is oriented 20 degrees east of south. The entire length of the perimeter zone in the laboratory is 10 m, with the façade divided into six window sections, separated by the internal frame. Each of the six sections was equipped with a different type of shading device. Therefore, in order to study the effect of a particular shading device, each section was separated with fabric curtains on each side to form an isolated experimental section. The isolated section is 1.5 m wide, 4.4 m high, and 2.3 m deep. The floor is black tile and was measured to have an absorptance of 80%. The back wall is white and measured to have an absorptance of 20%.

The façade of the experimental section is divided into a glazing section and a spandrel section. The spandrel extends 0.8 m from the floor and houses the perimeter heating system. The glazing section is divided into two parts, each 1.5 m x 1.3 m: an upper fritted section (50% grey ceramic frit) and lower “vision” section (Figure 3.3). The glazing for each part is double-glazed, with a low-*e* coating (outer side of interior pane) and argon filling. The glazing has a total solar transmittance ( $\tau_{solar}$ ) of 36% and a visible transmittance ( $\tau_V$ ) of 69%. The center-of-glass U-value is 1.6 W/m<sup>2</sup>K and the SHGC is 0.37.

Two different solar shading devices were used for measurements: roller shade and venetian blind. The roller shade is beige with an average reflectance of 55%, absorptance of 40%, and transmittance of 5%. The venetian blind is aluminum grey with an average diffuse reflectance of 75% and average specular reflectance of 5% (M. Collins, personal communication, May 6, 2007).

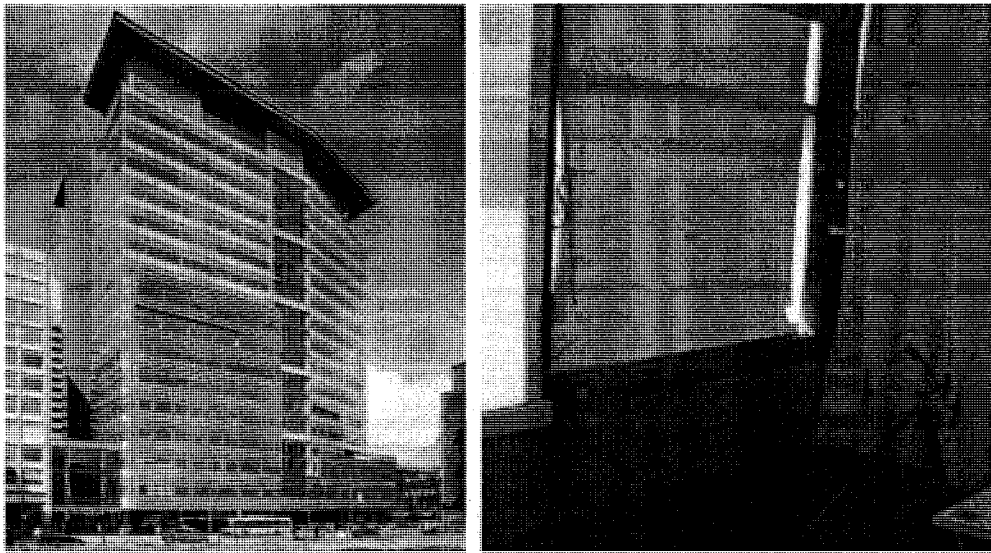


*Figure 3.1: The EV Building at Concordia University in Montreal where the experimental measurements were completed (KPMB Architects, 2006). The image on the right shows one of the experimental sections with a dividing curtain.*

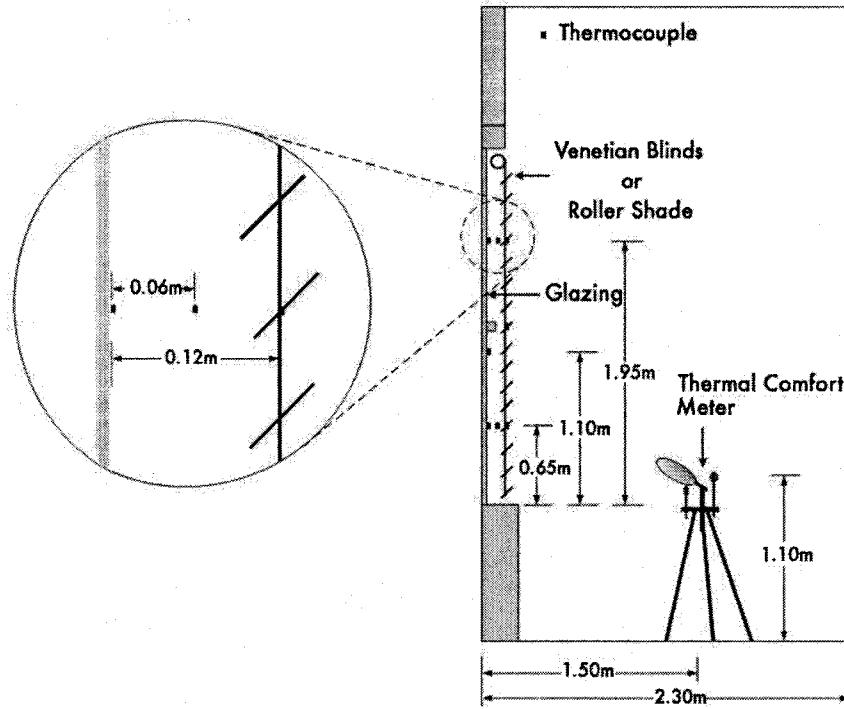


Figure 3.2: Schematic of experimental section used for measurements (not to scale)

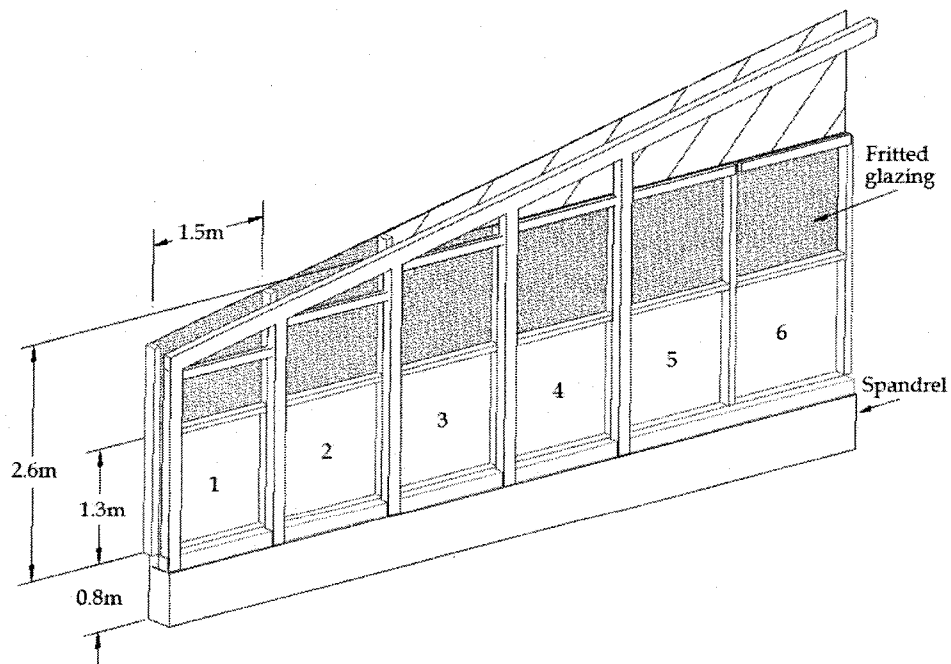


Figure 3.3: Schematic of the six sections of the experimental façade (interior view). The roller shade is used for section 4; the venetian blinds are used for section 5

### 3.2 Data acquisition system, sensors, and measurements

Climatic data was collected from exterior sensors placed outside next to the laboratory. Solar radiation incident on the façade was recorded using a Li-cor pyranometer. It is pre-calibrated against an Eppley precision spectral pyranometer under natural conditions. It has a spectral response from 280 - 2800 nm, a linear response up to 3000 W/m<sup>2</sup>, a cosine correction for an angle of incidence up to 80°, a response time of 0.01 ms, and an absolute error of 3%. Several T-type thermocouples (error = ±0.5 °C) were used to record the exterior air temperature. Thermocouples were also used to record the temperatures of all the interior surfaces (glazing, shading device, floor), the air gap between the glazing and shading device, and indoor air temperature. For the interior glazing surface, three thermocouples were used: in the center of the bottom vision section, 10 cm below the horizontal window frame in the bottom vision section, and the center of the upper fritted section. A thermocouple was placed below the horizontal window frame in the bottom section because the frame could act as a shade on part of the window during times of high solar altitude.

Indoor environmental conditions were measured using a Brüel & Kjaer Indoor Climate Analyzer (Type 1213), which is a collection of instruments and transducers that can measure individual indoor environmental parameters: air velocity, humidity, temperature, and plane radiant temperature (Figure 3.4). Plane radiant temperature is measured using a net radiometer. It consists of a small black plate element with a heat flow meter (thermopile) between the two

sides of the element. The radiant temperature asymmetry can be estimated by the difference in net heat flow between the two sides of the element. A thin polyethylene sphere covers the element to minimize the effect of air velocity (Blazejczyk et al., 1998).

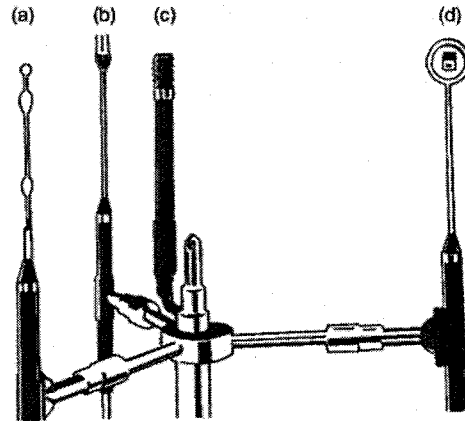


Figure 3.4: Instruments for measuring indoor environmental parameters: (a) air velocity; (b) shielded air temperature; (c) humidity; (d) plane radiant temperature. (Parsons, 2003)

No method exists for a direct measurement of MRT, although many prototype instruments have been developed such as a normal globe thermometer, polyethylene shield globe, and two- or three-sphere radiometer. The most common method for measuring MRT is the use of a black globe, which consists of a hollow, black sphere with a temperature sensor in its center. However, the globe shape (sphere) and colour (black) do not accurately represent the shape of a person or colour of clothing. Therefore, the use of an ellipsoid-shaped sensor is the preferred since its projected area factors may be considered a closer approximation of the shape of a human body. In a study testing the effect of solar radiation on an ellipsoid-shaped sensor, it was determined that measurements were most accurate when the sensor was a grey colour

(Blazejczyk et al., 1998). For this reason, a Brüel & Kjaer Thermal Comfort Meter (Type 1212) consisting of a grey-coloured ellipsoid-shaped transducer was used to measure the operative temperature. It was set at a 30° angle from the horizontal, to closely match the ratio of radiative heat loss to convective heat loss of a seated human body. The indoor climate analyzer and thermal comfort meter were placed 1.3 m from the façade at a height of 1.1 m.

Data was collected every minute from the exterior and interior sensors and transducers for a period of three months, from January to March 2007. The objective was to examine the impact of climatic conditions and shading devices on thermal comfort conditions near the façade during sunny and cloudy days. Therefore, the perimeter heating was turned off so that quasi-free-floating environmental conditions of the perimeter zone could be measured (although the section was affected by small air exchanges with the adjacent core zone of the laboratory as a result of small gaps between the curtains and floor/ceiling). The results of the measurements were also used to validate the simulation model (Chapter 4). The results for clear and cloudy representative days are presented in the next section.

### 3.3 Experimental results

#### 3.3.1 Clear winter day

The experimental results for the case with no shading for a clear winter day are shown in Figure 3.5. Even though the outdoor air temperature is about  $-15^{\circ}$ , the interior surface of the glass at the center of the bottom section reaches  $30^{\circ}\text{C}$ . Between 11:00 - 15:00 the operative temperature exceeds the upper limit of  $25^{\circ}\text{C}$ , reaching a maximum of  $31^{\circ}\text{C}$ . Room air temperature reaches a maximum of  $26^{\circ}\text{C}$ . Since the net radiometer used to measure radiant temperature asymmetry cannot measure plane radiant temperatures greater than  $50^{\circ}\text{C}$ , the results do not give an accurate portrayal of the actual radiant temperature asymmetry.

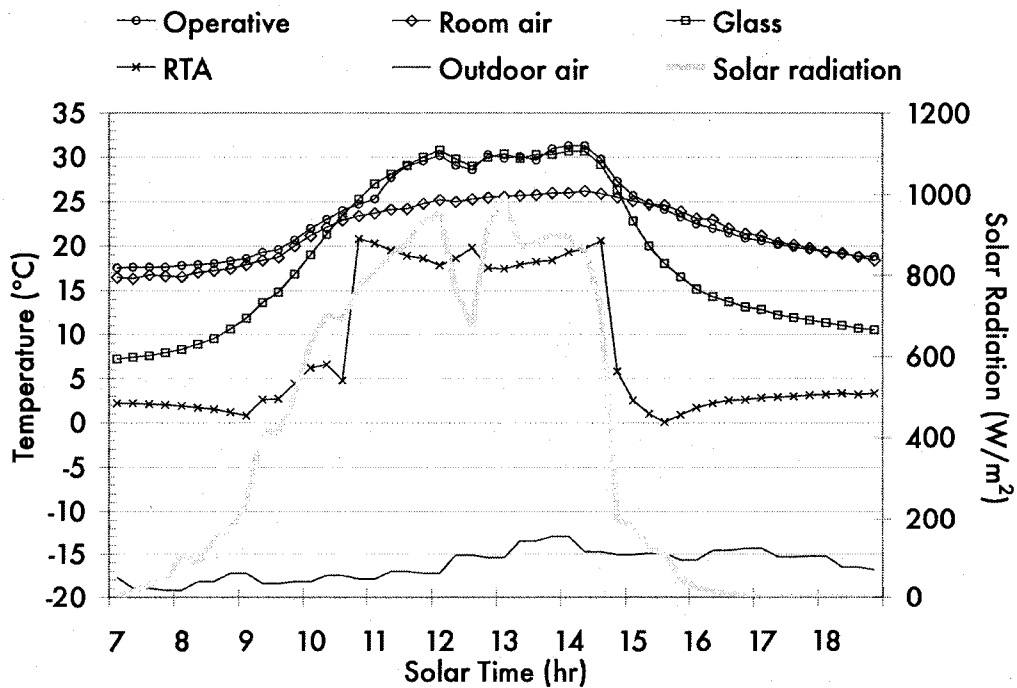


Figure 3.5: Temperature and total incident solar radiation measurements on clear day with no shading

When using a roller shade on a sunny day with slightly higher outdoor temperatures (Figure 3.6) both the shade and the interior surface of the window reached temperatures over 40 °C. However, since the shading device reduces the transmittance of direct solar radiation into the space, conditions remained within the comfort zone for most of the day (9:30 - 18:00). During this time period, the operative temperature was held between 20 - 26 °C, RTA remained at or below 5 °C, and the room air remained between 22 - 25 °C.

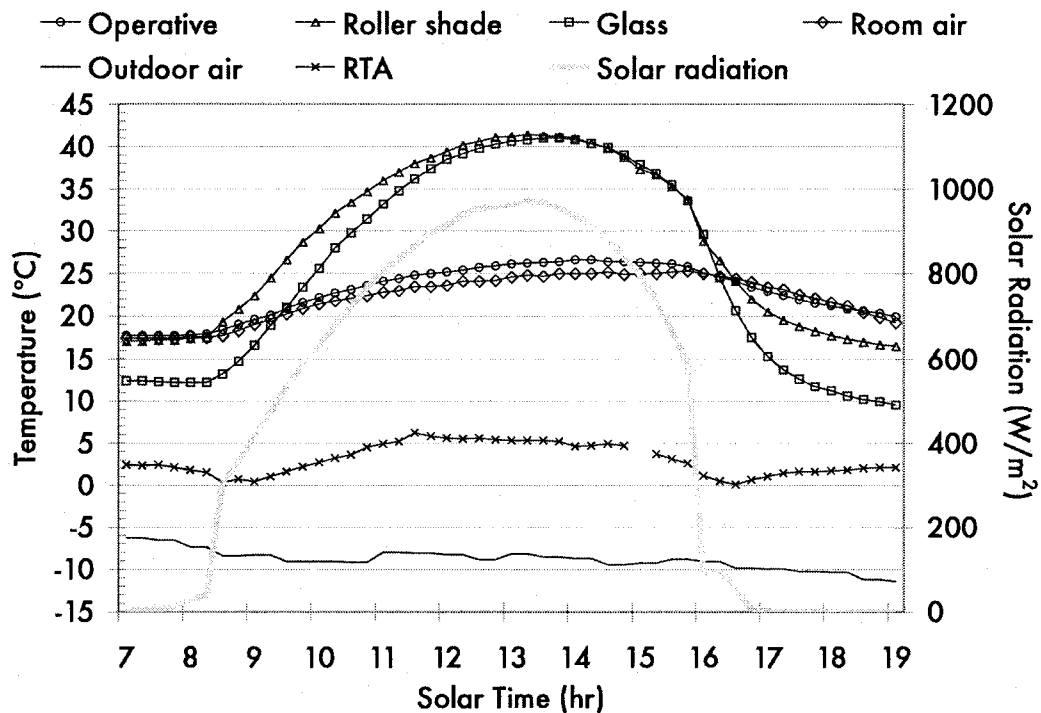


Figure 3.6: Temperature and total incident solar radiation measurements on a clear day with roller shade

With the venetian blind set at a horizontal position (slat tilt angle = 0°) on a similar cold and sunny day (Figure 3.7), the glazing and blind reached temperatures of 32 °C. Since the blind slats are in a horizontal position, part of the beam solar radiation is directly transmitted into the office. This can be

observed from the radiant temperature asymmetry results. Again, since the net radiometer cannot record plane radiant temperatures greater than 50 °C, the maximum RTA is only shown to be around 23 °C although it is expected to be much higher in reality. The “spikes” in the RTA value are due to intermittent shading of beam solar radiation on the net radiometer by the individual blind slats. An occupant would not experience these intermittent decreases in RTA since the surface of a human body is larger than the net radiometer and would therefore be simultaneously shaded and irradiated. The operative temperature remained above the comfort zone from 11:00 - 17:00, reaching a maximum of 31 °C. During this time, room air temperature ranged from 23 - 27 °C.

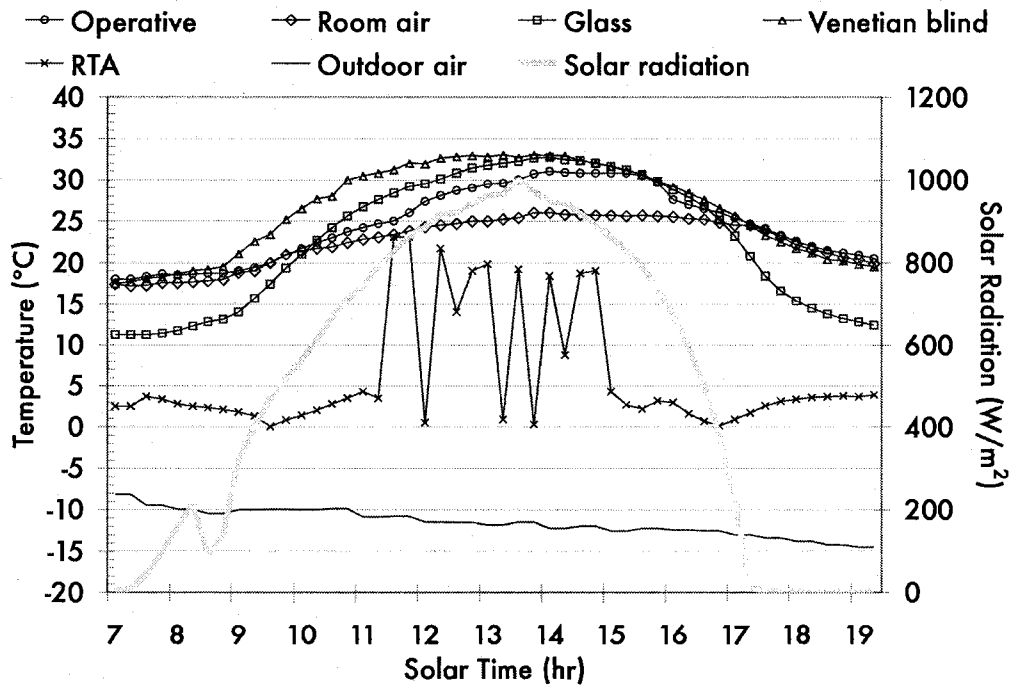


Figure 3.7: Temperature and total incident solar radiation measurements on a clear day with venetian blind (tilt = 0°)

Positioning the blind slats to a tilt of 45° has a significant effect on the thermal environment since it can decrease the amount of direct solar radiation entering the office (Figure 3.8). This can be seen in the significant reduction in RTA. The RTA is kept below 10 °C for the entire day, except for small intermittent increases in the afternoon when the sun's altitude is lower. The glazing reaches a maximum temperature of about 32 °C while the blind reaches slightly higher at 33 °C. Between 10:00 - 18:00 the operative temperature is maintained between 21 - 27 °C, exceeding the comfort zone between 12:30 - 16:30. During this time the air temperature ranges from 20 - 25 °C.

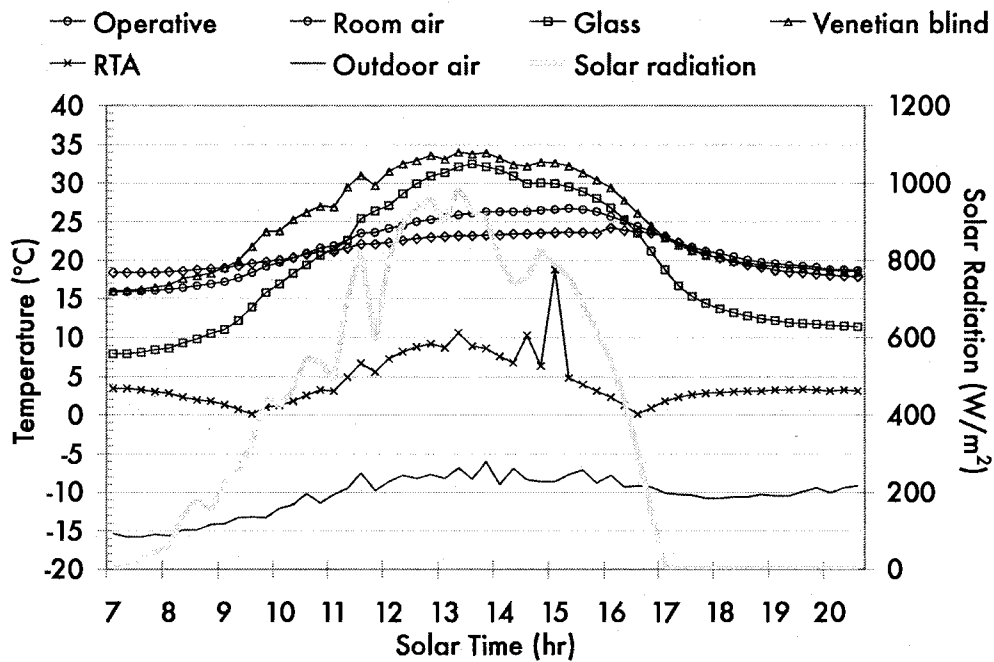


Figure 3.8: Temperature and total incident solar radiation measurements on a clear day with venetian blind (tilt = 45°)

Tilting the slats 90° to a closed position creates a vertical barrier between the glazing and indoor space (Figure 3.9). In this position the blind reaches a

maximum temperature of 34 °C. Operative temperature remains between 20 – 26 °C from 9:30 - 19:00. For most of the day, air temperature is essentially equal to the operative temperature. This means that the MRT is essentially the same as well. RTA is kept below 3 °C for the entire day. These results are similar to those obtained when using the roller shade.

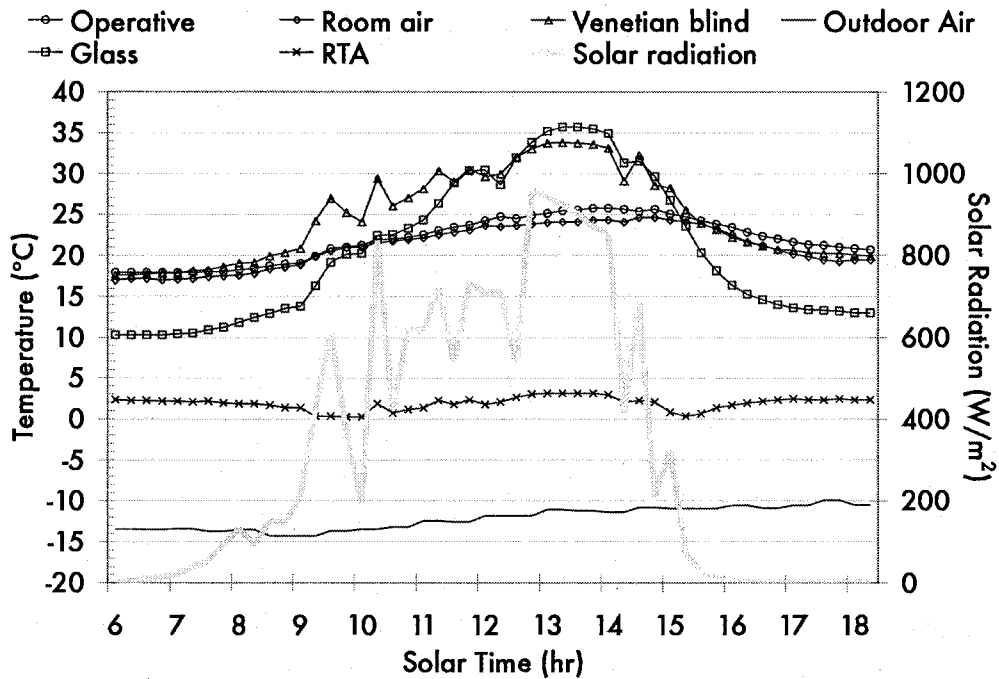


Figure 3.9: Temperature and total incident solar radiation measurements on a clear day with venetian blind (tilt = 90°)

### 3.3.2 Cloudy winter day

Measurements were also taken for a cloudy winter day to determine the thermal environmental conditions in the absence of direct solar radiation. Since the façade uses a relatively high-performance glazing, RTA never falls below 5 °C even when no shading is used.

Figure 3.10 presents results for the case with no shade. The interior surface of the glazing ranges between 13 - 19 °C from 9:00 - 17:00. Room air and operative temperature ranges between 18 - 21 °C and RTA is kept below 5 °C during this time.

With the venetian blind at a horizontal position (slat tilt = 0°) the room air, blind, and operative temperatures remained between 16 - 19 °C and glazing interior temperature remained between 11 - 13 °C for most of the day, while RTA does not exceed 4 °C.

Tilting the slats to an angle of 45°, operative temperature is between 20 - 23 °C and room air temperature is between 17 - 22 °C. RTA remains below 5 °C.

With the blinds fully closed (slat tilt = 90°), operative temperature never falls below 20 °C.

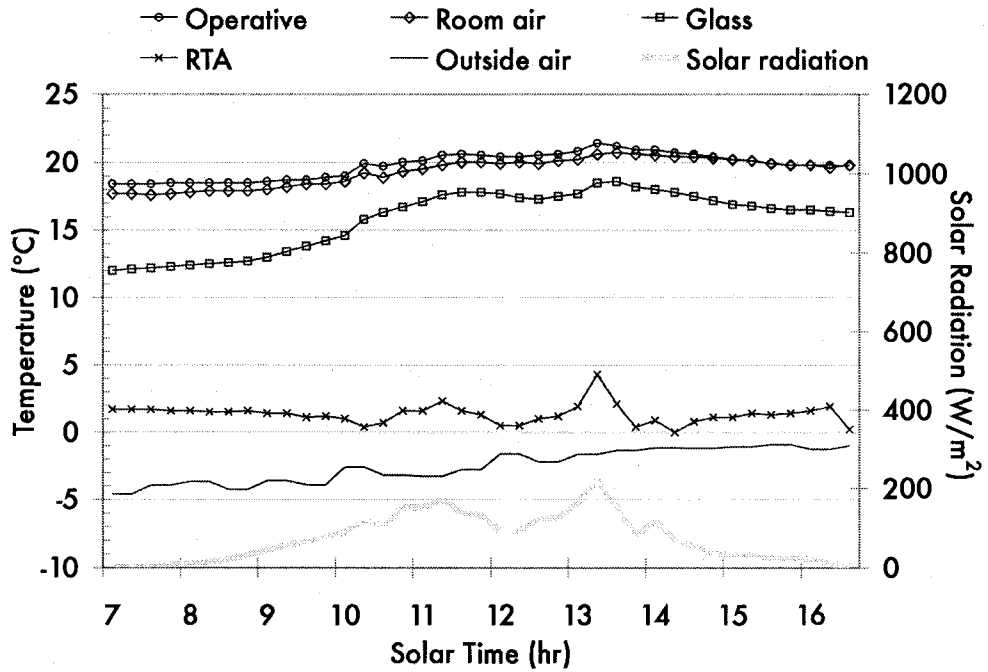


Figure 3.10: Temperature and total incident solar radiation measurements on cloudy day with no shading device

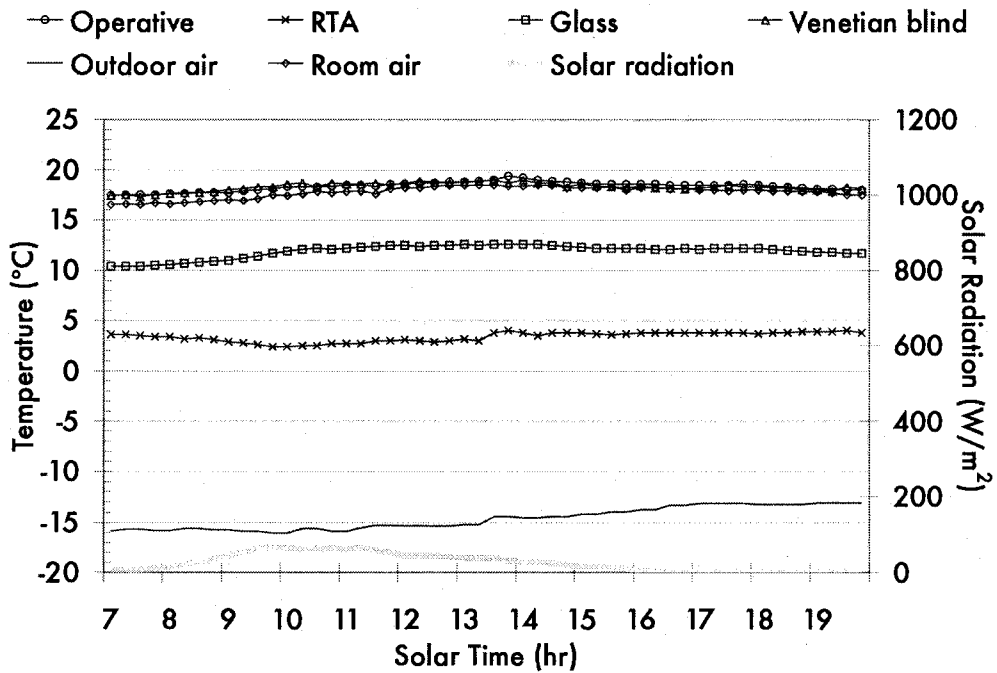


Figure 3.11: Temperature and total incident solar radiation measurements on a cloudy day with venetian blind (tilt = 0°)

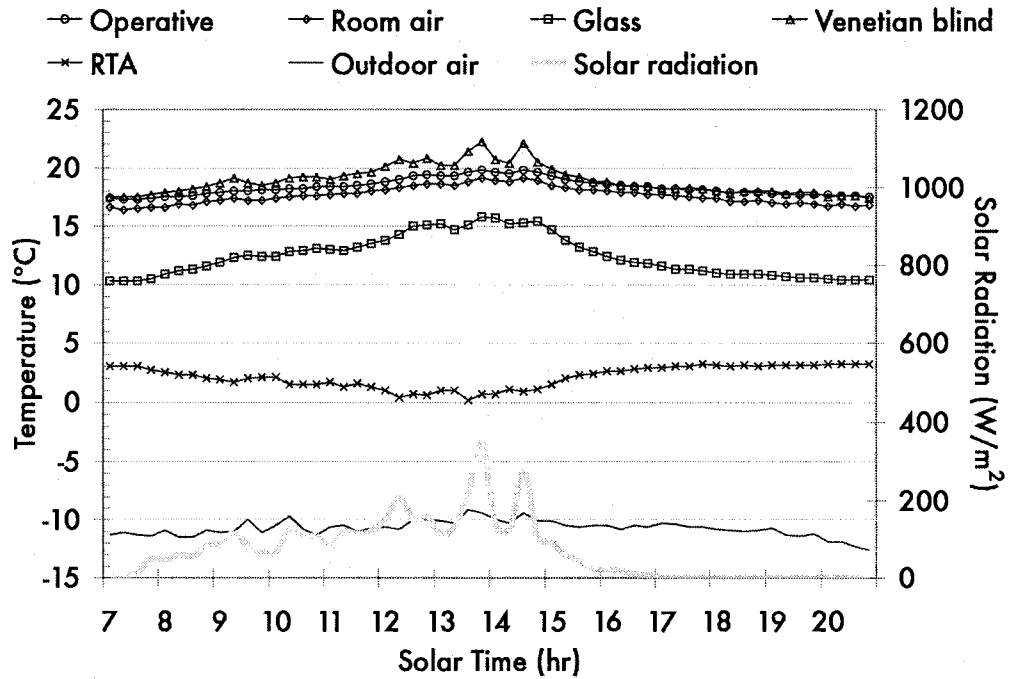


Figure 3.12: Temperature and total incident solar radiation measurements on a cloudy day with venetian blind (tilt = 45°)

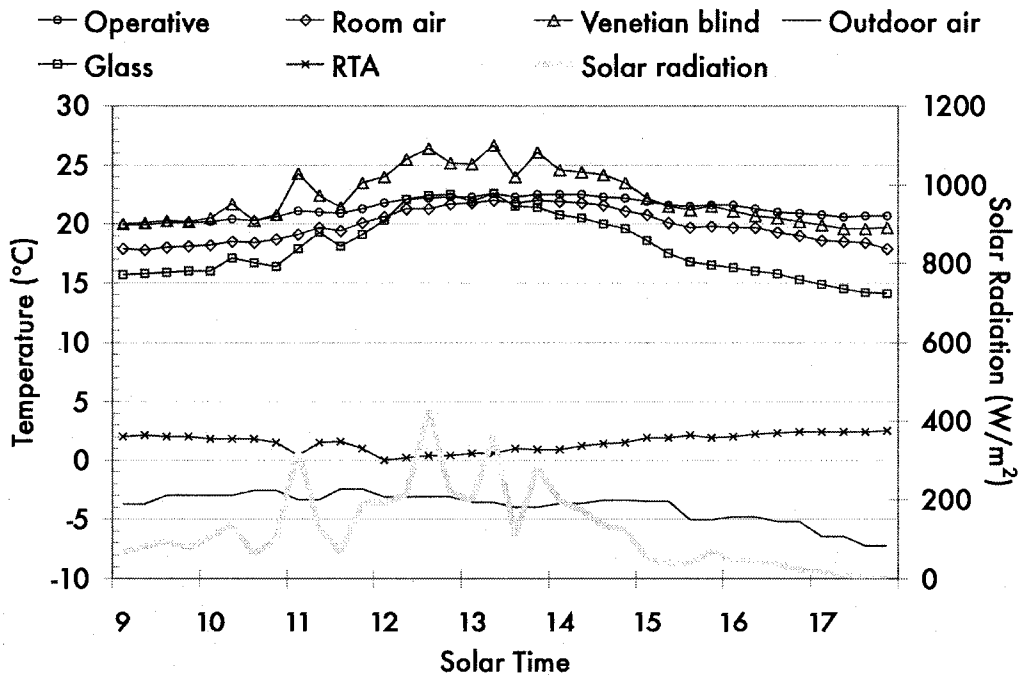


Figure 3.13: Temperature and total incident solar radiation measurements on a cloudy day with venetian blind (tilt = 90°)

### 3.4 Summary

The results of the experimental study show how outdoor climate affects indoor environmental and comfort conditions. The results also show how shading devices impact these conditions.

Using a roller shade on clear winter days can improve the indoor thermal environment (operative temperature and radiant temperature asymmetry) by minimizing the amount of direct solar radiation absorbed by the occupant. Using venetian blinds on clear winter days can also improve the indoor thermal environment but is dependent on the tilt angle of the slats. Maintaining slat angles at a horizontal position (tilt =  $0^\circ$ ) can still cause discomfort since a large amount of the incident beam solar radiation can still be transmitted into the space. A tilt of  $45^\circ$ , however, will decrease the amount of beam radiation entering the space and will, therefore, improve the indoor environment.

On cloudy winter days it was shown that shading devices can decrease the amount of heat loss through the façade and improve the thermal environment of the space. Once again, the venetian blinds set at a horizontal position showed no discernable effect compared with having no shading device since it shields only a small fraction of the glazing.

These results, however, are specific to the experimental façade. Even if the building envelope and blind properties are kept the same, a building at different latitude and with different orientation will have different results due to variation

in incident solar radiation. The purpose of the experimental study was to develop a general understanding of the impact of shading on indoor environmental conditions and to compare results with those generated with a numerical simulation study, which will be described and discussed in the next chapter. This numerical simulation study presents a model with which indoor environmental conditions can be assessed for different building envelope and blind properties and façade location and orientation.

## 4 NUMERICAL SIMULATION STUDY

This chapter presents the description and results of a numerical simulation study of a thermal analysis of a typical office in a highly glazed perimeter zone and its impact on thermal comfort. The results of the simulation study are compared with the experimental results discussed in Chapter 3. A numerical thermal simulation model of a typical office was developed using the Mathcad simulation software. A parametric analysis of the thermal response of the office was completed for different fenestration component properties (glazing and roller shade) and different climatic conditions. A numerical simulation study of thermal comfort was completed based on a transient two-node thermal comfort model. The results of the thermal comfort simulation are compared with experimental results found in the literature. Further investigation into the impact of heated air supply on airflow and comfort conditions using Computational Fluid Dynamics (CFD) is also presented.

### 4.1 Description of thermal simulation model

A transient building thermal simulation model of a typical office in a highly glazed perimeter zone was developed using the Mathcad simulation software. In Mathcad, the source code of the simulation program can be written in the form of mathematical expressions. The model uses the explicit finite-difference thermal

network approach. The entire simulation model is built upon several components:

- Typical Meteorological Year (TMY) weather data
- Solar radiation (Perez model)
- Geometry of perimeter zone office and angle factors
- Solar radiation transmission through glazing
- Building thermal simulation
- Thermal environmental conditions
- Transient thermal comfort modeling

#### **4.1.1 Typical meteorological year weather data**

An hourly weather data file for a Typical Meteorological Year (TMY) for Montreal was imported from an Energy Plus weather file database for use in the thermal simulation. The file contains hourly data for climatic variables including horizontal beam and diffuse irradiance, dry-bulb air temperature, dew-point temperature, humidity ratio, and wind speed.

#### **4.1.2 Solar radiation model**

The parameters in the simulation are expressed as a function of Julian day number ( $n$ ) and solar time ( $t$ ). Hourly values of solar position are determined by a three-dimensional angle with spherical coordinates based on longitude, latitude, altitude, surface azimuth ( $\psi$ ), surface tilt angle ( $\beta$ ), solar altitude ( $\alpha$ ), and solar azimuth ( $\varphi$ ) (Figure 4.1). These angles are a function of day number and

solar time. The solar incidence angle is the angle between the sun's rays and a line normal to the surface, calculated by (Athienitis, 1998):

$$\theta(n,t) = \cos^{-1}[\cos(\alpha(n,t)) \cdot \cos(\varphi(n,t) - \psi) \cdot \sin(\beta) - \sin(\alpha(n,t)) \cdot \cos(\beta)] \quad (4.1)$$

Hourly incident solar radiation on a tilted surface (façade) is calculated from horizontal irradiance values. Direct beam solar radiation on a tilted surface is calculated from:

$$I_b(n,t) = I_{bn}(n,t) \cdot \cos(\theta(n,t)) \quad (4.2)$$

where  $I_{bn}$  is the direct beam normal irradiance.

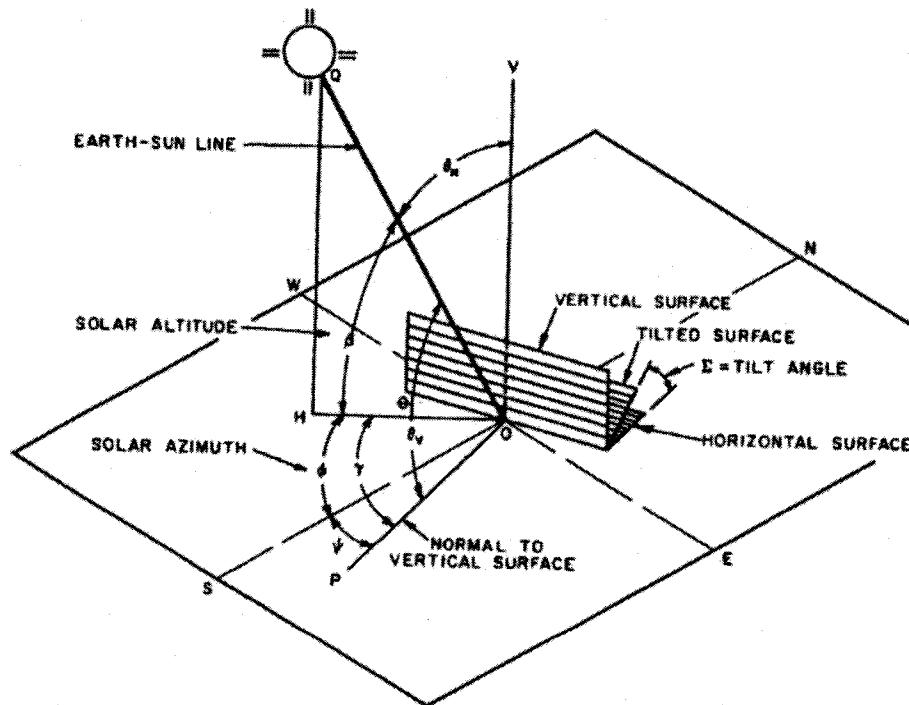


Figure 4.1: Solar angles for vertical and horizontal surfaces (ASHRAE Handbook of Fundamentals, 2005)

Diffuse sky radiation on a tilted surface is calculated using the Perez diffuse irradiance model (Perez et al., 1990). It consists of three components:

1. *Isotropic part*, received uniformly from the entire sky dome
2. *Circumsolar diffuse*, resulting from forward scattering of solar radiation and concentrated in the part of the sky around the sun
3. *Horizon brightening*, concentrated near the horizon and most pronounced in clear skies

The portion of diffuse irradiance coming from the sky can be calculated by:

$$I_{ds}(n, t) = I_{dh}(n, t) \cdot \left[ (1 - F_1) \cdot \left( \frac{1 + \cos \beta}{2} \right) + F_1 \cdot \frac{a}{b} + F_2 \cdot \sin \beta \right] \quad (4.3)$$

where:

$I_{dh}$  = sky diffuse horizontal irradiance;

$F_1$  = circumsolar brightening coefficient;

$F_2$  = horizon brightening coefficient;

$a$  = horizon brightness coefficient;

$b$  = horizon brightness coefficient;

The brightening coefficients are statistically derived and represent the degree of sky anisotropy. They are a function of solar altitude, sky clearness, and sky brightness.

The component of diffuse radiation that is reflected from the ground ( $I_{dg}$ ) is calculated by:

$$I_{dg} = (I_{bh} + I_{dh}) \cdot \rho_g \cdot \frac{1 - \cos \beta}{2} \quad (4.4)$$

where  $I_{bh}$  is the beam horizontal irradiance and  $\rho_g$  is the ground reflectance (albedo).

The total hemispherical diffuse solar radiation on a tilted surface ( $I_d$ ) is the summation of the sky diffuse component and the ground-reflected diffuse component:

$$I_d = I_{ds} + I_{dg} \quad (4.5)$$

Therefore, the total irradiance incident on a tilted surface is:

$$I = I_b + I_d \quad (4.6)$$

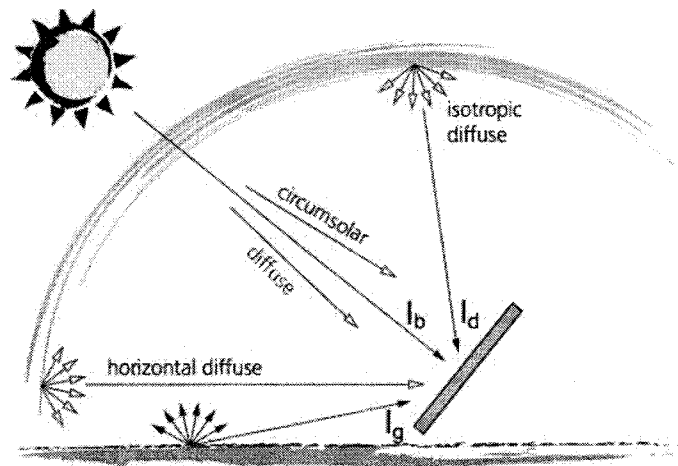


Figure 4.2: Direct radiation, ground reflected radiation, and different components of diffuse radiation (Fieber, 2005)

### 4.1.3 Geometry of perimeter zone office

The geometry of the office is needed for calculation of the view factors between each surface, which, in turn, is needed for radiation heat transfer calculation. The view factor from surface  $i$  to surface  $j$  ( $F_{ij}$ ) is equal to the fraction of diffuse radiation leaving surface  $i$  that is directly incident on surface  $j$ . For two perpendicular rectangles with a common edge, the view factor is given by (Athienitis, 1998):

$$F_{ij} = \frac{1}{\pi \cdot w} \left( w \cdot \tan^{-1}\left(\frac{1}{w}\right) + h \cdot \tan^{-1}\left(\frac{1}{h}\right) - \sqrt{h^2 + w^2} \cdot \tan^{-1}\left(\frac{1}{\sqrt{h^2 + w^2}}\right) \dots \right. \\ \left. + \frac{1}{4} \ln \left\{ \frac{(1+w^2)(1+h^2)}{1+w^2+h^2} \cdot \left[ \frac{w^2(1+w^2+h^2)}{(1+w^2)(w^2+h^2)} \right]^{w^2} \cdot \left[ \frac{h^2(1+h^2+w^2)}{(1+h^2)(h^2+w^2)} \right]^{h^2} \right\} \right) \quad (4.7)$$

where  $h = Z/X$  and  $w = Y/X$

For two parallel rectangular surfaces, the view factor is given by:

$$F_{ij} = \frac{2}{\pi \cdot w \cdot h} \cdot \left\{ \ln \sqrt{\frac{(1+h^2)(1+w^2)}{1+h^2+w^2}} + h\sqrt{1+w^2} \tan^{-1}\left(\frac{h}{\sqrt{1+w^2}}\right) \dots \right. \\ \left. + w\sqrt{1+h^2} \tan^{-1}\left(\frac{w}{\sqrt{1+h^2}}\right) - h \tan^{-1}(h) - w \tan^{-1}(w) \right\} \quad (4.8)$$

where  $h = X/L$  and  $w = Y/L$

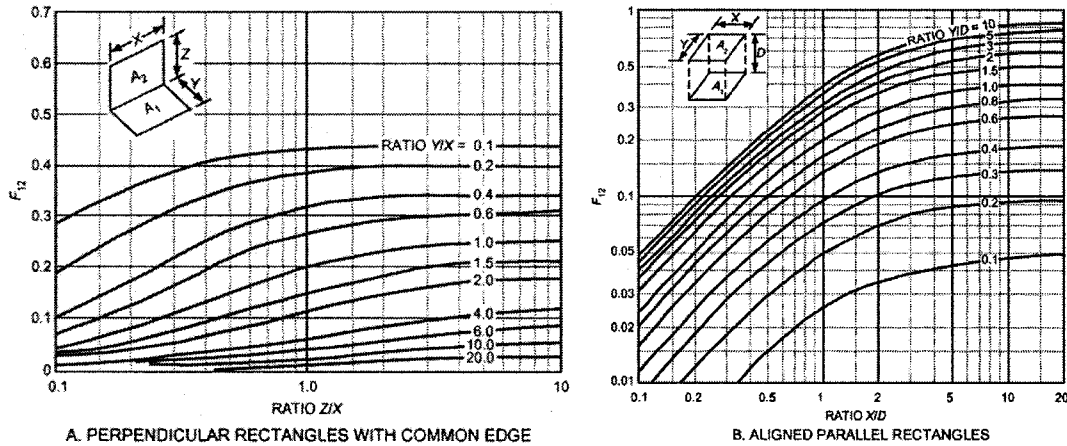


Figure 4.3: Graphical representation of view factors for radiation heat transfer calculation (ASHRAE Handbook of Fundamentals, 2005)

The view factors between all the room surfaces are calculated by applying the follow principles (Athienitis, 1998):

Reciprocity:  $A_i F_{ij} = A_j F_{ji}$  (4.9)

Symmetry:  $F_{ij} = F_{ik}$  (4.10)

Energy Conservation:  $\sum_j F_{ij} = 1$  (4.11)

#### 4.1.4 Solar radiation transmission through glazing

Typically, transmission of solar radiation into the interior space through non-opaque elements such as windows is calculated using the laws of optics. This method determines reflectance, absorptance and transmittance based on the element's thickness, extinction coefficient, refractive index, and angle of incidence. However, for the purposes of this simulation study, the glazing that

was used exhibit complex optical properties due to their selective coatings and tints. Therefore, solar-optical properties (absorptance, transmittance, and reflectance) were determined using the properties given in ASHRAE Handbook of Fundamentals (2005) which are given as a function of incidence angle for beam and diffuse radiation for each glazing layer.

Heat transfer through the fenestration system is determined by its U-value and is a function of the U-value for the window frame, edge-of-glass, and center-of-glass. For a curtain wall with aluminum frame, thermal break, and insulated spacer the frame U-value ( $U_f$ ) is taken to be  $9.26 \text{ W/m}^2\text{K}$  for all glazing types.

The edge-of-glass effects are assumed to extend over a 65 mm-wide band around the perimeter of the glazing. The U-value for the edge-of-glass ( $U_{eg}$ ) can vary from  $2.49 \text{ W/m}^2\text{K}$  for low- $e$  triple-glazed windows to  $3.36 \text{ W/m}^2\text{°C}$  for clear uncoated double-glazed windows (ASHRAE Handbook of Fundamentals, 2005).

The center-of-glass U-value ( $U_{cg}$ ) for double- and triple-glazed windows is approximately equal to the sum of the convective and radiative heat transfer coefficients between the panes of glass. For parallel plates, the convective heat transfer coefficient across a rectangular cavity is related to a number of dimensionless parameters: the Nusselt number (Nu), the Rayleigh number (Ra), and the Prandtl number (Pr) (ASHRAE Handbook of Fundamentals, 1989). The convective heat transfer coefficient ( $h_c$ ) is determined by:

$$h_c = \begin{cases} \frac{k_{air}}{L} \cdot (Nu_1) & \text{if } Nu_1 > Nu_2 \\ \frac{k_{air}}{L} \cdot (Nu_2) & \text{if } Nu_1 \leq Nu_2 \end{cases} \quad (4.12)$$

where  $k_{air}$  is the thermal conductivity of air and  $L$  is the length of the cavity. The thermal conductivity of air is calculated by:

$$k_{air} = \frac{0.002528 \cdot T_{mean}^{1.5}}{T_{mean} + 200} \quad (4.13)$$

where  $T_{mean}$  is the mean temperature of the hot and cold plates ( $^{\circ}\text{C}$ ). The Nusselt number is calculated by:

$$Nu_1 = 0.0605(Ra)^{1/3} \quad (4.14)$$

$$Nu_2 = \left[ 1 + \frac{0.104(Ra)^{0.293}}{\left[ 1 + \left( \frac{6310}{Ra} \right)^{1.36} \right]^3} \right]^{1/3} \quad (4.15)$$

For air the Rayleigh number,  $Ra$ , is determined by:

$$Ra = 2.737(1 + 2a)^2 \cdot a^4 \cdot (T_{hot} - T_{cold})(L)^3 \cdot p^2 \quad (4.16)$$

where  $p$  is the pressure in atmospheres, and  $a$  equals  $100^{\circ}\text{C}/T_{mean}$ .

Therefore, the overall U-value ( $U_0$ ) for a fenestration system becomes:

$$U_o = \frac{U_{cg}A_{cg} + U_{eg}A_{eg} + U_fA_f}{A_o} \quad (4.17)$$

#### 4.1.5 Building thermal simulation model

The building thermal simulation model uses the previous four modules (weather data, Perez irradiance model, room geometry and view factors, and solar transmission through glazing) as inputs. An explicit finite difference thermal network approach is used to simulate the transient thermal response of a perimeter zone office. The thermal network approach discretizes the space into a series of nodes with interconnecting paths through which energy flows. Thermal networks depend on a heat balance at each node to determine its temperature and energy flow between all connected nodes. Finite difference models are one of the most efficient techniques used for building simulation purposes (Tzempelikos, 2005).

For this simulation, each surface, mass layer, and air component is represented by a node that is connected by one or more thermal resistances to other adjacent nodes (Figure 4.4). The thermal resistances in the network ( $R$ ) represent the three heat flow mechanisms between two nodes: convection, radiation, and conduction. Non-linear heat transfer coefficients for convection and radiation are employed; therefore, resistances are a function not only of temperature, but also of time. Solar radiation absorbed in each layer is



$$h_c = 1.31(T_s - T_a)^{1/3} \quad (4.19)$$

Radiation heat transfer between all surfaces is modeled in detail using the radiosity method. Radiation view factors between surfaces are calculated and radiation heat exchange is represented with non-linear heat transfer coefficients.

It is calculated by:

$$h_{r,i \rightarrow j} = \frac{\sigma \cdot F_{\epsilon,ij} (T_i^4 - T_j^4)}{T_i - T_j} \quad (4.20)$$

where  $\sigma$  is the Stefan-Blotzmann constant,  $F_{\epsilon,ij}$  is the radiation exchange factor (*script F*) for the two surfaces (a function of view factors and emissivities) and  $T_i$  and  $T_j$  are the temperatures of surfaces  $i$  and  $j$  (degrees K), respectively.

Radiation exchange factors between surfaces are a function of their respective emissivities ( $\epsilon$ ):

$$F_{\epsilon,ij} = \frac{1}{\left( \frac{1}{\epsilon_i} + \frac{1}{\epsilon_j} \right) - 1} \quad (4.21)$$

For common building materials, emissivity is 0.9; low- $e$  coatings on glazing can have an emissivity as low as 0.05.

The total exterior heat transfer coefficient is the sum of the convection and radiation coefficients following the Energy Plus approach (Bauman et al., 1983).

The total convection coefficient is a combination of natural and forced convection coefficients, with the natural convection coefficient calculated by:

$$h_n = \frac{1.81 \cdot \sqrt[3]{T_s - T_o}}{1.382} \quad (4.22)$$

where  $T_o$  is the outside air temperature ( $^{\circ}\text{C}$ ). The total exterior convective heat transfer coefficient depends on the roughness of the surface exposed to the outside air (Bauman et al., 1983):

$$h_{co, glass} = \sqrt{h_n^2 + (\alpha \cdot v_o^\beta)^2} \quad \text{for smooth (glass) surfaces} \quad (4.23)$$

$$h_{co} = h_n + R_f \cdot (h_{co, glass} - h_n) \quad \text{for rough (cladding) surfaces} \quad (4.24)$$

where  $\alpha$  and  $\beta$  are constant modifiers for forced convection,  $v_o$  is the wind speed, and  $R_f$  is a surface roughness coefficient (1.6 for brick/concrete). The exterior radiation coefficient is a function of the temperature of the sky and the ground and their respective view factors. For simplicity, linearization is used:

$$h_{ro} = 4 \cdot \sigma \cdot \varepsilon_s \cdot T_m^3 \quad (4.25)$$

where  $\varepsilon_s$  is the effective emissivity of the exterior surface and  $T_m$  is the mean temperature of the sky, ground, and surface temperature. Therefore, the total exterior heat transfer coefficient is evaluated for each exterior surface and is calculated by:

$$h_o = h_{co} + h_{ro} \quad (4.26)$$

Heat storage in the building structure (walls, floor, ceiling) is modeled by using one or more thermal capacitances in the building mass nodes. The thermal capacitance ( $C$ ) is calculated by:

$$C = c_p \cdot \rho \cdot Vol \quad (4.27)$$

where  $c_p$  is the specific heat,  $\rho$  is the density, and  $Vol$  is the volume of each mass node.

The amount the solar radiation transmitted into the perimeter zone office is computed based on the hourly values of direct and diffuse solar radiation incident on the façade and the optical properties of the window system. The optical properties of the glazing depend on the type used, as described above. The roller shades are assumed to be perfect diffusers with constant transmittance (5%) over all wavelengths.

An energy balance is applied at each node for each time-step to determine the temperature of each node as a function of time. The system of simultaneous differential and algebraic non-linear equations is then solved numerically in Mathcad using an explicit finite difference technique. This involves going forward in time based on a set of initial conditions. The general form of the explicit finite difference model corresponding to node  $i$  and time-step  $p$  is (Athienitis, 1999):

$$T_i^{p+1} = \frac{\Delta t}{C_i} \cdot \left\{ q_i + \sum \frac{(T_j^p - T_i^p)}{R_{ij}} \right\} + T_i^p \quad (4.28)$$

where  $T$  is the temperature,  $p+1$  represents the next time-step,  $j$  represents all nodes connected to node  $i$ ,  $R_{ij}$  is the thermal resistance connected nodes  $i$  and  $j$ ,  $C_i$  is the capacitance of node  $i$ , and  $q$  is a heat source at node  $i$ . Using this equation, temperatures of all nodes are calculated at each time-step. The heating and cooling load is computed using appropriate proportional and integral control constants. Heating and cooling, if needed, is applied directly to the air node.

A short simulation time-step (five minutes) was selected based on numerical stability criteria. Since the thermal simulation must run on a five-minute time-step, the values of all simulation parameters must also be re-evaluated every five minutes. To do this, all parameters with hourly values were modelled by discrete Fourier Series and then applied with an inverse Fourier transform for the time-step (Athienitis, 1999).

#### 4.1.6 Indoor thermal environment

Once the building thermal simulation model has computed the interior surface temperatures, air temperature, and transmitted solar radiation into the space at each time-step, it is possible to determine the mean radiant temperature, operative temperature, and radiant temperature asymmetry.

To determine the mean radiant temperature, the view factors between a seated person and the surrounding surfaces ( $F_{P-A}$ ) are computed using a calculation method developed by Cannistraro et al. (1992):

$$F_{P-A} = F_{MAX} \left( 1 - \exp[-(a/c)\tau] \right) \cdot \left( 1 - \exp[-(b/c)/\gamma] \right) \quad (4.29)$$

where:

$$\tau = A + B \frac{a}{c} \quad (4.30)$$

$$\gamma = C + D \frac{b}{c} + E \frac{a}{c} \quad (4.31)$$

The coefficients  $a$ ,  $b$ , and  $c$  are show in Figure 2.1. The coefficients  $A$ ,  $B$ ,  $C$ ,  $D$ , and  $E$  can be found in Appendix D.

To determine the mean radiant temperature of a person irradiated by solar radiation, the projected area factor ( $f_p$ ) of the sun on the person is computed using a method developed by Rizzo et al. (1989):

$$f_p(\alpha, \beta) = \sum_{i=0}^4 A_i(\beta) \cdot \alpha^i \quad (4.32)$$

$$A_i(\beta) = \sum_{j=0}^3 A_{i,j} \cdot \beta^j \quad (4.33)$$

where  $\alpha$  is the azimuth angle between the front of the seated person and the sun and  $\beta$  is the solar altitude angle. The values for the coefficient  $A_{ij}$  can be found in the Appendix E.

The mean radiant temperature for a person exposed to solar radiation is then calculated using the algorithm developed by La Gennusa et al. (2005) described in detail in Chapter 2:

$$T_r^4 = \sum_i^N F_{p-i} T_i^4 + \frac{1}{\epsilon_s \sigma} \left( \alpha_{irr,d} \sum_{j=1}^M F_{p-j} I_{d,j} + \alpha_{irr,b} f_p I_b \right) \quad (4.34)$$

## 4.2 Comparison of thermal simulation model and measurements

The simulation model was compared with the results of the experimental measurements by using the climatic data from the measurements as inputs. The parameters used in the simulation for verification were modeled after the experimental façade section and therefore not considered to be representative of a “typical” office. For example, the interaction between the conditioned adjacent core zone and the unconditioned experimental section due to the divisions between the sections had to be taken into account. Nevertheless, adequate results could be generated using these parameters.

It should also be noted that verification of the experimental measurements were only completed for the cases with the roller shade and not for the venetian

blind, because there is currently no available method for calculating view factors between a person and complex surfaces such as tilted venetian blinds.

#### 4.2.1 Clear winter day: no shading

The following figures show a comparison of simulation results with measured values for a clear winter day with no shading. It can be seen from Figure 4.5 that the operative temperature in the simulation model increases quicker than with the measured data in the morning while the measured data decreases quicker at the end of the day. This could be due to greater surface-solar azimuth angles at sunrise and sunset that caused partial shading of the thermal comfort meter that was not taken into account in the model.

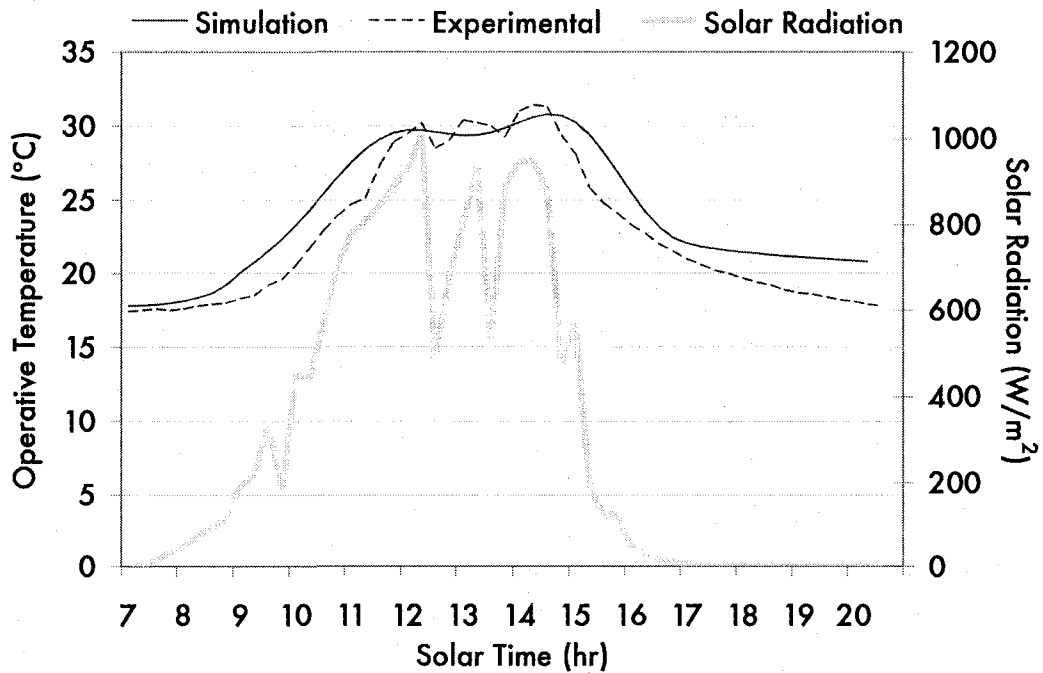


Figure 4.5: Operative temperature: verification of simulation model with measured values for a clear winter day with no shade

Results for comparison of the room air temperature were reasonable, with a difference of less than 2 °C for most of the day (Figure 4.6). Later in the day, however, simulation results diverge slightly from measured data, possibly due to difficulties in making assumptions about airflow between the adjacent zones and experimental section.

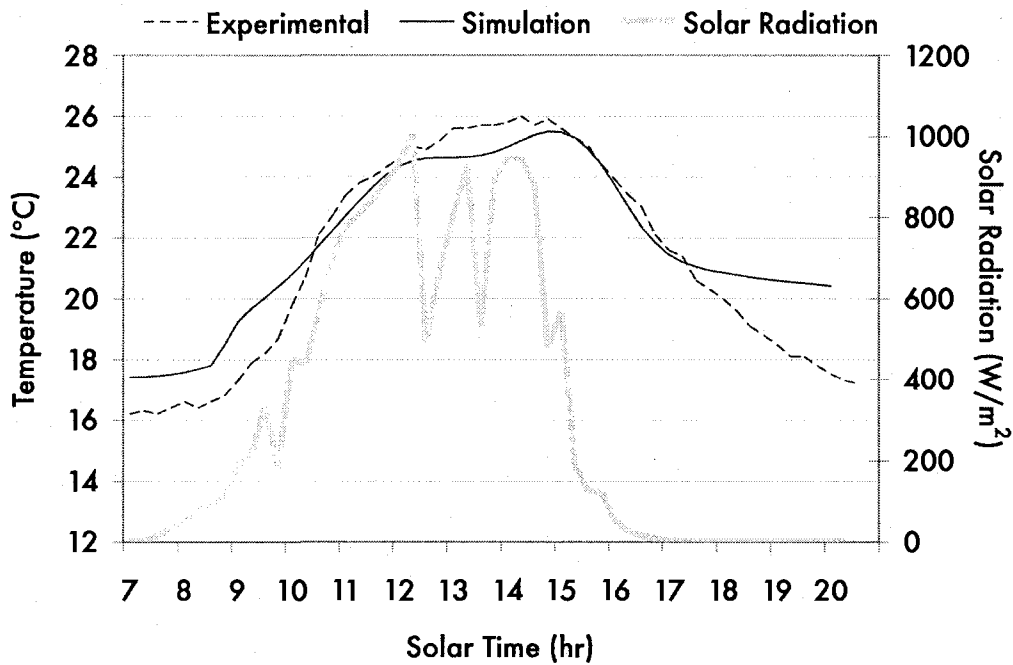


Figure 4.6: Room air temperature: verification of simulation model with measured values for a clear winter day with no shade

Simulated interior glass surface temperature follows closely with measured values for most of the day (Figure 4.7). There is a period when the simulation temperature is 5 °C higher than the measured value. This period is brief, however, since it occurs when the temperature is decreasing rapidly.

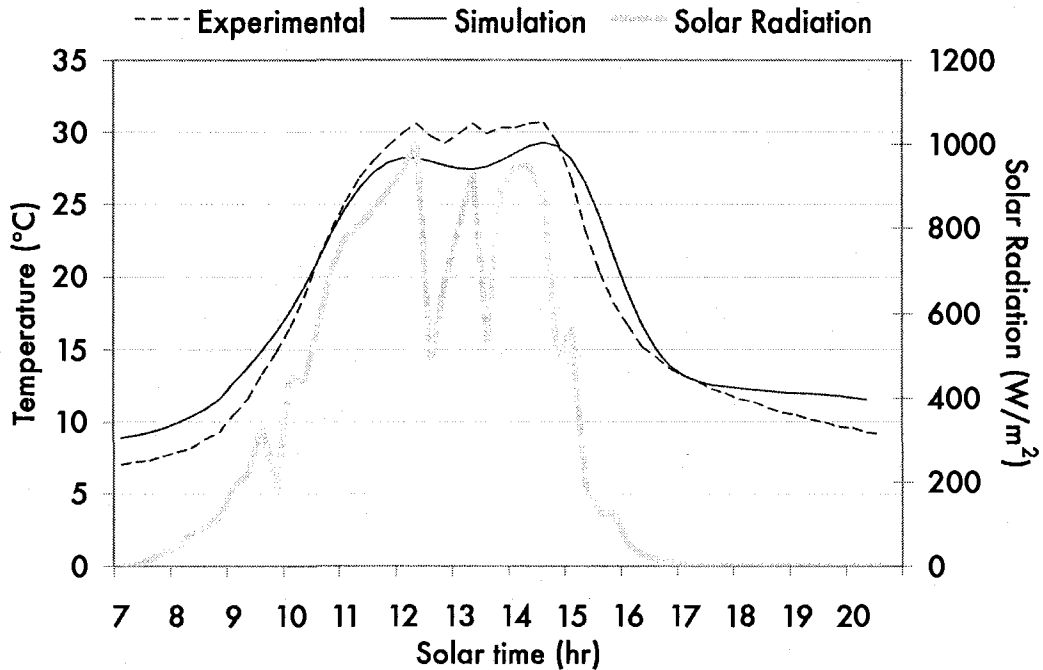


Figure 4.7: Interior glass surface temperature: verification of simulation model with measured values for a clear winter day with no shade

#### 4.2.2 Clear winter day: roller shade

The following figures show a comparison of simulation results with measured values for a clear winter day when using a roller shade. Figure 4.8 shows that the simulation results for operative temperature has a maximum difference of 2 °C from measured values. Simulated room air temperature follows closely with measured values except after 18:30 when there is a difference of over 3 °C. This could be due to difficulties in trying to model the airflow between the core zone and experimental zone correctly (Figure 4.9).

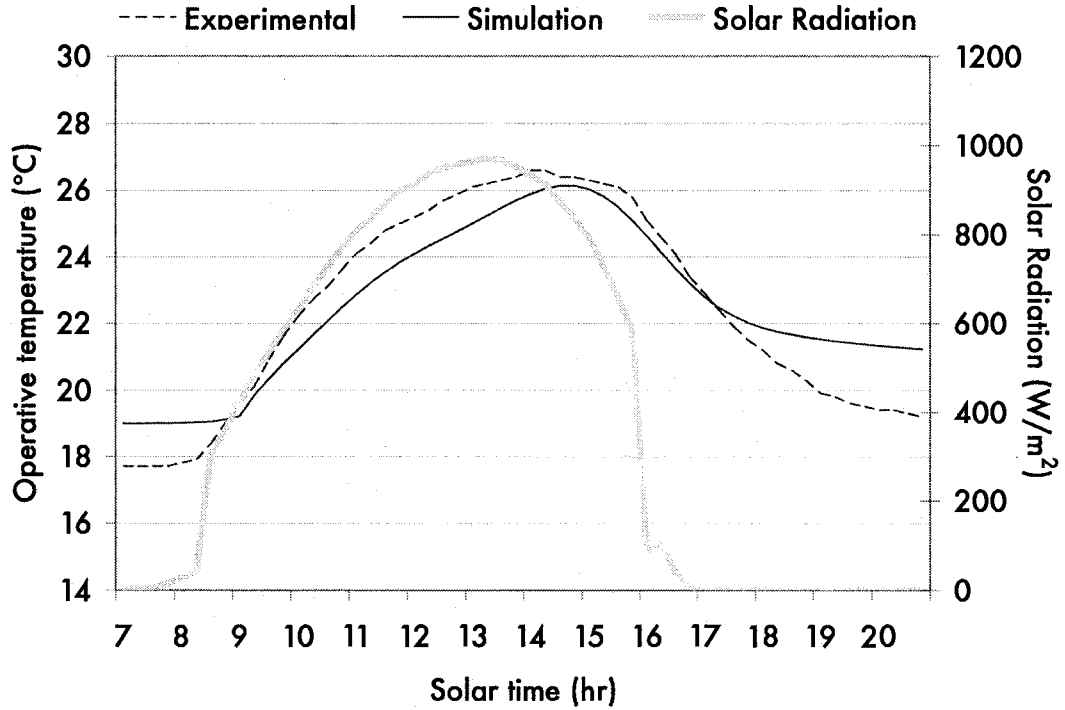


Figure 4.8: Operative temperature: verification of simulation model with measured values for a clear winter day with roller shade

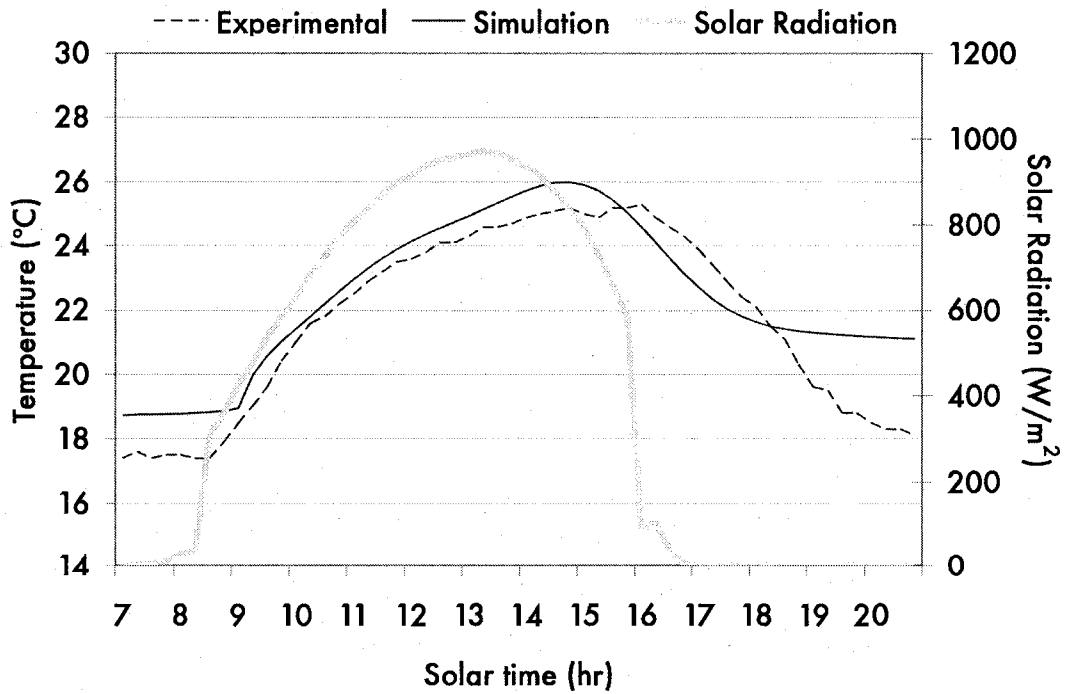


Figure 4.9: Room air temperature: verification of simulation model with measured values for a clear winter day with roller shade

Results of the interior glass surface temperature (Figure 4.10) and roller shade temperature (Figure 4.11) show that the simulated values slightly underestimate the values that were measured. Due to these components' rapid change in temperature due to rapidly increasing and decreasing incident solar radiation, these differences can be as much as 5 °C. The simulation results for RTA follow very closely with the measured values (Figure 4.12).

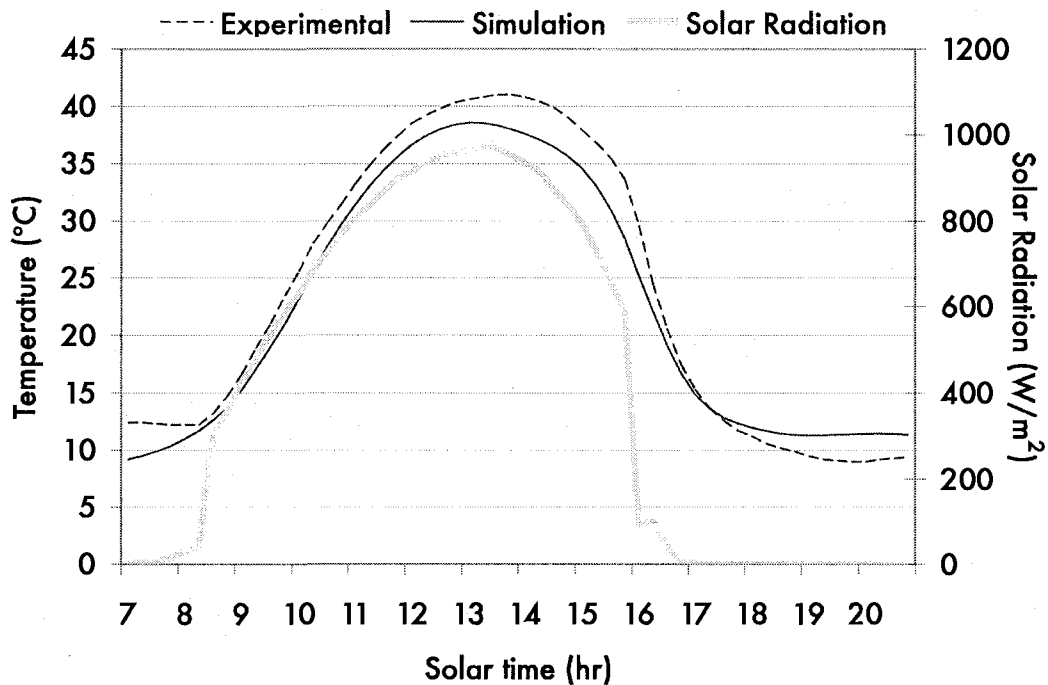


Figure 4.10: Interior glass surface temperature: verification of simulation model with measured values for a clear winter day with roller shade

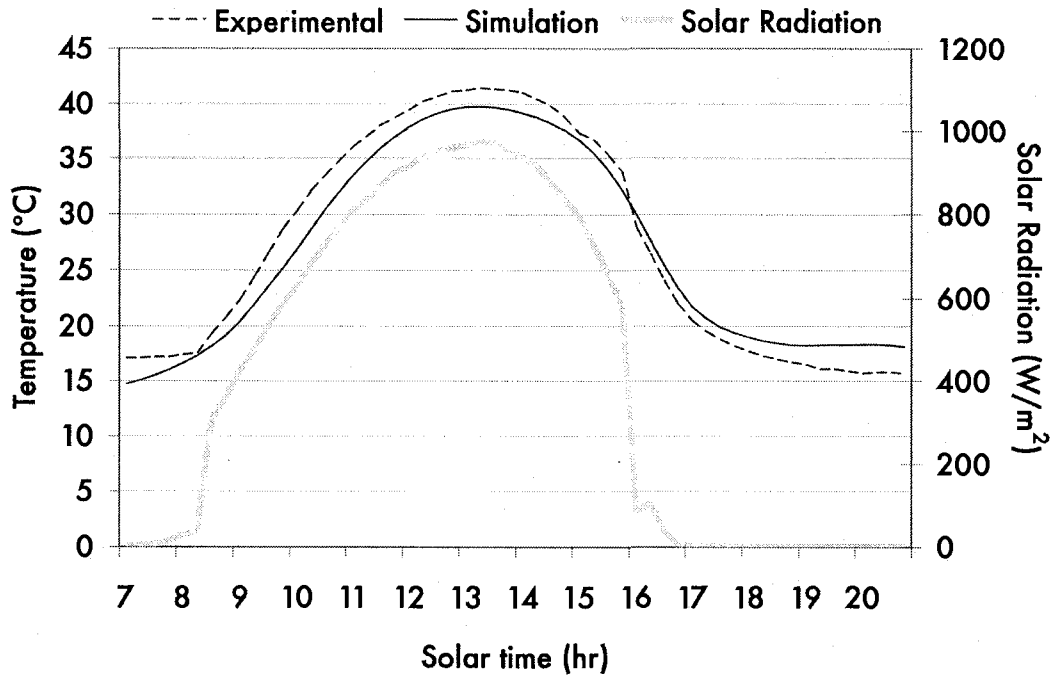


Figure 4.11: Roller shade: verification of simulation model with measured values for a clear winter day with roller shade

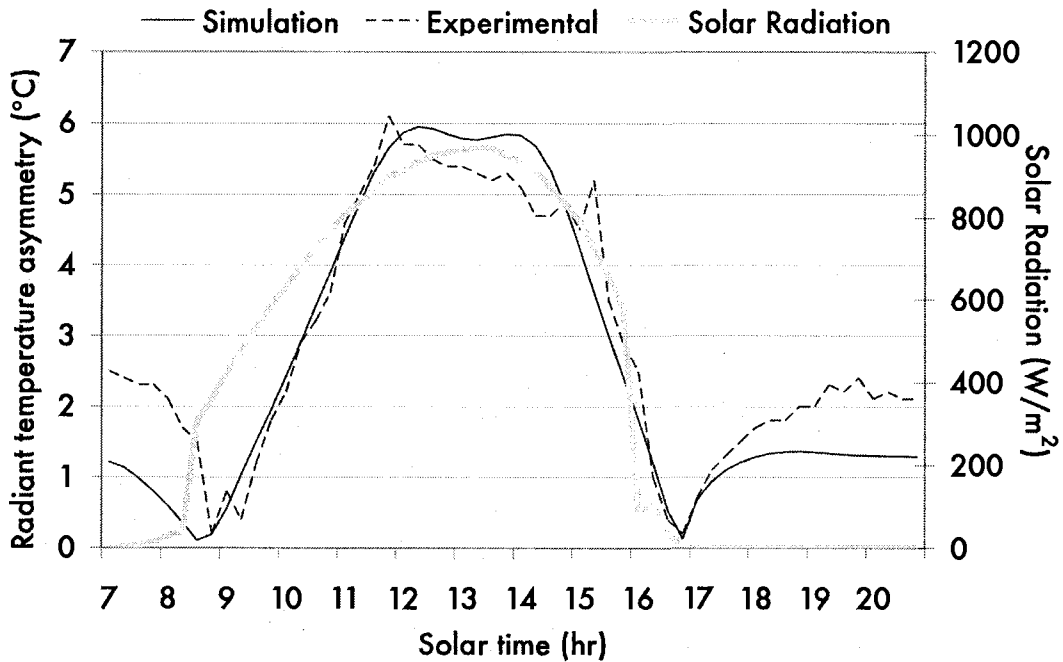


Figure 4.12: Radiant temperature asymmetry: verification of simulation model and measured values for a clear winter day with roller shade

### 4.2.3 Cloudy winter day: no shading

The following figures show a comparison of simulation results with measured values on a cloudy winter day when using no shading. Operative temperature (Figure 4.13) and room air temperature (Figure 4.14) fluctuate very little throughout the day due to low insolation. Simulation results of interior glass surface temperature differ by less than 2 °C compared with measured values (Figure 4.15).

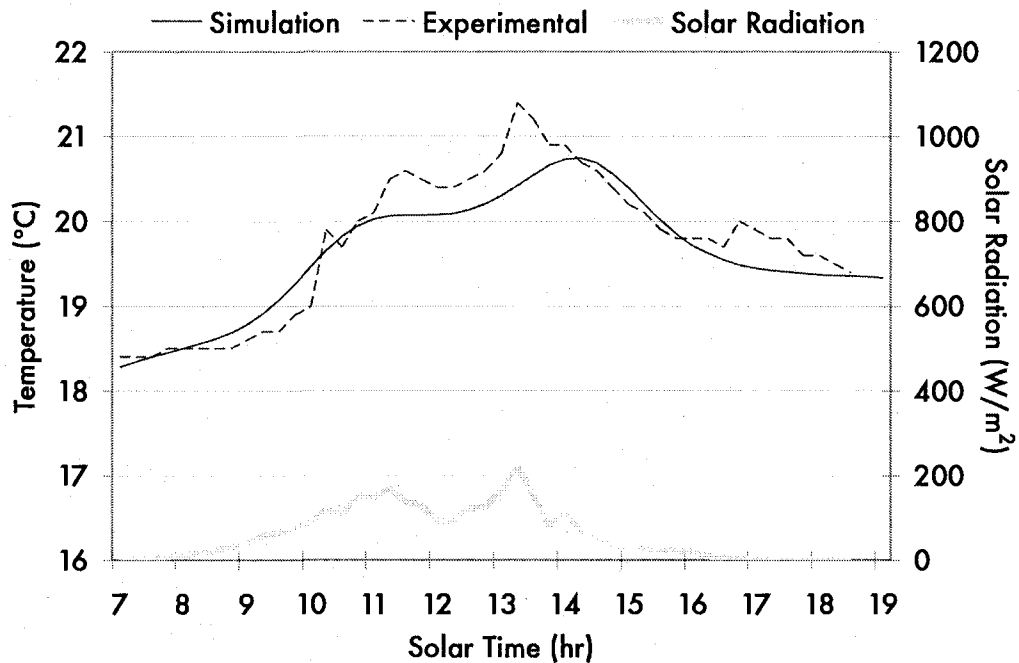


Figure 4.13: Operative temperature: verification of simulation model with measured values for a cloudy winter day with no shade

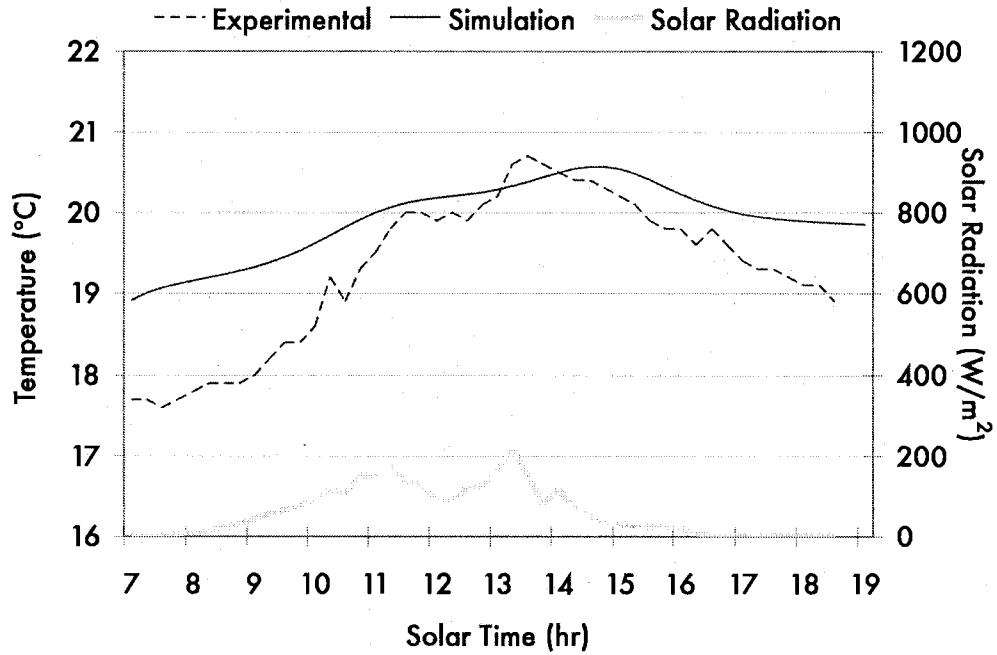


Figure 4.14: Room air temperature: verification of simulation model with measured values for a cloudy winter day with no shade

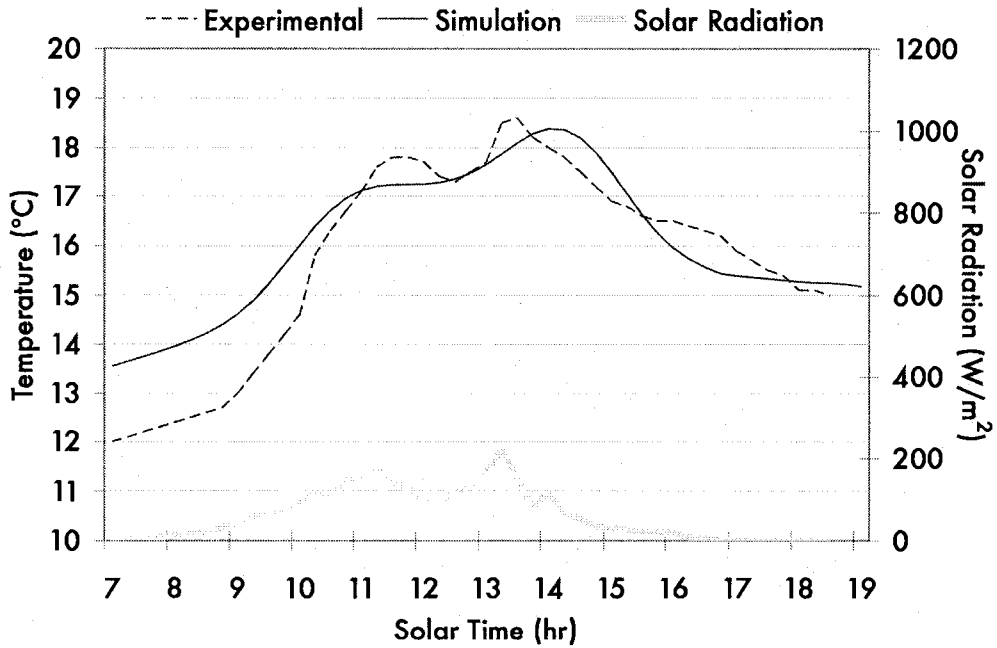


Figure 4.15: Glass temperature: verification of simulation model with measured values for a cloudy winter day with no shade

### 4.3 Description of thermal comfort model

A thermal comfort model was developed based on the transient two-node model of Gagge et al. (1970) which considers the human body as composed of two concentric thermal compartments: core and skin. This section describes the numerical methods used for developing this simulation model (ASHRAE Handbook of Fundamentals, 2005).

The rate of change of temperature of the core and skin is a function of its heat storage and heat capacity of the body:

$$\frac{dT_{cr}}{dt} = \frac{S_{cr} \cdot A_D}{(1 - \alpha_{sk}) \cdot m \cdot c_{p,b}} \quad (4.35)$$

$$\frac{dT_{sk}}{dt} = \frac{S_{sk} \cdot A_D}{\alpha_{sk} \cdot m \cdot c_{p,b}} \quad (4.36)$$

where:

$\alpha_{sk}$  = fraction of body mass concentrated in skin compartment

$m$  = body mass, kg

$c_{p,b}$  = specific heat capacity of body, J/kg · K

$A_D$  = DuBois surface area, m<sup>2</sup>

$T_{cr}$  = temperature of core compartment, °C

$T_{sk}$  = temperature of skin compartment, °C

$t$  = time, s

The heat storage in each compartment can be expressed as:

$$S_{cr} = M - W - (C_{res} - E_{res}) - Q_{crsk} \quad (4.37)$$

$$S_{sk} = Q_{crsk} - (C + R + E_{sk}) \quad (4.38)$$

where  $Q_{crsk}$  is the heat transfer from the core to the skin by convection through blood circulation and by conduction through the body tissue. It is calculated by:

$$Q_{crsk} = (k + c_{p,b} \cdot SKBF)(T_{cr} - T_{sk}) \quad (4.39)$$

where  $k$  is the thermal conductance between the core and the skin,  $c_{p,b}$  is the specific heat of blood, and  $SKBF$  is the rate of blood flow to the skin compartment.

During respiration, the body loses both sensible and latent heat by convection and evaporation of heat and water vapour. These heat losses can be determined by:

$$C_{res} = 0.0014M(34 - T_a) \quad (4.40)$$

$$E_{res} = 0.0173M(5.87 - P_a) \quad (4.41)$$

Convective and radiative heat losses from the outer surface of a clothed body are related to their respective heat transfer coefficients:

$$C = f_{cl}h_c(T_{cl} - T_a) \quad (4.42)$$

$$R = f_{cl} h_r (T_{cl} - T_{mrt}) \quad (4.43)$$

where:

$f_{cl}$  = clothing area factor

$h_c$  = convective heat transfer coefficient, W/m<sup>2</sup> °C

$h_r$  = linearized radiative heat transfer coefficient, W/m<sup>2</sup> °C

$T_{cl}$  = temperature of clothing, °C

$T_a$  = air temperature, °C

$T_{mrt}$  = mean radiant temperature, °C

Several different equations can be used to determine the convective heat transfer coefficient depending on the activity level of the person and the condition of the surrounding air. For conditions typical of an office environment, the following correlation can be used:

$$h_c = \max\left(8.3v_a^{0.6}, 3.1\right) \quad (4.44)$$

The linearized radiative heat transfer coefficient ( $h_r$ ) is given by:

$$h_r = 4\varepsilon\sigma \cdot (0.7) \cdot \left[273.2 + \frac{T_{cl} + T_{mrt}}{2}\right]^3 \quad (4.45)$$

where  $\varepsilon$  is the average emissivity of clothing (0.95) and  $\sigma$  is the Stefan-Boltzmann constant.

Evaporative heat loss from the skin is a function of the amount of moisture on the skin and the difference between the water vapour pressure at the skin and in the surrounding air. It can be calculated by:

$$E_{sk} = w \cdot h_e \cdot (P_{sk} - P_a) \quad (4.46)$$

where  $w$  is the fraction of the skin surface covered by water, or skin wettedness,  $h_e$  is the evaporative heat transfer coefficient,  $P_{sk}$  is the saturated water vapour pressure on the skin surface, and  $P_a$  is the partial pressure of water vapour at ambient conditions. These can be evaluated by:

$$w = 0.06 + \frac{0.94 \cdot E_{rsw}}{E_{max}} \quad (4.47)$$

$$h_e = 16.5 \cdot i_m \cdot h_c \quad (4.48)$$

where:

$E_{rsw}$  = rate of regulatory sweating, W/m<sup>2</sup>

$E_{max}$  = maximum rate of evaporative heat loss, W/m<sup>2</sup>

$i_m$  = moisture permeability of clothing

Skin temperatures and sweat rates required for comfort,  $t_{sk,req}$  and  $E_{rsw,req}$  depend upon activity level (ASHRAE Handbook of Fundamentals, 2005):

$$T_{sk,req} = 35.7 - 0.0275(M - W) \quad (4.49)$$

$$E_{rsw,req} = 0.42(M - W - 58.15) \quad (4.50)$$

The mean body temperature ( $T_b$ ) is therefore a weighted average of the skin and core temperatures:

$$T_b = \alpha_{sk} T_{sk} + (1 - \alpha_{sk}) T_{cr} \quad (4.51)$$

where  $\alpha_{sk}$  is the fraction of body mass concentrated in the skin compartment and is a function of the rate of blood flow from the core to the skin and the deviations of skin and core temperature from their respective set-points:

$$\alpha_{sk} = 0.1 + \frac{0.00028}{SKBF + 0.0011} \quad (4.52)$$

$$SKBF = \frac{6.3 + 200WSIG_{cr}}{3600(1 + 0.5CSIG_{sk})} \quad (4.53)$$

The rate of blood flow from the core to the skin is proportional with the difference between the actual temperature and corresponding set-point value for neutral condition:

Warm signal from the core:

$$WSIG_{cr} = \begin{cases} 0 & T_{cr} \leq T_{cr,n} \\ T_{cr} - T_{cr,n} & T_{cr} > T_{cr,n} \end{cases} \quad (4.54)$$

Cold signal from the core:

$$CSIG_{cr} = \begin{cases} T_{cr} - T_{cr,n} & T_{cr} < T_{cr,n} \\ 0 & T_{cr} \geq T_{cr,n} \end{cases} \quad (4.55)$$

Warm signal from the skin:

$$WSIG_{sk} = \begin{cases} 0 & T_{sk} \leq T_{sk,n} \\ T_{sk} - T_{sk,n} & T_{sk} > T_{sk,n} \end{cases} \quad (4.56)$$

Cold signal from the skin:

$$CSIG_{sk} = \begin{cases} T_{sk,n} - T_{sk} & T_{sk} < T_{sk,n} \\ 0 & T_{sk} \geq T_{sk,n} \end{cases} \quad (4.57)$$

Warm signal from the body:

$$WSIG_b = \begin{cases} 0 & T_b \leq T_{b,n} \\ T_b - T_{b,n} & T_b > T_{b,n} \end{cases} \quad (4.58)$$

where  $T_{cr,n} = 36.80$  °C,  $T_{b,n} = 33.70$  °C, and  $T_b = 36.49$  °C.

Thermal sensation (*TSENS*) is defined in terms of the deviation of the mean body temperature ( $T_b$ ) from cold and hot set points. The set points represent the lower (cold) and upper (hot) limit of the evaporation regulation zone ( $T_{b,c}$  and  $T_{b,h}$ , respectively) and are a function of the rate of internal heat production:

$$T_{b,c} = \frac{0.194}{58.15}(M - W) + 36.301 \quad (4.59)$$

$$T_{b,h} = \frac{0.347}{58.15}(M - W) + 36.669 \quad (4.60)$$

*TSENS* can then be calculated by:

$$TSENS = \begin{cases} 0.4685(T_b - T_{b,c}) & T_b > T_{b,c} \\ 3.995(T_b - T_{b,c}) / (T_{b,h} - T_{b,c}) & T_{b,c} \leq T_b \leq T_{b,h} \\ 3.995 + 0.4685(T_b - T_{b,h}) & T_{b,h} < T_b \end{cases} \quad (4.61)$$

Thermal discomfort (*DISC*) is numerically equal to *TSENS* when  $T_b < T_{b,c}$  and is related to skin wettedness when body temperature is regulated by sweating. *DISC* is calculated by:

$$DISC = \begin{cases} 0.4685(T_b - T_{b,c}) & T_b < T_{b,c} \\ \frac{4.7(E_{rsw} - E_{rsw,req})}{E_{max} - E_{rsw,req} - E_{dif}} & T_{b,c} \leq T_b \end{cases} \quad (4.62)$$

where  $E_{dif}$  is the heat flow from evaporation of moisture diffused through the skin.

The transient two-node thermal comfort model, like the building thermal simulation model, requires a time-step based on numerical stability criteria. To obtain numerical stability for the thermal comfort model, a time-step between 20 – 60 s is required (ASHRAE Standard 55, 2004); therefore, a 60 s time-step was selected. Since the thermal data from the previous simulation was run on a five-minute time-step it must be re-evaluated for the new 60 s time-step. This is done by using the discrete Fourier Series and applying an inverse Fourier transform at the 60 s time-step (Athienitis, 1998).

#### 4.4 Comparison of thermal comfort model with measurements

It is generally a difficult process to validate or verify thermal comfort models with measurements due to the assumptions used. Wissler (1988) suggests that a model can be deemed acceptable if the predicted and measured values of mean skin temperature agree within 2 °C. For comparison of thermal sensation, however, values can present large differences not only due to limitations in the mathematical model, but also due to experimental techniques used to assess the perception of the indoor environment (Zmeureanu and Doramajian, 1992).

The results of the two-node comfort model are compared with measurements taken by Grivel et al. (1989) The comfort model is also compared with the results of a computer program developed by Gagge et al. (1986). In both comparisons, mean radiant temperature is equal to air temperature.

Grivel et al. (1989) measured the skin temperature of six male and female subjects in a climate chamber under cyclical ambient conditions. The ambient temperature (air and mean radiant temperature) was kept constant at 28.8 °C for one hour. Then, at a rate of 2 °C every eight minutes, it was decreased to 20.8 °C, then increased to 34.8 °C, and then decreased again to 20.8 °C. The following parameters were used in the simulation: body mass = 63.1 kg, body surface area = 1.72 m<sup>2</sup>, clothing insulation = 0.1 clo, relative humidity = 50%, metabolic rate = 60 W/m<sup>2</sup>, and air velocity = 0.2 m/s. The simulated results and measurements are in good agreement, with differences smaller than 2 °C (Figure 4.16).

Values of thermal discomfort (DISC) generated by computer simulation and presented by Gagge et al. (1986) were compared with thermal discomfort values generated in the numerical simulation study. The following parameters were used in the simulation: body mass = 70 kg, body surface area = 1.8 m<sup>2</sup>, relative humidity = 50%, metabolic rate = 73 W/m<sup>2</sup>, clothing thermal insulation = 0.57 clo, moisture permeability = 0.45, and air velocity = 0.2 m/s. For ambient temperatures less than 28 °C, the predicted values for thermal discomfort (DISC) differ from the computer simulations presented by Gagge et al. by less than 0.25 (Figure 4.17). However, for ambient temperatures greater than 28 °C, predicted values for DISC differ by almost 0.5.

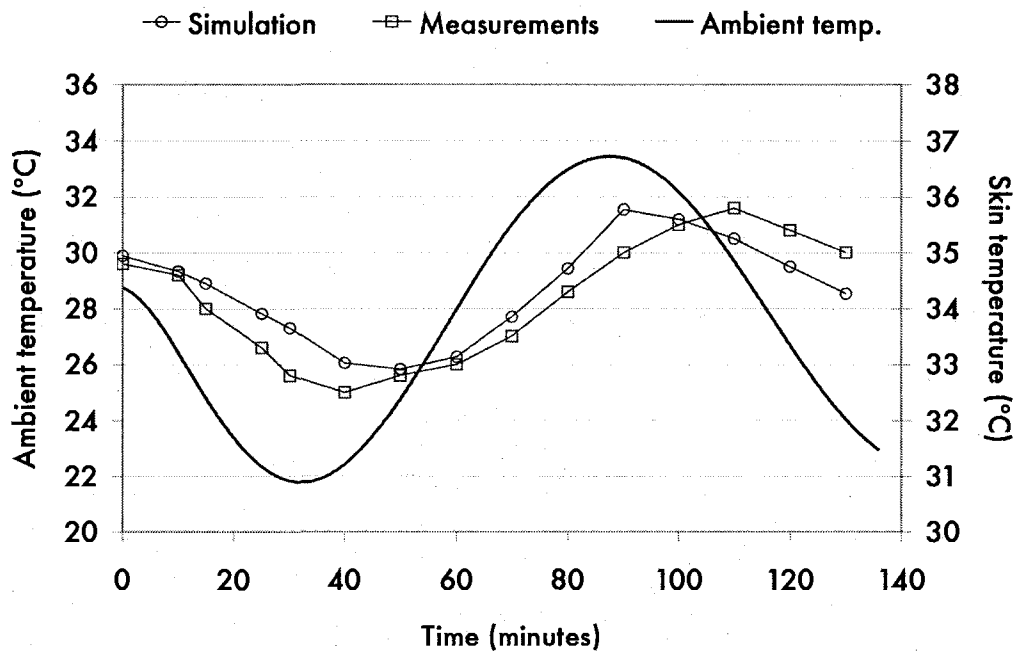


Figure 4.16: Comparison of skin temperature values for thermal comfort simulation model vs. Grivel experimental data

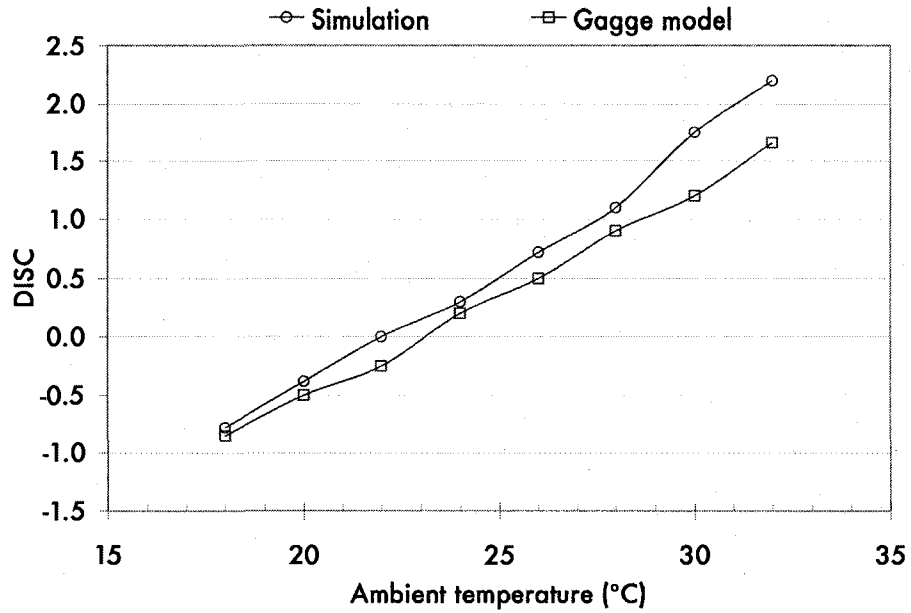


Figure 4.17: Comparison of thermal discomfort index for thermal comfort simulation model vs. Gagge computer model.

#### 4.5 Parameters and assumptions

A parametric analysis of a typical office with glass façade in a south-facing perimeter zone was completed in order to quantify the impact that different glazing types and shading properties have on thermal comfort. This section presents the parameters used and assumptions made for this analysis.

##### Climatic data

Representative days for winter conditions with clear and cloudy sky conditions were chosen (Table 4.1) from the TMY data.

Table 4.1: Climatic data for representative days used in simulations

Sky condition	Outdoor dry-bulb temperature (°C)		Maximum incident solar radiation (W/m <sup>2</sup> )		
	Min	Max	Beam	Diffuse	Total
Clear	-22	-16	735	310	1045
Cloudy	-19	-15	8	148	156

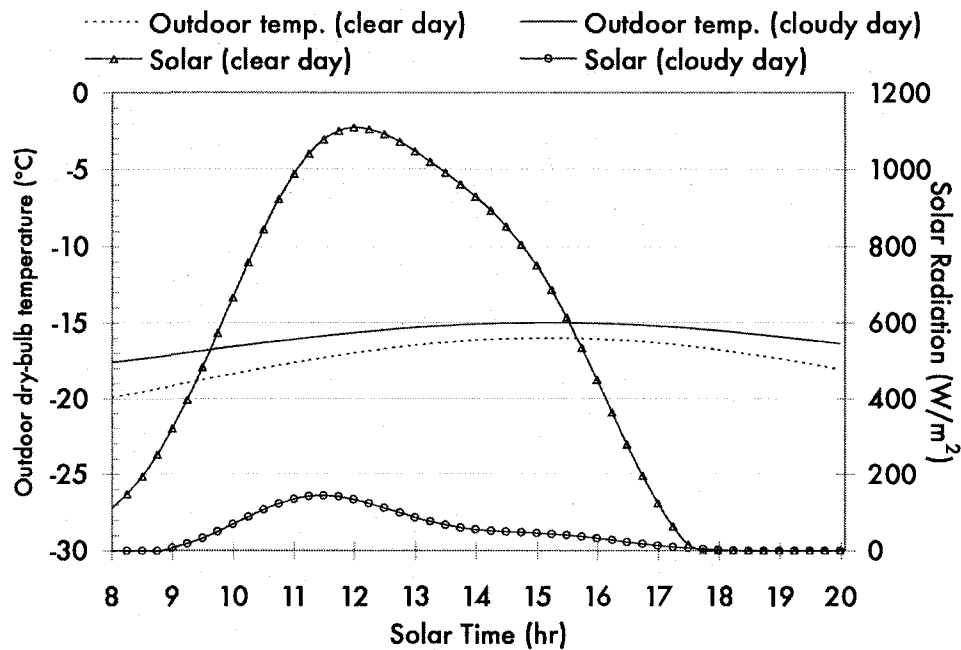


Figure 4.18: Climatic data for representative days used in simulation

### Room geometry

The geometry of the perimeter zone office is modeled as seven surfaces (ceiling, floor, side walls, back wall, window, and façade wall containing the window), with dimensions of 3.4 m x 3.0 m x 3.0 m (height x width x length). The window is 2.4 m x 2.8 m (height x width) above the spandrel of height 0.8 m.

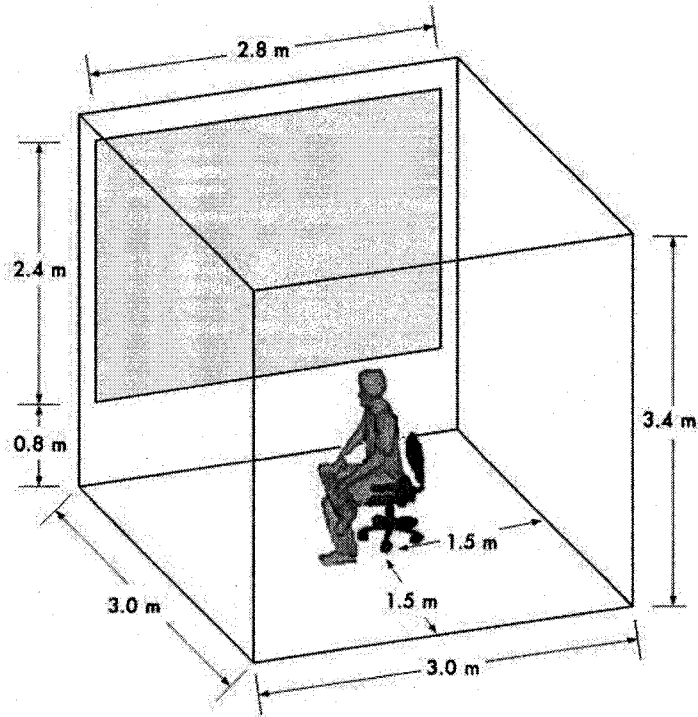


Figure 4.19: Schematic of typical office used for simulations (not to scale)

### Fenestration

Three different types of glazing were selected from the ASHRAE Handbook of Fundamentals (2005):

1. Double-glazing, uncoated
2. Double-glazing with low- $e$  ( $e = 0.1$ )
3. Triple-glazing with low- $e$  ( $e = 0.05$ )

Their optical properties, as a function of incidence angle, are presented in Figure 4.20 and Figure 4.21. Additional optical and thermal properties are presented in Table 4.2.

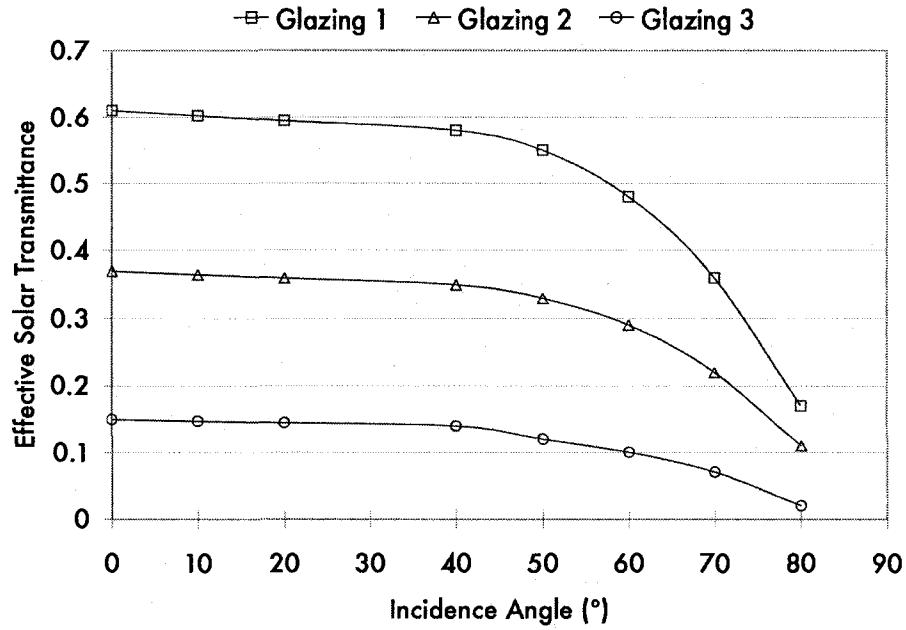


Figure 4.20: Effective solar transmittance of glazing as function of incidence angle

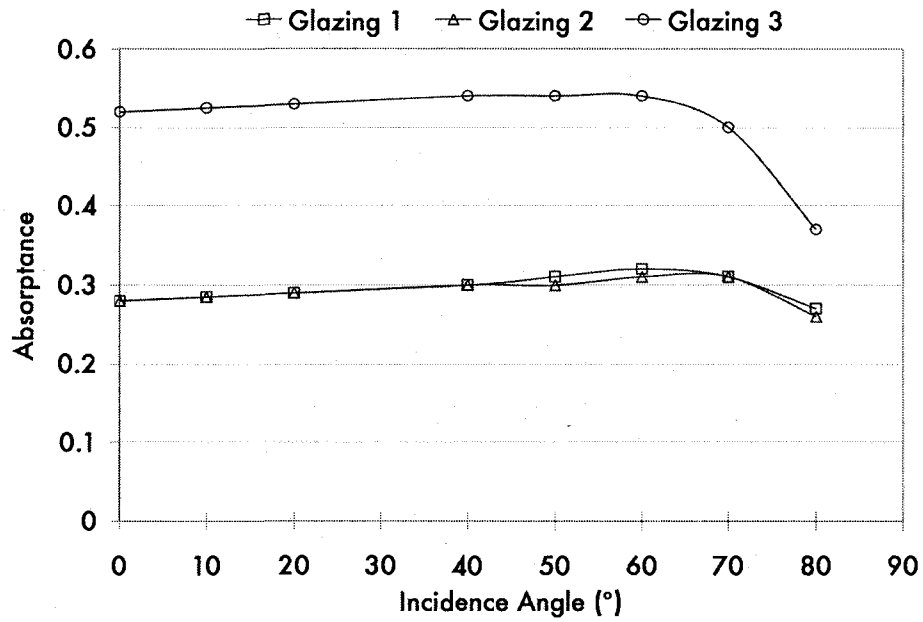


Figure 4.21: Absorptance of glazing as function of incidence angle

Table 4.2: Properties of the three different glazing types used for parametric analysis (ASHRAE Handbook of Fundamentals, 2005)

Glazing	Visible Transmittance	SHGC	U-value (W/m <sup>2</sup> °C)		
			Center-of-glass	Edge-of-glass	Total
1	0.78	0.7	2.73	3.36	3.51
2	0.53	0.27	1.7	2.60	2.63
3	0.55	0.26	1.53	2.49	2.43

The shading device type used for parametric analysis is a roller shade. Its transmittance is kept at 5%. For parametric analysis its absorptance is varied from 20% to 70%, and, hence, its reflectance is varied from 30% to 80%.

#### **Building material properties**

The floor, interior walls, and exterior façade have an absorptance of 80%, 20%, and 70%, respectively. Other thermal properties of the building materials are presented in Table 4.3.

Table 4.3: Thermal properties of building materials used for simulation

	Thickness (m)	Density (kg/m <sup>3</sup> )	Specific heat (J/kg °C)	Thermal conductivity (W/m °C)	Thermal resistance (m <sup>2</sup> °C/W)
<b>Floor</b>					
Concrete	0.2	2200	1400	1.7	
Insulation					0.5
<b>Exterior Wall</b>					
Cladding	0.1	1800	1005	1.3	
Gypsum board	0.02	800	750	0.16	
Insulation					3
<b>Interior walls</b>					
Gypsum board	0.02	800	750	0.16	
Insulation					2
<b>Ceiling</b>					
Gypsum board	0.02	800	750	0.16	
Concrete	0.2	2200	1400	1.7	
Insulation					2

### HVAC control

The HVAC system uses proportional-integral (PI) control for conditioning of the air. It was determined that a proportional control constant of 500 W/ °C and integral control constant of 0.03 W/s would be necessary to adequately condition the space. For heating, the set point temperature has a dead band of 1 °C.

### Occupancy schedule

Internal gains from people (67 W) and lights/equipment (100 W) are modeled as a heat source based on an occupancy schedule (8:00 – 20:00). Room air set point temperature is also based on occupancy schedules with a daytime (6:00 – 22:00) set point of 23 °C and nighttime (22:00 – 6:00) set point of 19 °C.

## Other issues

Since it can take several time-steps for some of the parameters to reach convergence in the building thermal simulation model, equivalent to several simulation days, it would be unrealistic to assume that the occupant is “in the space” for the time until convergence. This is because modeling the occupant as being in the space during the night (while approaching convergence), when conditions are outside of the comfort zone, would have an effect on the thermal comfort conditions during the occupied hours. In other words, the effect of discomfort caused by an occupant being modeled as being in the space during the night would carry on into the occupied hours, thereby giving a false sense of the actual comfort conditions that would occur in reality. Therefore, an important assumption is made in relation to how thermal comfort is modeled for an occupant while the building thermal simulation is running: during occupancy off-hours (20:00 – 08:00) the occupant is modeled to be in a thermally neutral state, i.e. room air and mean radiant temperature are forced to be 22 °C. Even though the actual room air and mean radiant temperature in the space are not these values, these parameters are used for the thermal comfort simulation model so that an analysis of comfort during the occupied hours can start at a reasonable value of DISC.

## Indoor environment and occupant properties

The occupant is modeled as being seated in the center of the room facing parallel to the façade. The solar absorptance of clothing is divided into beam ( $\alpha_{cl,b}$ ) and diffuse ( $\alpha_{cl,d}$ ) components, with  $\alpha_{cl,b} = 0.8$  (Blazejczyk et al., 1993) and  $\alpha_{cl,d} = 0.5$  (Lyons et al., 1999). Additional parameters related to the indoor environment and occupant properties used for the simulation are shown in Table 4.4.

Table 4.4: Parameters of indoor environmental conditions and occupant properties used for the thermal comfort simulation

Metabolic rate (met)	Body mass (kg)	DuBois area (m <sup>2</sup> )	Air speed (m/s)	Relative humidity (%)
1.2	80	1.80	0.1	50

### 4.6 Results of simulation study

This section presents the most important results of the simulation study, showing the impact that the three different glazing types and varying roller shade properties have on occupant thermal comfort under clear and cloudy sky conditions.

#### 4.6.1 Clear winter day

The effect of solar radiation on thermal comfort has its greatest impact during clear winter days. This is because a person has a larger projected area when the sun is at lower altitude, thereby absorbing more solar radiation. For the same reason, a vertical south-facing surface receives more incident solar radiation in

the winter months than in the summer months. Therefore, shading devices are critical on clear winter days in order to avoid overheating due to the presence of incident solar radiation. The properties of the shade, however, will determine the degree to which comfort can be maintained.

The importance of taking solar radiation into account when modeling thermal comfort in glazed perimeter zones can be seen in the results presented in Figure 4.22. There is a 16 °C difference between the mean radiant temperature due to the surrounding surfaces only and the mean radiant temperature due to the surrounding surfaces *and* solar radiation with an unshaded double-glazed uncoated window on a clear winter day.

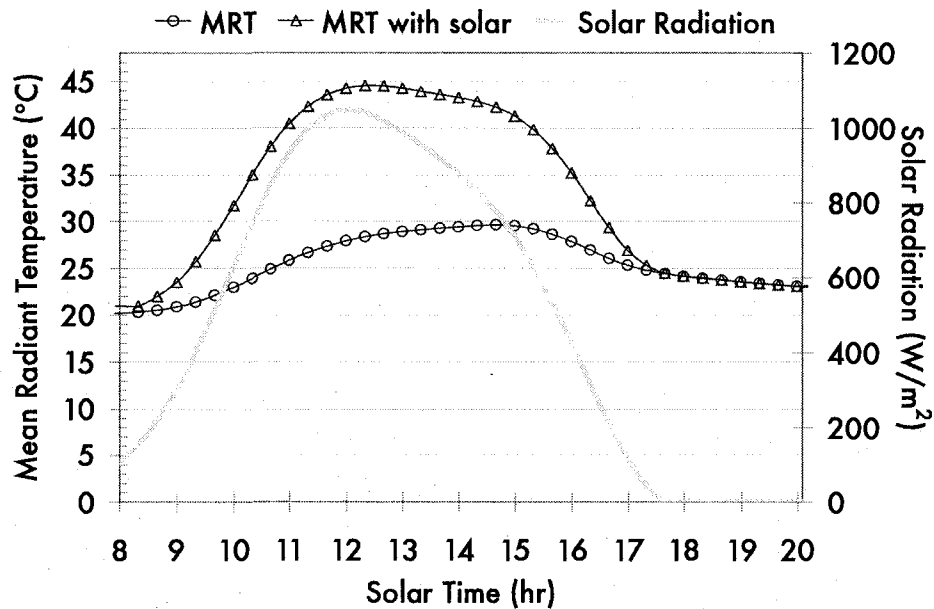


Figure 4.22: MRT due to surrounding surfaces only and MRT due to surrounding surfaces and solar radiation with an unshaded double-glazed window on a clear winter day

When using no shading device on clear winter days, the solar-optical properties of glazing have a pronounced effect on the mean radiant temperature

(Figure 4.24). During occupied hours (8:00 - 20:00), the predicted mean radiant temperature ranged between 20 - 38 °C with glazing 1, 20 - 31.5 °C with glazing 2, and 20 - 25.5 °C with glazing 3. Room air temperature can reach as high as 27 °C with glazing 1 but only 23 °C with glazing 3 due to differences in transmittance (Figure 4.25). The operative temperature ranged from 21 - 36.5 °C with glazing 1, 21 - 31.5 °C with glazing 2, and 21 - 26 °C with glazing 3 (Figure 4.26). Radiant temperature asymmetry reaches above the maximum allowable 20 °C for all three glazing types (Figure 4.27). Discomfort reaches a maximum DISC of +3.1 for glazing 1, +2.1 for glazing 2, and +0.9 for glazing 3 (Figure 4.28).

These results show how solar transmittance of glazing can affect the thermal radiant environment and overall discomfort, especially with the lower solar altitudes during winter.

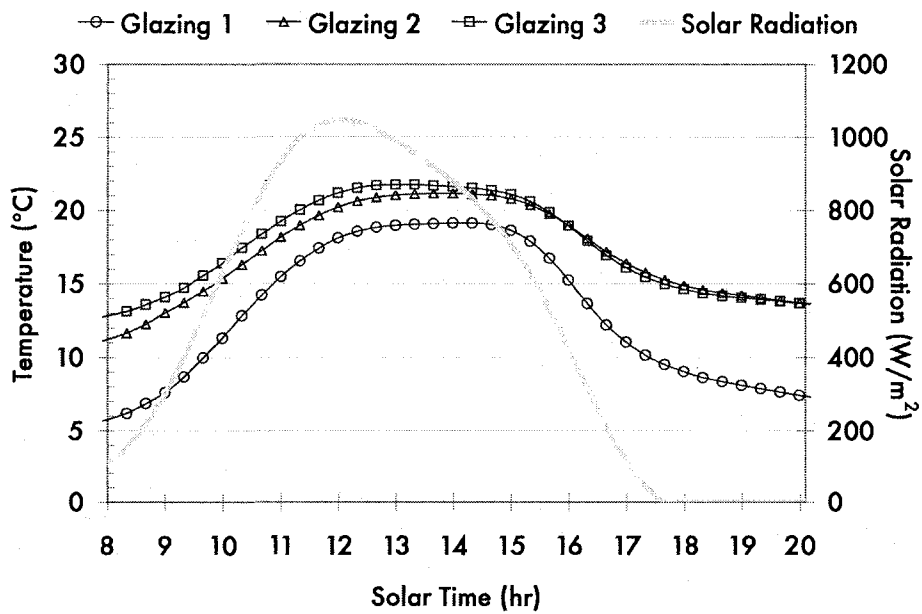


Figure 4.23: Effect of glazing type on interior window surface temperature on a clear winter day

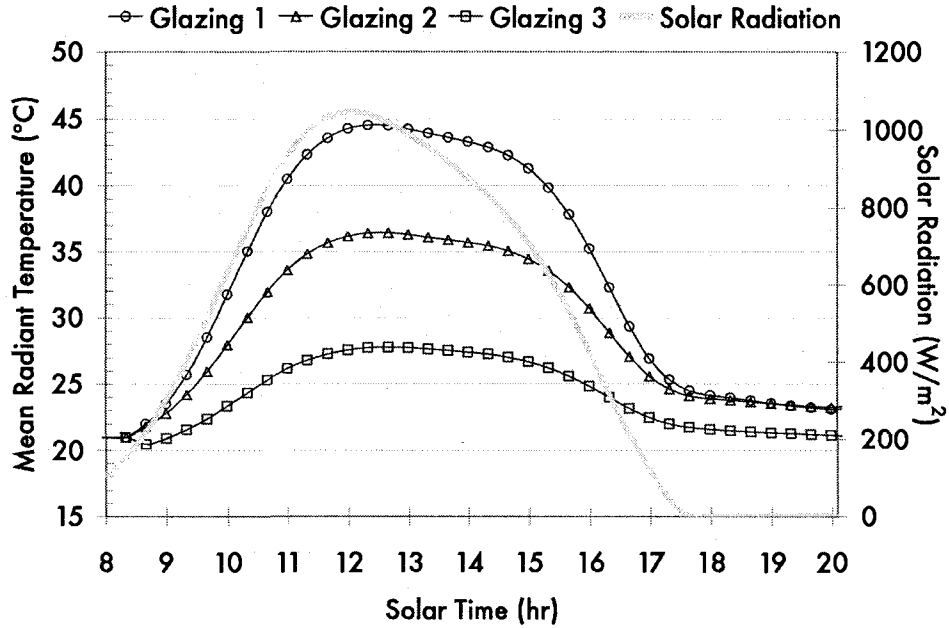


Figure 4.24: Effect of glazing type on mean radiant temperature for a clear winter day with no shading

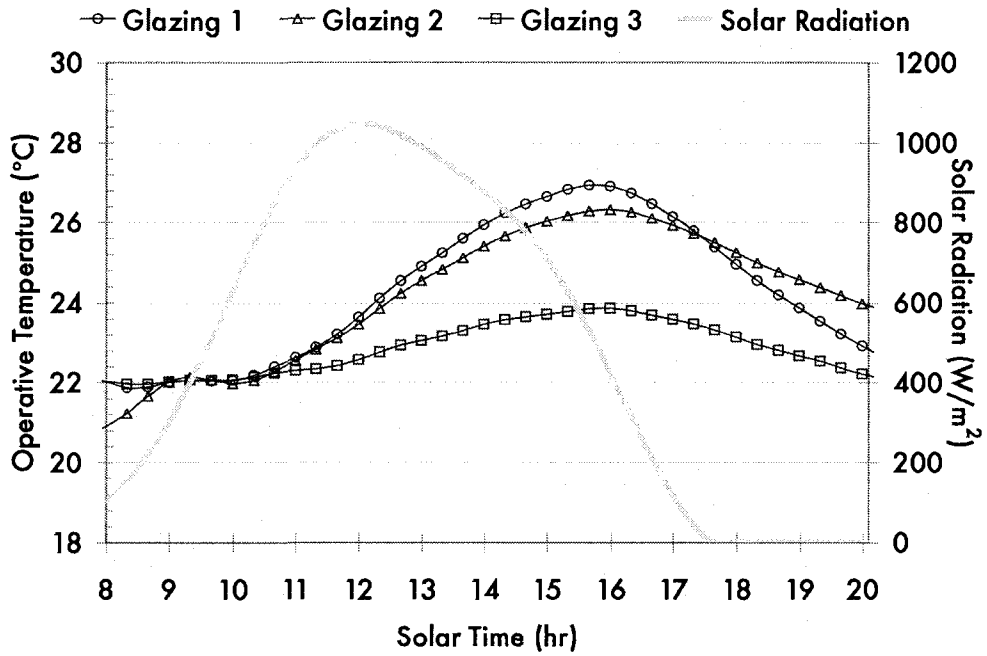


Figure 4.25: Effect of glazing type on room air temperature for a clear winter day with no shading

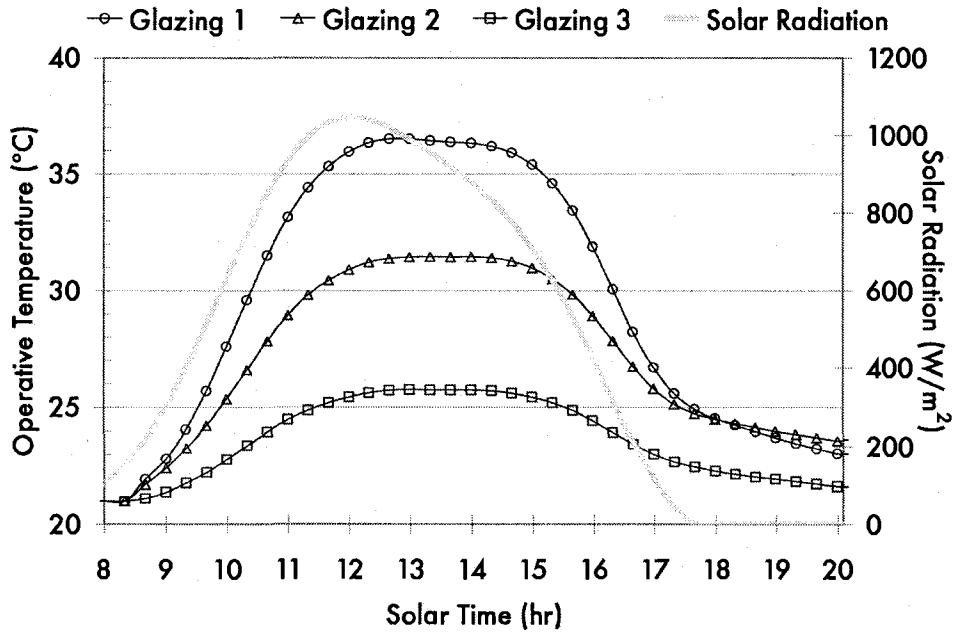


Figure 4.26: Effect of glazing type on operative temperature for a clear winter day with no shading

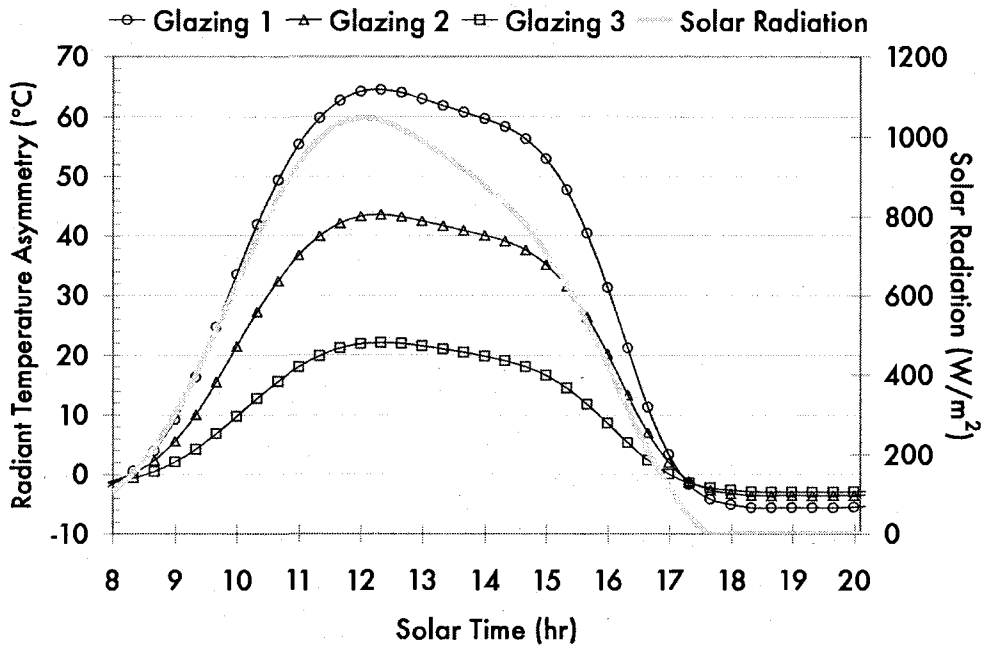


Figure 4.27: Effect of glazing type on radiant temperature asymmetry for a clear winter day with no shading

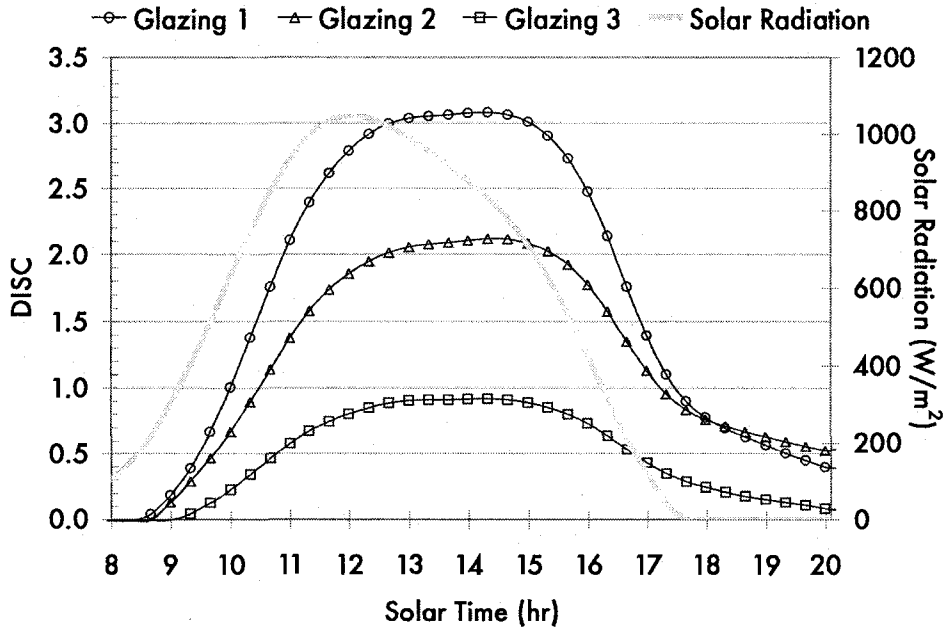


Figure 4.28: Effect of glazing type on thermal discomfort for a clear winter day with no shading

When using a shading device, the thermal environment is highly dependent upon the properties of the shade. An example of how shade temperature can change with varying absorptance can be seen in Figure 4.29. With a shade absorptance of 0.2 and 0.7, shade temperature with glazing 1 reaches a maximum of 28 °C and 44.5 °C, respectively; with glazing 2, maximum shade temperature reaches 26 °C and 37.5 °C, respectively; and with glazing 3, maximum shade temperature reaches 24 °C and 29 °C, respectively (Figure 4.30).

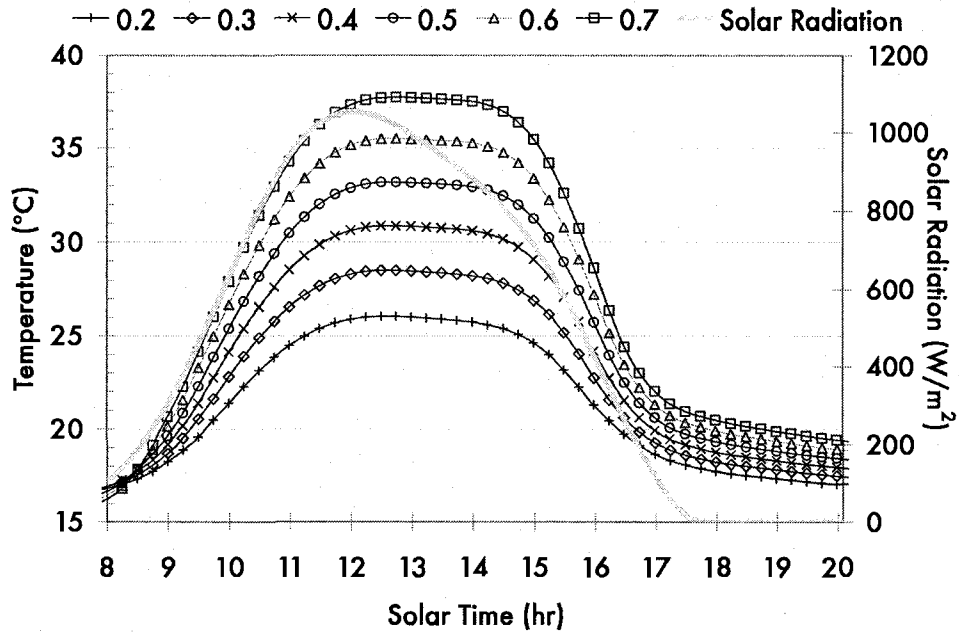


Figure 4.29: Effect of shade absorptance on shade temperature with glazing 2 (double-glazed, low-e) for a clear winter day

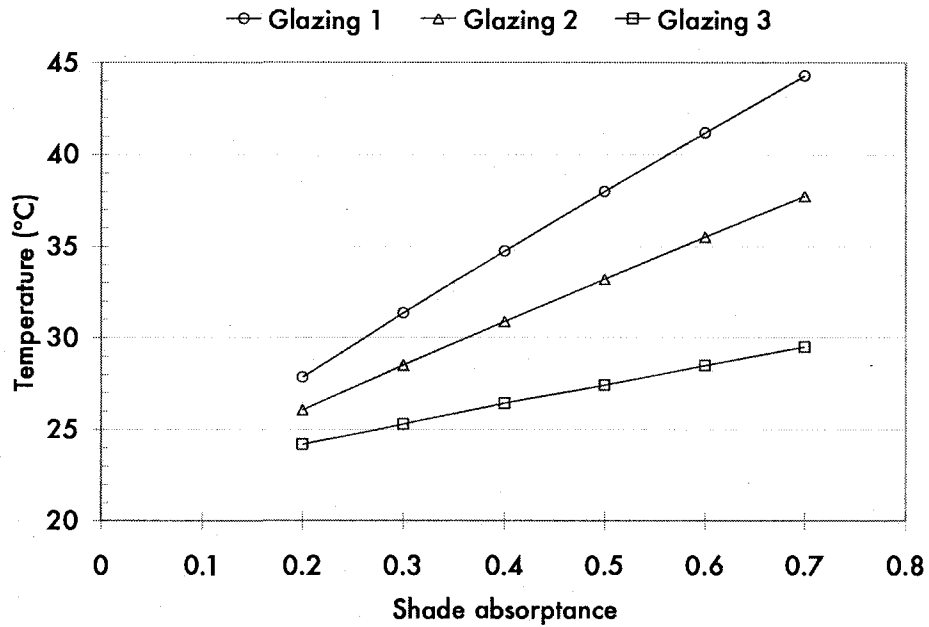


Figure 4.30: Effect of shade absorptance on maximum shade temperature for a clear winter day

With a shade absorptance of 0.2 and 0.7, the simulated mean radiant temperature with glazing 1 reaches a maximum of 23.5 °C and 29 °C,

respectively; with glazing 2, maximum mean radiant temperature reaches 23 °C and 27 °C, respectively; and with glazing 3, maximum mean radiant temperature reaches 22 °C and 23.5 °C, respectively (Figure 4.31).

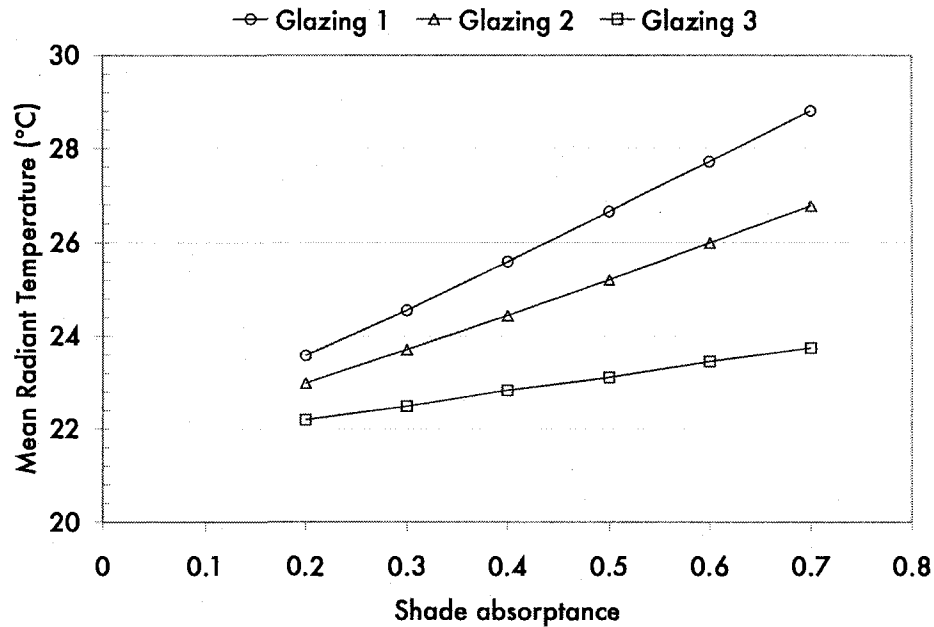


Figure 4.31: Effect of shade absorptance on maximum mean radiant temperature for a clear winter day

With shade absorptance between 0.2 and 0.7, the maximum room air temperature ranges from 24 – 30 °C for glazing 1; with glazing 2 it ranges from 23.5 – 28 °C; with glazing 3 it ranges from 23 – 25 °C (Figure 4.32).

With shade absorptance between 0.2 and 0.7, the maximum predicted operative temperature with glazing 1 ranges from 23.5 – 29 °C; with glazing 2, it ranges from 23 – 27 °C; and with glazing 3, it ranges from 22.5 °C and 24 °C, respectively (Figure 4.33).

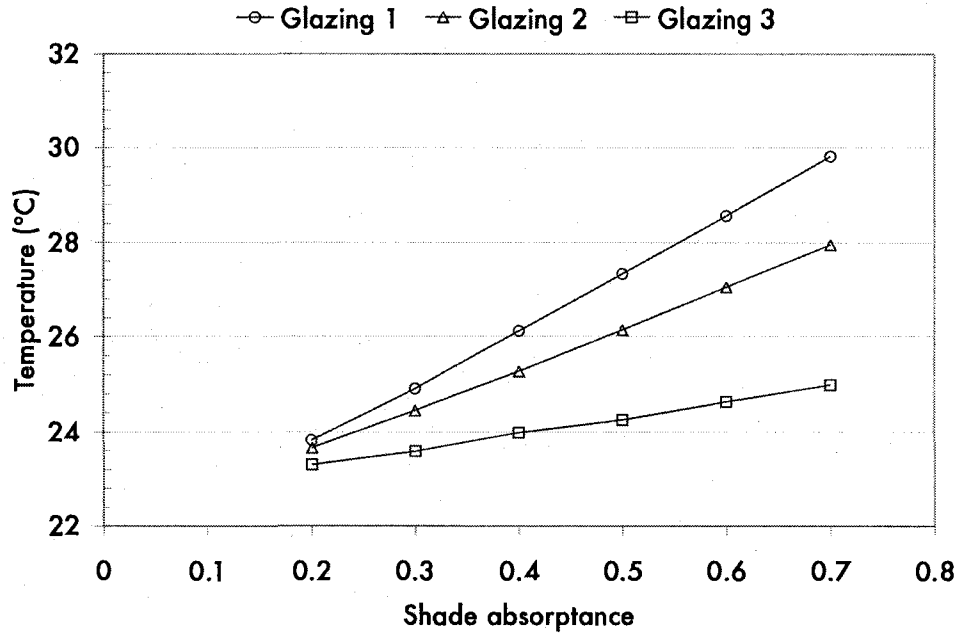


Figure 4.32: Effect of shade absorptance on maximum room air temperature for a clear winter day

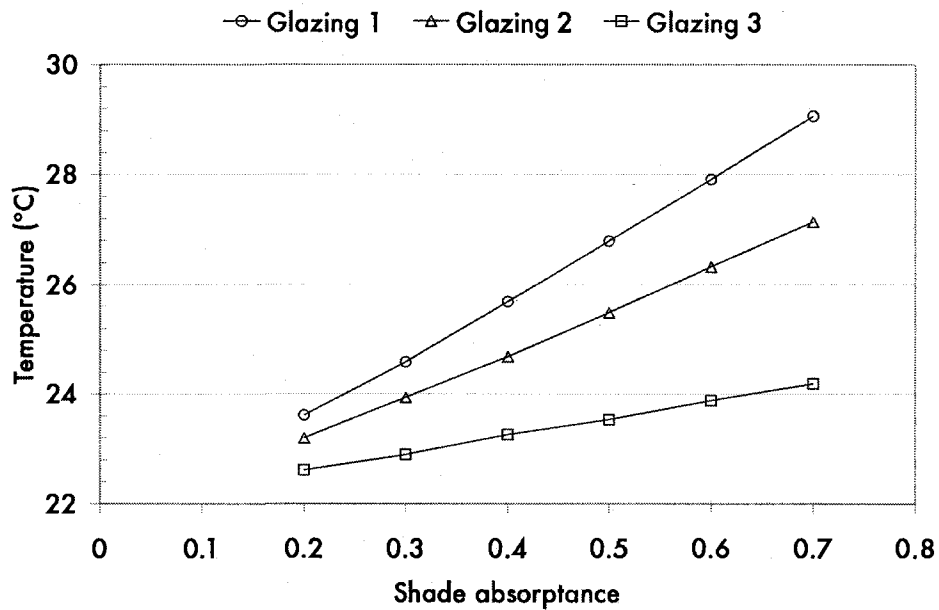


Figure 4.33: Effect of shade absorptance on maximum operative temperature for a clear winter day

When using a roller shade, the radiant temperature asymmetry is greatly reduced as compared to using no shading. For all glazing types and shade

absorptances, the RTA due to a warm wall is kept below the upper limit of 23 °C as recommended by ASHRAE Standard 55 (2004). The lowest radiant temperature asymmetry is 3 °C for glazing 3 and a shade absorptance of 0.2; the highest radiant temperature asymmetry is 18 °C for glazing 1 and a shade absorptance of 0.7 (Figure 4.34).

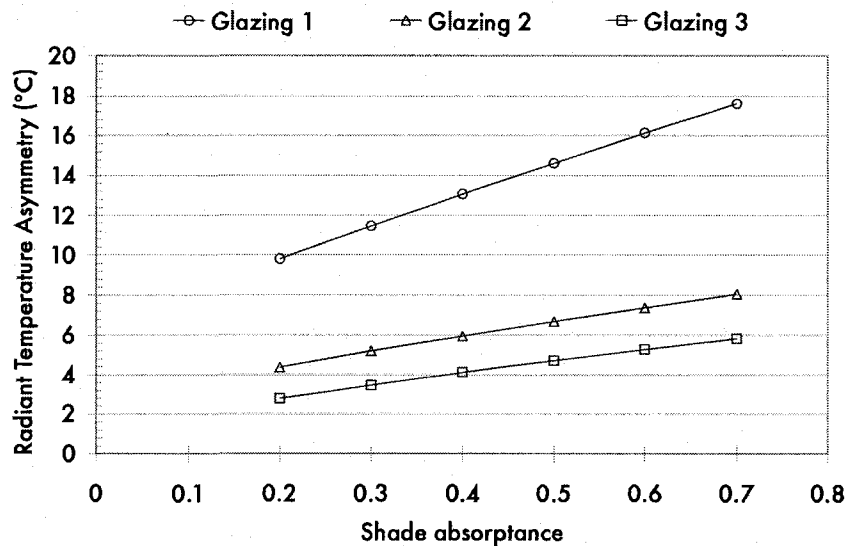


Figure 4.34: Effect of shade absorptance on maximum radiant temperature asymmetry for a clear winter day

The following three figures (Figure 4.35 - Figure 4.37) show the RTA at different distances from the façade for three different shade absorptances (0.2, 0.4, 0.7) for the three different glazing types. For each case the RTA is kept below 23 °C.

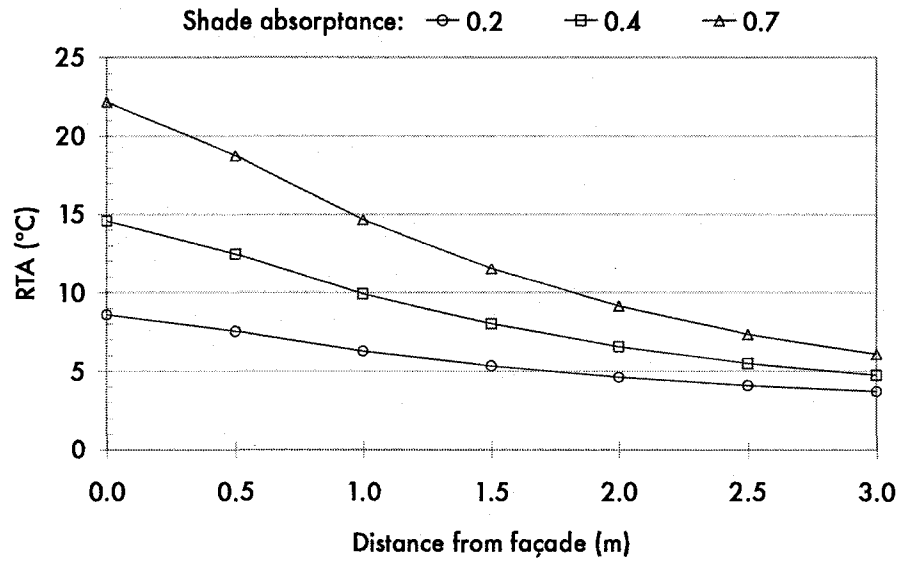


Figure 4.35: RTA as a function of distance from façade for three different shade absorptances using glazing 1

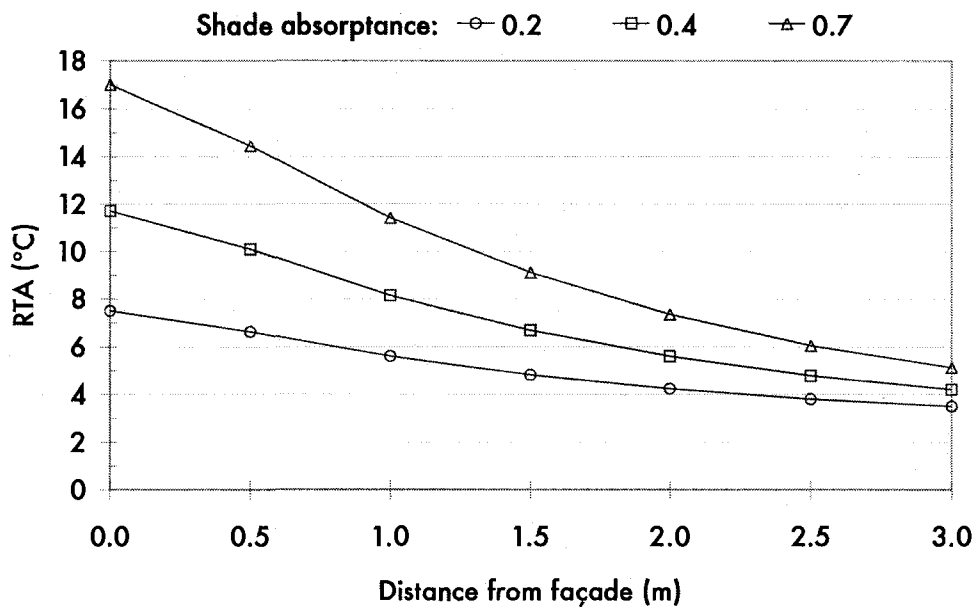


Figure 4.36: RTA as a function of distance from façade for three different shade absorptances using glazing 2

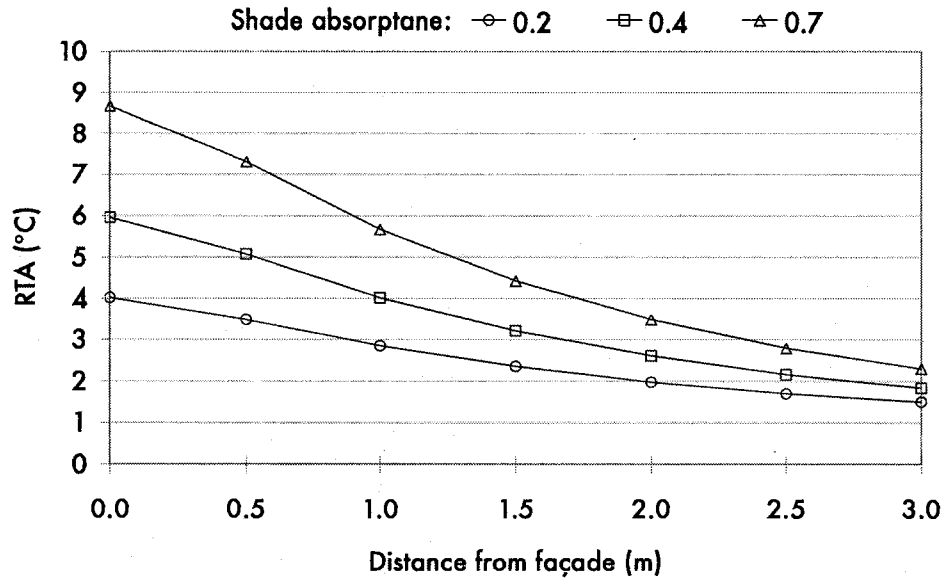


Figure 4.37: RTA as a function of distance from façade for three different shade absorptances using glazing 3

The maximum rating of discomfort on the DISC scale for glazing 1 ranges from +0.5 to +1.9 for shade absorptance between 0.2 and 0.7. For glazing 2, the maximum thermal discomfort ranges from +0.4 to +1.4. For glazing 3, the maximum thermal discomfort ranges from +0.3 to +0.7 (Figure 4.38).

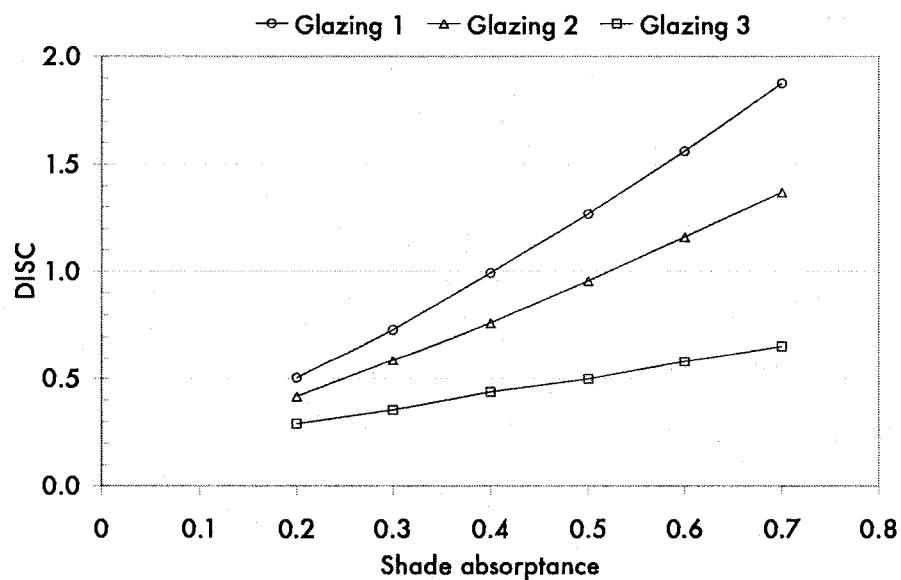


Figure 4.38: Effect of shade absorptance on maximum thermal discomfort for a clear winter day

For glazing 1, the number of hours in a day outside the comfort zone (DISC > +0.5) ranged from 0.5 hours to 9.5 hours, when using a shade with an absorptance of 0.2 and 0.7, respectively. For glazing 2, it ranged from three hours to just over nine hours when using a shade with an absorptance of 0.3 and 0.7, respectively. For glazing 3, the DISC only exceeds +0.5 with shade absorptances of 0.6 and 0.7, for three hours and over four hours, respectively (Figure 4.39).

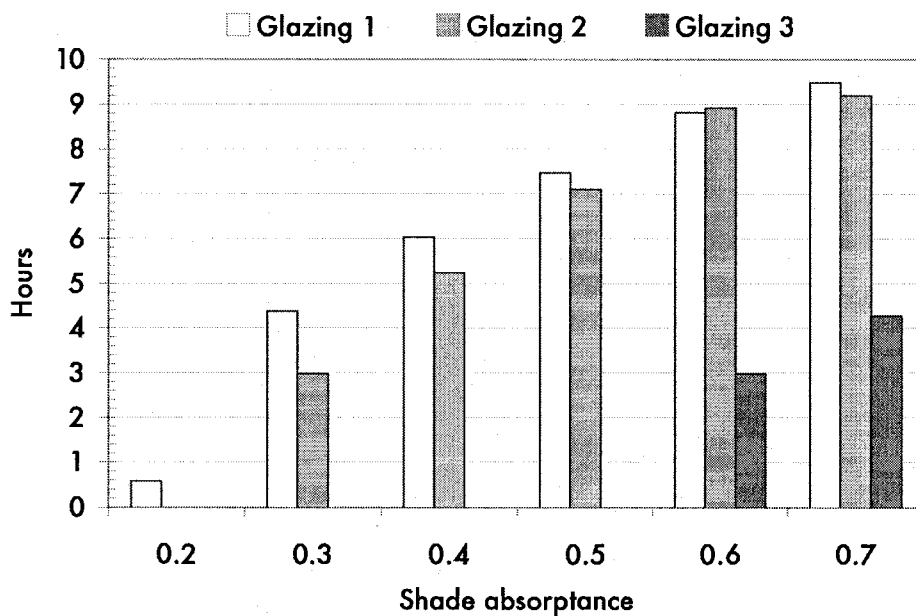


Figure 4.39: Effect of shade absorptance on number of hours per day in discomfort zone for a clear winter day

Increasing shade absorptance decreases the heating load of the space for all three glazing types (Figure 4.40). However, although glazing 3 has a slightly higher insulating value than glazing 2, it has a lower solar transmittance. Therefore, if using shading with an absorptance above 0.4 on clear winter days, more heating is needed with glazing 3 due to lower solar gains.

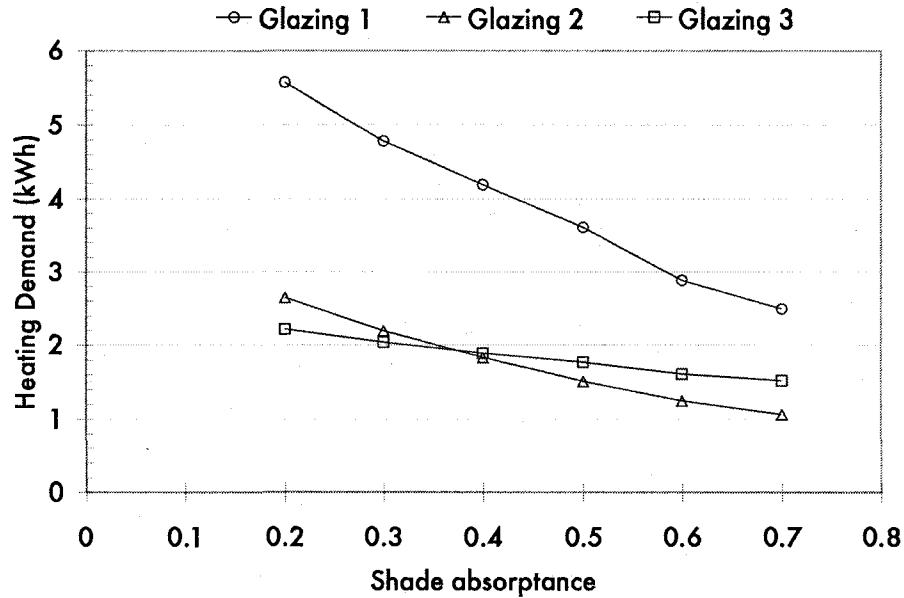


Figure 4.40: Effect of shade absorptance on daily total heating demand for a clear winter day

#### 4.6.2 Cloudy winter day

On overcast days in the winter, varying the shade absorptance has little effect on the indoor environmental conditions due to low (or no) direct solar radiation. Therefore, the comparison in this analysis only differentiates between the two cases of using shading and not using shading. For all glazing types, using a shading device increases the thermal performance of the façade: the shading device temperature is higher than that of the glazing interior surface and mean radiant temperature is increased to be closer to room air temperature; therefore, comfort conditions are improved. In addition, heating demand on cloudy winter days decreases due to shading device use.

As expected, increasing the R-value of the window increases its interior surface temperature to be closer to room air temperature (Figure 4.41). For all

windows, using shading increases the minimum surface temperature of fenestration component of the façade; the most drastic difference between shade temperature and interior window surface temperature, had the shade not been used, is for the window with the lowest R-value (glazing 1) which showed a 9 °C increase. The window with the highest R-value (glazing 3) showed a 4.5 °C increase.

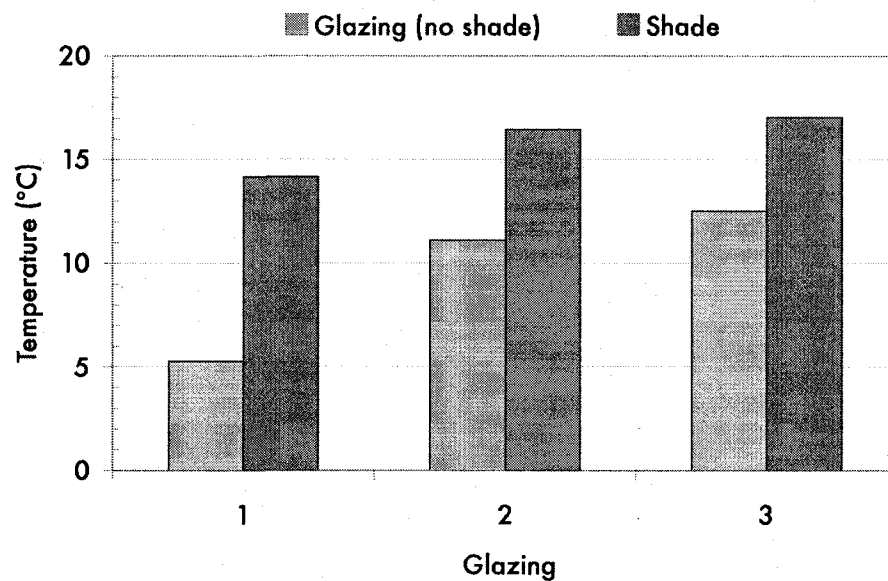


Figure 4.41: Minimum window surface temperature (glazing or shade): Effect of glazing type for a cloudy winter day

The mean radiant temperature is affected by window R-value and shading (Figure 4.42). Minimum mean radiant temperature can be increased by as much as 2 °C (glazing 1) if shading is used. Correspondingly, the minimum operative temperature also increases with increasing window R-value and shading use (Figure 4.43). Therefore, the minimum thermal discomfort rating decreases with increasing window R-value (Figure 4.44) and shading use.

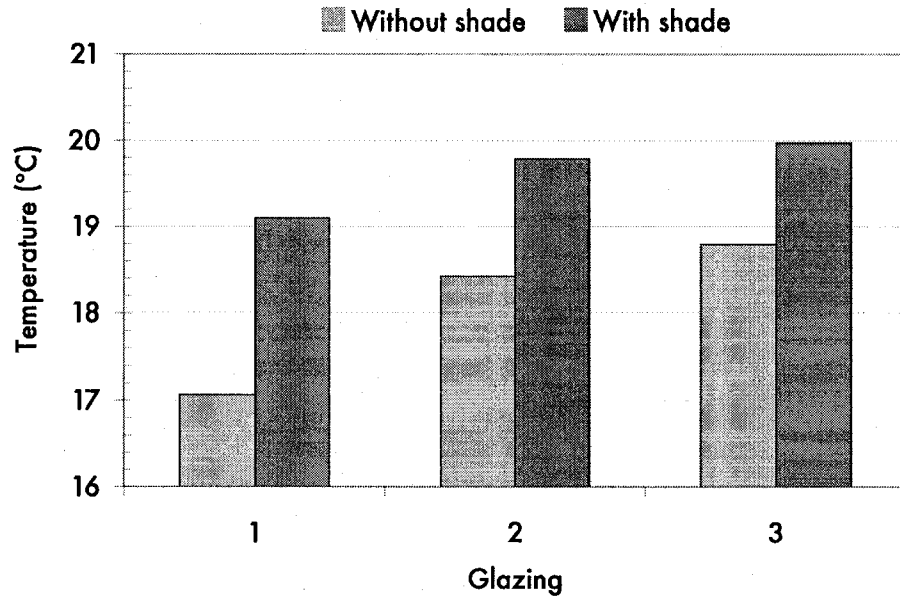


Figure 4.42: Minimum mean radiant temperature: Effect of glazing type for a cloudy winter day

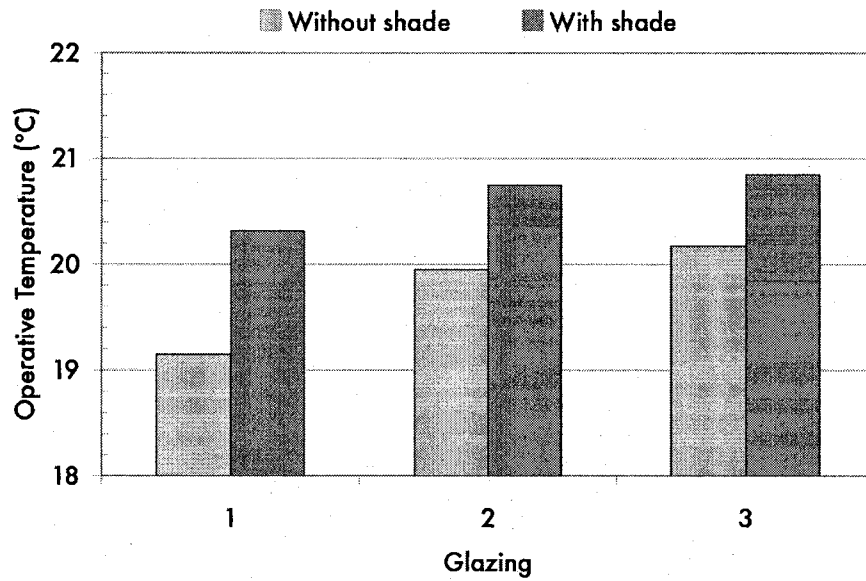


Figure 4.43: Minimum operative temperature: Effect of glazing type for a cloudy winter day

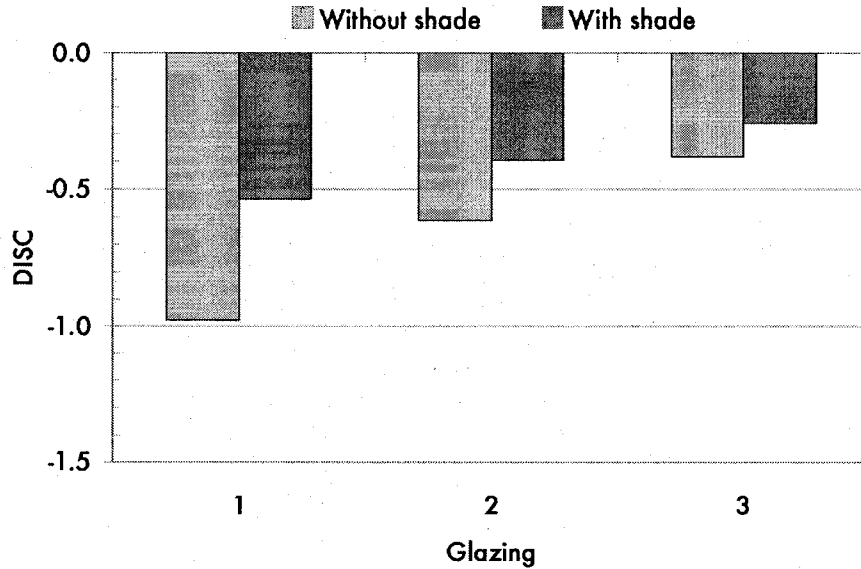


Figure 4.44: Minimum thermal discomfort rating: Effect of glazing type for a cloudy winter day

Similarly, increasing the window's R-value decreases the heating energy demand for the office and even more so if shading is used (Figure 4.45). A daily heating demand of 16.3, 8.3, and 6.7 kWh is needed when using glazing 1, 2, and 3, respectively. If using a shading device, however, this demand can be reduced by 42%, 41%, and 40%, respectively.

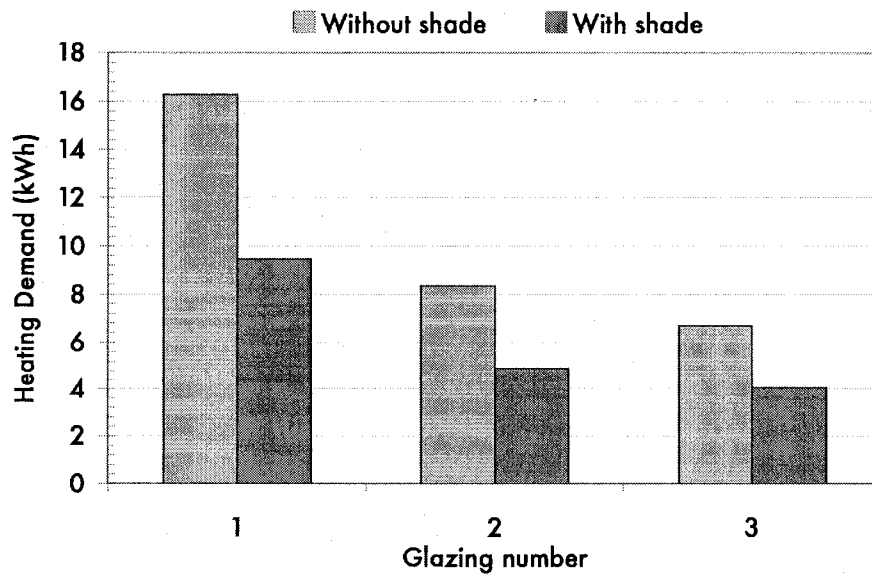


Figure 4.45: Daily heating demand: Effect of glazing type for a cloudy winter day

The following three figures (Figure 4.46 - Figure 4.48) show the RTA at different distances from the façade for each glazing with and without shading. For each case, RTA is kept below the 10 °C limit recommended by ASHRAE Standard 55 (2004) for cool walls. The only exception is for the case with very close to the façade with glazing 1 and no shading.

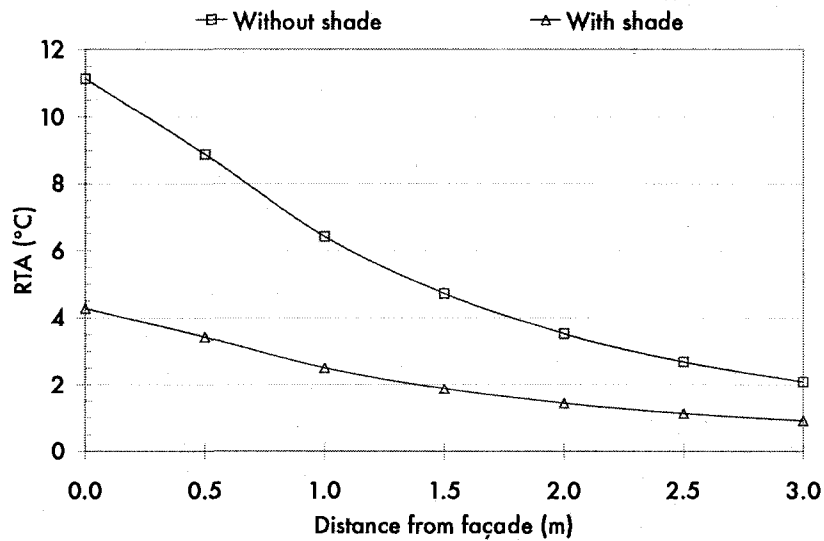


Figure 4.46: RTA as a function of distance from façade for glazing 1 with and without shading

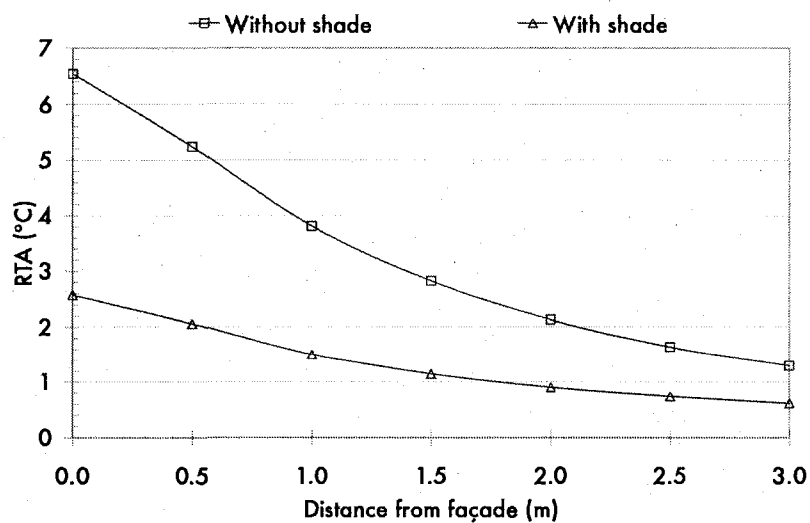


Figure 4.47: RTA as a function of distance from façade for glazing 2 with and without shading

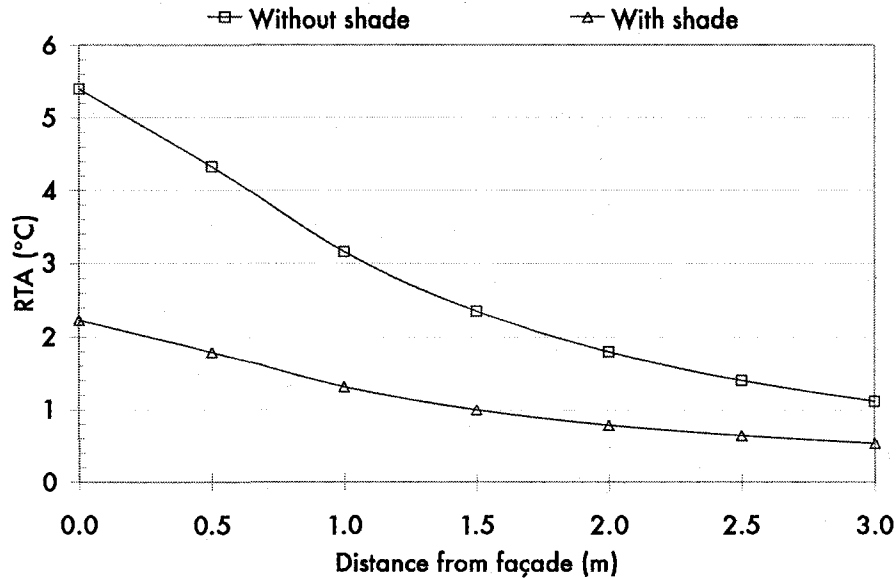


Figure 4.48: RTA as a function of distance from façade for glazing 3 with and without shading

It should be noted that using a shade on a cloudy day is not typical since occupants are more likely to take advantage of the view when the chance of glare is minimal. Therefore, the results generated for the case with no shade would be more indicative of reality. However, shading devices could be employed at night to minimize heat loss through the façade and increase comfort.

#### 4.7 Further investigation using CFD

Although the finite-difference network model is adequate for performing simulation of transient thermal environments, it handles air temperature as a single node and air velocity as an input variable, and is, therefore, unable to model the complex airflow and temperature stratifications that can occur within the office. Thus, it cannot be used to predict local discomfort caused by

temperature stratification or air speed. For this reason, Computational Fluid Dynamics (CFD) was employed for further analysis.

CFD is an established, state-of-the-art approach for quantitative prediction and analysis of fluid flow and heat and mass transfer. For this study, the commercial CFD software tool used was Airpak, which uses FLUENT as its solver engine (Airpak 3.0 User's Guide, 2007). Airpak uses a finite-volume formulation of governing differential equations used in CFD and can model basic fluid flow, heat transfer (including radiation), turbulence, and contaminant transport. These governing equations are adapted forms of the continuity equation, the Navier-Stokes (or momentum) equations, and the energy equations, based respectively on the fundamental principles of conservation of mass, momentum, and energy. A detailed account of these equations can be found in the literature.

#### **4.7.1 Description of CFD model**

A representative perimeter zone office was modeled with dimensions 3.4 m x 3.0 m x 3.0 m. The exterior wall has a window of dimensions 2.4 m x 2.8 m above a spandrel of height 0.8 m. The part of the exterior façade on both sides of the window has a width and thickness of 0.2 m. Both the spandrel and exterior façade section have a thermal conductivity of 0.07 W/m·K. The glazing is modeled as having a U-value of 2 W/m<sup>2</sup>·K (double-glazed, low-e).

An airflow analysis was completed for the case of a heated office under winter conditions with the diffuser for supply heating at different locations on the ceiling, with its center located 0.7 m, 1.1 m, and 1.5 m away from the window.

Heating is supplied to the space through a diffuser at 30 °C and 1.5 m/s. For boundary conditions in the model, outdoor air temperature is -20 °C and all surfaces not exposed to outside (back wall, floor, ceiling, side walls) are assumed to be adiabatic (no heat flux).

For an indoor air set-point temperature of 22 °C, the design heating load was calculated to be:

$$\begin{aligned}
 Q &= (U_{window} \cdot A_{window} + U_{exterior} \cdot A_{exterior}) \cdot (T_R - T_o) \\
 &= \left[ \left( 2 \frac{\text{W}}{\text{m}^2 \cdot ^\circ\text{C}} \right) \cdot 7.28 \text{m}^2 + \left( \frac{1}{3} \frac{\text{W}}{\text{m}^2 \cdot ^\circ\text{C}} \right) \cdot 3.6 \text{m}^2 \right] \cdot [22^\circ\text{C} - (-20^\circ\text{C})] \\
 &= 662 \text{W}
 \end{aligned}$$

The approximate size of the supply diffuser was then determined to be:

$$\begin{aligned}
 Q = 662 \text{W} &= \dot{m} \cdot c_p \cdot (T_{supply} - T_{return}) \\
 Q = 662 \text{W} &= A_{supply} \cdot v_{supply} \cdot \rho \cdot c_p \cdot (T_{supply} - T_{return})
 \end{aligned}$$

$$\therefore A_{supply} = 0.042 \text{m}^2 \approx 0.2 \text{m} \times 0.2 \text{m}$$

Therefore, the diffuser was modeled to have an area of 0.2 m x 0.2 m. The return vent was assumed to be 0.4 m x 0.4 m located 0.2 m from the back wall

(2.8 m from the window). The indoor zero-equation turbulence model was selected for the flow regime since it was developed specifically for indoor airflow simulations and is ideally suited for predicting indoor air flows that consider natural convection, forced convection, and displacement ventilation (Airpak 3.0 User's Guide, 2007). Under-relaxation values for pressure (0.2) and momentum (0.1) were selected based on convergence criteria for flow and energy. After refining the grid size for the mesh, it was determined that a 0.095 m x 0.095 m mesh would be sufficient to generate adequate results. A more refined mesh was generated for components such as diffuser (0.02 m x 0.02 m) and return air vent (0.04 m x 0.04 m). In total, the model contained 83,790 elements and 89,700 nodes.

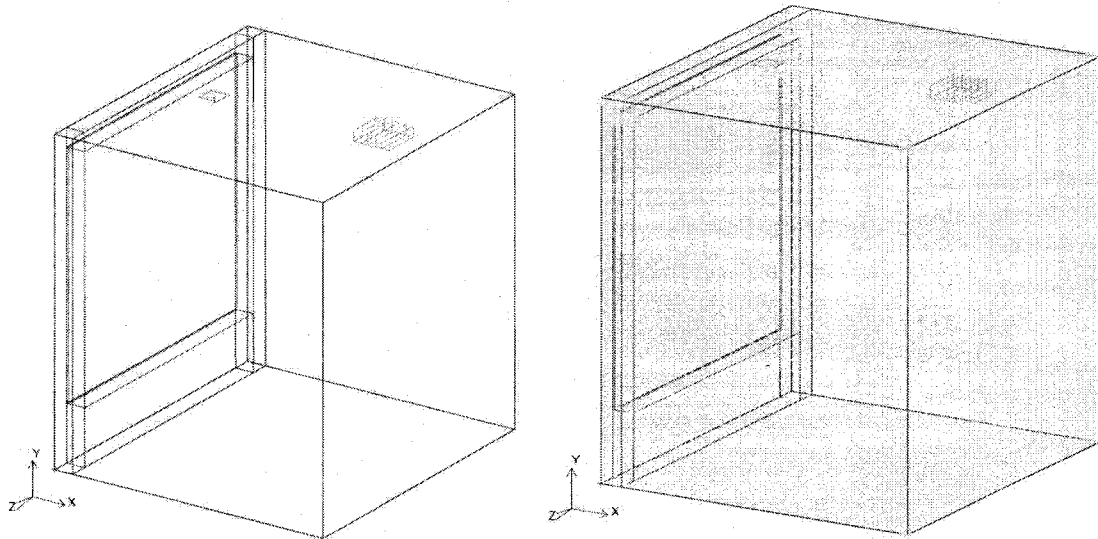


*Figure 4.49: Model of perimeter zone office used for Airpak simulation (left); representation of mesh (right)*

## 4.7.2 Results of CFD investigation

The resulting mean interior window surface temperature is 16 °C and the actual heat loss through the façade is calculated to be 554 W. Inner surfaces have a mean temperature of about 23 °C. The calculated supply airflow rate is 5.80 L/s (0.0687 kg/s), the mean temperature of supply air is 29 °C, and the mean return air temperature is 26 °C. Therefore, the heat gain from the heating system is:

$$\begin{aligned} Q &= \dot{m} \cdot c_p \cdot (T_{\text{supply}} - T_{\text{return}}) \\ &= 0.0678 \frac{\text{kg}}{\text{s}} \cdot 1005 \frac{\text{J}}{\text{kg} \cdot \text{K}} \cdot (34^\circ\text{C} - 26^\circ\text{C}) \\ &= 552 \text{ W} \end{aligned}$$

The variation in air speed as a function of distance from the window was taken at three different heights from the floor, 0.1 m, 0.6 m, and 1.1 m, corresponding to the heights of measurement of the ankle, chest, and head of a seated occupant (ASHRAE Standard 55-2004). The following figures show the differences in air speed at these heights for the diffuser at three different distances from the window: 0.7 m (Figure 4.50), 1.1 m (Figure 4.51), and 1.5 m (Figure 4.52).

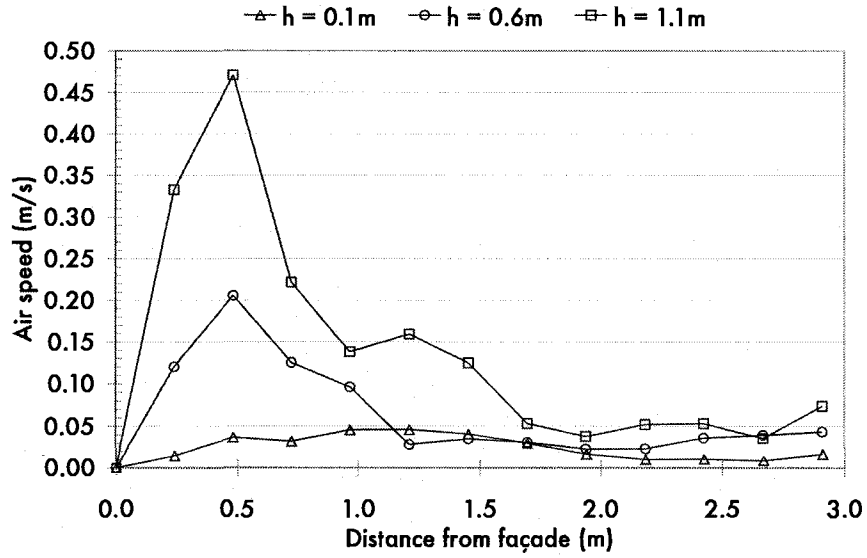


Figure 4.50: Variation in air speed at three different heights with diffuser 0.7 m from window ( $T_{supply} = 30\text{ }^{\circ}\text{C}$ ;  $v_{supply} = 1.5\text{ m/s}$ )

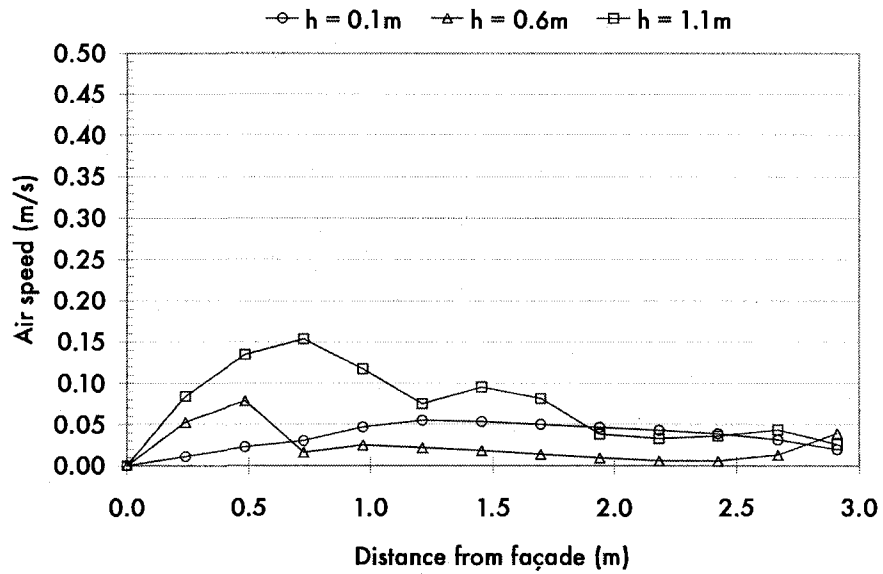


Figure 4.51: Variation in air speed at three different heights with diffuser 1.1 m from window ( $T_{supply} = 30\text{ }^{\circ}\text{C}$ ;  $v_{supply} = 1.5\text{ m/s}$ )

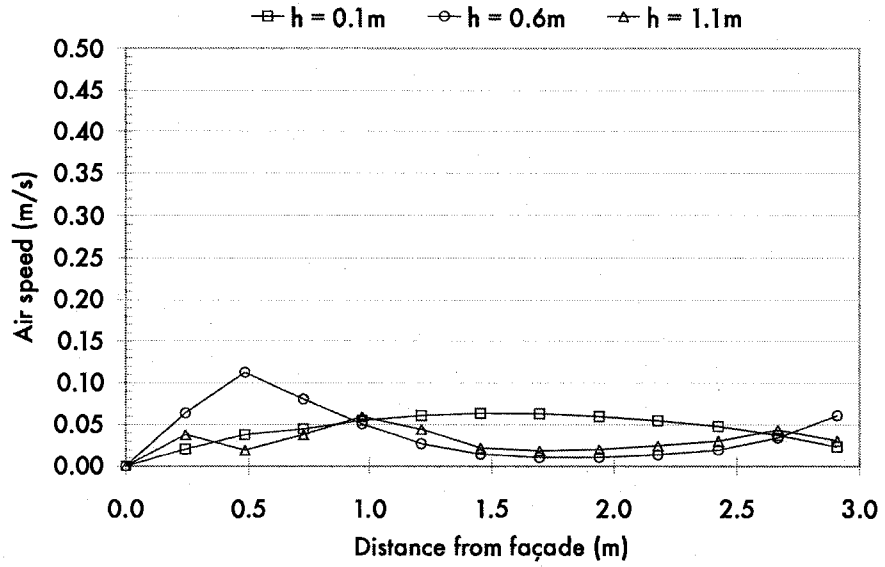


Figure 4.52: Variation in air speed at three different heights with diffuser 1.5 m from window ( $T_{supply} = 30\text{ }^{\circ}\text{C}$ ;  $v_{supply} = 1.5\text{ m/s}$ )

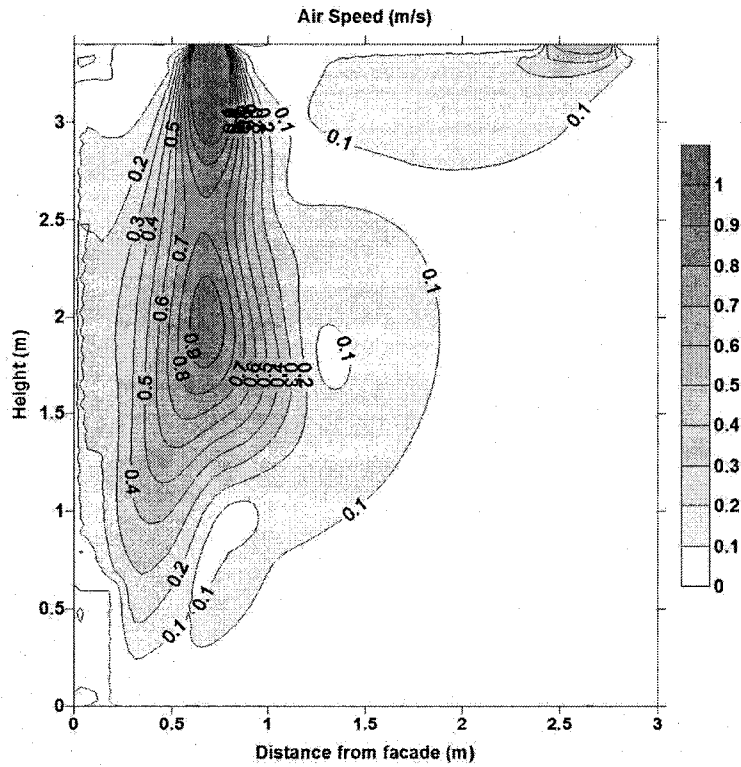


Figure 4.53: Cross sectional contour plot of air speed with diffuser 0.7 m from window

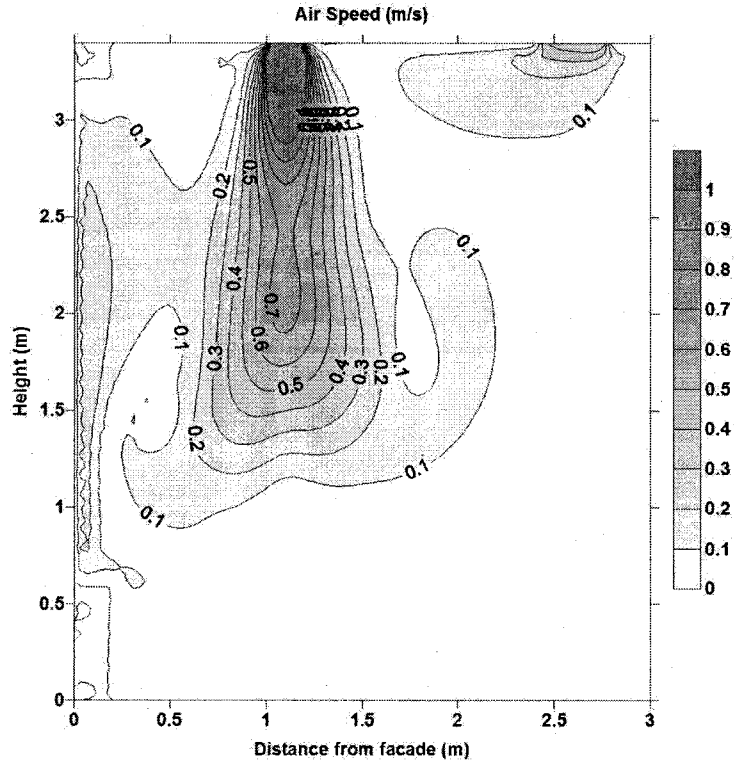


Figure 4.54: Cross sectional contour plot of air speed with diffuser 1.1 m from window

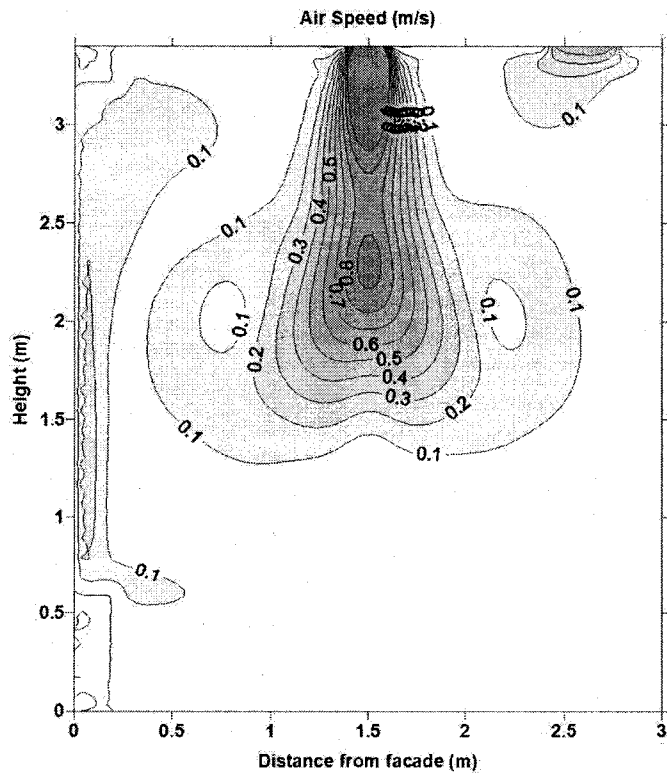


Figure 4.55: Cross sectional contour plot of air speed with difusser 1.5 m from window

There is not a large variation in operative temperature with the diffuser at different locations (Figure 4.56 - Figure 4.58). For heights  $\leq 1.1$  m, operative temperature is kept between 23 - 23.5 °C with the diffuser located 0.7 m from the window, between 21.5 - 23.5 °C with the diffuser located 1.1 m from the window, and between 21.5 - 22.5 °C with the diffuser located 1.5 m from the window. In addition, vertical temperature stratification between ankle and head level is less than 3 °C, meeting the requirement of ASHRAE Standard 55 (2004). This shows that primary heating is sufficient in providing the conditions necessary for comfort in terms of operative temperature.

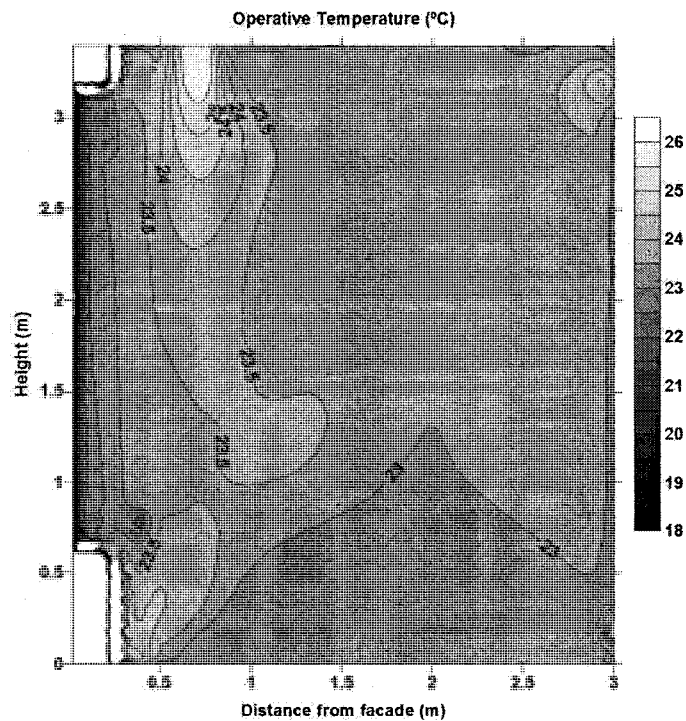


Figure 4.56: Cross sectional contour plot of operative temperature with diffuser 0.7 m from window

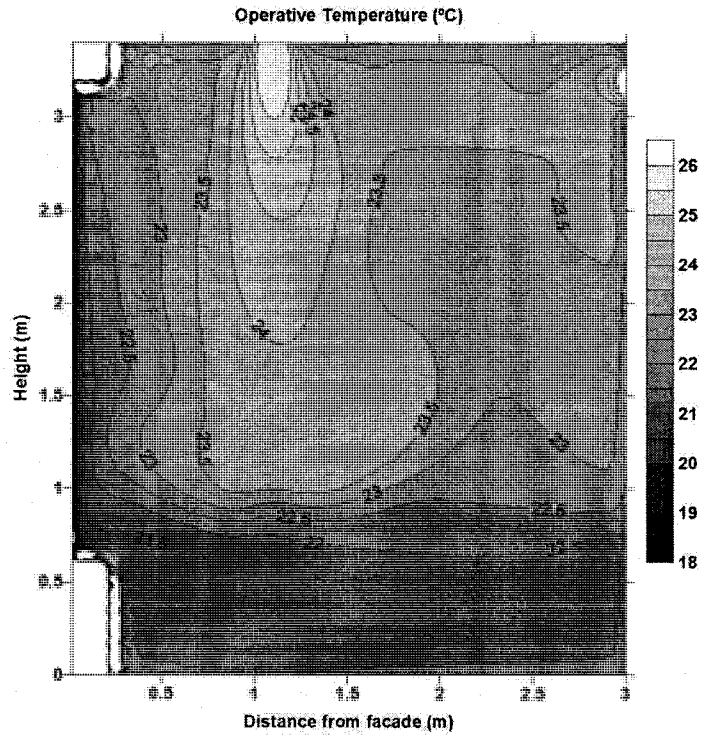


Figure 4.57: Cross sectional contour plot of operative temperature with diffuser 1.1 m from window

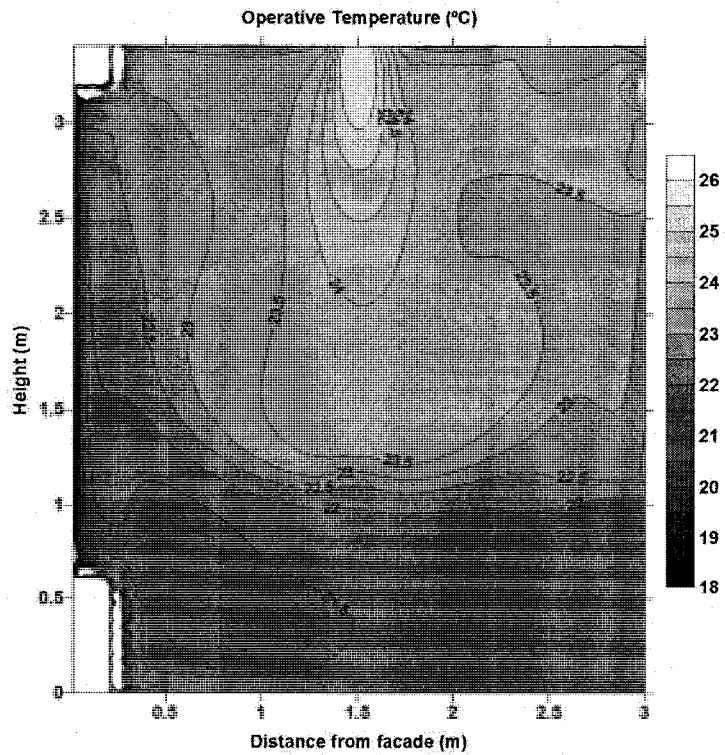


Figure 4.58: Cross sectional contour plot of operative temperature with diffuser 1.5 m from window

The results from Airpak demonstrate the need for proper placement of the diffuser in order to maintain comfort for occupants near the façade. Although comfortable operative temperature is attained in each case, placing the diffuser close to the window (0.7 m) would cause discomfort due to air speeds exceeding 0.45 m/s at the head level. The results also suggest that secondary perimeter heating is not needed to mitigate cold downdraft or to increase operative temperature near the façade.

## 5 CONCLUSIONS AND RECOMMENDATIONS

### 5.1 Conclusions

This thesis has considered:

1. Thermal comfort in a perimeter zone office with glass façade;
2. How exterior climate (air temperature and solar radiation) directly and indirectly affects interior thermal conditions and thermal comfort; and
3. Shading device properties and glazing type and their use as a means to improve thermal comfort.

An explicit finite-difference mathematical model was developed to analyze the thermal conditions of highly glazed perimeter zones. A transient two-node thermal comfort mathematical model was also developed to provide a prediction of thermal comfort. The effect of shading properties on thermal comfort was quantified.

Measurements were taken in an experimental perimeter zone using thermocouples and an indoor climate analyzer to investigate the effect that the exterior climate and shading devices have on the indoor thermal environment. It was determined through the experimental study that shading devices can have a positive impact on thermal comfort conditions in perimeter zones, preventing

overheating (minimizing operative temperature) on clear winter days and increasing operative temperature on cloudy winter days. For both of these sky conditions, the venetian blinds only showed an improvement in comfort when the slats were tilted at 45° or 90° (fully closed). A good agreement between the measurements of the experimental study and simulation model was obtained.

Clear days in winter are the most complex conditions in terms maintaining comfort and managing space conditioning. This is because the climate exhibits contrasting thermal interactions: high incident solar radiation and cold air temperature. Furthermore, comfort can be more difficult to manage due to low solar altitude. This study has shown that not only the thermal resistance of glazing, but also its solar transmittance, has a profound effect on thermal comfort. Rooms that use glazing with low insulating value and high transmittance exhibit the greatest fluctuations of the indoor thermal environment. Rooms that use glazing with a higher insulating value and lower transmittance create conditions which are more comfortable and less affected by the exterior climate; however, there is a relationship between lower transmittance of the glazing and increased demand of primary heating needed to be supplied to the space due to decreased solar gains. It is evident that the selection of fenestration components becomes a trade-off between energy, thermal comfort, and lighting needs.

For cloudy winter days the indoor environmental conditions remain more stable. For this case, indoor thermal conditions are dependent on the window

thermal transmittance. Even on very cold cloudy days, a highly insulating window (i.e. triple glazed, low-*e*) can maintain comfort conditions. Regardless of glazing type, using a roller shade can improve comfort conditions by decreasing radiant temperature asymmetry and increasing operative temperature. For the cases considered, perimeter heating could be eliminated when using a triple glazed, low-*e* window or a double glazed, low-*e* window with roller shade. However, it is not suggested to rely on the occupant using a shade on a cloudy day since these climatic conditions provide an optimum scenario to take advantage of glare-free daylighting and view.

Using CFD to analyze the airflow patterns in an office with double glazed low-*e* windows on a cold cloudy day, it was determined that placing the diffuser in the ceiling near the window (0.7 m) will cause discomfort near the window due to elevated downdraft, with air speeds exceeding 0.45 m/s at head level. It was also determined that secondary perimeter heating was not needed since the primary heating could provide adequate thermal conditions by maintaining the operative temperature in the comfort zone.

As noted in Chapter 4, it is generally a difficult process to validate or verify thermal comfort models with measurements due to the assumptions used. Furthermore, these assumptions (clothing insulation and absorptance, position in the room, metabolic rates) are more complex in reality since they can vary from person to person or even with respect to time. However, this work has been able to show in general terms how thermal comfort in perimeter zones is affected by

glazing and roller shade properties and location of primary heating systems. It was determined that with a high-quality building envelope (glazing U-value =  $2.0 \text{ W/m}^2 \text{ }^\circ\text{C}$ ) and the diffuser for primary heating located away from the glazing (1.1 m), cold air downdraft near the glazing would be reduced and operative temperatures could be maintained within the comfort zone, thereby eliminating the need for secondary perimeter heating.

## **5.2 Recommendations for future work**

There are several possibilities for extension of current work. The work presented in this thesis investigates whole-body thermal comfort. An investigation into the impact of perimeter zones on local discomfort could be developed with a thermal comfort simulation model for individual body segments.

Another possible extension would be to model the impact of venetian blinds on thermal comfort. It is currently difficult to model this since there is no information in the literature on how to take complex surfaces into account for mean radiant temperature; the process becomes even more difficult when considering the varying amounts of solar radiation falling on the occupant due to openings in the blinds. Therefore, it would be interesting to see if a model could be developed based on experimental data.

Most importantly, however, would be the development of a model that considers thermal comfort, visual comfort, daylighting, and energy management.

Since shading devices play an important role for all these parameters, control strategies could be developed to optimize some or all of these criteria. Furthermore, models that also consider or take into account occupant behaviour would be advantageous since it is difficult to develop an automated control strategy that predicts operating conditions when occupants have some control over their work environment (i.e. shade position).

As with all thermal comfort prediction methods, which aim to provide recommendations for building design in order to achieve comfort, there will be a range of variability in the comfort conditions actually experienced by real people under real conditions. Once a building is in use, it is important to consider thermal comfort as part of the commissioning strategy by completing a post-occupancy evaluation and adjusting any control strategy as necessary.

By considering comfort as a key element in building design from the initial design stage to the occupancy stage, it can be ensured that new sustainable high-performance and passive solar buildings are not only aesthetically pleasing and energy-efficient, but also comfortable and enjoyable places to work and live.

## REFERENCES

- Architectural Energy Corporation (2004). *Improving indoor environmental quality and energy performance of California K-12 schools*. No. D-2.2d - Final CFD Analysis and Documentation Report.
- ASHRAE. (2004). *Standard 55 - Thermal environmental conditions for human occupancy*. Atlanta: American Society of Heating, Refrigerating, and Air-Conditioning Engineers, Inc.
- ASHRAE. (2005). *Handbook of fundamentals*. Atlanta: American Society of Heating, Refrigerating, and Air-Conditioning Engineers, Inc.
- Athienitis, A. K. (1998). *Building thermal analysis* (2nd ed.) Mathcad electronic book, Mathsoft.
- Athienitis, A. K. & Santamouris, M. (2002). *Thermal analysis and design of passive solar buildings*. London: James and James.
- Ayoub, J., Dignard-Bailey, L., & Filion, A. (2000). *Photovoltaics for buildings: Opportunities for Canada: A discussion paper*. No. CEDRL-2000-72 (TR). Varennes, Quebec: CANMET Energy Diversification Research Laboratory, Natural Resources Canada.

- Bauman, F., Andersson, B., Carroll, W., Kammerud, R. C., & Friedman, N. E. (1983). Verification of BLAST by comparison with measurements of a solar-dominated test cell and a thermally massive building. *ASME Journal of Solar Engineering*, 105(2), 207-216.
- Blazejczyk, K., Holmer, I., & Nilsson, H. (1998). Absorption of solar radiation by an ellipsoid sensor simulated the human body. *Journal of Physiological Anthropology*, 17(6), 267-273.
- Blazejczyk, K., Nilsson, H., & Holmer, I. (1993). Solar heat load on man: Review of different methods of estimation. *International Journal of Biometeorology*, 37, 125-132.
- Cabanac, M. (1996). Pleasure and joy, and their role in human life. *Proceedings of Indoor Air '96*.
- Cannistraro, G., Franzitta, G., Giaconia, C., & Rizzo, G. (1992). Algorithms for the calculation of the view factors between human body and rectangular surfaces in parallelepiped environments. *Energy and Buildings*, 19(1), 51-60.
- Carmody, J., Selkowitz, S., Lee, E. S., Arasteh, D., & Willmert, T. (2004). *Window systems for high-performance buildings* (First ed.). New York: W.W. Norton & Company, Inc.

- Chaiyapinunt, S., Phueakphongsuriya, B., Mongkornsaksit, K., & Khomporn, N. (2005). Performance rating of glass windows and glass windows with films in aspect of thermal comfort and heat transmission. *Energy and Buildings*, 37, 725-738.
- Chapman, K. S., & Sengupta, J. (2003). *Development of a simplified methodology to incorporate fenestration systems into occupant thermal comfort calculations*. No. 1071. ASHRAE.
- Clarke, J. A., Janak, M., & Ruyssevelt, P. (1998). Assessing the overall performance of advanced glazing systems. *Solar Energy*, 63(4), 231-241.
- Collins, M., Harrison, S. J., Naylor, D., & Oosthuizen, P. H. (2002). Heat transfer from an isothermal vertical surface with adjacent heated horizontal louvers: Numerical analysis. *Journal of Heat Transfer*, 124, 1072-1077.
- Fang, Y., Eames, P. C., & Hyde, T. J. (2006) *Electrochemical vacuum glazing may improve thermal comfort in buildings*. The International Society for Optical Engineering.
- Fanger, P. O. (1973). *Thermal comfort*. New York: McGraw-Hill Book Co.
- Fanger, P. O., Melikov, A. K., Hanzawa, H., & Ring, J. (1988). Air turbulence and sensation of draught. *Energy and Buildings*, 12, 21-29.

Fieber, A. (2005). Building integration of solar energy: A multifunctional approach. (Licentiate Thesis, Department of Construction and Architecture, Division of Energy and Building Design, Lund University, Sweden).

Fluent Inc. (2007). *Airpak 3.0. User's Guide*.

Gagge, A. P., Fobelets, A. P., & Berglund, L. G. (1986). A standard predictive index and human response to the thermal environment. *ASHRAE Transactions*, 92(2), 709-731.

Gagge, A. P., Stolwijk, J., & Nishi, Y. (1970). An effective temperature scale based on a simple model of human physiological regulatory response. *ASHRAE Transactions*,

Ge, H., & Fazio, P. (2004). Experimental investigations of cold drafts induced by two different types of glazing panels in metal curtain walls. *Building and Environment*, 39, 115-125.

Grivel, F., Hoefl, A., & Candas, V. (1989). Body temperatures and thermal perceptions during warm and cool periodic transients: Influence of clothing. *Proceedings of the Annual International Industrial Ergonomics and Safety Conference*, 217-224.

- Hawthorne, W., & Reilly, M. S. (2000). The impact of glazing selection on residential duct design and comfort. *ASHRAE Transactions*, 106(1).
- Heiselberg, P., Overby, H., & Bjorn, E. (1995). Energy-efficient measures to avoid downdraft from large glazed facades. *ASHRAE Transactions*, 101(2), 1127-1135.
- Hensen, J. L. M. (1990). Literature review on thermal comfort in transient conditions. *Building and Environment*, 25(4), 309.
- Hodder, S. G., & Parsons, K. (2007). The effects of solar radiation on thermal comfort. *International Journal of Biometeorology*, 51(3), 233-250.
- Huizenga, C., Zhang, H., Mattelaer, P., Yu, T., Arens, E., & Lyons, P. (2006). *Window performance for human thermal comfort*. Final report to the National Fenestration Rating Council. (Center for the Built Environment, University of California, Berkeley).
- Humphreys, M. A., Nicol, J. F., & McCartney, J. K. (2002). An analysis of some subjective assessments of indoor air quality in five European countries. *Proceedings of the 9th International Conference on Indoor Air*, Santa Cruz, USA. 86-91.

Hutcheon, N. B., & Handegord, G. O. P. (1995). *Building science for a cold climate*.

Institute for Research in Construction, National Research Council Canada.

KPMB Architects. Retrieved 11/01, 2007, from <http://www.kpmb.com>.

Kubaha, K., Fiala, D., Toftum, J., & Taki, A. H. (2004). Human projected area factors for detailed direct and diffuse solar radiation analysis. *International Journal of Biometeorology*, 49, 113-129.

Kuhn, T. E., Bühler, C., & Platzer, W. J. (2000). Evaluation of overheating protection with sun-shading systems. *Solar Energy*, 69(6), 59-74.

La Gennusa, M., Nucara, A., Rizzo, G., & Scaccianoce, G. (2005). The calculation of the mean radiant temperature of a subject exposed to the solar radiation— a generalised algorithm. *Building and Environment*, 40(3), 367-375.

Laforgue, P., Souyri, B., & Achard, G. (1997). Simulation of visual and thermal comfort related to daylighting and solar radiation in office buildings. Paper presented at the *International Building Performance Simulation Association*.

Larsson, U., & Moshfegh, B. (2002). Experimental investigation of downdraught from well-insulated windows. *Building and Environment*, 37, 1073-1082.

- Lyons, P., Arates, D., & Huizenga, C. (1999). Window performance for human thermal comfort. *ASHRAE Transactions*, 73(2), 4.0-4.20.
- Manz, H., & Frank, T. (2004). Analysis of thermal comfort near cold vertical surfaces by means of computational fluid dynamics. *Indoor and Built Environment*, 13, 233-242.
- McIntyre, D. A. (1980). *Indoor climate*. Essex, England: Applied Science Publishers, Ltd.
- Nicol, F. (1993). *Thermal comfort: A handbook of field studies toward an adaptive model*. London: University of East London.
- Nicol, F. (2003). Thermal comfort. In M. Santamouris (Ed.), *Solar thermal technologies for buildings* (pp. 164). London: James & James Ltd.
- Nicol, F. (2004). *Thermal comfort*. Freiburg Solar Academy.
- Nicol, J. F., & Humphreys, M. A. (2002). Adaptive thermal comfort and sustainable thermal standards for buildings. *Energy and Buildings*, 34, 563-572.

- Park, C., Augenbroe, A., & Messadi, T. (2003). Daylighting optimization in smart façade systems. *Eight International IBPSA Conference*, Eindhoven, Netherlands.
- Parsons, K. (2003). *Human thermal environments: The effects of hot, moderate, and cold environments on human health, comfort, and performance* (2nd ed.). London: Taylor & Francis.
- Perez, R., Ineichen, P., Seals, R., Michalsky, J., & Stewart, R. (1990). Modeling daylight availability and irradiance components from direct and global irradiance. *Solar Energy*, 50(3), 235-245.
- Poirazis, H. (2005). Single skin glazed office buildings: Energy use and indoor climate simulations. (Licentiate Thesis, Department of Construction and Architecture, Division of Energy and Building Design, Lund University, Sweden).
- Rizzo, G., Franzitta, G., & Cannistraro, G. (1991). Algorithms for the calculation of the mean projected area factors of seated and standing persons. *Energy and Buildings*, 17(3), 221-230.

- Rueegg, T., Dorer, V., & Steinemann, U. (2001). Must cold air down draughts be compensated using highly insulating windows? *Energy and Buildings*, 33, 489-493.
- Shahid, H., & Naylor, D. (2005). Energy performance assessment of a window with a horizontal venetian blind. *Energy and Buildings*, 37, 836-843.
- Shahid, H., & Naylor, D. (2005). Energy performance assessment of a window with a horizontal venetian blind. *Energy and Buildings*, 37, 836-843.
- Tzempelikos, A., & Athienitis, A. K. (2007). The impact of shading design and control on building cooling and lighting demand. *Solar Energy*, 81(3), 369-382.
- Tzempelikos, A. (2001). A methodology for detailed calculations of illuminance levels and light dimming factors in a room with motorized blinds integrated in an advanced window. (Master of Applied Science, Department of Building, Civil, and Environmental Engineering, Concordia University).
- Tzempelikos, A. and Athienitis, A.K. (2003). Modeling and evaluation of a window with integrated motorized venetian blinds. *Proceedings of 3<sup>rd</sup> International Solar Energy Society World Congress*, Göteborg, Sweden, June 2003.

- Tzempelikos, A. (2005). A methodology for integrating daylighting and thermal analysis of buildings. (PhD, Department of Building, Civil, and Environmental Engineering, Concordia University).
- Tzempelikos, A., Athienitis, A. K., & Karava, P. (2007). Simulation of facade and envelope design options for a new institutional building. *Solar Energy*, 81(9), 1088-1103.
- U.S. Green Building Council (2007). Retrieved 07/01, 2007, from [www.usgbc.org](http://www.usgbc.org)
- Wissler, E. W. (1988). A review of human thermal models. In I. B. Mekjavic, E. W. Banister & J. B. Morrison (Eds.), *Environmental Ergonomics* (pp. 267-285) Taylor and Francis.
- Zhang, H., Huizenga, C., Arens, E., & Wang, D. (2004). Thermal sensation and comfort in transient non-uniform thermal environments. *European Journal of Applied Physiology*, 92, 728-733.
- Zmeureanu, R., & Doramajian, A. (1992). Thermally acceptable temperature drifts can reduce the energy consumption for cooling in office buildings. *Building and Environment*, 27(4), 469-481.

Zmeureanu, R., Iliescu, S., & Jacob, Y. (2003). Radiation from cold or warm windows: Computer model development and experimental validation. *Building and Environment*, 38, 427-434.

## **APPENDIX A: Perez irradiance model**

## SOLAR RADIATION MODELING: PEREZ MODEL

Perez R., Ineichen P., Seals R., Michalsky J., Stewart R., "Modeling daylight availability and irradiance components from direct and global irradiance", Solar Energy, Vol. 44 (5), pp. 271-289, 1990.

### Surface and Location Data:

Latitude:	LAT := 45.5·deg
Longitude:	LNG := 74·deg
Local Standard Meridian:	LSM := 75·deg
Altitude:	Alt := 50·m
Surface azimuth:	$\psi$ := 0deg
Surface tilt angle:	$\beta$ := 90·deg
Ground reflectance:	$\rho_g$ := 0.7

### Solar Geometry:

Equation of time:

$$ET(n) := \left( 9.87 \cdot \sin\left(4 \cdot \pi \cdot \frac{n - 81}{364}\right) - 7.53 \cdot \cos\left(2 \cdot \pi \cdot \frac{n - 81}{364}\right) - 1.5 \cdot \sin\left(2 \cdot \pi \cdot \frac{n - 81}{364}\right) \right) \cdot \text{min}$$

$$\text{Apparent Solar Time: } AST(n, t) := t \cdot \text{hr} + ET(n) + \frac{(LSM - LNG) \cdot \text{hr}}{15 \cdot \text{deg}} \quad s(n, t) := AST(n, t) - 12 \cdot \text{hr}$$

$$\text{Solar declination: } \delta(n) := 23.45 \cdot \text{deg} \cdot \sin\left(360 \cdot \frac{284 + n}{365} \cdot \text{deg}\right)$$

$$\text{Hour angle: } H(n, t) := (AST(n, t) - 12 \cdot \text{hr}) \cdot \left(15 \cdot \frac{\text{deg}}{\text{hr}}\right)$$

$$\text{Sunset hour angle: } h_s(n) := \left(\text{acos}\left(-\tan(LAT) \cdot \tan(\delta(n))\right)\right)$$

$$\text{Sunset time: } t_s(n) := h_s(n) \cdot \frac{\text{hr}}{15 \cdot \text{deg}}$$

$$\text{Surface sunset time: } t_{ss}(n) := \min\left(h_s(n), \text{acos}\left(-\tan(LAT - \beta) \cdot \tan(\delta(n))\right)\right) \cdot \frac{\text{hr}}{15 \cdot \text{deg}}$$

Solar altitude:

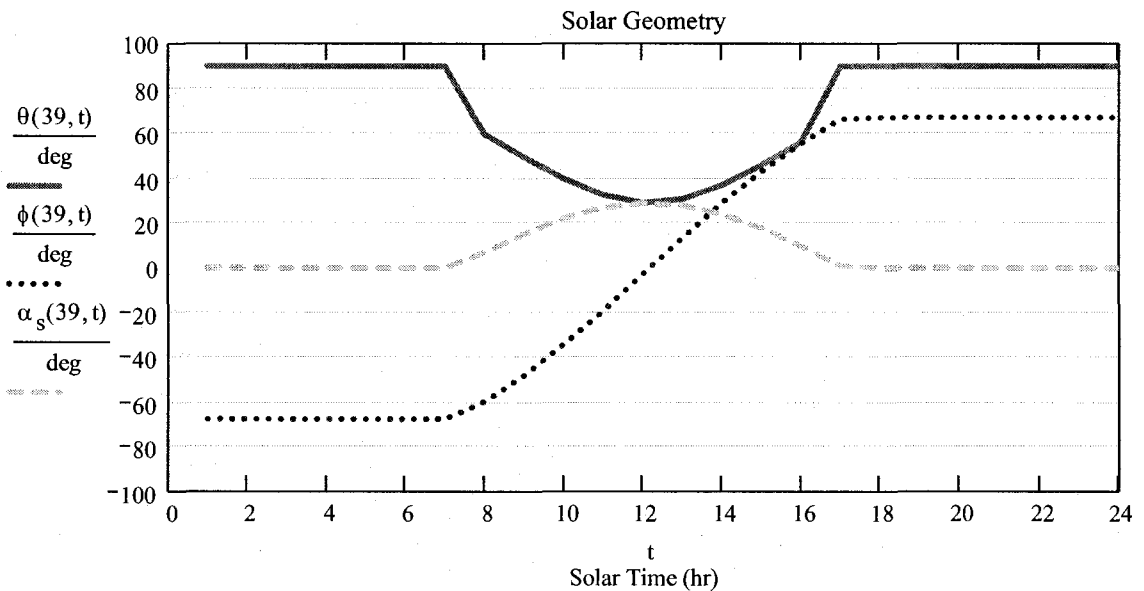
$$\alpha_s(n, t) := \begin{cases} \text{asin}\left[\frac{(\cos(LAT)) \cdot \cos(\delta(n)) \cdot \cos(H(n, t)) \dots}{+[(\sin(LAT)) \cdot \sin(\delta(n))]} \right] & \text{if } \text{asin}\left[\frac{(\cos(LAT)) \cdot \cos(\delta(n)) \cdot \cos(H(n, t)) \dots}{+[(\sin(LAT)) \cdot \sin(\delta(n))]} \right] > 0 \cdot \text{deg} \\ 0 \cdot \text{deg} & \text{otherwise} \end{cases}$$

Solar azimuth: 
$$\phi(n, t) := \operatorname{acos}\left(\frac{\sin(\alpha_s(n, t)) \cdot \sin(\text{LAT}) - \sin(\delta(n))}{\cos(\alpha_s(n, t)) \cdot \cos(\text{LAT})}\right) \cdot \frac{H(n, t)}{|H(n, t)|}$$

Surface solar azimuth: 
$$\gamma_s(n, t) := \phi(n, t) - \psi$$

The angle of incidence, is: 
$$\theta(n, t) := \cos(\alpha_s(n, t)) \cdot \cos(|\gamma_s(n, t)|) \cdot \sin(\beta) + \sin(\alpha_s(n, t)) \cdot \cos(\beta)$$

$$\theta(n, t) := \begin{cases} \operatorname{acos}\left(\frac{\theta\theta(n, t) + |\theta\theta(n, t)|}{2}\right) & \text{if } (12\text{hr} - t_{ss}(n)) < t\text{-hr} < (12\text{hr} + t_{ss}(n)) \\ (90\text{deg}) & \text{otherwise} \end{cases}$$



Solar constant: 
$$I_{sc} := 1367 \cdot \frac{\text{W}}{\text{m}^2}$$

Normal extraterrestrial solar radiation: 
$$I_{exn}(n) := I_{sc} \cdot \left(1 + 0.033 \cdot \cos\left(\frac{360 \cdot n}{365} \cdot \text{deg}\right)\right)$$

Hourly average global horizontal irradiance for Montreal:

$$I_h(n, t) = [I_{bn}(n, t) \cdot (\sin(\alpha_s(n, t))) + I_{dh}(n, t)] \cdot \frac{\text{W}}{\text{m}^2}$$

Incident beam radiation on an inclined surface:

$$I_b(n, t) := (I_{bn}(n, t) \cdot \cos(\theta(n, t))) \cdot \frac{\text{W}}{\text{m}^2}$$

$$I_{bh}(n, t) := I_{bn}(n, t) \cdot \sin(\alpha_s(n, t))$$

### Perez diffuse irradiance model:

Diffuse radiation consists of three components:

1. Isotropic part, received uniformly from all the sky dome
2. Circumsolar diffuse, resulting from forward scattering of solar radiation and concentrated in the part of the sky around the sun.
3. Horizon brightening, concentrated near the horizon, most pronounced in clear skies.

Anisotropic sky models have been produced initially by Hay & Davies (1980), and further developed by Reindl et al (1990). An anisotropy index is used to account for a portion of diffuse radiation which is treated as forward scattered. More recently, Perez et al (1988, 1990, 1993) produced more accurate models for treating the three parts of diffuse radiation on a tilted surface.

### **Horizon brightness coefficients:**

$$a_p(n, t) := \max(0, \cos(\theta(n, t))) \quad b_p(n, t) := \max(\cos(85\text{-deg}), \sin(\alpha_s(n, t)))$$

### **Relative optical air mass:**

$$m_{\text{opt}}(n, t) := \frac{1}{\sin(\alpha_s(n, t)) + 0.15 \cdot \left( \alpha_s(n, t) \cdot \frac{\pi}{180 \cdot \text{deg}} + 3.885 \right)^{-1.253}}$$

### **Sky brightness:**

$$\Delta(n, t) := m_{\text{opt}}(n, t) \cdot \frac{I_{\text{dh}}(n, t) \cdot \frac{W}{m^2}}{I_{\text{exn}}(n)}$$

### **Sky clearness:**

$$\varepsilon(n, t) := \begin{cases} \frac{\frac{I_{\text{dh}}(n, t) + I_{\text{bn}}(n, t)}{I_{\text{dh}}(n, t)} + 5.535 \cdot 10^{-6} \cdot (90\text{-deg} - \alpha_s(n, t))^3}{1 + 5.535 \cdot 10^{-6} \cdot (90\text{-deg} - \alpha_s(n, t))^3} & \text{if } I_{\text{dh}}(n, t) > 0 \\ 0 & \text{otherwise} \end{cases}$$

Statistically derived irradiance coefficients for Perez model:

$$f_{11}(n,t) := \begin{cases} -0.008 & \text{if } \varepsilon(n,t) \leq 1.065 \\ 0.130 & \text{if } 1.065 < \varepsilon(n,t) \leq 1.23 \\ 0.330 & \text{if } 1.23 < \varepsilon(n,t) \leq 1.5 \\ 0.568 & \text{if } 1.5 < \varepsilon(n,t) \leq 1.95 \\ 0.873 & \text{if } 1.95 < \varepsilon(n,t) \leq 2.8 \\ 1.132 & \text{if } 2.8 < \varepsilon(n,t) \leq 4.5 \\ 1.060 & \text{if } 4.5 < \varepsilon(n,t) \leq 6.2 \\ 0.678 & \text{otherwise} \end{cases} \quad f_{12}(n,t) := \begin{cases} 0.588 & \text{if } \varepsilon(n,t) \leq 1.065 \\ 0.683 & \text{if } 1.065 < \varepsilon(n,t) \leq 1.23 \\ 0.487 & \text{if } 1.23 < \varepsilon(n,t) \leq 1.5 \\ 0.187 & \text{if } 1.5 < \varepsilon(n,t) \leq 1.95 \\ -0.392 & \text{if } 1.95 < \varepsilon(n,t) \leq 2.8 \\ -1.237 & \text{if } 2.8 < \varepsilon(n,t) \leq 4.5 \\ -1.600 & \text{if } 4.5 < \varepsilon(n,t) \leq 6.2 \\ -0.327 & \text{otherwise} \end{cases}$$

$$f_{21}(n,t) := \begin{cases} -0.060 & \text{if } \varepsilon(n,t) \leq 1.065 \\ -0.019 & \text{if } 1.065 < \varepsilon(n,t) \leq 1.23 \\ 0.055 & \text{if } 1.23 < \varepsilon(n,t) \leq 1.5 \\ 0.109 & \text{if } 1.5 < \varepsilon(n,t) \leq 1.95 \\ 0.226 & \text{if } 1.95 < \varepsilon(n,t) \leq 2.8 \\ 0.288 & \text{if } 2.8 < \varepsilon(n,t) \leq 4.5 \\ 0.264 & \text{if } 4.5 < \varepsilon(n,t) \leq 6.2 \\ 0.156 & \text{otherwise} \end{cases} \quad f_{22}(n,t) := \begin{cases} 0.072 & \text{if } \varepsilon(n,t) \leq 1.065 \\ 0.066 & \text{if } 1.065 < \varepsilon(n,t) \leq 1.23 \\ -0.064 & \text{if } 1.23 < \varepsilon(n,t) \leq 1.5 \\ -0.152 & \text{if } 1.5 < \varepsilon(n,t) \leq 1.95 \\ -0.462 & \text{if } 1.95 < \varepsilon(n,t) \leq 2.8 \\ -0.823 & \text{if } 2.8 < \varepsilon(n,t) \leq 4.5 \\ -1.127 & \text{if } 4.5 < \varepsilon(n,t) \leq 6.2 \\ -1.377 & \text{otherwise} \end{cases}$$

$$f_{13}(n,t) := \begin{cases} -0.062 & \text{if } \varepsilon(n,t) \leq 1.065 \\ -0.151 & \text{if } 1.065 < \varepsilon(n,t) \leq 1.23 \\ -0.221 & \text{if } 1.23 < \varepsilon(n,t) \leq 1.5 \\ -0.295 & \text{if } 1.5 < \varepsilon(n,t) \leq 1.95 \\ -0.362 & \text{if } 1.95 < \varepsilon(n,t) \leq 2.8 \\ -0.412 & \text{if } 2.8 < \varepsilon(n,t) \leq 4.5 \\ -0.359 & \text{if } 4.5 < \varepsilon(n,t) \leq 6.2 \\ -0.25 & \text{otherwise} \end{cases} \quad f_{23}(n,t) := \begin{cases} -0.022 & \text{if } \varepsilon(n,t) \leq 1.065 \\ -0.029 & \text{if } 1.065 < \varepsilon(n,t) \leq 1.23 \\ -0.026 & \text{if } 1.23 < \varepsilon(n,t) \leq 1.5 \\ -0.014 & \text{if } 1.5 < \varepsilon(n,t) \leq 1.95 \\ -0.001 & \text{if } 1.95 < \varepsilon(n,t) \leq 2.8 \\ 0.056 & \text{if } 2.8 < \varepsilon(n,t) \leq 4.5 \\ 0.131 & \text{if } 4.5 < \varepsilon(n,t) \leq 6.2 \\ 0.251 & \text{otherwise} \end{cases}$$

**Brightness coefficients:**

$$F_1(n,t) := \max \left[ 0, f_{11}(n,t) + f_{12}(n,t) \cdot \Delta(n,t) + \pi \cdot \frac{(90\text{-deg} - \alpha_s(n,t))}{180\text{-deg}} \cdot f_{13}(n,t) \right]$$

$$F_2(n,t) := \max \left[ 0, f_{21}(n,t) + f_{22}(n,t) \cdot \Delta(n,t) + \pi \cdot \frac{(90\text{-deg} - \alpha_s(n,t))}{180\text{-deg}} \cdot f_{23}(n,t) \right]$$

**Sky diffuse radiation on a tilted surface is calculated by:**

$$I_{sd}(n,t) := I_{dh}(n,t) \cdot \left[ (1 - F_1(n,t)) \cdot \left( \frac{1 + \cos(\beta)}{2} \right) + F_1(n,t) \cdot \frac{a_p(n,t)}{b_p(n,t)} + F_2(n,t) \cdot \sin(\beta) \right] \cdot \frac{W}{m^2}$$

**Ground-reflected radiation on a tilted surface:**

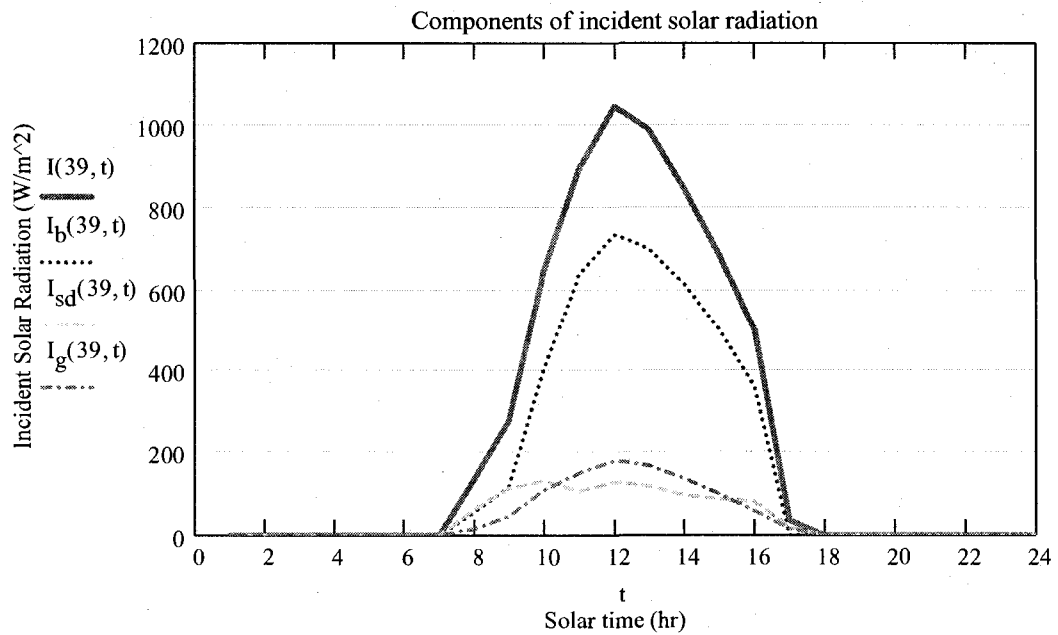
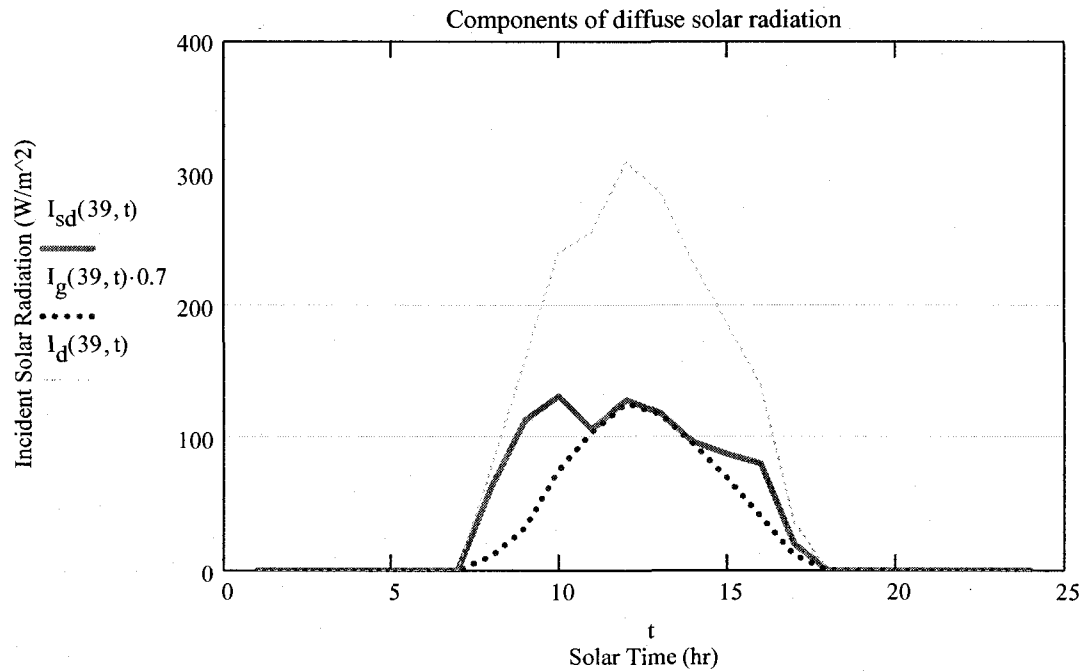
$$I_g(n, t) := \left[ (I_{bh}(n, t) + I_{dh}(n, t)) \cdot \rho_g \cdot \frac{1 - \cos(\beta)}{2} \right] \frac{W}{m^2}$$

**Total diffuse radiation on a tilted surface:**

$$I_d(n, t) := I_{sd}(n, t) + I_g(n, t)$$

**The total incident solar radiation on a tilted surface is equal to:**

$$I(n, t) := I_b(n, t) + I_{sd}(n, t) + I_g(n, t)$$



## **APPENDIX B: Room geometry and view factors**

## ROOM DIMENSIONS AND CALCULATION OF VIEW FACTORS

This file details the geometric dimensions of an office with one window. With this information, view factors between each surface can then be calculated to be used for radiation heat transfer analysis in the thermal simulation model.

### Room Dimensions:

$$W_{\text{rm}} := 3.2 \cdot \text{m} \quad \dots \text{width of room (along facade)}$$

$$D_{\text{rm}} := 3 \cdot \text{m} \quad \dots \text{depth of room}$$

$$H_{\text{rm}} := 3.0 \cdot \text{m} \quad \dots \text{height of room}$$

$$H_{\text{win}} := 2.0 \cdot \text{m} \quad \dots \text{height of window}$$

$$H_{\text{sp}} := 0.8 \cdot \text{m} \quad \dots \text{height of spandrel (distance from window to floor)}$$

$$W_{\text{win}} := W_{\text{rm}} - 0.0001 \cdot \text{m} \quad \dots \text{width of window (equal to width of room)}$$

Window area (assume window is horizontally located at the middle of the wall):

$$D_{\text{win}} := H_{\text{rm}} - H_{\text{sp}} - H_{\text{win}} + 0.0001 \cdot \text{m} \quad \dots \text{distance from top of window to ceiling}$$

$$D_{\text{win}} = 0.2 \cdot \text{m}$$

$$A_{\text{win\_south}} := W_{\text{win}} \cdot H_{\text{win}} \quad A_{\text{win\_south}} = 6.4 \cdot \text{m}^2 \quad \dots \text{window area}$$

Wall net areas:

$$A_{\text{south}} := H_{\text{rm}} \cdot W_{\text{rm}} - A_{\text{win\_south}} \quad A_{\text{south}} = 3.2 \cdot \text{m}^2 \quad \dots \text{area of wall minus window}$$

$$\text{WWR} := \frac{A_{\text{win\_south}}}{H_{\text{rm}} \cdot W_{\text{rm}}} \quad \text{WWR} = 0.667 \quad \dots \text{window-to-wall ratio}$$

$$A_{\text{east}} := D_{\text{rm}} \cdot H_{\text{rm}} \quad A_{\text{west}} := A_{\text{east}}$$

$$A_{\text{north}} := H_{\text{rm}} \cdot W_{\text{rm}} \quad A_{\text{north}} = 9.6 \cdot \text{m}^2$$

$$A_{\text{ceiling}} := W_{\text{rm}} \cdot D_{\text{rm}} \quad A_{\text{floor}} := A_{\text{ceiling}}$$

$$\text{Vol} := A_{\text{floor}} \cdot H_{\text{rm}} \quad \text{Vol} = 28.8 \cdot \text{m}^3$$

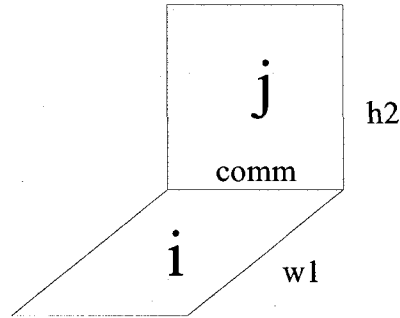
Wall/window azimuth angles:

$$\Psi_{\text{south}} := 19.6 \cdot \text{deg}$$

$$\Psi_{\text{north}} := 199.6 \cdot \text{deg}$$

## View Factors Between Internal Surfaces:

The view factors for the room below are determined after first calculating the view factor between two rectangular finite surfaces inclined at 90 degrees to each other with one common edge:



Define the following intermediate variables for calculating view factor from surface i to surface j:

$$w = \frac{w1}{comm}$$

$$h = \frac{h2}{comm}$$

$$A(h, w) := h^2 + w^2$$

$$B(w) := 1 + w^2$$

$$C(h) := 1 + h^2$$

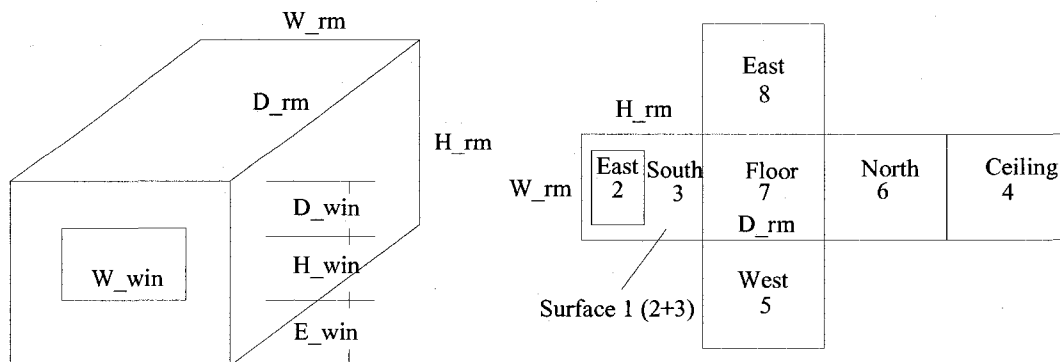
$$D(h, w) := 1 + (h^2 + w^2)$$

$$E(w) := w^2$$

$$G(h) := h^2$$

View factor  $F_{ij}$  from i to j:

$$F_{ij}(w, h) := \frac{\left( w \cdot \operatorname{atan}\left(\frac{1}{w}\right) + h \cdot \operatorname{atan}\left(\frac{1}{h}\right) - \sqrt{A(h, w)} \cdot \operatorname{atan}\left(\frac{1}{\sqrt{A(h, w)}}\right) \right) \dots + 0.25 \cdot \ln \left[ \frac{E(w) \cdot D(h, w)}{B(w) \cdot A(h, w)} \right]^{E(w)} \cdot \left[ \frac{G(h) \cdot D(h, w)}{C(h) \cdot A(h, w)} \right]^{G(h)} \cdot \frac{B(w) \cdot C(h)}{D(h, w)}}{\pi \cdot w}$$



The other view factors between the room surfaces are calculated by applying the following principles:

1. Reciprocity:  $A_i \cdot F_{i,j} = A_j \cdot F_{j,i}$

2. Symmetry, e.g.:  $F_{7,5} = F_{7,8}$

3. Energy conservation:  $\sum_j F_{i,j} = 1$  (for any surface i)

$i := 1, 2 \dots 8$

$j := 1, 2 \dots 8$  indices for surfaces

Areas of surfaces:

$A_1 := W_{\text{rm}} \cdot H_{\text{rm}}$

$A_2 := W_{\text{win}} \cdot H_{\text{win}}$

$A_3 := A_1 - A_2$

$A_4 := W_{\text{rm}} \cdot D_{\text{rm}}$

$A_5 := D_{\text{rm}} \cdot H_{\text{rm}}$

$A_7 := A_4$

$A_8 := A_5$

$A_6 := A_1$

Calculate view factors for all surfaces except 2, 3 (window and wall around window):



$w1 := H_{\text{rm}}$

$h2 := D_{\text{rm}}$

$\text{comm} := W_{\text{rm}}$

$w := \frac{w1}{\text{comm}}$

$h := \frac{h2}{\text{comm}}$

$F_{6,7} := F_{ij}(w, h)$

$F_{7,6} := A_6 \cdot \frac{F_{6,7}}{A_7}$

$$\begin{array}{lll}
F_{6,4} := F_{6,7} & F_{4,6} := F_{7,6} & F_{4,1} := F_{4,6} \\
F_{1,4} := F_{6,7} & F_{1,7} := F_{6,7} & F_{7,1} := F_{4,6} \\
w1 := W_{\text{rm}} & h2 := D_{\text{rm}} & \text{comm} := H_{\text{rm}} \\
w := \frac{w1}{\text{comm}} & h := \frac{h2}{\text{comm}} & \\
F_{6,5} := \text{Fij}(w,h) & F_{5,6} := A_6 \cdot \frac{F_{6,5}}{A_5} & F_{6,8} := F_{6,5} \\
F_{8,6} := F_{5,6} & F_{1,5} := F_{6,8} & F_{5,1} := F_{8,6} \\
F_{1,8} := F_{6,8} & F_{8,1} := F_{8,6} & \\
w1 := H_{\text{rm}} & h2 := W_{\text{rm}} & \text{comm} := D_{\text{rm}} \\
w := \frac{w1}{\text{comm}} & h := \frac{h2}{\text{comm}} & \\
F_{8,7} := \text{Fij}(w,h) & F_{7,8} := A_8 \cdot \frac{F_{8,7}}{A_7} & F_{5,7} := F_{8,7} \\
F_{7,5} := F_{7,8} & F_{4,5} := F_{7,8} & F_{5,4} := F_{8,7} \\
F_{8,4} := F_{8,7} & F_{4,8} := F_{7,8} &
\end{array}$$

... from symmetry



Determine the view factors for parallel opposite surfaces using the rule that:

$$\sum_j F_{i,j} = 1$$

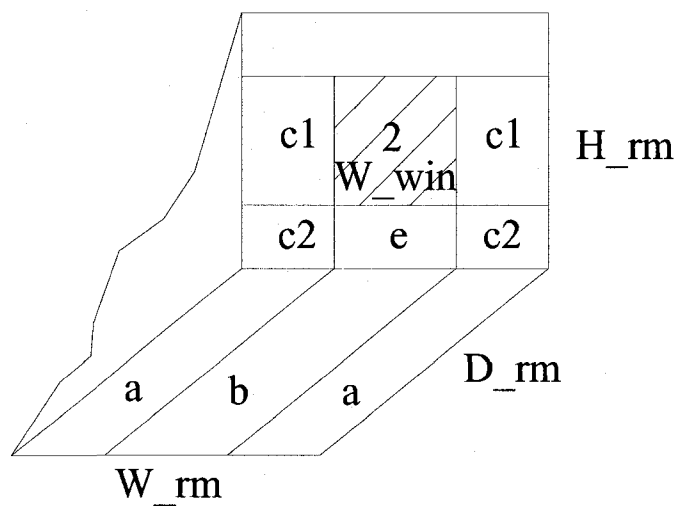
$$F_{1,6} := 1 - 2 \cdot F_{1,8} - 2 \cdot F_{1,4} \quad F_{6,1} := F_{1,6}$$

$$F_{5,8} := 1 - 2 \cdot F_{5,4} - 2 \cdot F_{5,6} \quad F_{8,5} := F_{5,8}$$

$$F_{4,7} := 1 - 2 \cdot F_{4,8} - 2 \cdot F_{4,6} \quad F_{7,4} := F_{4,7}$$

Determine the view factor between the window and the floor. Note that the same equations may be used to determine the view factor between the window and all other surfaces except the back wall (6).  $F_{2,6}$  can be calculated from the fact that the sum of the view factors to all surfaces is equal to 1.

## Calculation for view factors between window (surface 2) and floor (surface 7).



$$A_b := W_{win} \cdot D_{rm}$$

$$A_2 := W_{win} \cdot H_{win}$$

$$A_e := W_{win} \cdot H_{sp}$$

$$DIS := \frac{W_{rm} - W_{win}}{2}$$

$$A_{c1} := H_{win} \cdot DIS$$

$$A_{c2} := H_{sp} \cdot DIS$$

$$A_a := DIS \cdot D_{rm}$$

$$A_{ab} := D_{rm} \cdot (DIS + W_{win})$$

$$w_1 := D_{rm}$$

$$h_2 := H_{win} + H_{sp}$$

$$comm := W_{win}$$

$$w := \frac{w_1}{comm}$$

$$h := \frac{h_2}{comm}$$

$$F_{b\_2e} := F_{ij}(w, h)$$

...F from  $A_b$  to  $A_2 + A_e$

$$F_{b\_2e} = 0.2$$

$$w_1 := D_{rm}$$

$$h_2 := H_{sp}$$

$$comm := W_{win}$$

$$w := \frac{w_1}{comm}$$

$$h := \frac{h_2}{comm}$$

$$F_{b\_e} := F_{ij}(w, h)$$

$$F_{b\_e} = 0.098$$

$$w_1 := D_{rm}$$

$$h_2 := H_{sp}$$

comm := DIS

$$w := \frac{w1}{comm}$$

$$h := \frac{h2}{comm}$$

Fa\_c2 := Fij(w, h)

$$Fa\_c2 = 2.957 \times 10^{-5}$$

$$Fa\_c2 = 2.957 \times 10^{-5}$$

w1 := D<sub>rm</sub>

h2 := H<sub>win</sub> + H<sub>sp</sub>

comm := DIS

$$w := \frac{w1}{comm}$$

$$h := \frac{h2}{comm}$$

Fa\_c1c2 := Fij(w, h)

...F from Aa to Ac1+Ac2

$$Fa\_c1c2 = 3.215 \times 10^{-5}$$

w1 := D<sub>rm</sub>

h2 := H<sub>win</sub> + H<sub>sp</sub>

comm := W<sub>win</sub> + DIS

$$w := \frac{w1}{comm}$$

$$h := \frac{h2}{comm}$$

Fab\_c1c2e2 := Fij(w, h)

...F from Aab to Ac1+Ac2+Ae+A2

$$Fab\_c1c2e2 = 0.2$$

w1 := D<sub>rm</sub>

h2 := H<sub>sp</sub>

comm := W<sub>win</sub> + DIS

$$w := \frac{w1}{comm}$$

$$h := \frac{h2}{comm}$$

Fab\_c2e := Fij(w, h)

$$Fab\_c2e = 0.098$$

$$F2\_b := (Fb\_2e - Fb\_e) \cdot \frac{Ab}{A2}$$

$$Fa\_2e := \frac{Aab \cdot Fab\_c1c2e2 - Aa \cdot Fa\_c1c2 - Ab \cdot Fb\_2e}{2 \cdot Aa}$$

$$Fa\_2e = 0.132$$

$$Fa_e := \frac{Aab \cdot Fab_{c2e} - Aa \cdot Fa_{c2} - Ab \cdot Fb_e}{2 \cdot Aa}$$

$$F2_a := (Fa_{2e} - Fa_e) \cdot \frac{Aa}{A2}$$

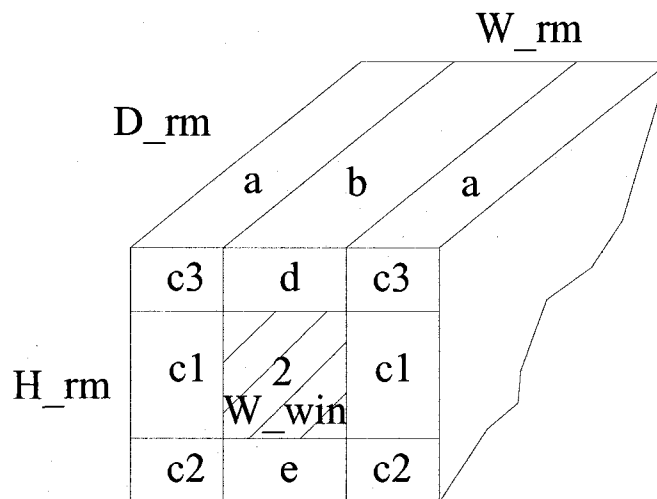
$$F_{2,7} := 2 \cdot F2_a + F2_b$$

$$F_{7,2} := A2 \cdot \frac{F_{2,7}}{A7}$$

$$F_{2,7} = 0.153$$

### Calculation for view factors between window, surface 2, and ceiling, surface 4

Similar to calculation for windows to ceiling: switch E\_win to D\_win.



$$Ad := W_{win} \cdot D_{win}$$

$$Ac3 := D_{win} \cdot DIS$$

$$w1 := D_{rm}$$

$$h2 := H_{win} + D_{win} \quad comm := W_{win}$$

$$w := \frac{w1}{comm}$$

$$h := \frac{h2}{comm}$$

$$Fb_{2d} := Fij(w, h)$$

...F from Ab to A2+Ad

$$Fb_{2d} = 0.181$$

$$w1 := D_{rm}$$

$$h2 := D_{win}$$

$$comm := W_{win}$$

$$w := \frac{w1}{comm}$$

$$h := \frac{h2}{comm}$$

$$Fb_d := Fij(w, h)$$

$$Fb_d = 0.03$$

$$Fb_d = 0.03$$

$$w1 := D_{rm} \qquad h2 := D_{win} \qquad comm := DIS$$

$$w := \frac{w1}{comm} \qquad h := \frac{h2}{comm}$$

$$Fa_{c3} := Fij(w, h) \qquad Fa_{c3} = 2.597 \times 10^{-5}$$

$$w1 := D_{rm} \qquad h2 := H_{win} + D_{win} \qquad comm := DIS$$

$$w := \frac{w1}{comm} \qquad h := \frac{h2}{comm}$$

$$Fa_{c1c3} := Fij(w, h) \qquad \dots F \text{ from } Aa \text{ to } Ac1+Ac3 \qquad Fa_{c1c3} = 3.177 \times 10^{-5}$$

$$w1 := D_{rm} \qquad h2 := H_{win} + D_{win} \qquad comm := W_{win} + DIS$$

$$w := \frac{w1}{comm} \qquad h := \frac{h2}{comm}$$

$$Fab_{2c1c3d} := Fij(w, h) \qquad \dots F \text{ from } Aab \text{ to } Ac1+Ac2+Ad+A2 \qquad Fab_{2c1c3d} = 0.181$$

$$w1 := D_{rm} \qquad h2 := D_{win} \qquad comm := W_{win} + DIS$$

$$w := \frac{w1}{comm} \qquad h := \frac{h2}{comm}$$

$$Fab_{c3d} := Fij(w, h) \qquad Fab_{c3d} = 0.03$$

$$F2_b := (Fb_{2d} - Fb_d) \cdot \frac{Ab}{A2} \qquad \text{Since } Fa_{2d} = Fb_{c1c2}$$

$$Fa_{2d} := \frac{Aab \cdot Fab_{2c1c3d} - Aa \cdot Fa_{c1c3} - Ab \cdot Fb_{2d}}{2 \cdot Aa} \qquad Fa_{2d} = 0.117$$

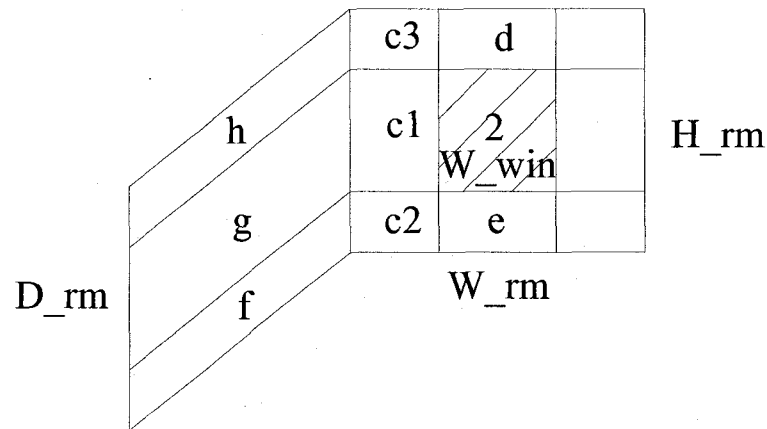
$$Fa_d := \frac{Aab \cdot Fab_{c3d} - Aa \cdot Fa_{c3} - Ab \cdot Fb_d}{2 \cdot Aa}$$

$$F2_a := (Fa_{2d} - Fa_d) \cdot \frac{Aa}{A2}$$

$$F_{2,4} := 2 \cdot F_{2,a} + F_{2,b} \quad F_{4,2} := A_2 \cdot \frac{F_{2,4}}{A_4} \quad F_{2,4} = 0.226 \quad F_{4,2} = 0.151$$

**Calculation for view factors between window, surface 2, and west/east wall, surface 5 /8.**

Similar to calculation for windows to floor.



$$\begin{aligned} A_d &:= W_{win} \cdot D_{win} & A_e &:= W_{win} \cdot H_{sp} & A_g &:= D_{rm} \cdot H_{win} & A_h &:= D_{win} \cdot D_{rm} & A_f &:= H_{sp} \cdot D_{rm} \\ A_{c1} &:= H_{win} \cdot DIS & A_{c2} &:= H_{sp} \cdot DIS & A_{c3} &:= D_{win} \cdot DIS & A_{gh} &:= A_g + A_h & A_{gf} &:= A_g + A_f \end{aligned}$$

$$w1 := D_{rm} \quad h2 := W_{win} + DIS \quad comm := H_{win}$$

$$w := \frac{w1}{comm} \quad h := \frac{h2}{comm}$$

$$Fg\_2c1 := F_{ij}(w, h) \quad \dots F \text{ from } A_g \text{ to } A_2 + A_{c1} \quad Fg\_2c1 = 0.174$$

$$w1 := D_{rm} \quad h2 := DIS \quad comm := H_{win}$$

$$w := \frac{w1}{comm} \quad h := \frac{h2}{comm}$$

$$Fg\_c1 := F_{ij}(w, h) \quad Fg\_c1 = 8.333 \times 10^{-6}$$

$$w1 := D_{rm} \quad h2 := DIS \quad comm := D_{win}$$

$$w := \frac{w1}{comm} \quad h := \frac{h2}{comm}$$

$$Fh\_c3 := Fij(w, h) \quad Fh\_c3 = 8.327 \times 10^{-6}$$

$$w1 := D_{rm} \quad h2 := W_{win} + DIS \quad comm := D_{win}$$

$$w := \frac{w1}{comm} \quad h := \frac{h2}{comm}$$

$$Fh\_dc3 := Fij(w, h) \quad \dots F \text{ from Ah to Ac3+Ad} \quad Fh\_dc3 = 0.041$$

$$w1 := D_{rm} \quad h2 := W_{win} + DIS \quad comm := H_{win} + D_{win}$$

$$w := \frac{w1}{comm} \quad h := \frac{h2}{comm}$$

$$Fgh\_c1c3d2 := Fij(w, h) \quad \dots F \text{ from Agh to Ac1+Ac3+Ad+A2} \quad Fgh\_c1c3d2 = 0.181$$

$$w1 := D_{rm} \quad h2 := DIS \quad comm := H_{win} + D_{win}$$

$$w := \frac{w1}{comm} \quad h := \frac{h2}{comm}$$

$$Fgh\_c1c3 := Fij(w, h) \quad Fgh\_c1c3 = 8.333 \times 10^{-6}$$

$$F2\_g := (Fg\_2c1 - Fg\_c1) \cdot \frac{Ag}{A2}$$

$$Fh\_2c1 := \frac{Agh \cdot Fgh\_c1c3d2 - Ah \cdot Fh\_dc3 - Ag \cdot Fg\_2c1}{2 \cdot Ah} \quad Fh\_2c1 = 0.106$$

$$Fh\_c1 := \frac{Agh \cdot Fgh\_c1c3 - Ah \cdot Fh\_c3 - Ag \cdot Fg\_c1}{2 \cdot Ah} \quad Fh\_c1 = 3.202 \times 10^{-9}$$

$$F2\_h := (Fh\_2c1 - Fh\_c1) \cdot \frac{Ah}{A2}$$

$$w1 := D_{rm} \quad h2 := DIS \quad comm := H_{sp}$$

$$w := \frac{w1}{comm} \quad h := \frac{h2}{comm}$$

$$Ff\_c2 := Fij(w, h) \quad Ff\_c2 = 8.331 \times 10^{-6}$$

$$w1 := D_{rm} \quad h2 := W_{win} + DIS \quad comm := H_{sp}$$

$$w := \frac{w1}{comm} \quad h := \frac{h2}{comm}$$

$$Ff\_ec2 := Fij(w, h) \quad \dots F \text{ from } Ah \text{ to } Ac2+Ae \quad Ff\_ec2 = 0.107$$

$$w1 := D_{rm} \quad h2 := W_{win} + DIS \quad comm := H_{win} + H_{sp}$$

$$w := \frac{w1}{comm} \quad h := \frac{h2}{comm}$$

$$Fgf\_c1c2e2 := Fij(w, h) \quad \dots F \text{ from } Agf \text{ to } Ac1+Ac2+Ae+A2 \quad Fgf\_c1c2e2 = 0.199$$

$$w1 := D_{rm} \quad h2 := DIS \quad comm := H_{win} + H_{sp}$$

$$w := \frac{w1}{comm} \quad h := \frac{h2}{comm}$$

$$Fgf\_c1c2 := Fij(w, h) \quad Fgf\_c1c2 = 8.333 \times 10^{-6}$$

$$Ff\_2c1 := \frac{Agf \cdot Fgf\_c1c2e2 - Af \cdot Ff\_ec2 - Ag \cdot Fg\_2c1}{2 \cdot Af} \quad Ff\_2c1 = 0.078$$

$$Ff\_c1 := \frac{Agf \cdot Fgf\_c1c2 - Af \cdot Ff\_c2 - Ag \cdot Fg\_c1}{2 \cdot Af} \quad Ff\_c1 = 8.869 \times 10^{-10}$$

$$F2\_f := (Ff\_2c1 - Ff\_c1) \cdot \frac{Af}{A2}$$



$$F2\_f = 0.029$$

$$F2\_g = 0.163$$

$$F2\_h = 9.987 \times 10^{-3}$$

$$F_{2,5} := F2\_h + F2\_g + F2\_f \quad F_{5,2} := A2 \cdot \frac{F_{2,5}}{A_5}$$

$$F_{2,8} := F_{2,5}$$

$$F_{8,2} := F_{5,2}$$

$$F_{2,6} := 1 - 2 \cdot F_{2,5} - F_{2,7} - F_{2,4}$$

$$F_{6,2} := F_{2,6} \cdot \frac{A2}{A_6}$$

$$\text{num} := 4, 5 \dots 8$$

$$F_{\text{num},3} := F_{\text{num},1} - F_{\text{num},2}$$

$$F_{3,\text{num}} := F_{\text{num},3} \cdot \frac{A_{\text{num}}}{A_3}$$

F =

	1	2	3	4	5	6	7	8
1	0	0	0	0.204	0.191	0.208	0.204	0.191
2	0	0	0	0.226	0.202	0.216	0.153	0.202
3	0	0	0	0.161	0.17	0.192	0.307	0.17
4	0.204	0.151	0.054	0	0.191	0.204	0.208	0.191
5	0.204	0.144	0.06	0.204	0	0.204	0.204	0.183
6	0.208	0.144	0.064	0.204	0.191	0	0.204	0.191
7	0.204	0.102	0.102	0.208	0.191	0.204	0	0.191
8	0.204	0.144	0.06	0.204	0.183	0.204	0.204	0

$$\text{surf} := 2, 3 \dots 8$$

$$F_{\text{sum}_i} := \sum_{\text{surf}} F_{i,\text{surf}}$$

$$F_{\text{sum}} =$$

- (1)
- 1
- 1
- 1
- 1
- 1
- 1
- 1

## **APPENDIX C: Building thermal simulation model**

---

## BUILDING THERMAL SIMULATION MODEL

This file is used for thermal analysis of the highly-glazed office space. The properties and dimensions of the surfaces and components are initially defined. Hourly values of incident solar radiation (beam and diffuse) are read from the Perez model. Representative days are selected for parametric analysis. Solar gains, thermal mass, heat transfer (convection, conduction, and radiation), and internal gains are modeled in detail. Glazing properties are modeled after data given in ASHRAE Handbook - Fundamentals, 2005 (Chapter 31, Fenestration). Therefore, the optical (transmittance, absorptance) and thermal properties of glazing were fitted to curves in Excel and used in Mathcad. Initial values of temperature and heat transfer coefficients are assumed; heat transfer coefficients are computed as a function of temperature at each time-step and the system of non-linear equations is solved explicitly in matrix form.

The results shown here are for an office with a south-facing facade in Montreal on a clear day in the winter. Shading with transmittance of 5% and absorptance 40% is used in conjunction with a double-glazed low-e window.

---

$$\text{degC} \equiv 1 \quad \sigma := 5.67 \cdot 10^{-8} \cdot \frac{\text{watt}}{\text{m}^2 \cdot \text{K}^4}$$

### Season and sky conditions:

The user can select the season (winter or summer) and sky conditions (clear or overcast)

$$\text{season} := 2 \quad (\text{summer} = 1 \text{ or winter} = 2) \quad \text{sky} := 1 \quad (\text{clear} = 1 \text{ or overcast} = 2)$$

$$n := \begin{cases} 38 & \text{if season} = 2 \wedge \text{sky} = 2 \\ 39 & \text{if season} = 2 \wedge \text{sky} = 1 \\ 180 & \text{if season} = 1 \wedge \text{sky} = 1 \\ 178 & \text{if season} = 1 \wedge \text{sky} = 2 \end{cases} \quad \begin{array}{l} \dots \text{representative days} \\ \text{selected from the} \\ \text{Perez model.} \end{array}$$

### Roller shade properties:

$$\text{shade} := 1 \quad \dots \text{ set to 1 if shade is down, 0 if no shade is used}$$

$$\alpha_{\text{sh}} := 0.4 \quad \dots \text{ absorptance of shade} \quad \tau_{\text{sh}} := 0.05 \quad \dots \text{ transmittance of shade}$$

---

### GLAZING PROPERTIES:

This file can six different types of glazing chosen from ASHRAE. Only three types were used in parametric analysis (1,4,6)

- 1 = ID #5b (uncoated double-glazing)
- 2 = ID #21a
- 3 = ID #21d (low-e (e=0.1) double glazing)
- 4 = ID #25a (low e (e=0.05) double glazing)
- 5 = ID #40a
- 6 = ID #40d (low e (e=0.05) triple glazing)

$$\text{ID} := 1 \quad \dots \text{ selection of glazing type based on ID descriptions above.}$$

**Effective solar transmittance as a function of solar incidence angle:**

$$\tau_e(n, t) := \begin{cases} \frac{-0.2152 \left(\frac{\theta(n, t)}{\text{deg}}\right)^3 + 13.81 \left(\frac{\theta(n, t)}{\text{deg}}\right)^2 - 278.54 \frac{\theta(n, t)}{\text{deg}} + 61350}{100000} & \text{if ID} = 1 \\ \frac{-0.2206 \left(\frac{\theta(n, t)}{\text{deg}}\right)^3 + 15.152 \left(\frac{\theta(n, t)}{\text{deg}}\right)^2 - 315.26 \frac{\theta(n, t)}{\text{deg}} + 59408}{100000} & \text{if ID} = 2 \\ \frac{-0.1338 \left(\frac{\theta(n, t)}{\text{deg}}\right)^3 + 7.78624 \left(\frac{\theta(n, t)}{\text{deg}}\right)^2 - 151.47 \frac{\theta(n, t)}{\text{deg}} + 42118}{100000} & \text{if ID} = 3 \\ \frac{-0.1221 \left(\frac{\theta(n, t)}{\text{deg}}\right)^3 + 7.737 \left(\frac{\theta(n, t)}{\text{deg}}\right)^2 - 163.1 \frac{\theta(n, t)}{\text{deg}} + 37169}{100000} & \text{if ID} = 4 \\ \frac{-0.0867 \left(\frac{\theta(n, t)}{\text{deg}}\right)^3 + 4.675 \left(\frac{\theta(n, t)}{\text{deg}}\right)^2 - 122.02 \frac{\theta(n, t)}{\text{deg}} + 28987}{100000} & \text{if ID} = 5 \\ \frac{-0.0407 \left(\frac{\theta(n, t)}{\text{deg}}\right)^3 + 1.6892 \left(\frac{\theta(n, t)}{\text{deg}}\right)^2 - 36.026 \frac{\theta(n, t)}{\text{deg}} + 14981}{100000} & \text{if ID} = 6 \\ 0 & \text{otherwise} \end{cases} \quad \text{if } I_b(n, t) > 0 \frac{\text{W}}{\text{m}^2}$$

**Solar transmittance of first layer of glazing as a function of solar incidence angle:**

$$\tau(n, t) := \begin{cases} \frac{-0.2668 \left(\frac{\theta(n, t)}{\text{deg}}\right)^3 + 17.956 \left(\frac{\theta(n, t)}{\text{deg}}\right)^2 - 340.58 \frac{\theta(n, t)}{\text{deg}} + 72542}{100000} & \text{if ID} = 1 \\ \frac{-0.2442 \left(\frac{\theta(n, t)}{\text{deg}}\right)^3 + 17.103 \left(\frac{\theta(n, t)}{\text{deg}}\right)^2 - 331.26 \frac{\theta(n, t)}{\text{deg}} + 65519}{100000} & \text{if ID} = 2 \\ \frac{-0.227 \left(\frac{\theta(n, t)}{\text{deg}}\right)^3 + 16.165 \left(\frac{\theta(n, t)}{\text{deg}}\right)^2 - 300.8 \frac{\theta(n, t)}{\text{deg}} + 57552}{100000} & \text{if ID} = 3 \\ \frac{-0.151 \left(\frac{\theta(n, t)}{\text{deg}}\right)^3 + 10.871 \left(\frac{\theta(n, t)}{\text{deg}}\right)^2 - 255.34 \frac{\theta(n, t)}{\text{deg}} + 41328}{100000} & \text{if ID} = 4 \\ \frac{-0.151 \left(\frac{\theta(n, t)}{\text{deg}}\right)^3 + 9.5141 \left(\frac{\theta(n, t)}{\text{deg}}\right)^2 - 184.46 \frac{\theta(n, t)}{\text{deg}} + 45176}{100000} & \text{if ID} = 5 \\ \frac{-0.0995 \left(\frac{\theta(n, t)}{\text{deg}}\right)^3 + 6.4989 \left(\frac{\theta(n, t)}{\text{deg}}\right)^2 - 145.88 \frac{\theta(n, t)}{\text{deg}} + 33140}{100000} & \text{if ID} = 6 \\ 0 & \text{otherwise} \end{cases} \quad \text{if } I_b(n, t) > 0 \frac{\text{W}}{\text{m}^2}$$

## Diffuse transmittance and absorptance:

$$\tau_d := \begin{cases} 0.7 & \text{if ID} = 1 \\ 0.65 & \text{if ID} = 2 \\ 0.56 & \text{if ID} = 3 \\ 0.35 & \text{if ID} = 4 \\ 0.39 & \text{if ID} = 5 \\ 0.39 & \text{if ID} = 6 \end{cases} \quad \dots \text{diffuse transmittance} \\ \text{of first glazing layer}$$

$$\tau_{de} := \begin{cases} 0.51 & \text{if ID} = 1 \\ 0.5 & \text{if ID} = 2 \\ 0.35 & \text{if ID} = 3 \\ 0.31 & \text{if ID} = 4 \\ 0.23 & \text{if ID} = 5 \\ 0.23 & \text{if ID} = 6 \end{cases} \quad \dots \text{effective diffuse} \\ \text{transmittance}$$

$$\alpha_{di} := \begin{cases} 0.19 & \text{if ID} = 1 \\ 0.2 & \text{if ID} = 2 \\ 0.21 & \text{if ID} = 3 \\ 0.26 & \text{if ID} = 4 \\ 0.28 & \text{if ID} = 5 \\ 0.35 & \text{if ID} = 6 \end{cases} \quad \dots \text{diffuse absorptance} \\ \text{of inner glazing layer}$$

$$\alpha_{do} := \begin{cases} 0.11 & \text{if ID} = 1 \\ 0.27 & \text{if ID} = 2 \\ 0.16 & \text{if ID} = 3 \\ 0.04 & \text{if ID} = 4 \\ 0.08 & \text{if ID} = 5 \\ 0.03 & \text{if ID} = 6 \end{cases} \quad \dots \text{diffuse absorptance} \\ \text{of outer glazing layer}$$

$$\alpha_{dmid} := \begin{cases} 0 & \text{if ID} = 1 \\ 0 & \text{if ID} = 2 \\ 0 & \text{if ID} = 3 \\ 0 & \text{if ID} = 4 \\ 0.07 & \text{if ID} = 5 \\ 0.14 & \text{if ID} = 6 \end{cases} \quad \dots \text{diffuse absorptance} \\ \text{of middle glazing layer}$$

**Solar transmittance of outer glazing as a function of solar incidence angle:**

$$\alpha_o(n, t) := \begin{cases} \frac{-0.0013 \left(\frac{\theta(n, t)}{\text{deg}}\right)^4 + 0.1873 \left(\frac{\theta(n, t)}{\text{deg}}\right)^3 - 7.2357 \left(\frac{\theta(n, t)}{\text{deg}}\right)^2 + 101.12 \frac{\theta(n, t)}{\text{deg}} + 16949}{100000} & \text{if ID} = 1 \\ \frac{-0.0013 \left(\frac{\theta(n, t)}{\text{deg}}\right)^4 + 0.1602 \left(\frac{\theta(n, t)}{\text{deg}}\right)^3 - 5.9329 \left(\frac{\theta(n, t)}{\text{deg}}\right)^2 + 88.986 \frac{\theta(n, t)}{\text{deg}} + 19948}{100000} & \text{if ID} = 2 \\ \frac{-0.0013 \left(\frac{\theta(n, t)}{\text{deg}}\right)^4 + 0.1873 \left(\frac{\theta(n, t)}{\text{deg}}\right)^3 - 7.2357 \left(\frac{\theta(n, t)}{\text{deg}}\right)^2 + 101.12 \frac{\theta(n, t)}{\text{deg}} + 18949}{100000} & \text{if ID} = 3 \\ \frac{-0.0027 \left(\frac{\theta(n, t)}{\text{deg}}\right)^4 + 0.3629 \left(\frac{\theta(n, t)}{\text{deg}}\right)^3 - 14.836 \left(\frac{\theta(n, t)}{\text{deg}}\right)^2 + 221.83 \frac{\theta(n, t)}{\text{deg}} + 23841}{100000} & \text{if ID} = 4 \\ \frac{-0.0037 \left(\frac{\theta(n, t)}{\text{deg}}\right)^4 + 0.5178 \left(\frac{\theta(n, t)}{\text{deg}}\right)^3 - 20.764 \left(\frac{\theta(n, t)}{\text{deg}}\right)^2 + 281.7 \frac{\theta(n, t)}{\text{deg}} + 24809}{100000} & \text{if ID} = 5 \\ \frac{-0.0035 \left(\frac{\theta(n, t)}{\text{deg}}\right)^4 + 0.4481 \left(\frac{\theta(n, t)}{\text{deg}}\right)^3 - 17.392 \left(\frac{\theta(n, t)}{\text{deg}}\right)^2 + 242.39 \frac{\theta(n, t)}{\text{deg}} + 33841}{100000} & \text{if ID} = 6 \\ 0 & \text{otherwise} \end{cases}$$

**Solar transmittance of middle layer of glazing as a function of solar incidence angle:**

$$\alpha_{\text{mid}}(n, t) := \begin{cases} 0 & \text{if ID} = 1 \\ 0 & \text{if ID} = 2 \\ 0 & \text{if ID} = 3 \\ 0 & \text{if ID} = 4 \\ \frac{-0.0007 \left(\frac{\theta(n, t)}{\text{deg}}\right)^4 + 0.0607 \left(\frac{\theta(n, t)}{\text{deg}}\right)^3 - 1.6316 \left(\frac{\theta(n, t)}{\text{deg}}\right)^2 + 36.844 \frac{\theta(n, t)}{\text{deg}} + 7001.9}{100000} & \text{if ID} = 5 \\ \frac{-0.0007 \left(\frac{\theta(n, t)}{\text{deg}}\right)^4 + 0.057 \left(\frac{\theta(n, t)}{\text{deg}}\right)^3 - 1.3312 \left(\frac{\theta(n, t)}{\text{deg}}\right)^2 + 8.2881 \frac{\theta(n, t)}{\text{deg}} + 15002}{100000} & \text{if ID} = 6 \\ 0 & \text{otherwise} \end{cases}$$

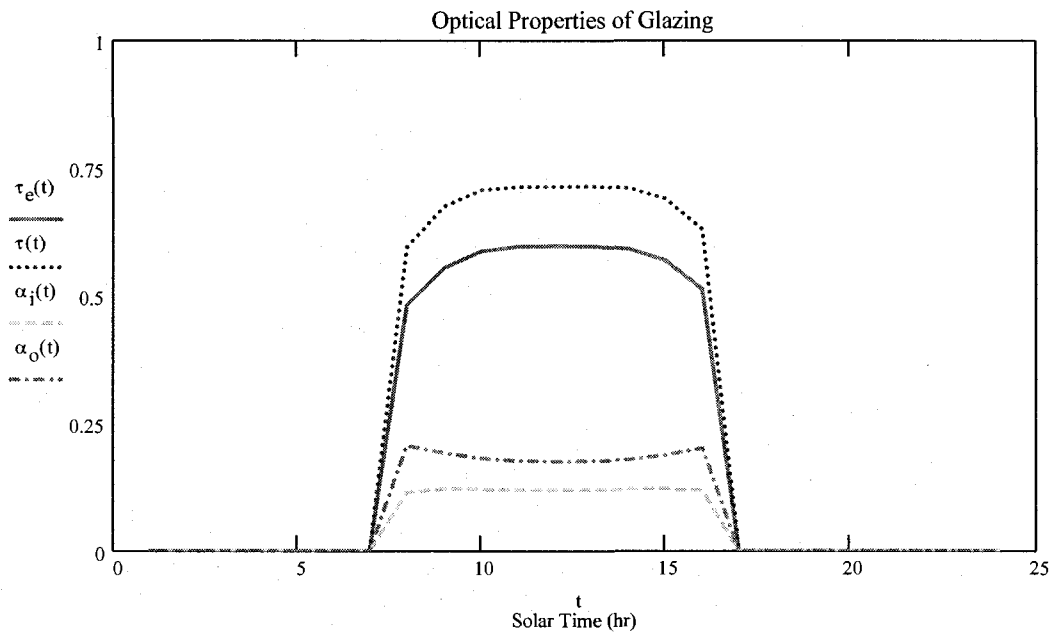
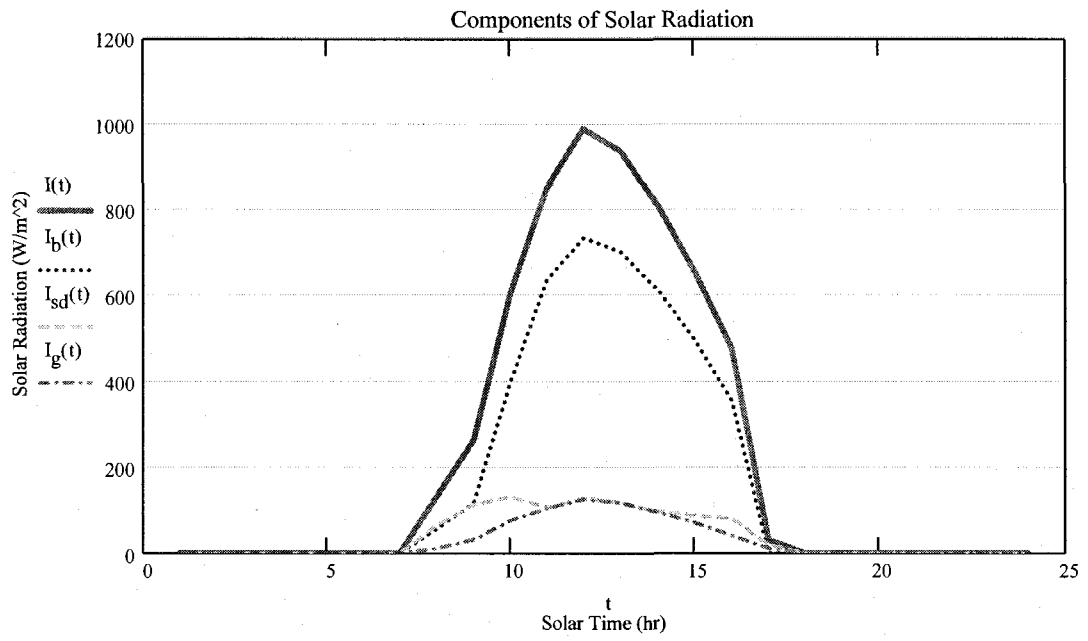
## Solar transmittance of inner layer of glazing as a function of solar incidence a

$$\alpha_i(n, t) := \begin{cases} \frac{-0.0007 \left(\frac{\theta(n, t)}{\text{deg}}\right)^4 + 0.0607 \left(\frac{\theta(n, t)}{\text{deg}}\right)^3 - 1.6316 \left(\frac{\theta(n, t)}{\text{deg}}\right)^2 + 36.844 \frac{\theta(n, t)}{\text{deg}} + 11002}{100000} & \text{if ID} = 1 \\ \frac{-0.0009 \left(\frac{\theta(n, t)}{\text{deg}}\right)^4 + 0.0983 \left(\frac{\theta(n, t)}{\text{deg}}\right)^3 - 2.796 \left(\frac{\theta(n, t)}{\text{deg}}\right)^2 + 18.218 \frac{\theta(n, t)}{\text{deg}} + 7013.3}{100000} & \text{if ID} = 2 \\ \frac{-0.0022 \left(\frac{\theta(n, t)}{\text{deg}}\right)^4 + 0.2739 \left(\frac{\theta(n, t)}{\text{deg}}\right)^3 - 10.396 \left(\frac{\theta(n, t)}{\text{deg}}\right)^2 + 138.93 \frac{\theta(n, t)}{\text{deg}} + 15905}{100000} & \text{if ID} = 3 \\ \frac{0.0002 \left(\frac{\theta(n, t)}{\text{deg}}\right)^4 - 0.0426 \left(\frac{\theta(n, t)}{\text{deg}}\right)^3 + 2.0696 \left(\frac{\theta(n, t)}{\text{deg}}\right)^2 - 27.171 \frac{\theta(n, t)}{\text{deg}} + 4031.9}{100000} & \text{if ID} = 4 \\ \frac{-0.00004 \left(\frac{\theta(n, t)}{\text{deg}}\right)^4 + 0.0103 \left(\frac{\theta(n, t)}{\text{deg}}\right)^3 - 0.762 \left(\frac{\theta(n, t)}{\text{deg}}\right)^2 + 14.074 \frac{\theta(n, t)}{\text{deg}} + 7013}{100000} & \text{if ID} = 5 \\ \frac{-0.0002 \left(\frac{\theta(n, t)}{\text{deg}}\right)^4 + 0.0142 \left(\frac{\theta(n, t)}{\text{deg}}\right)^3 - 0.162 \left(\frac{\theta(n, t)}{\text{deg}}\right)^2 + 2.2007 \frac{\theta(n, t)}{\text{deg}} + 3010.4}{100000} & \text{if ID} = 6 \\ 0 & \text{otherwise} \end{cases}$$

### Conversion of outdoor variables for the day of interest:

$$\begin{array}{llll} T_o(t) := T_o(n, t) & \gamma_s(t) := \gamma_s(n, t) & \alpha_o(t) := \alpha_o(n, t) & \alpha_i(t) := \alpha_i(n, t) \\ \alpha_{\text{mid}}(t) := \alpha_{\text{mid}}(n, t) & \alpha_s(t) := \alpha_s(n, t) & \rho(t) := \rho(n, t) & \tau(t) := \tau(n, t) \\ \tau_e(t) := \tau_e(n, t) & T_{\text{dp}}(t) := T_{\text{dp}}(n, t) & I_b(t) := I_b(n, t) & I_{\text{sd}}(t) := I_{\text{sd}}(n, t) \\ I_g(t) := I_g(n, t) & I_g(t) := I_g(t) \cdot \rho_g & I_d(t) := I_{\text{sd}}(t) + I_g(t) & I(t) := I_b(t) + I_d(t) \end{array}$$

$\rho_g := \text{if}(\text{season} = 1, 0.2, 0.7)$  ...ground reflectance depends on season



## THERMAL PROPERTIES OF GLAZING:

$L_{\text{cavity}} :=$	12.7mm if ID = 1	...width of cavity between panes	$\varepsilon_w :=$	0.9 if ID = 1	...emissivity of outside of inner pane
	12.7mm if ID = 2			0.1 if ID = 2	
	12.7mm if ID = 3			0.1 if ID = 3	
	12.7mm if ID = 4			0.05 if ID = 4	
	6.4mm if ID = 5			0.05 if ID = 5	
	6.4mm if ID = 6			0.05 if ID = 6	

$U_{\text{eg}} :=$	$3.36 \frac{W}{m^2 \text{degC}}$ if ID = 1	...edge-of-glass U-value.  Edge of glass effects assumed to extend over 65mm band around perimeter of each glazing unit
	$2.7 \frac{W}{m^2 \text{degC}}$ if ID = 2	
	$2.7 \frac{W}{m^2 \text{degC}}$ if ID = 3	
	$2.6 \frac{W}{m^2 \text{degC}}$ if ID = 4	
	$2.49 \frac{W}{m^2 \text{degC}}$ if ID = 5	
	$2.49 \frac{W}{m^2 \text{degC}}$ if ID = 6	

### Radiative coefficients:

$$F_{\varepsilon} := \frac{1}{\left(\frac{1}{0.9} + \frac{1}{0.9}\right) - 1} \quad F_{\varepsilon} = 0.818 \quad \text{...emissivity factor}$$

$$F_{\varepsilon \text{window}} := \frac{1}{\left(\frac{1}{\varepsilon_w} + \frac{1}{0.9}\right) - 1} \quad F_{\varepsilon \text{window}} = 0.818 \quad \text{...emissivity factor of window}$$

$$U_{\text{fr}} := 9.26 \frac{W}{m^2 \text{degC}} \quad \text{... window frame U-value for double-glazed curtain wall with aluminum frame with thermal break and insulated spacer (ASHRAE Fundamentals, 2005)}$$

$$U_o = \frac{U_{\text{cg}} \cdot A_{\text{cg}} + U_{\text{eg}} \cdot A_{\text{eg}} + U_{\text{fr}} \cdot A_{\text{fr}}}{A_{\text{win}}_{\text{south}}} \quad \text{...Total U-value for fenestration is weighted-average of center-of-glass, edge-of-glass, and frame}$$

$$A_{cg} := [W_{win} - 2 \cdot 2(65\text{mm})] \cdot [H_{win} - 2 \cdot 2(65\text{mm})] \quad A_{cg} = 5.115 \text{ m}^2$$

$$A_{eg} := [W_{win} - 2(65\text{mm})] \cdot [H_{win} - 2(65\text{mm})] - A_{cg} \quad A_{eg} = 0.625 \text{ m}^2$$

$$A_{fr} := (W_{win} \cdot H_{win}) - A_{cg} - A_{eg} \quad A_{fr} = 0.659 \text{ m}^2$$

$$W_{win} \cdot H_{win} = 6.4 \text{ m}^2$$

$$A_{cg} + A_{eg} + A_{fr} = 6.4 \text{ m}^2$$

### Convection within cavity:

$$P_{atm} := 1 \quad T_{win\_mean\_p} = \frac{T_{gout\_p} + T_{gin\_p}}{2} + 273 \quad \dots \text{mean temperature of inner and outer glazing} \quad a_{win\_p} = \frac{100 \cdot \text{degC}}{T_{win\_mean\_p}}$$

$$k_{win\_p} = \frac{0.002528 \cdot (T_{win\_mean\_p})^{1.5}}{T_{win\_mean\_p} + 200} \quad \text{watt} \quad \dots \text{thermal conductivity of air in window} \quad \text{m} \cdot \text{degC}$$

$$Ra_p = 2.737 \cdot (1 + 2 \cdot a_{win\_p})^2 \cdot (a_{win\_p})^4 \cdot (|T_{gout\_p} - T_{gin\_p}|) \cdot \left(\frac{L_{cavity}}{\text{mm}}\right)^3 \cdot P_{atm}^2 \quad \dots \text{Rayleigh number}$$

$$Nu1_p = 0.0605 \cdot (Ra_p)^{\frac{1}{3}} \quad Nu2_p = \left[ 1 + \frac{0.104 \cdot (Ra_p)^{0.293}}{\left[ 1 + \left(\frac{6310}{Ra_p}\right)^{1.36} \right]^3} \right]^{\frac{1}{3}} \quad \dots \text{Nusselt number}$$

$$h_{cglass\_p} = \frac{k_{air\_p}}{L_{cavity}} \cdot \text{if}(Nu1_p > Nu2_p, Nu1_p, Nu2_p) \quad \dots \text{convective heat transfer coefficient within glazing cavity}$$

### OTHER PARAMETERS:

$$\alpha_f := 0.8 \quad \dots \text{absorptance of floor} \quad h_{conv} := 3.5 \cdot \frac{W}{\text{m}^2 \cdot \text{degC}} \quad \dots \text{convective heat transfer coefficient between floor and basement}$$

$$\alpha_{ex} := 0.7 \quad \dots \text{absorptance of exterior wall} \quad \alpha_{walls} := 0.2 \quad \dots \text{interior walls absorptance}$$

$$R_{insglass} := 0.021 \cdot \text{m}^2 \cdot \frac{\text{degC}}{W} \quad \dots \text{insulated glazing unit}$$

### Temperature of adjacent rooms:

$$T_{adj}(t) := \text{if} \left[ \text{season} = 1, \left[ \begin{array}{l} (26\text{degC}) \text{ if } 1 \leq t \leq 6 \vee 22 \leq t \leq 24 \\ (24\text{degC}) \text{ otherwise} \end{array} \right], \left[ \begin{array}{l} (19\text{degC}) \text{ if } 1 \leq t \leq 6 \vee 22 \leq t \leq 24 \\ (23\text{degC}) \text{ otherwise} \end{array} \right] \right]$$

## Exterior Heat Transfer Coefficients

$$h_{co} = \sqrt{h_n^2 + [\alpha (V_o)^b]^2} \quad \dots \text{outdoor conv. h.t. coeff. for glass}$$

$\alpha$  and  $b$  are modifiers (2.5 and 0.75 on average, respectively).

$$V_o := \begin{cases} 24 & \text{if season} = 2 \\ 10 & \text{otherwise} \end{cases} \quad \dots \text{wind speed} \quad h_n = \frac{1.81^3 \cdot \sqrt{T_{go} - T_o}}{1.382} \quad \dots \text{Natural conv. coeff. for vertical surfaces}$$

The radiative coeff. is calculated from the sky and ground temp. and their respective view factors.

$$h_{ro} = 4 \cdot \sigma \cdot \epsilon_w \cdot T_m^3 \quad \text{where } T_m \text{ is the mean temp of the outer glazing and outdoors:} \quad T_m = \frac{T_o + T_{go}}{2} + 273$$

$$h_o = h_{co} + h_{ro} \quad \dots \text{combined convective and radiative exterior heat transfer coefficient}$$

Exterior heat transfer coeff. for outer glazing:

$$h_o = \sqrt{\left[ \left( \frac{1.81^3 \cdot \sqrt{T_{go} - T_o}}{1.382} \right)^2 + [2.5 \cdot (V_o)^{0.75}]^2 \right] \cdot \frac{W}{m^2 \cdot K} + 4 \cdot \sigma \cdot \epsilon_w \cdot \left[ \left( \frac{T_o + T_{go}}{2} + 273 \right) \cdot K \right]^3}$$

Exterior heat transfer coeff. for wall surface:

$$h_{ex} = \left( \frac{1.81^3 \cdot \sqrt{T_{ex} - T_o}}{1.382} \right) + 1.6 \sqrt{\left[ \left( \frac{1.81^3 \cdot \sqrt{T_{go} - T_o}}{1.382} \right)^2 + [2.5 \cdot (V_o)^{0.75}]^2 \right] \cdot \frac{W}{m^2 \cdot K} - \frac{1.81^3 \cdot \sqrt{T_{ex} - T_o}}{1.382}} \dots + 4 \cdot \sigma \cdot \epsilon_w \cdot \left[ \left( \frac{T_{ex} + T_o}{2} + 273 \right) \cdot K \right]^3$$

## Interior Heat Transfer Coefficients

For convection of interior surfaces, the following correlation is used:

$$h_{ci} = 1.31 \Delta T^{\frac{1}{3}} \quad \text{where } \Delta T \text{ is the temp diff. between the surface and air temp.}$$

For radiation of interior surfaces, the following correlation is used:

$$h_{12} = \frac{\sigma \cdot \left[ \left[ (T_1 + 273) K \right]^4 - \left[ (T_2 + 273) K \right]^4 \right] \cdot F_{\epsilon 12} \cdot F_{12} \cdot A_1}{|T_1 - T_2|} \quad \dots \text{radiation between interior surfaces}$$

## Infiltration Conductances:

### Between room air and outside:

$$\begin{aligned} V_{\text{rm}} &:= A_{\text{floor}} \cdot H_{\text{rm}} & V_{\text{rm}} &= 26.88 \text{ m}^3 & \text{...volume of room} & \text{ach}_{\text{ext}} &:= 0.01 & \text{...air changes per hour} \\ c_{\text{p,air}} &:= 1000 \frac{\text{joule}}{\text{kg} \cdot \text{degC}} & \rho_{\text{air}} &:= 1.2 \frac{\text{kg}}{\text{m}^3} \\ U_{\text{infex}} &:= \frac{\text{ach}_{\text{ext}} \cdot V_{\text{rm}}}{3600 \text{sec}} \cdot \rho_{\text{air}} \cdot c_{\text{p,air}} & U_{\text{infex}} &= 0.09 \frac{\text{W}}{\text{degC}} & R_{\text{infex}} &:= \frac{1}{U_{\text{infex}}} \end{aligned}$$

### Between room air and adjacent room:

$$\begin{aligned} v_{\text{room}} &:= 0.001 \frac{\text{m}}{\text{sec}} & \text{...velocity of air leaving section} \\ m_{\text{room}} &:= v_{\text{room}} \cdot 0.9 \text{m} \cdot 2.0 \text{m} & m_{\text{room}} &= 1.8 \times 10^{-3} \frac{\text{m}^3}{\text{s}} & \text{...mass flow rate of air leaving} \\ \text{ach}_{\text{adj}} &:= \frac{m_{\text{room}} \cdot 3600 \text{sec}}{V_{\text{rm}}} & \text{ach}_{\text{adj}} &= 0.241 & \text{...air changes per hour} \\ U_{\text{infadj}} &:= \frac{\text{ach}_{\text{adj}} \cdot V_{\text{rm}}}{3600 \text{sec}} \cdot \rho_{\text{air}} \cdot c_{\text{p,air}} & U_{\text{infadj}} &= 2.16 \frac{\text{W}}{\text{degC}} & R_{\text{infadj}} &:= \frac{1}{U_{\text{infadj}}} \end{aligned}$$

### Between air gap and room air:

$$\begin{aligned} V_{\text{airgap}} &:= H_{\text{win}} \cdot W_{\text{win}} \cdot 0.15 \text{m} & V_{\text{airgap}} &= 0.96 \text{ m}^3 \\ v_{\text{gap}} &:= 0.25 \frac{\text{m}}{\text{sec}} & m_{\text{gap}} &:= (0.03 \text{m} + 0.07 \text{m}) \cdot H_{\text{win}} \cdot v_{\text{gap}} & m_{\text{gap}} &= 0.05 \frac{\text{m}^3}{\text{s}} \\ \text{ach}_{\text{gaproom}} &:= \frac{m_{\text{gap}} \cdot 3600 \text{sec}}{V_{\text{airgap}}} & \text{ach}_{\text{gaproom}} &= 187.506 & \text{...air changes per hour} \\ U_{\text{infgaproom}} &:= \frac{\text{ach}_{\text{gaproom}} \cdot V_{\text{airgap}}}{3600 \text{sec}} \cdot \rho_{\text{air}} \cdot c_{\text{p,air}} & U_{\text{infgaproom}} &= 60 \frac{\text{W}}{\text{degC}} & R_{\text{infgaproom}} &:= \frac{1}{U_{\text{infgaproom}}} \end{aligned}$$

Between air gap and outside:

$$V_{\text{airgap}} := H_{\text{win}} \cdot W_{\text{win}} \cdot 0.15\text{m}$$

$$V_{\text{airgap}} = 0.96 \text{ m}^3$$

$$\text{ach}_{\text{gapext}} := 0.01 \quad \dots \text{air changes per hour}$$

$$U_{\text{infgapext}} := \frac{\text{ach}_{\text{gapext}} \cdot V_{\text{airgap}}}{3600\text{sec}} \cdot \rho_{\text{air}} \cdot c_{\text{p,air}}$$

$$U_{\text{infgapext}} = 3.2 \times 10^{-3} \frac{\text{W}}{\text{degC}}$$

$$R_{\text{infgapext}} := \frac{1}{U_{\text{infgapext}}}$$

## Thermal Properties of Building Materials

### Floor:

Concrete blocks:  $L_{\text{floor}} := 0.2\text{m}$   $k_{\text{floor}} := 1.7 \frac{\text{watt}}{\text{m} \cdot \text{degC}}$

$$\rho_{\text{floor}} := 2200 \frac{\text{kg}}{\text{m}^3} \quad c_{\text{floor}} := 1400 \frac{\text{joule}}{\text{kg} \cdot \text{degC}}$$

$$R_{\text{floor}} := \frac{L_{\text{floor}}}{k_{\text{floor}} \cdot A_{\text{floor}}} \quad R_{\text{floor}} = 0.012 \frac{\text{degC}}{\text{W}}$$

Insulation:  $R_{\text{insf}} := 0.5 \frac{\text{m}^2 \text{degC}}{\text{watt}}$   $R_{\text{insf}} := \frac{R_{\text{insf}}}{A_{\text{floor}}}$   $R_{\text{insf}} = 0.052 \frac{\text{degC}}{\text{watt}}$

$$C_{\text{floor}} := c_{\text{floor}} \cdot \rho_{\text{floor}} \cdot A_{\text{floor}} \cdot L_{\text{floor}} \quad C_{\text{floor}} = 5.914 \times 10^6 \text{ J} \quad \dots \text{thermal capacitance of floor}$$

### Exterior (south) wall:

Brick:  $L_{\text{ex}} := 0.1 \cdot \text{m}$   $\rho_{\text{ex}} := 1800 \frac{\text{kg}}{\text{m}^3}$   $c_{\text{ex}} := 1004.8 \frac{\text{joule}}{\text{kg} \cdot \text{degC}}$   $k_{\text{ex}} := 1.3 \frac{\text{watt}}{\text{m} \cdot \text{degC}}$

$$R_{\text{ex}} := \frac{L_{\text{ex}}}{k_{\text{ex}} \cdot A_{\text{south}}} \quad R_{\text{ex}} = 0.03 \frac{\text{degC}}{\text{W}}$$

Insulation:  $R_{\text{insex}} := 3 \cdot \frac{\text{m}^2}{\text{degC} \cdot \text{W}}$   $R_{\text{insex}} := \frac{R_{\text{insex}}}{A_{\text{south}}}$

$$C_{\text{ex}} := c_{\text{ex}} \cdot \rho_{\text{ex}} \cdot A_{\text{south}} \cdot L_{\text{ex}} \quad C_{\text{ex}} = 4.63 \times 10^5 \text{ J} \quad \dots \text{thermal capacitance of exterior wall}$$

### East/west/north walls:

Gypsum board:  $L_{\text{east}} := 0.02 \cdot \text{m}$      $\rho_{\text{east}} := 800 \cdot \frac{\text{kg}}{\text{m}^3}$      $k_{\text{east}} := 0.16 \cdot \frac{\text{watt}}{\text{m} \cdot \text{degC}}$      $c_{\text{east}} := 750 \cdot \frac{\text{joule}}{\text{kg} \cdot \text{degC}}$

$$L_{\text{west}} := L_{\text{east}} \quad \rho_{\text{west}} := \rho_{\text{east}} \quad k_{\text{west}} := k_{\text{east}} \quad c_{\text{west}} := c_{\text{east}}$$

$$L_{\text{north}} := L_{\text{east}} \quad \rho_{\text{north}} := \rho_{\text{east}} \quad k_{\text{north}} := k_{\text{east}} \quad c_{\text{north}} := c_{\text{east}}$$

If considered as one:  $A_{\text{wall}} := A_{\text{north}} + A_{\text{west}} + A_{\text{east}}$      $A_{\text{wall}} = 25.76 \text{ m}^2$

$$L_{\text{wall}} := L_{\text{east}} + L_{\text{west}} + L_{\text{north}}$$

$$R_{\text{wall}} := \frac{L_{\text{wall}}}{k_{\text{east}} \cdot A_{\text{wall}}} \quad R_{\text{wall}} = 0.015 \frac{\text{degC}}{\text{W}}$$

Insulation:  $R_{\text{inswall}} := 2 \cdot \frac{\text{m}^2}{\text{degC} \cdot \text{W}}$      $R_{\text{inswall}} := \frac{R_{\text{inswall}}}{A_{\text{wall}}}$

$$C_{\text{wall}} := c_{\text{east}} \cdot \rho_{\text{east}} \cdot A_{\text{wall}} \cdot L_{\text{wall}} \quad C_{\text{wall}} = 9.274 \times 10^5 \text{ J}$$

### Ceiling:

Gypsum board:  $L_{\text{ceil}} := 0.02 \cdot \text{m}$      $\rho_{\text{ceil}} := 800 \cdot \frac{\text{kg}}{\text{m}^3}$      $k_{\text{ceil}} := 0.16 \cdot \frac{\text{watt}}{\text{m} \cdot \text{degC}}$      $c_{\text{ceil}} := 750 \cdot \frac{\text{joule}}{\text{kg} \cdot \text{degC}}$

$$R_{\text{ceil}} := \frac{L_{\text{ceil}}}{k_{\text{ceil}} \cdot A_{\text{floor}}} \quad R_{\text{ceil}} = 0.012 \frac{\text{degC}}{\text{W}}$$

Concrete blocks:  $L_{\text{ceil}} := 0.2 \text{ m}$      $k_{\text{ceil}} := 1.7 \cdot \frac{\text{watt}}{\text{m} \cdot \text{degC}}$      $\rho_{\text{ceil}} := 2200 \cdot \frac{\text{kg}}{\text{m}^3}$      $c_{\text{ceil}} := 1400 \cdot \frac{\text{joule}}{\text{kg} \cdot \text{degC}}$

$$R_{\text{ceil}} := \frac{L_{\text{ceil}}}{k_{\text{ceil}} \cdot A_{\text{floor}}} \quad R_{\text{ceil}} = 0.012 \frac{\text{degC}}{\text{W}}$$

Insulation:  $R_{\text{insceil}} := 2 \cdot \frac{\text{m}^2}{\text{degC} \cdot \text{W}}$      $R_{\text{insceil}} := \frac{R_{\text{insceil}}}{A_{\text{wall}}}$

$$C_{\text{ceil}} := c_{\text{ceil}} \cdot \rho_{\text{ceil}} \cdot A_{\text{floor}} \cdot L_{\text{ceil}} \quad C_{\text{ceil}} = 5.914 \times 10^6 \text{ J}$$

## Air:

$$k_{\text{air}} := 0.0257 \frac{\text{watt}}{\text{m} \cdot \text{degC}}$$

$$c_{\text{air}} := 1005 \frac{\text{joule}}{\text{kg} \cdot \text{degC}}$$

$$\rho_{\text{air}} := 1.22 \frac{\text{kg}}{\text{m}^3}$$

$$C_{\text{air}} := c_{\text{air}} \cdot \rho_{\text{air}} \cdot (A_{\text{floor}} \cdot H_{\text{rm}})$$

$$C_{\text{air}} = 3.296 \times 10^4 \text{ J}$$

Since the room also contains furniture and other objects that can act as thermal mass, using the properties of air only is inadequate. Therefore, an estimate is made as to how the furniture can be lumped with the air capacitance to make an "equivalent air capacitance" based on the ratio of furniture thermal capacitance (using wood as the material) to room air thermal capacitance:

$$c_{\text{wood}} := 1700 \frac{\text{joule}}{\text{kg} \cdot \text{K}}$$

$$\rho_{\text{wood}} := 400 \frac{\text{kg}}{\text{m}^3}$$

$$\text{Vol} := 2.5\text{m} \cdot 1\text{m} \cdot 0.75\text{m} = 1.875 \text{ m}^3$$

$$C_{\text{wood}} := c_{\text{wood}} \cdot \rho_{\text{wood}} \cdot (\text{Vol})$$

$$C_{\text{wood}} = 1.275 \times 10^6 \text{ J}$$

$$\frac{C_{\text{wood}}}{C_{\text{air}}} = 38.686$$

...therefore, the equivalent room air capacitance should be a factor of about 40 greater than air capacitance alone.

$$C_{\text{air}} := C_{\text{air}} \cdot 40$$

$$C_{\text{air}} = 1.318 \times 10^6 \text{ J}$$

---

## View Factors:

$$F_{\text{sh}_g} := 1$$

$$F_{\text{sky}} := 0.5$$

### Between floor and other surfaces:

$$F_{\text{floor\_ceiling}} := F_{7,4}$$

$$F_{\text{floor\_ceiling}} = 0.227$$

$$F_{\text{floor\_win}} := F_{7,2}$$

$$F_{\text{floor\_win}} = 0.116$$

$$F_{\text{floor\_south}} := F_{7,3}$$

$$F_{\text{floor\_south}} = 0.084$$

$$F_{\text{floor\_walls}} := 1 - F_{\text{floor\_south}} - F_{\text{floor\_win}} - F_{\text{floor\_ceiling}}$$

$$F_{\text{floor\_walls}} = 0.573$$

### Between exterior (south) wall and other surfaces:

$$F_{\text{south\_floor}} := \frac{A_{\text{floor}}}{A_{\text{south}}} \cdot F_{\text{floor\_south}}$$

$$F_{\text{south\_floor}} = 0.314$$

$$F_{\text{south\_ceiling}} := F_{3,4}$$

$$F_{\text{south\_ceiling}} = 0.183$$

$$F_{\text{south\_walls}} := 1 - F_{\text{south\_ceiling}} - F_{\text{south\_floor}}$$

$$F_{\text{south\_walls}} = 0.504$$

Between window (or shade) and other surfaces:

$$F_{\text{win\_floor}} := \frac{A_{\text{floor}}}{A_{\text{win\_south}}} \cdot F_{\text{floor\_win}}$$

$$F_{\text{win\_floor}} = 0.174$$

$$F_{\text{win\_ceiling}} := F_{2,4}$$

$$F_{\text{win\_ceiling}} = 0.226$$

$$F_{\text{win\_walls}} := 1 - F_{\text{win\_ceiling}} - F_{\text{win\_floor}}$$

$$F_{\text{win\_walls}} = 0.6$$

Between ceiling and other surfaces:

$$F_{\text{ceiling\_win}} := \frac{A_{\text{win\_south}}}{A_{\text{floor}}} \cdot F_{\text{win\_ceiling}}$$

$$F_{\text{ceiling\_win}} = 0.151$$

$$F_{\text{ceiling\_floor}} := F_{\text{floor\_ceiling}}$$

$$F_{\text{ceiling\_floor}} = 0.227$$

$$F_{\text{ceiling\_south}} := \frac{A_{\text{south}}}{A_{\text{floor}}} \cdot F_{\text{south\_ceiling}}$$

$$F_{\text{ceiling\_south}} = 0.049$$

$$F_{\text{ceiling\_walls}} := 1 - F_{\text{ceiling\_win}} - F_{\text{ceiling\_floor}} - F_{\text{ceiling\_south}}$$

$$F_{\text{ceiling\_walls}} = 0.573$$

Between walls and other surfaces:

$$F_{\text{walls\_win}} := \frac{A_{\text{win\_south}}}{A_{\text{wall}}} \cdot F_{\text{win\_walls}}$$

$$F_{\text{walls\_win}} = 0.149$$

$$F_{\text{walls\_south}} := \frac{A_{\text{south}}}{A_{\text{wall}}} \cdot F_{\text{south\_walls}}$$

$$F_{\text{walls\_south}} = 0.05$$

$$F_{\text{walls\_floor}} := \frac{A_{\text{floor}}}{A_{\text{wall}}} \cdot F_{\text{floor\_walls}}$$

$$F_{\text{walls\_floor}} = 0.214$$

$$F_{\text{walls\_ceiling}} := 1 - F_{\text{walls\_win}} - F_{\text{walls\_south}} - F_{\text{walls\_floor}}$$

$$F_{\text{walls\_ceiling}} = 0.587$$

**Selection of Simulation Time Step:**

$$TS := \left( \frac{C_{\text{floor}}}{\frac{1}{\frac{R_{\text{floor}}}{2}} + \frac{1}{R_{\text{insf}}} + \frac{1}{\frac{R_{\text{floor}}}{2}} + h_{\text{conv}} \cdot A_{\text{floor}}} \quad \frac{C_{\text{ceil}}}{\frac{1}{\frac{R_{\text{ceil}}}{2}} + \frac{1}{R_{\text{insceil}}} + \frac{1}{\frac{R_{\text{ceil}}}{2}} + h_{\text{conv}} \cdot A_{\text{ceiling}}} \quad \frac{C_{\text{ex}}}{\frac{1}{\frac{R_{\text{ex}}}{2}} + \frac{1}{R_{\text{insex}}}} \right)^{-1}$$

$\Delta t := \min(TS)$

$dt := 300 \cdot \text{sec} \quad \dots \text{simulation timestep}$

$n_{\text{days}} := 7 \text{ day} \quad \dots \text{number of days to run simulation}$

$\frac{n_{\text{days}}}{dt} = 2.016 \times 10^3$

$p := 1, 2, \dots, \frac{n_{\text{days}}}{dt} \quad \dots \text{number of timesteps}$

**Transformation from hourly simulation to selected time-step:**

**Fourier transform:**

$nn := 1, 2, \dots, 7$

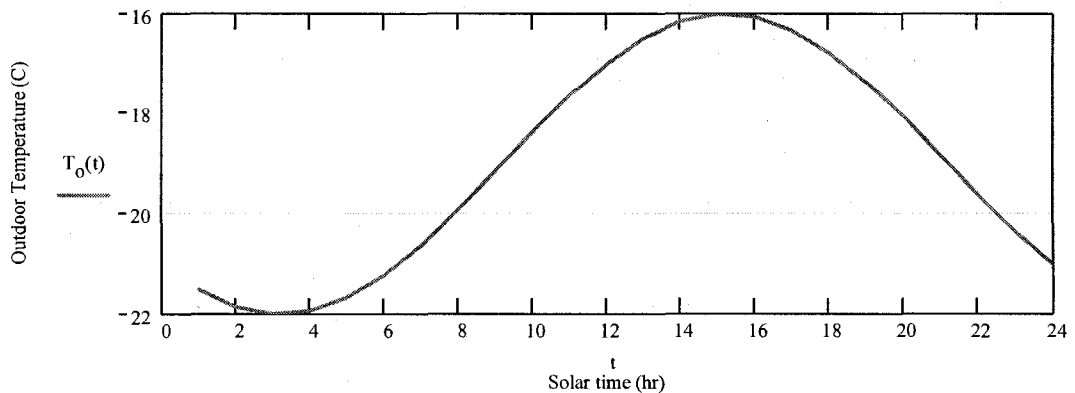
$j := \sqrt{-1}$

$\omega_{nn} := \frac{2 \cdot \pi \cdot (nn - 1)}{24 \cdot \text{hr}}$

$\omega\omega := 2.0 \cdot \frac{\pi}{24}$

$$T_o(t) := \begin{cases} -17 - 2 \cdot \cos\left(\omega\omega \cdot t + 5.2 \cdot \frac{\pi}{3}\right) \cdot \text{degC} & \text{if season} = 2 \wedge \text{sky} = 2 \\ -19 - 3 \cdot \cos\left(\omega\omega \cdot t + 5.2 \cdot \frac{\pi}{3}\right) \cdot \text{degC} & \text{if season} = 2 \wedge \text{sky} = 1 \\ 28 - 3 \cdot \cos\left(\omega\omega \cdot t + 5.2 \cdot \frac{\pi}{3}\right) \cdot \text{degC} & \text{if season} = 1 \wedge \text{sky} = 1 \\ 24 - 2 \cdot \cos\left(\omega\omega \cdot t + 5.2 \cdot \frac{\pi}{3}\right) \cdot \text{degC} & \text{if season} = 1 \wedge \text{sky} = 2 \end{cases}$$

$\dots$ outdoor temperature for representative days



$$\text{TT}_{o_{nn}} := \sum_t T_o(t) \cdot \frac{\exp(-j \cdot \omega_{nn} \cdot t \cdot \text{hr})}{24}$$

$$\text{TT}_{dp_{nn}} := \sum_t T_{dp}(t) \cdot \frac{\exp(-j \cdot \omega_{nn} \cdot t \cdot \text{hr})}{24}$$

$$\text{II}_{nn} := \sum_t I(t) \cdot \frac{\exp(-j \cdot \omega_{nn} \cdot t \cdot \text{hr})}{24}$$

$$\text{II}_{b_{nn}} := \sum_t I_b(t) \cdot \frac{\exp(-j \cdot \omega_{nn} \cdot t \cdot \text{hr})}{24}$$

$$\text{II}_{d_{nn}} := \sum_t I_d(t) \cdot \frac{\exp(-j \cdot \omega_{nn} \cdot t \cdot \text{hr})}{24}$$

$$\tau\tau_{nn} := \sum_t \tau(t) \cdot \frac{\exp(-j \cdot \omega_{nn} \cdot t \cdot \text{hr})}{24}$$

$$\alpha\alpha_{i_{nn}} := \sum_t \alpha_i(t) \cdot \frac{\exp(-j \cdot \omega_{nn} \cdot t \cdot \text{hr})}{24}$$

$$\tau\tau_{e_{nn}} := \sum_t \tau_e(t) \cdot \frac{\exp(-j \cdot \omega_{nn} \cdot t \cdot \text{hr})}{24}$$

$$\alpha\alpha_{o_{nn}} := \sum_t \alpha_o(t) \cdot \frac{\exp(-j \cdot \omega_{nn} \cdot t \cdot \text{hr})}{24}$$

$$\tau\tau_{nn} := \sum_t \tau(t) \cdot \frac{\exp(-j \cdot \omega_{nn} \cdot t \cdot \text{hr})}{24}$$

$$\gamma\gamma_{s_{nn}} := \sum_t \gamma_s(t) \cdot \frac{\exp(-j \cdot \omega_{nn} \cdot t \cdot \text{hr})}{24}$$

$$\alpha\alpha_{s_{nn}} := \sum_t \alpha_s(t) \cdot \frac{\exp(-j \cdot \omega_{nn} \cdot t \cdot \text{hr})}{24}$$

$$\text{TT}_{adj_{nn}} := \sum_t T_{adj}(t) \cdot \frac{\exp(-j \cdot \omega_{nn} \cdot t \cdot \text{hr})}{24}$$

$$\alpha\alpha_{mid_{nn}} := \sum_t \alpha_{mid}(t) \cdot \frac{\exp(-j \cdot \omega_{nn} \cdot t \cdot \text{hr})}{24}$$

$t_p := p \cdot dt$  ...times at which simulation will be performed

### Generation of data for each time step (back in time domain):

$nl := 2, 3.. 7$

$$T_{o_p} := \text{TT}_{o_1} + 2 \left( \sum_{nl} \text{Re} \left( \text{TT}_{o_{nl}} \cdot \exp(j \cdot \omega_{nl} \cdot t_p) \right) \right)$$

$$I_{b_p} := \text{if} \left[ \text{II}_{b_1} + 2 \cdot \left( \sum_{nl} \text{Re} \left( \text{II}_{b_{nl}} \cdot \exp(j \cdot \omega_{nl} \cdot t_p) \right) \right) > 0 \cdot \frac{W}{m^2}, \text{II}_{b_1} + 2 \cdot \left( \sum_{nl} \text{Re} \left( \text{II}_{b_{nl}} \cdot \exp(j \cdot \omega_{nl} \cdot t_p) \right) \right), 0 \cdot \frac{W}{m^2} \right]$$

$$I_{d_p} := \text{if} \left[ \text{II}_{d_1} + 2 \cdot \left( \sum_{nl} \text{Re} \left( \text{II}_{d_{nl}} \cdot \exp(j \cdot \omega_{nl} \cdot t_p) \right) \right) > 0 \cdot \frac{W}{m^2}, \text{II}_{d_1} + 2 \cdot \left( \sum_{nl} \text{Re} \left( \text{II}_{d_{nl}} \cdot \exp(j \cdot \omega_{nl} \cdot t_p) \right) \right), 0 \cdot \frac{W}{m^2} \right]$$

$$I_p := \text{if} \left[ \text{II}_1 + 2 \cdot \left( \sum_{nl} \text{Re} \left( \text{II}_{nl} \cdot \exp(j \cdot \omega_{nl} \cdot t_p) \right) \right) > 0 \cdot \frac{W}{m^2}, \text{II}_1 + 2 \cdot \left( \sum_{nl} \text{Re} \left( \text{II}_{nl} \cdot \exp(j \cdot \omega_{nl} \cdot t_p) \right) \right), 0 \cdot \frac{W}{m^2} \right]$$

$$\alpha_{o_p} := \text{if} \left[ \alpha\alpha_{o_1} + 2 \cdot \left( \sum_{nl} \text{Re}(\alpha\alpha_{o_{nl}} \cdot \exp(j \cdot \omega_{nl} \cdot t_p)) \right) > 0, \alpha\alpha_{o_1} + 2 \cdot \left( \sum_{nl} \text{Re}(\alpha\alpha_{o_{nl}} \cdot \exp(j \cdot \omega_{nl} \cdot t_p)) \right), 0 \right]$$

$$\alpha_{i_p} := \text{if} \left[ \alpha\alpha_{i_1} + 2 \cdot \left( \sum_{nl} \text{Re}(\alpha\alpha_{i_{nl}} \cdot \exp(j \cdot \omega_{nl} \cdot t_p)) \right) > 0, \alpha\alpha_{i_1} + 2 \cdot \left( \sum_{nl} \text{Re}(\alpha\alpha_{i_{nl}} \cdot \exp(j \cdot \omega_{nl} \cdot t_p)) \right), 0 \right]$$

$$\alpha_{mid_p} := \text{if} \left[ \alpha\alpha_{mid_1} + 2 \cdot \left( \sum_{nl} \text{Re}(\alpha\alpha_{mid_{nl}} \cdot \exp(j \cdot \omega_{nl} \cdot t_p)) \right) > 0, \alpha\alpha_{mid_1} + 2 \cdot \left( \sum_{nl} \text{Re}(\alpha\alpha_{mid_{nl}} \cdot \exp(j \cdot \omega_{nl} \cdot t_p)) \right), 0 \right]$$

$$\tau_{e_p} := \text{if} \left[ \tau\tau_{e_1} + 2 \cdot \left( \sum_{nl} \text{Re}(\tau\tau_{e_{nl}} \cdot \exp(j \cdot \omega_{nl} \cdot t_p)) \right) > 0, \tau\tau_{e_1} + 2 \cdot \left( \sum_{nl} \text{Re}(\tau\tau_{e_{nl}} \cdot \exp(j \cdot \omega_{nl} \cdot t_p)) \right), 0 \right]$$

$$\tau_p := \text{if} \left[ \tau\tau_1 + 2 \cdot \left( \sum_{nl} \text{Re}(\tau\tau_{nl} \cdot \exp(j \cdot \omega_{nl} \cdot t_p)) \right) > 0, \tau\tau_1 + 2 \cdot \left( \sum_{nl} \text{Re}(\tau\tau_{nl} \cdot \exp(j \cdot \omega_{nl} \cdot t_p)) \right), 0 \right]$$

$$\gamma_{s_p} := \gamma\gamma_{s_1} + 2 \cdot \left( \sum_{nl} \text{Re}(\gamma\gamma_{s_{nl}} \cdot \exp(j \cdot \omega_{nl} \cdot t_p)) \right)$$

$$\alpha_{s_p} := \text{if} \left[ \alpha\alpha_{s_1} + 2 \cdot \left( \sum_{nl} \text{Re}(\alpha\alpha_{s_{nl}} \cdot \exp(j \cdot \omega_{nl} \cdot t_p)) \right) > 0, \alpha\alpha_{s_1} + 2 \cdot \left( \sum_{nl} \text{Re}(\alpha\alpha_{s_{nl}} \cdot \exp(j \cdot \omega_{nl} \cdot t_p)) \right), 0 \right]$$

$$T_{adj_p} := TT_{adj_1} + 2 \cdot \left( \sum_{nl} \text{Re}(TT_{adj_{nl}} \cdot \exp(j \cdot \omega_{nl} \cdot t_p)) \right)$$

$$T_{dp_p} := TT_{dp_1} + 2 \cdot \left( \sum_{nl} \text{Re}(TT_{dp_{nl}} \cdot \exp(j \cdot \omega_{nl} \cdot t_p)) \right)$$

$$T_{sky_p} := (T_{o_p}) \cdot \left( 0.8 + \frac{T_{dp_p}}{250} \right)^{\frac{1}{4}}$$

---

### **Internal gains:**

$Q_{int_p} := \text{if}(8 \cdot 3600\text{sec} \leq \text{mod}(p \cdot dt, 24 \cdot 3600\text{sec}) \leq 20 \cdot 3600\text{sec}, 167\text{W}, 0\text{W})$  ...internal gains from equipment (100 W) and person (67 W) during occupied hours

---

### **CONTROLS:**

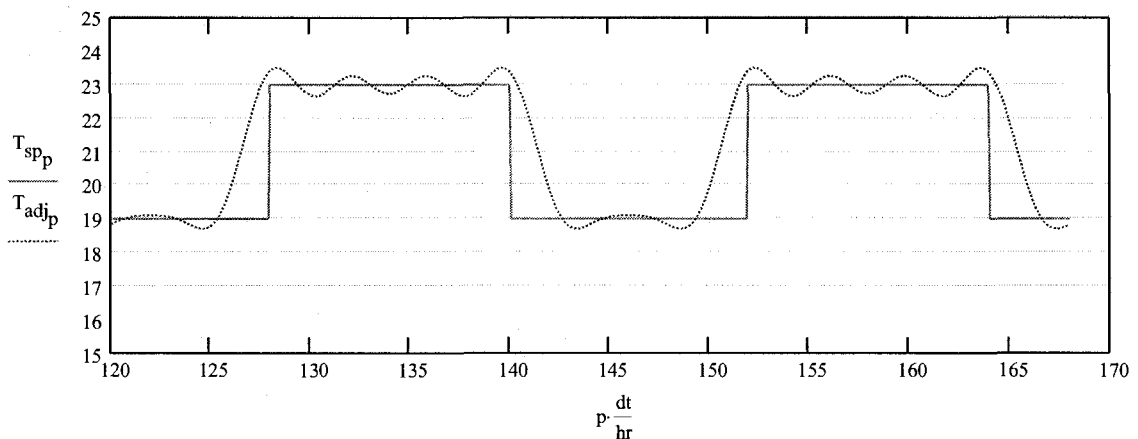
Set-point temperatures vary between summer and winter and between night and day.  
 Conditioning of the air is modeled with proportional-integral (PI) control.

$$T_{sp_p} := \text{if} \left( \text{season} = 1, \begin{cases} 24\text{degC} & \text{if } 8 \cdot 3600\text{sec} \leq \text{mod}(p \cdot dt, 24 \cdot 3600\text{sec}) \leq 20 \cdot 3600\text{sec} \\ 26\text{degC} & \text{otherwise} \end{cases}, \begin{cases} 23\text{degC} & \text{if } 8 \cdot 3600\text{sec} \leq \text{mod}(p \cdot dt, 24 \cdot 3600\text{sec}) \leq 20 \cdot 3600\text{sec} \\ 19\text{degC} & \text{otherwise} \end{cases} \right)$$

$$K_p := \begin{cases} (600\text{W}) & \text{if } \text{season} = 1 \\ (500\text{W}) & \text{if } \text{season} = 2 \end{cases} \quad \dots \text{proportional control constant} \quad K_I := 0.03 \frac{\text{W}}{\text{sec}} \quad \dots \text{integral control}$$

$$\text{startt} := \frac{n_{\text{days}} - 1 \text{day}}{dt} \quad \text{startt} = 1.728 \times 10^3 \quad \text{endt} := \frac{n_{\text{days}}}{dt} \quad \text{endt} = 2.016 \times 10^3$$

$$\text{offset} := 0\text{degC}$$

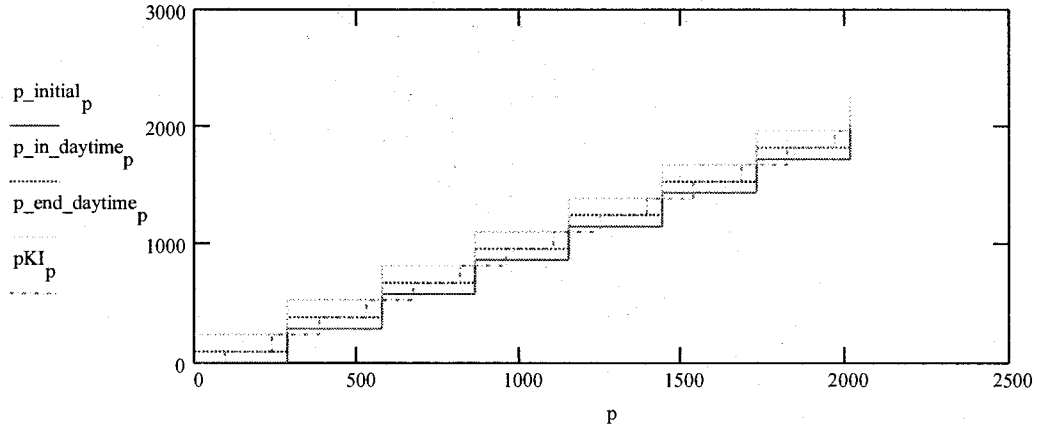


When using PI control, control of the air conditioning is based on an integration of the deviation of actual air temperatures at previous time steps from the desired set-point temperature. Integral control is based on deviations of air temperature from set-point temperatures at previous time-steps. Since the set-point temperature changes from day to night, the PI control must only take into account deviations of previous values of air temperature from the set-point (not necessarily at the present time-step). For this reason, the time-step "counter" must be "reset" at each change of set-point temperature. The following lines outline the modeling needed in order to take this into account:

$$\text{ppday} := \frac{24\text{hr}}{dt} \quad p_{\text{initial}_p} := \text{floor} \left( \frac{p}{\text{ppday}} \right) \cdot \text{ppday}$$

$$p_{\text{in\_daytime}_p} := p_{\text{initial}_p} + 8 \frac{\text{hr}}{dt} \quad p_{\text{end\_daytime}_p} := p_{\text{initial}_p} + 20 \frac{\text{hr}}{dt}$$

$$pKI_p := \begin{cases} 1 & \text{if } p < 8 \frac{\text{hr}}{dt} \\ p_{\text{in\_daytime}_p} & \text{if } 8 \cdot 3600\text{sec} \leq \text{mod}(p \cdot dt, 24 \cdot 3600\text{sec}) \leq 20 \cdot 3600\text{sec} \\ \text{otherwise} & \begin{cases} p_{\text{end\_daytime}_p} & \text{if } \text{mod}(p \cdot dt, 24 \cdot 3600\text{sec}) > 20 \cdot \text{hr} \\ (p_{\text{end\_daytime}_p} - \text{ppday}) & \text{if } \text{mod}(p \cdot dt, 24 \cdot 3600\text{sec}) < 8\text{hr} \end{cases} \end{cases}$$



$$p\_initial \leftarrow \text{floor}\left(\frac{p}{ppday}\right) \cdot ppday$$

$$p\_in\_daytime \leftarrow p\_initial + 8 \frac{\text{hr}}{\text{dt}}$$

$$p\_end\_daytime \leftarrow p\_initial + 20 \frac{\text{hr}}{\text{dt}}$$

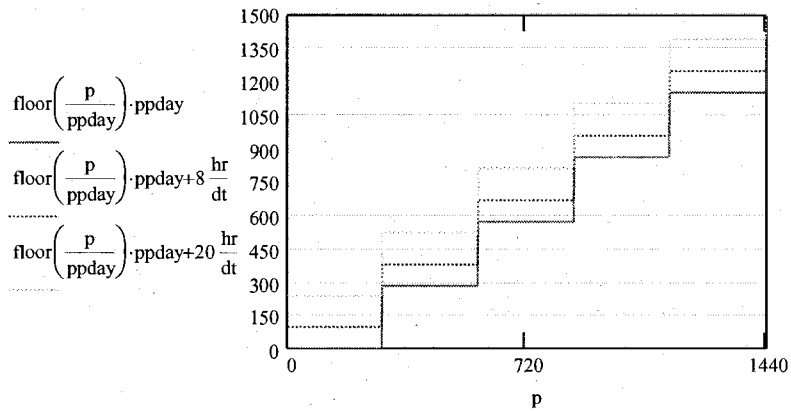
$$pKI \leftarrow p\_in\_daytime \text{ if } 8 \cdot 3600 \text{sec} \leq \text{mod}(p \cdot \text{dt}, 24 \cdot 3600 \text{sec}) \leq 20 \cdot 3600 \cdot \text{sec}$$

$$pKI \leftarrow p\_end\_daytime \text{ otherwise}$$

$$K_p \cdot (T_{sp_p} - T_{R_p} + \text{offset}) + K_I \cdot \sum_{p=1}^p (T_{sp_p} - T_{R_p}) dt \text{ if } T_{sp_p} - T_{R_p} < -1 \cdot \text{degC}$$

$$K_p \cdot (T_{sp_p} - T_{R_p} + \text{offset}) + K_I \cdot \sum_{p=1}^p (T_{sp_p} - T_{R_p}) dt \text{ if } T_{sp_p} - T_{R_p} > 1 \cdot \text{degC}$$

$$(0 \cdot \text{watt}) \text{ otherwise}$$



## INITIAL CONDITIONS:

Node temperatures:

$T_{\text{floormass}_1}$	
$T_{\text{floorin}_1}$	
$T_{\text{wallsmass}_1}$	
$T_{\text{wallsin}_1}$	24.1
$T_{\text{exmass}_1}$	21
$T_{\text{exin}_1}$	22
$T_{\text{exout}_1}$	23
$T_{\text{ceilingmass}_1}$	24
$T_{\text{ceilingin}_1}$	25
$T_{\text{gin}_1}$	26.5
$T_{\text{gout}_1}$	22.1
$T_{\text{sh}_1}$	22.5
$T_{\text{gap}_1}$	29
$T_{\text{R}_1}$	10
$T_{\text{gmid}_1}$	20.2
$T_{\text{sp}_1}$	20.1
	22.7
	12
	18

:= · degC

## CONVECTIVE AND RADIATIVE COEFFICIENTS- initial values

Exterior heat transfer coefficient for window surface:

$$h_{og_1} := \left[ \sqrt{\left[ \frac{1.81 \cdot \sqrt[3]{|T_{o_1} - (T_{gout})_1|}}{1.382} \right]^2 + (2.5 \cdot V_o^{0.75})^2} \cdot \frac{W}{m^2 \cdot K} + 4 \cdot \epsilon_w \cdot \sigma \cdot \left[ \left( \frac{T_{gout}_1 + T_{o_1}}{2} + 273 \right) \cdot K \right]^3 \right] \cdot \frac{K}{degC}$$

$$h_{og_1} = 31.325 \frac{1}{m^2} \frac{W}{degC}$$

Exterior heat transfer coefficient for wall surface:

$$h_{oex_1} := \left[ \frac{1.81 \cdot \sqrt[3]{|T_{o_1} - T_{exout_1}|}}{1.382} + 1.6 \cdot \sqrt[2]{\left[ \left( \frac{1.81 \cdot \sqrt[3]{|T_{o_1} - T_{exout_1}|}}{1.382} \right)^2 + (2.5 \cdot V_o^{0.75}) \right]} - \frac{1.81 \cdot \sqrt[3]{|T_{o_1} - T_{exout_1}|}}{1.382} \right] \cdot \frac{W}{m^2 \cdot K} + 4 \cdot \epsilon_w \cdot \sigma \cdot \left[ \left( \frac{T_{o_1} + T_{exout_1}}{2} + 273 \right) \cdot K \right]^3$$

**Radiation coefficients:**

$$h_{rg_1} := \frac{\sigma \cdot \left[ \left[ (T_{gin_1} + 273) K \right]^4 - \left[ (T_{gout_1} + 273) K \right]^4 \right] \cdot F_{\epsilon window}}{|T_{gin_1} - T_{gout_1}|}$$

$$h_{rgmid1_1} := \frac{\sigma \cdot \left[ \left[ (T_{gin_1} + 273) K \right]^4 - \left[ (T_{gmid_1} + 273) K \right]^4 \right] \cdot F_{\epsilon window}}{|T_{gin_1} - T_{gmid_1}|}$$

$$h_{rgmid2_1} := \frac{\sigma \cdot \left[ \left[ (T_{gout_1} + 273) K \right]^4 - \left[ (T_{gmid_1} + 273) K \right]^4 \right] \cdot F_{\epsilon window}}{|T_{gout_1} - T_{gmid_1}|}$$

$$h_{sh_g_1} := \frac{\sigma \cdot \left[ \left[ (T_{sh_1} + 273) K \right]^4 - \left[ (T_{gin_1} + 273) K \right]^4 \right] \cdot F_{\epsilon} \cdot F_{sh_g}}{|T_{sh_1} - T_{gin_1}|}$$

... between shade and glazing

$$h_{sh_floor_1} := \frac{\sigma \cdot \left[ \left[ (T_{sh_1} + 273) K \right]^4 - \left[ (T_{floorin_1} + 273) K \right]^4 \right] \cdot F_{\epsilon} \cdot F_{win\_floor}}{|T_{sh_1} - T_{floorin_1}|}$$

...between shade and floor

$$h_{sh\_ceiling_1} := \frac{\sigma \cdot \left[ \left[ (T_{sh_1} + 273) K \right]^4 - \left[ (T_{ceilingin_1} + 273) K \right]^4 \right] \cdot F_{\epsilon} \cdot F_{win\_ceiling}}{|T_{sh_1} - T_{ceilingin_1}|}$$

...between shade and ceiling

$$h_{sh\_walls_1} := \frac{\sigma \cdot \left[ \left[ (T_{sh_1} + 273) K \right]^4 - \left[ (T_{wallsin_1} + 273) K \right]^4 \right] \cdot F_{\epsilon} \cdot F_{win\_walls}}{|T_{sh_1} - T_{wallsin_1}|}$$

...between shade and walls

$$h_{g\_floor_1} := \frac{\sigma \cdot \left[ \left[ (T_{gin_1} + 273) K \right]^4 - \left[ (T_{floorin_1} + 273) K \right]^4 \right] \cdot F_{\epsilon} \cdot F_{win\_floor}}{|T_{gin_1} - T_{floorin_1}|}$$

...between glazing and floor

$$h_{g\_ceiling_1} := \frac{\sigma \cdot \left[ \left[ (T_{gin_1} + 273) K \right]^4 - \left[ (T_{ceilingin_1} + 273) K \right]^4 \right] \cdot F_{\epsilon} \cdot F_{win\_ceiling}}{|T_{gin_1} - T_{ceilingin_1}|} \quad \dots \text{between glazing and ceiling}$$

$$h_{g\_walls_1} := \frac{\sigma \cdot \left[ \left[ (T_{gin_1} + 273) K \right]^4 - \left[ (T_{wallsin_1} + 273) K \right]^4 \right] \cdot F_{\epsilon} \cdot F_{win\_walls}}{|T_{gin_1} - T_{wallsin_1}|} \quad \dots \text{between glazing and walls}$$

$$h_{floor\_ex_1} := \frac{\sigma \cdot \left[ \left[ (T_{floorin_1} + 273) K \right]^4 - \left[ (T_{exin_1} + 273) K \right]^4 \right] \cdot F_{\epsilon} \cdot F_{floor\_south}}{|T_{floorin_1} - T_{exin_1}|} \quad \dots \text{between floor and south wall}$$

$$h_{floor\_walls_1} := \frac{\sigma \cdot \left[ \left[ (T_{floorin_1} + 273) K \right]^4 - \left[ (T_{wallsin_1} + 273) K \right]^4 \right] \cdot F_{\epsilon} \cdot F_{floor\_walls}}{|T_{floorin_1} - T_{wallsin_1}|} \quad \dots \text{between floor and walls}$$

$$h_{floor\_ceiling_1} := \frac{\sigma \cdot \left[ \left[ (T_{floorin_1} + 273) K \right]^4 - \left[ (T_{ceilingin_1} + 273) K \right]^4 \right] \cdot F_{\epsilon} \cdot F_{floor\_south}}{|T_{floorin_1} - T_{ceilingin_1}|} \quad \dots \text{between floor and ceiling}$$

$$h_{ceiling\_ex_1} := \frac{\sigma \cdot \left[ \left[ (T_{ceilingin_1} + 273) K \right]^4 - \left[ (T_{exin_1} + 273) K \right]^4 \right] \cdot F_{\epsilon} \cdot F_{ceiling\_south}}{|T_{ceilingin_1} - T_{exin_1}|} \quad \dots \text{between ceiling and south wall}$$

$$h_{ceiling\_walls_1} := \frac{\sigma \cdot \left[ \left[ (T_{ceilingin_1} + 273) K \right]^4 - \left[ (T_{wallsin_1} + 273) K \right]^4 \right] \cdot F_{\epsilon} \cdot F_{ceiling\_walls}}{|T_{ceilingin_1} - T_{wallsin_1}|} \quad \dots \text{between ceiling and west wall}$$

$$h_{ex\_walls_1} := \frac{\sigma \cdot \left[ \left[ (T_{exin_1} + 273) K \right]^4 - \left[ (T_{wallsin_1} + 273) K \right]^4 \right] \cdot F_{\epsilon} \cdot F_{south\_walls}}{|T_{exin_1} - T_{wallsin_1}|} \quad \dots \text{south wall to walls}$$

### Convection coefficients:

$$h_{cglass_1} := 2.5 \frac{\text{watt}}{\text{m}^2 \text{degC}}$$

$$h_{cglass\_mid1_1} := 2.5 \frac{\text{watt}}{\text{m}^2 \text{degC}}$$

$$h_{cglass\_mid2_1} := 2.5 \frac{\text{watt}}{\text{m}^2 \text{degC}}$$

$$Nu1_1 := 1.18$$

$$Nu1\_mid1_1 := 1.18$$

$$Nu1\_mid2_1 := 1.18$$

$$Nu2_1 := 1.1$$

$$Nu2\_mid1_1 := 1.1$$

$$Nu2\_mid2_1 := 1.1$$

$$k_{win_1} := 0.0235 \frac{\text{watt}}{\text{m} \cdot \text{degC}}$$

$$k_{win\_mid1_1} := 0.0235 \frac{\text{watt}}{\text{m} \cdot \text{degC}}$$

$$k_{win\_mid2_1} := 0.0235 \frac{\text{watt}}{\text{m} \cdot \text{degC}}$$

$$Ra_1 := 7500$$

$$Ra_{mid1_1} := 7500$$

$$Ra_{mid2_1} := 7500$$

$$a_{win_1} := 0.1$$

$$a_{win_{mid1_1}} := 0.1$$

$$a_{win_{mid2_1}} := 0.1$$

$$T_{g\_mean\_p} := 10\text{degC}$$

$$U_{cg_1} := 1.8 \frac{W}{m^2 \text{degC}}$$

$$U_{o_1} := 2.5 \frac{\text{watt}}{m^2 \text{degC}}$$

$$h_{cfloor_1} := \left[ 1.31 \cdot \left( |T_{R_1} - T_{floorin_1}| \right)^{\frac{1}{3}} \cdot \frac{W \cdot \text{degC}^{\frac{-4}{3}}}{m^2} \right] \quad \dots \text{ room air to floor}$$

$$h_{cwalls_1} := \left[ 1.31 \cdot \left( |T_{R_1} - T_{wallsin_1}| \right)^{\frac{1}{3}} \cdot \frac{W \cdot \text{degC}^{\frac{-4}{3}}}{m^2} \right] \quad \dots \text{ room air to walls}$$

$$h_{cex_1} := \left[ 1.31 \cdot \left( |T_{R_1} - T_{exin_1}| \right)^{\frac{1}{3}} \cdot \frac{W \cdot \text{degC}^{\frac{-4}{3}}}{m^2} \right] \quad \dots \text{ room air to south exterior wall}$$

$$h_{cg_1} := \left[ 1.31 \cdot \left( |T_{R_1} - T_{gin_1}| \right)^{\frac{1}{3}} \cdot \frac{W \cdot \text{degC}^{\frac{-4}{3}}}{m^2} \right] \quad \dots \text{ room air to glass}$$

$$h_{csh_1} := \left[ 1.31 \cdot \left( |T_{R_1} - T_{sh_1}| \right)^{\frac{1}{3}} \cdot \frac{W \cdot \text{degC}^{\frac{-4}{3}}}{m^2} \right] \quad \dots \text{ room air to shade}$$

$$h_{gapsh_1} := \left[ 1.31 \cdot \left( |T_{gap_1} - T_{sh_1}| \right)^{\frac{1}{3}} \cdot \frac{W \cdot \text{degC}^{\frac{-4}{3}}}{m^2} \right] \quad \dots \text{ air gap to shade}$$

$$h_{cceiling_1} := \left[ 1.31 \cdot \left( |T_{R_1} - T_{ceilingin_1}| \right)^{\frac{1}{3}} \cdot \frac{W \cdot \text{degC}^{\frac{-4}{3}}}{m^2} \right] \quad \dots \text{ room air to ceiling}$$

$$h_{gapg_1} := \left[ 1.31 \cdot \left( |T_{gap_1} - T_{gin_1}| \right)^{\frac{1}{3}} \cdot \frac{W \cdot \text{degC}^{\frac{-4}{3}}}{m^2} \right] \quad \dots \text{ air gap to glass}$$

**FINITE DIFFERENCE MODEL (SYSTEM OF EQUATIONS) MATRIX:**

$$\left[ \frac{1.81 \cdot \sqrt[3]{T_o - T_{exout}_p}}{1.382} + 1.6 \cdot \sqrt{\left[ \frac{1.81 \cdot \sqrt[3]{T_o - T_{exout}_p}}{1.382} \right]^2 + (2.5 \cdot V_o)^2} - \frac{W}{m^2 \cdot K} + 4 \cdot \epsilon_w \cdot \sigma \cdot \left[ \left( \frac{T_{gout}_p + T_{sky}_p}{2} + 273 \right) \cdot K \right]^3 \right] \cdot \frac{K}{degC}$$

$$\left[ \frac{1.81 \cdot \sqrt[3]{T_o - T_{exout}_p}}{1.382} \right]^2 + \frac{1.81 \cdot \sqrt[3]{T_o - T_{exout}_p}}{1.382} \cdot \frac{W}{m^2 \cdot K} + 4 \cdot \epsilon_w \cdot \sigma \cdot \left[ \left( \frac{T_{sky}_p + T_{exout}_p}{2} + 273 \right) \cdot K \right]^3 \right] \cdot \frac{K}{degC}$$

$$\sigma \cdot \left[ \frac{\left[ (T_{gin}_p + 273) \cdot K \right]^4 - \left[ (T_{gout}_p + 273) \cdot K \right]^4 \right]}{\left[ T_{gin}_p - T_{gout}_p \right]} \cdot F_{swindow}$$

$$\sigma \cdot \left[ \frac{\left[ (T_{gin}_1 + 273) \cdot K \right]^4 - \left[ (T_{gmid}_1 + 273) \cdot K \right]^4 \right]}{\left[ T_{gin}_1 - T_{gmid}_1 \right]} \cdot F_{swindow}$$

$$\sigma \cdot \left[ \frac{\left[ (T_{gout}_1 + 273) \cdot K \right]^4 - \left[ (T_{gmid}_1 + 273) \cdot K \right]^4 \right]}{\left[ T_{gout}_1 - T_{gmid}_1 \right]} \cdot F_{swindow}$$

$$\sigma \cdot \left[ \frac{\left[ (T_{sh}_p + 273) \cdot K \right]^4 - \left[ (T_{gin}_p + 273) \cdot K \right]^4 \right]}{\left[ T_{sh}_p - T_{gin}_p \right]} \cdot F_{\epsilon} \cdot F_{sh_g}$$

$$\sigma \cdot \left[ \frac{\left[ (T_{sh}_p + 273) \cdot K \right]^4 - \left[ (T_{floorin}_p + 273) \cdot K \right]^4 \right]}{\left[ T_{sh}_p - T_{floorin}_p \right]} \cdot F_{\epsilon} \cdot F_{win\_floor}$$

$$\sigma \cdot \left[ \frac{\left[ (T_{sh}_p + 273) \cdot K \right]^4 - \left[ (T_{ceilingin}_p + 273) \cdot K \right]^4 \right]}{\left[ T_{sh}_p - T_{ceilingin}_p \right]} \cdot F_{\epsilon} \cdot F_{win\_ceiling}$$

$$\sigma \cdot \left[ \left[ \left[ \left( T_{sh_p} + 273 \right) \cdot K \right]^4 - \left[ \left( T_{wallsin_p} + 273 \right) \cdot K \right]^4 \right] \cdot F_{\varepsilon} \cdot F_{win\_walls} \right] - \frac{T_{sh_p} - T_{wallsin_p}}{\left[ \left[ \left( T_{gin_p} + 273 \right) \cdot K \right]^4 - \left[ \left( T_{floorin_p} + 273 \right) \cdot K \right]^4 \right] \cdot F_{\varepsilon} \cdot F_{win\_floor}}$$

$$\sigma \cdot \left[ \left[ \left[ \left( T_{gin_p} + 273 \right) \cdot K \right]^4 - \left[ \left( T_{ceilingin_p} + 273 \right) \cdot K \right]^4 \right] \cdot F_{\varepsilon} \cdot F_{win\_ceiling} \right] - \frac{T_{gin_p} - T_{ceilingin_p}}{\left[ \left[ \left( T_{gin_p} + 273 \right) \cdot K \right]^4 - \left[ \left( T_{wallsin_p} + 273 \right) \cdot K \right]^4 \right] \cdot F_{\varepsilon} \cdot F_{win\_walls}}$$

$$\sigma \cdot \left[ \left[ \left[ \left( T_{floorin_p} + 273 \right) \cdot K \right]^4 - \left[ \left( T_{exin_p} + 273 \right) \cdot K \right]^4 \right] \cdot F_{\varepsilon} \cdot F_{floor\_south} \right] - \frac{T_{floorin_p} - T_{exin_p}}{\left[ \left[ \left( T_{floorin_p} + 273 \right) \cdot K \right]^4 - \left[ \left( T_{wallsin_p} + 273 \right) \cdot K \right]^4 \right] \cdot F_{\varepsilon} \cdot F_{floor\_walls}}$$

$$\sigma \cdot \left[ \left[ \left[ \left( T_{floorin_p} + 273 \right) \cdot K \right]^4 - \left[ \left( T_{ceilingin_p} + 273 \right) \cdot K \right]^4 \right] \cdot F_{\varepsilon} \cdot F_{floor\_south} \right] - \frac{T_{floorin_p} - T_{ceilingin_p}}{\left[ \left[ \left( T_{ceilingin_p} + 273 \right) \cdot K \right]^4 - \left[ \left( T_{exin_p} + 273 \right) \cdot K \right]^4 \right] \cdot F_{\varepsilon} \cdot F_{ceiling\_south}}$$

$$\sigma \cdot \left[ \left[ \left[ \left( T_{ceilingin_p} + 273 \right) \cdot K \right]^4 - \left[ \left( T_{exin_p} + 273 \right) \cdot K \right]^4 \right] \cdot F_{\varepsilon} \cdot F_{ceiling\_south} \right] - \frac{T_{ceilingin_p} - T_{exin_p}}{\left[ \left[ \left( T_{ceilingin_p} + 273 \right) \cdot K \right]^4 - \left[ \left( T_{exin_p} + 273 \right) \cdot K \right]^4 \right] \cdot F_{\varepsilon} \cdot F_{ceiling\_south}}$$

$$\sigma \cdot \left[ \left[ \left[ \left( T_{\text{ceiling}_p} + 273 \right) \cdot K \right]^4 - \left[ \left( T_{\text{wallsin}_p} + 273 \right) \cdot K \right]^4 \right] \cdot F_{\varepsilon} \cdot F_{\text{ceiling\_walls}} \right]$$

$$\frac{\left[ T_{\text{ceiling}_p} - T_{\text{wallsin}_p} \right]}{\left[ \left( T_{\text{ceiling}_p} + 273 \right) \cdot K \right]^4 - \left[ \left( T_{\text{wallsin}_p} + 273 \right) \cdot K \right]^4} \cdot F_{\varepsilon} \cdot F_{\text{ceiling\_walls}}$$

$$\sigma \cdot \left[ \left[ \left[ \left( T_{\text{exin}_p} + 273 \right) \cdot K \right]^4 - \left[ \left( T_{\text{wallsin}_p} + 273 \right) \cdot K \right]^4 \right] \cdot F_{\varepsilon} \cdot F_{\text{south\_walls}} \right]$$

$$\frac{\left[ T_{\text{exin}_p} - T_{\text{wallsin}_p} \right]}{\left[ \left( T_{\text{exin}_p} + 273 \right) \cdot K \right]^4 - \left[ \left( T_{\text{wallsin}_p} + 273 \right) \cdot K \right]^4} \cdot F_{\varepsilon} \cdot F_{\text{south\_walls}}$$

$$1.31 \cdot \left( \left( T_{R_p} - T_{\text{floorin}_p} \right) \right)^{\frac{-4}{3}} \cdot \frac{1}{3} \cdot \frac{W \cdot \text{degC}}{\text{m}^2}$$

$$1.31 \cdot \left( \left( T_{R_p} - T_{\text{wallsin}_p} \right) \right)^{\frac{-4}{3}} \cdot \frac{1}{3} \cdot \frac{W \cdot \text{degC}}{\text{m}^2}$$

$$1.31 \cdot \left( \left( T_{R_p} - T_{\text{exin}_p} \right) \right)^{\frac{-4}{3}} \cdot \frac{1}{3} \cdot \frac{W \cdot \text{degC}}{\text{m}^2}$$

$$1.31 \cdot \left( \left( T_{R_p} - T_{\text{ceiling}_p} \right) \right)^{\frac{-4}{3}} \cdot \frac{1}{3} \cdot \frac{W \cdot \text{degC}}{\text{m}^2}$$

$$1.31 \cdot \left( \left( T_{R_p} - T_{\text{gin}_p} \right) \right)^{\frac{-4}{3}} \cdot \frac{1}{3} \cdot \frac{W \cdot \text{degC}}{\text{m}^2}$$

$$1.31 \cdot \left( \left( T_{R_p} - T_{\text{sh}_p} \right) \right)^{\frac{-4}{3}} \cdot \frac{1}{3} \cdot \frac{W \cdot \text{degC}}{\text{m}^2}$$

$$1.31 \cdot \left( \left( T_{\text{gap}_p} - T_{\text{sh}_p} \right) \right)^{\frac{-4}{3}} \cdot \frac{1}{3} \cdot \frac{W \cdot \text{degC}}{\text{m}^2}$$

$$1.31: \left( T_{gap,p} - T_{g,in,p} \right)^{-4} \frac{1}{3} \frac{W \cdot degC}{m^2}$$

$$\frac{k_{win,p}}{L_{cavity}} \cdot \text{if}(Nu1_p > Nu2_p, Nu1_p, Nu2_p)$$

$$\frac{k_{win\_mid1}}{L_{cavity}} \cdot \text{if}(Nu1\_mid1_p > Nu2\_mid1_p, Nu1\_mid1_p, Nu2\_mid1_p)$$

$$\frac{k_{win\_mid2}}{L_{cavity}} \cdot \text{if}(Nu1\_mid2_p > Nu2\_mid2_p, Nu1\_mid2_p, Nu2\_mid2_p)$$

$$\left( \frac{1}{\frac{1}{h_{og,p}} + \frac{1}{h_{eglass\_mid2,p} + h_{rgmid2,p}} + \frac{1}{h_{eglass\_mid1,p} + h_{rgmid1,p}} + \frac{1}{h_{cg,p} + h_{g\_floor,p} + h_{g\_ceiling,p} + h_{g\_walls,p}}} \right) \cdot \text{if shade} = 0$$

$$\left( \frac{1}{\frac{1}{h_{og,p}} + \frac{1}{h_{rg,p} + h_{eglass\_mid2,p} + h_{rgmid2,p}} + \frac{1}{h_{eglass\_mid1,p} + h_{rgmid1,p}} + \frac{1}{h_{gap,p} + h_{sh\_g,p}}} \right) \cdot \text{if shade} = 1$$

$$\left( \frac{1}{\frac{1}{h_{og,p}} + \frac{1}{h_{eglass\_p} + h_{rg,p}} + \frac{1}{h_{cg,p} + h_{g\_floor,p} + h_{g\_ceiling,p} + h_{g\_walls,p}}} \right) \cdot \text{if shade} = 0$$

$$\left( \frac{1}{\frac{1}{h_{og,p}} + \frac{1}{h_{rg,p} + h_{eglass\_p} + h_{rgmid,p}} + \frac{1}{h_{gap,p} + h_{sh\_g,p}}} \right) \cdot \text{if shade} = 1$$

$$\left( \frac{1}{\frac{1}{h_{og,p+1}} + \frac{1}{h_{ogex\_p+1}} + \frac{1}{h_{rg\_p+1}} + \frac{1}{h_{rgmid\_p+1}}} \right) \cdot \text{otherwise}$$

if ID = 5 ∨ ID = 6

$h_{og,p+1}$   
 $h_{ogex\_p+1}$   
 $h_{rg\_p+1}$   
 $h_{rgmid\_p+1}$

$h_{rgmid2_{p+1}}$	$\frac{U_{cg} \cdot A_{cg} + U_{eg} \cdot A_{eg} + U_{fr} \cdot A_{fr}}{A_{win\_south}}$
$h_{sh\_g_{p+1}}$	$\frac{1}{3}$
$h_{sh\_floor_{p+1}}$	$0.0605 \cdot (Ra_p)^{\frac{1}{3}}$
$h_{sh\_ceiling_{p+1}}$	$0.0605 \cdot (Ra_{mid1_p})^{\frac{1}{3}}$
$h_{sh\_walls_{p+1}}$	$0.0605 \cdot (Ra_{mid2_p})^{\frac{1}{3}}$
$h_{g\_floor_{p+1}}$	$\frac{1}{3} \left[ \frac{0.104 \cdot (Ra_p)^{0.293}}{1 + \left( \frac{6310}{Ra_p} \right)^{1.36}} \right]^{\frac{1}{3}}$
$h_{g\_ceiling_{p+1}}$	$\frac{1}{3} \left[ \frac{0.104 \cdot (Ra_{mid1_p})^{0.293}}{1 + \left( \frac{6310}{Ra_{mid1_p}} \right)^{1.36}} \right]^{\frac{1}{3}}$
$h_{g\_walls_{p+1}}$	$\frac{1}{3} \left[ \frac{0.104 \cdot (Ra_{mid2_p})^{0.293}}{1 + \left( \frac{6310}{Ra_{mid2_p}} \right)^{1.36}} \right]^{\frac{1}{3}}$
$h_{floor\_ex_{p+1}}$	$\frac{T_{gout_p} + T_{gout_p} + 273}{2}$
$h_{floor\_walls_{p+1}}$	$\frac{100 \cdot degC}{2}$
$h_{floor\_ceiling_{p+1}}$	$\frac{100 \cdot degC}{2}$
$h_{ceiling\_ex_{p+1}}$	$\frac{100 \cdot degC}{2}$
$h_{ceiling\_walls_{p+1}}$	$\frac{100 \cdot degC}{2}$
$h_{ex\_walls_{p+1}}$	$\frac{100 \cdot degC}{2}$
$h_{cfloor_{p+1}}$	$\frac{100 \cdot degC}{2}$
$h_{cwalls_{p+1}}$	$\frac{100 \cdot degC}{2}$
$h_{cex_{p+1}}$	$\frac{100 \cdot degC}{2}$

$h_{\text{ceiling}_{p+1}}$	$\frac{100 \cdot \text{degC}}{\left( \frac{T_{\text{gin}_p} + T_{\text{gmid}_p}}{2} + 273 \right)}$
$h_{\text{cg}_{p+1}}$	$\frac{100 \cdot \text{degC}}{\left( \frac{T_{\text{gout}_p} + T_{\text{gmid}_p}}{2} + 273 \right)}$
$h_{\text{csh}_{p+1}}$	$0.002528 \cdot \left( \frac{T_{\text{gin}_p} + T_{\text{gout}_p}}{2} + 273 \right)^{1.5}$
$h_{\text{gapsh}_{p+1}}$	$\frac{\text{watt}}{\text{m-degC}}$
$h_{\text{glass}_{p+1}}$	$\frac{T_{\text{gin}_p} + T_{\text{gout}_p}}{2} + 273 + 200$
$h_{\text{cglass\_mid1}_{p+1}}$	$\frac{\text{watt}}{\text{m-degC}}$
$h_{\text{cglass\_mid2}_{p+1}}$	$0.002528 \cdot \left( \frac{T_{\text{gin}_p} + T_{\text{gmid}_p}}{2} + 273 \right)^{1.5}$
$U_{\text{cg}_{p+1}}$	$\frac{\text{watt}}{\text{m-degC}}$
$U_{\text{o}_{p+1}}$	$\frac{T_{\text{gin}_p} + T_{\text{gmid}_p}}{2} + 273 + 200$
$\text{Nu1}_{p+1}$	$\frac{\text{watt}}{\text{m-degC}}$
$\text{Nu1\_mid1}_{p+1}$	$\frac{\text{watt}}{\text{m-degC}}$
$\text{Nu1\_mid2}_{p+1}$	$0.002528 \cdot \left( \frac{T_{\text{gout}_p} + T_{\text{gmid}_p}}{2} + 273 \right)^{1.5}$
$\text{Nu2}_{p+1}$	$\frac{\text{watt}}{\text{m-degC}}$
$\text{Nu2\_mid1}_{p+1}$	$\frac{\text{watt}}{\text{m-degC}}$
$\text{Nu2\_mid2}_{p+1}$	$\frac{\text{watt}}{\text{m-degC}}$
$a_{\text{win}_{p+1}}$	$2.737 \cdot (1 + 2 \cdot a_{\text{win}_p})^2 \cdot (a_{\text{win}_p})^4 \cdot ( T_{\text{gout}_p} - T_{\text{gin}_p} ) \cdot \left( \frac{L_{\text{cavity}}}{\text{mm}} \right)^3 \cdot P_{\text{atm}}^2$
$a_{\text{win\_mid1}_{p+1}}$	

$a_{win\_mid2\_p-1}$	$2.737 \left(1 + 2 \cdot a_{win\_mid1\_p}\right)^2 \left(a_{win\_mid1\_p}\right)^4 \left(T_{gmid\_p} - T_{gin\_p}\right) \left(\frac{L_{cavity}}{num}\right)^3 \cdot P_{atm}^2$
$k_{win\_p-1}$	
$k_{win\_mid1\_p-1}$	$2.737 \left(1 + 2 \cdot a_{win\_mid2\_p}\right)^2 \left(a_{win\_mid2\_p}\right)^4 \left(T_{gou\_p} - T_{gmid\_p}\right) \left(\frac{L_{cavity}}{num}\right)^3 \cdot P_{atm}^2$
$k_{win\_mid2\_p-1}$	
$Ra_{p-1}$	$\frac{dt}{C_{floor}} \left( \frac{T_{adj\_p} - T_{floormass\_p}}{1 + \frac{R_{floor}}{h_{conv} \cdot A_{floor}}} + \frac{T_{floorin\_p} - T_{floormass\_p}}{\frac{R_{floor}}{2}} \right) + T_{floormass\_p}$
$Ra\_mid1\_p-1$	
$Ra\_mid2\_p-1$	
$T_{floormass\_p-1}$	$T_{floorin\_p} + \frac{T_{exin\_p}}{1 + \frac{h_{floor\_ex\_p} \cdot A_{floor}}{h_{floor\_walls\_p} \cdot A_{floor}}} + \frac{T_{sh\_p}}{1 + \frac{I_{sh\_p}}{h_{sh\_floor\_p} \cdot A_{win\_south}}} + \frac{T_{R\_p}}{1 + \frac{I_{R\_p}}{h_{cfloor\_p} \cdot A_{floor}}} + I_b \cdot \tau_e \cdot \tau_{sh} \cdot \alpha_f \cdot A_{floor} \cdot 0.7 + I_d \cdot \tau_{de} \cdot \tau_{sh} \cdot \frac{\alpha_f}{5} \cdot A_{floor} \cdot 0.5$
$T_{floorin\_p-1}$	if shade = 1
$T_{wallmass\_p-1}$	$\frac{1}{\frac{R_{floor}}{2} + h_{floor\_walls\_p} \cdot A_{floor} + h_{floor\_ex\_p} \cdot A_{floor} + h_{floor\_ceiling\_p} \cdot A_{floor} + h_{sh\_floor\_p} \cdot A_{win\_south} + h_{cfloor\_p} \cdot A_{floor}}$
$T_{wallsin\_p-1}$	
$T_{exmass\_p-1}$	$\frac{T_{floormass\_p}}{2} + \frac{T_{wallsin\_p}}{1 + \frac{h_{floor\_walls\_p} \cdot A_{floor}}{h_{floor\_ceiling\_p} \cdot A_{floor}}} + \frac{T_{ceilingin\_p}}{1 + \frac{T_{ceilingin\_p}}{h_{floor\_ceiling\_p} \cdot A_{floor}}} + \frac{T_{gin\_p}}{1 + \frac{T_{R\_p}}{h_{cfloor\_p} \cdot A_{floor}}} + h_b \cdot \tau_e \cdot \alpha_f \cdot A_{floor} \cdot 0.7 + I_d \cdot \tau_{de} \cdot \frac{\alpha_f}{5} \cdot A_{floor} \cdot 0.5$
$T_{exin\_p-1}$	
$T_{exout\_p-1}$	otherwise
$T_{ceilingmass\_p-1}$	$\frac{1}{\frac{R_{floor}}{2} + h_{floor\_walls\_p} \cdot A_{floor} + h_{floor\_ex\_p} \cdot A_{floor} + h_{floor\_ceiling\_p} \cdot A_{floor} + h_{g\_floor\_p} \cdot A_{win\_south} + h_{floor\_p} \cdot A_{floor}}$
$T_{ceilingin\_p-1}$	$\frac{dt}{C_{wall}} \left( \frac{T_{adj\_p} - T_{wallmass\_p}}{1 + \frac{R_{wall}}{h_{conv} \cdot A_{wall}}} + \frac{T_{wallsin\_p} - T_{wallmass\_p}}{\frac{R_{wall}}{2}} \right) + T_{wallmass\_p}$
$T_{gin\_p-1}$	

$T_{gout}^{p+1}$   
 $T_{gmid}^{p+1}$   
 $T_{sh}^{p+1}$   
 $T_{gap}^{p+1}$   
 $T_R^{p+1}$   
 $Q_{aux}^{p+1}$

$$\frac{T_{wallsmass}_p}{R_{wall}} + \frac{T_{floorin}_p}{1} + \frac{T_{exin}_p}{h_{ex\_walls\_A\_floor}} + \frac{T_{ceilingin}_p}{1} + \frac{T_{sh}_p}{1} + \frac{T_{R}_p}{h_{walls\_A\_wall}} + I_b \cdot \tau_e \cdot \tau_{sh} \cdot \alpha_{walls} \cdot A_{floor} \cdot 0.3 + I_d \cdot \tau_d \cdot \tau_{sh} \cdot \frac{\alpha_{walls}}{5} \cdot A_{floor} \cdot 0.5$$

if shade = 1

$$\frac{1}{R_{wall}} + \frac{h_{floor\_walls\_A\_floor} + h_{ex\_walls\_A\_south} + h_{ceiling\_walls\_A\_ceiling} - h_{sh\_walls\_A\_win\_south} + h_{ceiling\_walls\_A\_ceiling} + h_{ex\_walls\_A\_wall}}{2}$$

$$\frac{T_{wallsmass}_p}{R_{wall}} + \frac{T_{floorin}_p}{1} + \frac{T_{exin}_p}{h_{ex\_walls\_A\_south}} + \frac{T_{ceilingin}_p}{1} + \frac{T_{gin}_p}{1} + \frac{T_{R}_p}{h_{walls\_A\_wall}} + I_b \cdot \tau_e \cdot \alpha_{walls} \cdot A_{floor} \cdot 0.3 + I_d \cdot \tau_d \cdot \frac{\alpha_{walls}}{5} \cdot A_{floor} \cdot 0.5$$

$$\frac{1}{R_{wall}} + \frac{h_{floor\_walls\_A\_floor} + h_{ex\_walls\_A\_south} + h_{ceiling\_walls\_A\_ceiling} + h_{g\_walls\_A\_win\_south} + h_{ceiling\_walls\_A\_ceiling} + h_{ex\_walls\_A\_wall}}{2}$$

otherwise

$$\frac{dt}{C_{ex}} \left[ \frac{T_{exout}_p - T_{exmass}_p}{R_{ex}} + \frac{T_{exin}_p - T_{exmass}_p}{2} + T_{exmass}_p \right]$$

$$\frac{T_{exmass}_p}{R_{ex}} + \frac{T_{floorin}_p}{1} + \frac{T_{ceilingin}_p}{1} + \frac{T_{wallin}_p}{1} + \frac{T_{R}_p}{1} + \frac{R_{ex}}{2} + R_{insex} \cdot \frac{h_{floor\_ex\_p} \cdot A_{floor}}{h_{ceiling\_ex\_p} \cdot A_{ceiling}} + \frac{h_{ex\_walls\_A\_south}}{h_{ceiling\_ex\_p} \cdot A_{ceiling}} + \frac{1}{l_{ceiling\_p} \cdot A_{ceiling}}$$

$$\frac{1}{R_{ex}} + \frac{R_{insex}}{2} + \frac{h_{floor\_ex\_p} \cdot A_{floor} + h_{ceiling\_ex\_p} \cdot A_{ceiling} + h_{ex\_walls\_A\_south} + h_{ceiling\_ex\_p} \cdot A_{ceiling}}{2}$$

$$\frac{T_{\text{exmass}}}{R_{\text{ex}}} + \frac{T_{\text{O}}}{1} + \frac{T_{\text{p}}}{1} + \frac{T_{\text{p}} \cdot \alpha \cdot \text{ex} \cdot A_{\text{south}}}{h_{\text{og}} \cdot A_{\text{south}}}$$

$$\frac{1}{R_{\text{ex}}} + \frac{h_{\text{og}} \cdot A_{\text{south}}}{2}$$

$$\frac{dt}{C_{\text{ceiling}}} \left( \frac{T_{\text{adj}_p} - T_{\text{ceilingmass}_p}}{h_{\text{conv}} \cdot A_{\text{ceiling}}} + \frac{T_{\text{ceilingin}_p} - T_{\text{ceilingmass}_p}}{R_{\text{ceiling}}} + T_{\text{ceilingmass}_p} \right)$$

$$\frac{T_{\text{ceilingmass}_p}}{R_{\text{ceiling}}} + \frac{T_{\text{floorin}_p}}{h_{\text{floor\_ceiling}_p} \cdot A_{\text{floor}}} + \frac{T_{\text{exin}_p}}{1} + \frac{T_{\text{wallsin}_p}}{1} + \frac{T_{\text{sh}_p}}{1} + \frac{T_{\text{R}_p}}{1}$$

$$\frac{1}{R_{\text{ceiling}}} + \frac{h_{\text{floor\_ceiling}_p} \cdot A_{\text{floor}} + h_{\text{ceiling\_ex}_p} \cdot A_{\text{ceiling}} + h_{\text{ceiling\_walls}_p} \cdot A_{\text{ceiling}} + h_{\text{sh\_ceiling}_p} \cdot A_{\text{ceiling}} + h_{\text{ceiling}_p} \cdot A_{\text{ceiling}}}{2}$$

$$\frac{T_{\text{ceilingmass}_p}}{R_{\text{ceiling}}} + \frac{T_{\text{floorin}_p}}{h_{\text{floor\_ceiling}_p} \cdot A_{\text{floor}}} + \frac{T_{\text{exin}_p}}{1} + \frac{T_{\text{wallsin}_p}}{1} + \frac{T_{\text{gin}_p}}{1} + \frac{T_{\text{R}_p}}{1}$$

$$\frac{1}{R_{\text{ceiling}}} + \frac{h_{\text{floor\_ceiling}_p} \cdot A_{\text{floor}} + h_{\text{ceiling\_ex}_p} \cdot A_{\text{ceiling}} + h_{\text{ceiling\_walls}_p} \cdot A_{\text{ceiling}} + h_{\text{g\_ceiling}_p} \cdot A_{\text{ceiling}} + h_{\text{ceiling}_p} \cdot A_{\text{ceiling}}}{2}$$

otherwise

if shade = 1

$$\begin{aligned}
& \frac{T_{gap_p}}{1} + \frac{T_{gmid_p}}{1} + \frac{T_{sh_p}}{1} + I_b \cdot \tau_p \cdot \alpha_i \cdot A_{win\_south} + I_d \cdot \tau_d \cdot \alpha_d \cdot A_{win\_south} \\
& \frac{h_{gap_p} \cdot A_{win\_south}}{(h_{cglass\_mid1_p} + h_{gmid1_p}) \cdot A_{win\_south}} + \frac{h_{sh\_g_p} \cdot A_{win\_south}}{h_{sh\_g_p} \cdot A_{win\_south}} \\
& \frac{h_{gap_p} \cdot A_{win\_south}}{h_{gap_p} \cdot A_{win\_south} + (h_{cglass\_mid1_p} + h_{gmid1_p}) \cdot A_{win\_south}} + \frac{h_{sh\_g_p} \cdot A_{win\_south}}{h_{sh\_g_p} \cdot A_{win\_south}} \\
& \frac{T_{ceilingin_p}}{1} + \frac{T_{wallsin_p}}{1} + \frac{T_{gmid_p}}{1} + \frac{T_{Rp}}{1} + I_b \cdot \tau_p \cdot \alpha_i \cdot A_{win\_south} + I_d \cdot \tau_d \cdot \alpha_d \cdot A_{win\_south} \\
& \frac{h_{g\_floor\_p} \cdot A_{win\_south}}{h_{g\_ceiling_p} \cdot A_{win\_south}} + \frac{h_{g\_walls\_p} \cdot A_{win\_south}}{h_{g\_walls\_p} \cdot A_{win\_south}} + \frac{h_{g\_ceiling\_p} \cdot A_{win\_south}}{(h_{cglass\_mid1_p} + h_{gmid1_p}) \cdot A_{win\_south}} + \frac{h_{Rp}}{h_{cgp\_p} \cdot A_{win\_south}} \\
& \frac{h_{g\_floor\_p} \cdot A_{win\_south} + h_{g\_ceiling\_p} \cdot A_{win\_south} + h_{g\_walls\_p} \cdot A_{win\_south} + (h_{cglass\_mid1_p} + h_{gmid1_p}) \cdot A_{win\_south}}{h_{g\_ceiling\_p} \cdot A_{win\_south} + h_{g\_walls\_p} \cdot A_{win\_south} + (h_{cglass\_mid1_p} + h_{gmid1_p}) \cdot A_{win\_south}} + \frac{h_{Rp}}{h_{cgp\_p} \cdot A_{win\_south}}
\end{aligned}$$

if ID = 5 v ID = 6

otherwise

$$\begin{aligned}
& \frac{T_{gap_p}}{1} + \frac{T_{gout_p}}{1} + \frac{T_{sh_p}}{1} + I_b \cdot \tau_p \cdot \alpha_i \cdot A_{win\_south} + I_d \cdot \tau_d \cdot \alpha_d \cdot A_{win\_south} \\
& \frac{h_{gap_p} \cdot A_{win\_south}}{(h_{cglass\_p} + h_{gp_p}) \cdot A_{win\_south}} + \frac{h_{sh\_g_p} \cdot A_{win\_south}}{h_{sh\_g_p} \cdot A_{win\_south}} \\
& \frac{h_{gap_p} \cdot A_{win\_south} + (h_{cglass\_p} + h_{gp_p}) \cdot A_{win\_south}}{h_{gap_p} \cdot A_{win\_south} + (h_{cglass\_p} + h_{gp_p}) \cdot A_{win\_south}} + \frac{h_{sh\_g_p} \cdot A_{win\_south}}{h_{sh\_g_p} \cdot A_{win\_south}} \\
& \frac{T_{ceilingin_p}}{1} + \frac{T_{wallsin_p}}{1} + \frac{T_{gout_p}}{1} + \frac{T_{Rp}}{1} + I_b \cdot \tau_p \cdot \alpha_i \cdot A_{win\_south} + I_d \cdot \tau_d \cdot \alpha_d \cdot A_{win\_south} \\
& \frac{h_{g\_floor\_p} \cdot A_{win\_south}}{h_{g\_ceiling_p} \cdot A_{win\_south}} + \frac{h_{g\_walls\_p} \cdot A_{win\_south}}{h_{g\_walls\_p} \cdot A_{win\_south}} + \frac{h_{g\_ceiling\_p} \cdot A_{win\_south}}{(h_{cglass\_p} + h_{gp_p}) \cdot A_{win\_south}} + \frac{h_{Rp}}{h_{cgp\_p} \cdot A_{win\_south}} \\
& \frac{h_{g\_floor\_p} \cdot A_{win\_south} + h_{g\_ceiling\_p} \cdot A_{win\_south} + h_{g\_walls\_p} \cdot A_{win\_south} + (h_{cglass\_p} + h_{gp_p}) \cdot A_{win\_south}}{h_{g\_ceiling\_p} \cdot A_{win\_south} + h_{g\_walls\_p} \cdot A_{win\_south} + (h_{cglass\_p} + h_{gp_p}) \cdot A_{win\_south}} + \frac{h_{Rp}}{h_{cgp\_p} \cdot A_{win\_south}}
\end{aligned}$$

otherwise

$$\begin{aligned}
& \frac{T_{o_p}}{1} + \frac{T_{gmid_p}}{1} + I_b \cdot \alpha_o \cdot A_{win\_south} + I_d \cdot \alpha_d \cdot A_{win\_south} \\
& \frac{h_{og\_p} \cdot A_{win\_south}}{(h_{cglass\_mid2_p} + h_{gmid2_p}) \cdot A_{win\_south}} + \frac{h_{og\_p} \cdot A_{win\_south}}{(h_{cglass\_mid2_p} + h_{gmid2_p}) \cdot A_{win\_south}} \\
& \frac{h_{og\_p} \cdot A_{win\_south} + (h_{cglass\_mid2_p} + h_{gmid2_p}) \cdot A_{win\_south}}{h_{og\_p} \cdot A_{win\_south} + (h_{cglass\_mid2_p} + h_{gmid2_p}) \cdot A_{win\_south}} \\
& \frac{T_{o_p}}{1} + \frac{T_{gun_p}}{1} + I_b \cdot \alpha_o \cdot A_{win\_south} + I_d \cdot \alpha_d \cdot A_{win\_south} \\
& \frac{h_{og\_p} \cdot A_{win\_south}}{(h_{cglass\_p} + h_{gp_p}) \cdot A_{win\_south}} + \frac{h_{og\_p} \cdot A_{win\_south}}{(h_{cglass\_p} + h_{gp_p}) \cdot A_{win\_south}} \\
& \frac{h_{og\_p} \cdot A_{win\_south} + (h_{cglass\_p} + h_{gp_p}) \cdot A_{win\_south}}{h_{og\_p} \cdot A_{win\_south} + (h_{cglass\_p} + h_{gp_p}) \cdot A_{win\_south}}
\end{aligned}$$

if ID = 5 v ID = 6

otherwise

$$\frac{T_{gout\_p}}{1} + \frac{T_{gin\_p}}{1 + I_b \cdot \alpha_{mid} \cdot \tau_p \cdot Awin\_south + I_d \cdot \tau_d \cdot \alpha_{dmid} \cdot Awin\_south}$$

$$\frac{(h_{glass\_mid1\_p} + h_{igmid1\_p}) \cdot Awin\_south}{(h_{glass\_mid1\_p} + h_{igmid1\_p}) \cdot Awin\_south} + \frac{(h_{glass\_mid2\_p} + h_{igmid2\_p}) \cdot Awin\_south}{(h_{glass\_mid2\_p} + h_{igmid2\_p}) \cdot Awin\_south}$$

$$\frac{T_{gap\_p}}{1} + \frac{T_{floorin\_p}}{1} + \frac{T_{ceilingin\_p}}{1} + \frac{T_{walkin\_p}}{1} + \frac{T_{R\_p}}{1} + I_b \cdot \tau_e \cdot \alpha_{sh} \cdot Awin\_south + I_d \cdot \tau_d \cdot \alpha_{dmid} \cdot Awin\_south$$

$$\frac{h_{sh\_fp} \cdot Awin\_south}{h_{sh\_fp} \cdot Awin\_south} + \frac{h_{sh\_ceilingp} \cdot Awin\_south}{h_{sh\_ceilingp} \cdot Awin\_south} + \frac{h_{sh\_wallsp} \cdot Awin\_south}{h_{sh\_wallsp} \cdot Awin\_south} + \frac{h_{sh\_ceilingp} \cdot Awin\_south}{h_{sh\_ceilingp} \cdot Awin\_south}$$

$$h_{gapsh} \cdot Awin\_south + h_{sh\_floor} \cdot Awin\_south + h_{sh\_ceiling} \cdot Awin\_south + h_{sh\_walls} \cdot Awin\_south + h_{csh} \cdot Awin\_south$$

$$\frac{T_{gin\_p}}{1} + \frac{T_{sh\_p}}{1} + \frac{T_{o\_p}}{1} + \frac{T_{R\_p}}{1}$$

$$\frac{h_{gapg} \cdot Awin\_south + h_{gapsh} \cdot Awin\_south}{h_{gapg} \cdot Awin\_south + h_{gapsh} \cdot Awin\_south} + \frac{1}{R_{infgapext}} + \frac{1}{R_{infgaproom}}$$

$$\frac{dt}{C_{air}} \left( \frac{T_{floorin\_p} - T_{R\_p}}{1} + \frac{T_{ceilingin\_p} - T_{R\_p}}{1} + \frac{T_{wallsin\_p} - T_{R\_p}}{1} + \frac{T_{sh\_p} - T_{R\_p}}{1} + \frac{T_{exin\_p} - T_{R\_p}}{1} + \frac{T_{o\_p} - T_{R\_p}}{1} + \frac{T_{adj\_p} - T_{R\_p}}{1} + \frac{T_{gap\_p} - T_{R\_p}}{1} + Q_{int\_p} + Q_{aux\_p} + T_{R\_p} \right) \text{ if shade} = 1$$

$$\frac{dt}{C_{air}} \left( \frac{T_{floorin\_p} - T_{R\_p}}{1} + \frac{T_{ceilingin\_p} - T_{R\_p}}{1} + \frac{T_{wallsin\_p} - T_{R\_p}}{1} + \frac{T_{gin\_p} - T_{R\_p}}{1} + \frac{T_{exin\_p} - T_{R\_p}}{1} + \frac{T_{o\_p} - T_{R\_p}}{1} + \frac{T_{adj\_p} - T_{R\_p}}{1} + \frac{T_{gap\_p} - T_{R\_p}}{1} + Q_{int\_p} + Q_{aux\_p} + T_{R\_p} \right) \text{ otherwise}$$

$$K_p \left( T_{sp\_p} - T_{R\_p} + offset \right) + K_I \sum_{p=pKI}^p \left( T_{sp\_p} - T_{R\_p} \right) dt \text{ if } \left( T_{sp\_p} - T_{R\_p} \right) < -0.5 \text{ degC} \wedge K_p \left( T_{sp\_p} - T_{R\_p} + offset \right) + K_I \sum_{p=pKI}^p \left( T_{sp\_p} - T_{R\_p} \right) dt \leq 0 \text{ watt}$$

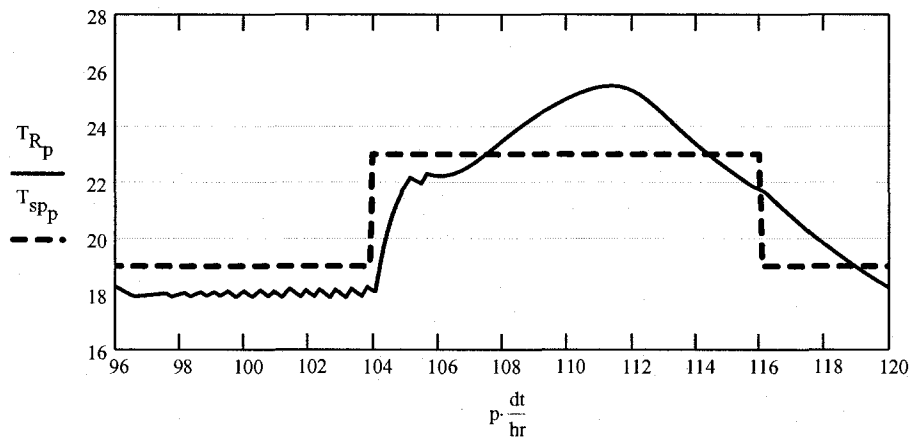
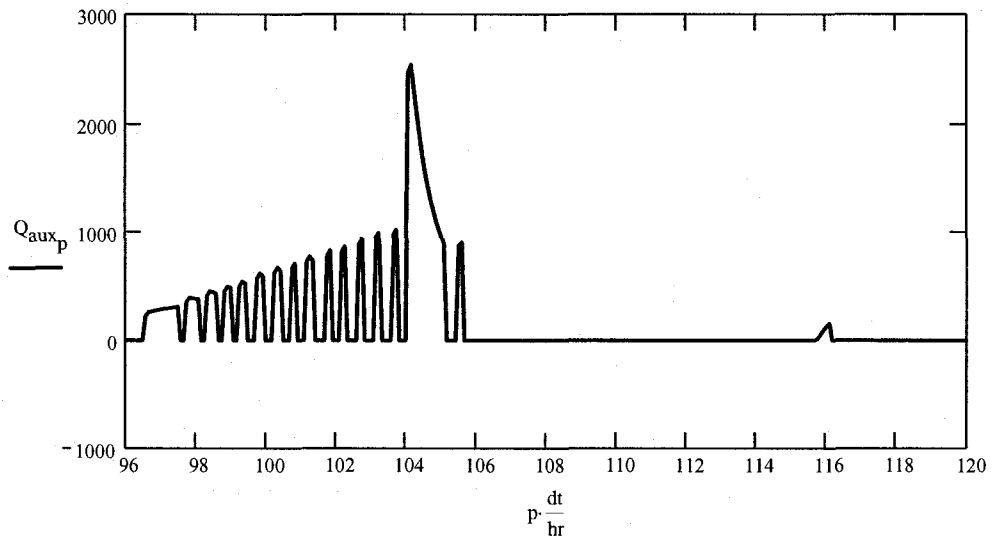
(0-watt) otherwise

$$K_p \left( T_{sp\_p} - T_{R\_p} + offset \right) + K_I \sum_{p=pKI}^p \left( T_{sp\_p} - T_{R\_p} \right) dt \text{ if } \left( T_{sp\_p} - T_{R\_p} \right) \leq -2 \text{ degC} \wedge (6 \cdot 3600 \cdot \text{sec} < \text{mod}(p \cdot dt, 24 \cdot 3600 \cdot \text{sec}) < 22 \cdot 3600 \cdot \text{sec})$$

if season = 2

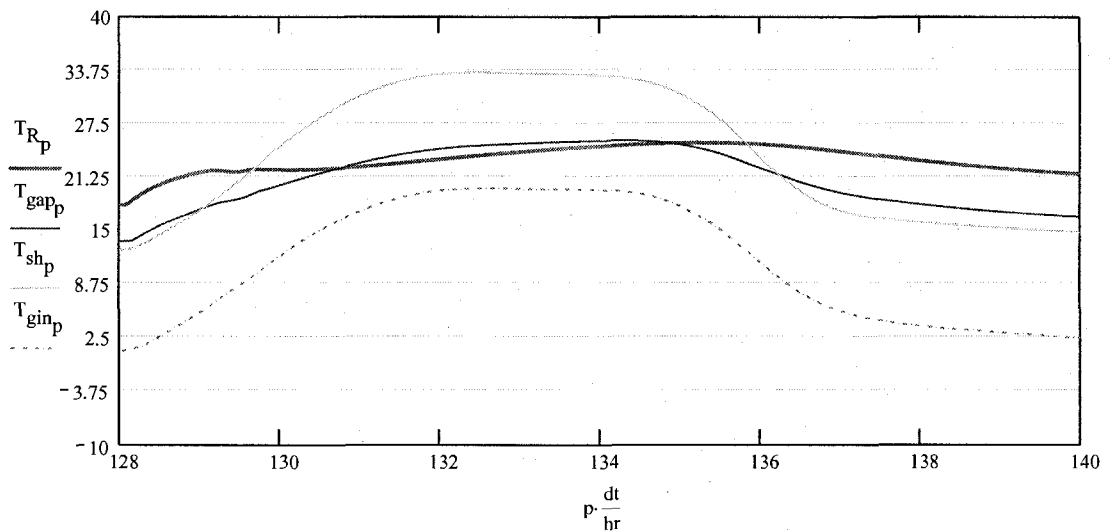
$$K_p \left( T_{sp\_p} - T_{R\_p} + offset \right) + K_I \sum_{p=pKI}^p \left( T_{sp\_p} - T_{R\_p} \right) dt \text{ if } \left( T_{sp\_p} - T_{R\_p} \right) \geq 1 \text{ degC}$$

(0-watt) otherwise

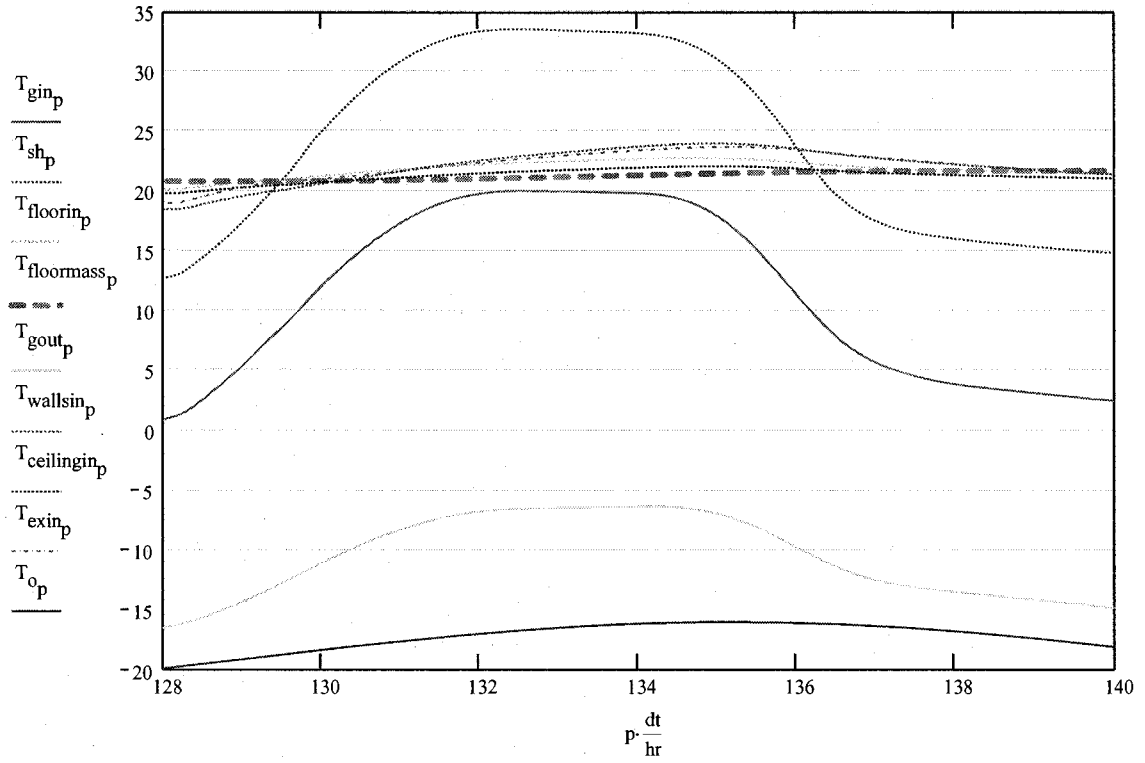


## Results:

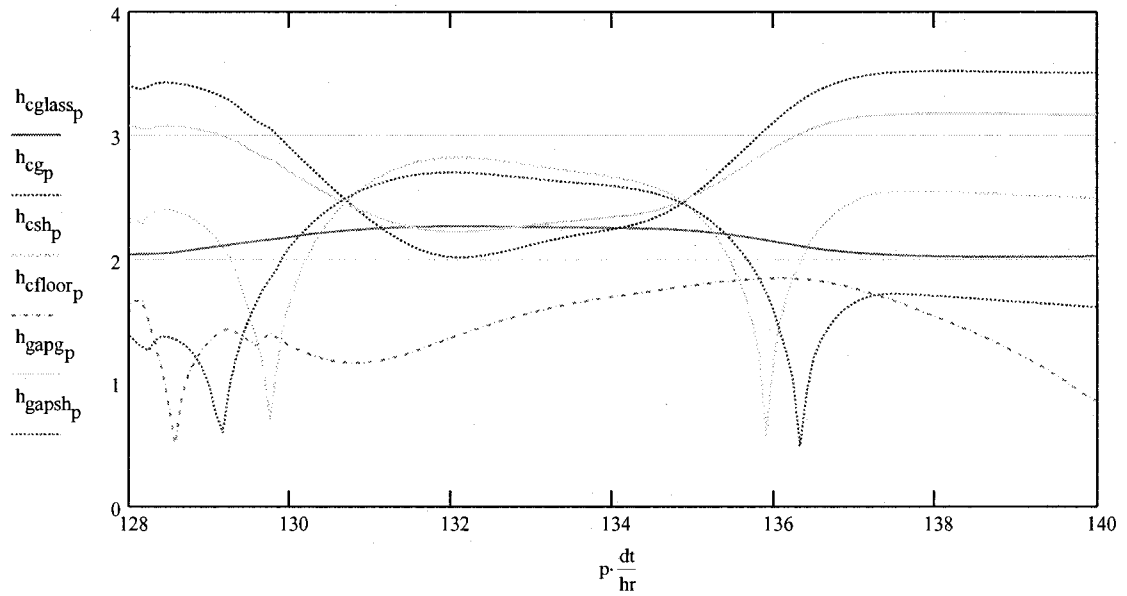
### AIR TEMPERATURES:



## SURFACE TEMPERATURES



## CONVECTIVE HEAT TRANSFER COEFFICIENTS





$$n_p := \left[ \frac{n_{\text{days}} - 1 \text{ day}}{dt}, \left( \frac{n_{\text{days}} - 1 \text{ day}}{dt} + 1 \right) \dots \left( \frac{n_{\text{days}}}{dt} \right) \right]$$

...timesteps for last day

$$I_{n_p} = \frac{\text{kg}}{\text{s}^3}$$

	1
1	12.713
2	11.754
3	10.569
4	9.183
5	7.626
6	5.931
7	4.135
8	2.273
9	0.385
10	0

$$T_{O_{n_p}} =$$

	1
1	-21.007
2	-21.056
3	-21.103
4	-21.149
5	-21.194
6	-21.238
7	-21.281
8	-21.323
9	-21.364
10	-21.404

$$T_{gin_{n_p}} =$$

	1
1	-0.351
2	-0.394
3	-0.437
4	-0.481
5	-0.525
6	-0.571
7	-0.617
8	-0.663
9	-0.699
10	-0.729

$$T_{sh_{n_p}} =$$

	1
1	12.267
2	12.225
3	12.183
4	12.14
5	12.098
6	12.055
7	12.012
8	11.979
9	11.956
10	11.94

$$T_{R_{n_p}} =$$

	1
1	18.198
2	18.142
3	18.088
4	18.035
5	17.982
6	17.93
7	17.924
8	17.925
9	17.929
10	17.933

$$Q_{aux_{n_p}} = \text{W}$$

	1
1	0
2	0
3	0
4	0
5	0
6	201.399
7	237.116
8	249.631
9	258.54
10	266.471

## Total fenestration U-value:

### Center of Glass:

$$U_{g_p} = \frac{1}{\frac{1}{h_{og_p}} + \frac{1}{h_{cglass_p} + h_{rg_p}} + R_{insglass} + \frac{1}{h_{cg_p} + h_{g\_floor_p} + h_{g\_ceiling_p} + h_{g\_walls_p}}}$$

**Total Window:**

$$U_{o_p} = \frac{U_{cg_p} \cdot A_{cg} + U_{eg} \cdot A_{eg} + U_{fr} \cdot A_{fr}}{A_{win\_south}}$$

$$U_{o_{48hr}} = 3.539 \frac{kg}{s^3}$$

$$U_{cg_{48hr}} = 2.824 \frac{kg}{s^3}$$

**Total window and shade**

$$U_{o\_sh_p} := \begin{cases} \frac{1}{\frac{1}{h_{og_p}} + \frac{1}{h_{cglass_p} + h_{rg_p}} + R_{insglass} + \frac{1}{h_{gapg_p} + h_{sh\_g_p}} + \frac{1}{h_{gapsh_p}} + \frac{1}{h_{csh_p} + h_{sh\_walls_p} + h_{sh\_floor_p} + h_{sh\_}}} & \\ 0 \frac{\text{watt}}{m^2 \text{degC}} & \text{otherwise} \end{cases}$$

$$U_{o\_sh_{48hr}} = 0.804 \frac{\text{watt}}{m^2 \text{degC}}$$

$$U_{o\_sh_{48hr}} \cdot A_{win\_south} = 5.147 \frac{\text{watt}}{\text{degC}}$$

**Therefore:**

$$U_{window_p} := \text{if}(\text{shade} = 0, U_{o_p}, U_{o\_sh_p})$$

$$U_{window_1} := 1 \frac{\text{watt}}{m^2 \text{degC}}$$

$$U_{window_{48hr}} = 0.804 \frac{kg}{s^3}$$

$$U_{o_{144hr}} = 3.534 \frac{kg}{s^3}$$

**Exterior South Wall U-value**

$$U_{ex_p} := \frac{1}{\frac{1}{h_{oex_p}} + R_{insex} \cdot A_{south} + R_{ex} \cdot A_{south} + \frac{1}{(h_{cex_p} + h_{floor\_ex_p} + h_{ceiling\_ex_p} + h_{ex\_walls_p})}}$$

$$U_{ex_{48hr}} = 0.301 \frac{\text{watt}}{m^2}$$

**Total U-Value (Glazing, Shade, exterior wall):**

$$U_{\text{facade}_p} := \frac{1}{\frac{1}{U_{\text{window}_p}} \cdot (\text{WWR}) + \frac{1}{U_{\text{ex}_p}} \cdot (1 - \text{WWR})}$$

$$U_{\text{facade}_{48 \frac{\text{hr}}{\text{dt}}}} = 0.544 \frac{1}{\text{m}^2} \frac{\text{watt}}{\text{degC}}$$

$$U_{\text{facade}_{48 \frac{\text{hr}}{\text{dt}}}} \cdot (W_{\text{rm}} \cdot H_{\text{rm}}) = 4.877 \frac{\text{watt}}{\text{degC}}$$

**SUMMARY:**

**Center-of-glass:**

$$U_{\text{cg}_{144 \frac{\text{hr}}{\text{dt}}}} = 2.816 \frac{\text{kg}}{\text{s}^3}$$

**Total window:**

$$U_{\text{O}_{144 \frac{\text{hr}}{\text{dt}}}} = 3.534 \frac{\text{kg}}{\text{s}^3}$$

**Total window and shade:**

$$U_{\text{window}_{48 \frac{\text{hr}}{\text{dt}}}} = 0.804 \frac{\text{kg}}{\text{s}^3}$$

**Exterior Wall:**

$$U_{\text{ex}_{48 \frac{\text{hr}}{\text{dt}}}} = 0.301 \frac{\text{kg}}{\text{s}^3}$$

**Total facade:**

$$U_{\text{facade}_{48 \frac{\text{hr}}{\text{dt}}}} = 0.544 \frac{\text{kg}}{\text{s}^3}$$

## **APPENDIX D: Indoor thermal environment and thermal comfort model**

# INDOOR THERMAL ENVIRONMENT & THERMAL COMFORT MODEL

The following methodology is referred to *Algorithms for the calculation of the view factors between human body and rectangular surfaces in parallelepiped environments* by G. Cannistraro, G. Franzitta, C. Giaconia and G. Rizzo, *energy and buildings*, 19 (1992) 51-60

Drawings and calculation procedure in this section courtesy of Yu Xiang Chen

## Parameters for seated person with known orientation

- SEK 1: Vertical rectangle in front of person and above their centre, or behind and below his center
- SEK 2: Vertical rectangle in front of person and below their centre, or behind and above his center
- SEK 3: Vertical rectangle on side wall above and forward of their centre, or below and behind his centre
- SEK 4: Vertical rectangle on side wall below and forward of their centre, or above and behind his centre
- SEK 5: Horizontal rectangle in ceiling and forward of their centre, or on floor and behind his center
- SEK 6: Horizontal rectangle in ceiling and behind their centre, or on floor and forward of his center

$$F_{\max} := \begin{pmatrix} 0.132 \\ 0.103 \\ 0.131 \\ 0.104 \\ 0.130 \\ 0.101 \end{pmatrix} \quad A := \begin{pmatrix} 1.14505 \\ 1.33522 \\ 1.41607 \\ 1.15253 \\ 1.31858 \\ 1.51966 \end{pmatrix} \quad B := \begin{pmatrix} 0.14524 \\ 0.14454 \\ 0.09957 \\ 0.13945 \\ 0.12807 \\ 0.12266 \end{pmatrix} \quad C := \begin{pmatrix} 0.74379 \\ 0.60637 \\ 0.76196 \\ 0.73371 \\ 1.00432 \\ 0.84923 \end{pmatrix} \quad D := \begin{pmatrix} 0.10312 \\ 0.14678 \\ 0.07182 \\ 0.09442 \\ 0.03802 \\ 0.10471 \end{pmatrix} \quad E := \begin{pmatrix} 0.02967 \\ 0.04628 \\ 0.05578 \\ 0.03688 \\ 0.06189 \\ 0.05704 \end{pmatrix}$$

$$F(a, b, c) := \begin{pmatrix} F_{\max_1} \left[ \frac{-\frac{a}{c}}{1 - e^{\frac{-\frac{a}{c}}{A_1 + B_1 \left(\frac{a}{c}\right)}}} \right] \left[ \frac{-\frac{b}{c}}{1 - e^{\frac{-\frac{b}{c}}{C_1 + D_1 \left(\frac{b}{c}\right) + E_1 \left(\frac{a}{c}\right)}}} \right] \\ F_{\max_2} \left[ \frac{-\frac{a}{c}}{1 - e^{\frac{-\frac{a}{c}}{A_2 + B_2 \left(\frac{a}{c}\right)}}} \right] \left[ \frac{-\frac{b}{c}}{1 - e^{\frac{-\frac{b}{c}}{C_2 + D_2 \left(\frac{b}{c}\right) + E_2 \left(\frac{a}{c}\right)}}} \right] \\ F_{\max_3} \left[ \frac{-\frac{a}{c}}{1 - e^{\frac{-\frac{a}{c}}{A_3 + B_3 \left(\frac{a}{c}\right)}}} \right] \left[ \frac{-\frac{b}{c}}{1 - e^{\frac{-\frac{b}{c}}{C_3 + D_3 \left(\frac{b}{c}\right) + E_3 \left(\frac{a}{c}\right)}}} \right] \\ F_{\max_4} \left[ \frac{-\frac{a}{c}}{1 - e^{\frac{-\frac{a}{c}}{A_4 + B_4 \left(\frac{a}{c}\right)}}} \right] \left[ \frac{-\frac{b}{c}}{1 - e^{\frac{-\frac{b}{c}}{C_4 + D_4 \left(\frac{b}{c}\right) + E_4 \left(\frac{a}{c}\right)}}} \right] \\ F_{\max_5} \left[ \frac{-\frac{a}{c}}{1 - e^{\frac{-\frac{a}{c}}{A_5 + B_5 \left(\frac{a}{c}\right)}}} \right] \left[ \frac{-\frac{b}{c}}{1 - e^{\frac{-\frac{b}{c}}{C_5 + D_5 \left(\frac{b}{c}\right) + E_5 \left(\frac{a}{c}\right)}}} \right] \\ F_{\max_6} \left[ \frac{-\frac{a}{c}}{1 - e^{\frac{-\frac{a}{c}}{A_6 + B_6 \left(\frac{a}{c}\right)}}} \right] \left[ \frac{-\frac{b}{c}}{1 - e^{\frac{-\frac{b}{c}}{C_6 + D_6 \left(\frac{b}{c}\right) + E_6 \left(\frac{a}{c}\right)}}} \right] \end{pmatrix} \quad \dots F() \text{ function for 6 SEKs}$$

**Convert room geometry into dimensionless quantities:**

DSC := 0.1      ... distance from wall for calculation to start (m)

H<sub>p</sub> := 0.6      ... seated subject center

$$w_{rm} := \frac{W_{rm}}{m} \qquad d_{rm} := \frac{D_{rm}}{m} \qquad h_{rm} := \frac{H_{rm}}{m} \qquad dis_{win} := \frac{DIS}{m}$$

$$w_{win} := \frac{W_{win}}{m} \qquad d_{win} := \frac{D_{win}}{m} \qquad e_{win} := \frac{H_{sp}}{m} \qquad dis_{win} := 0.001$$

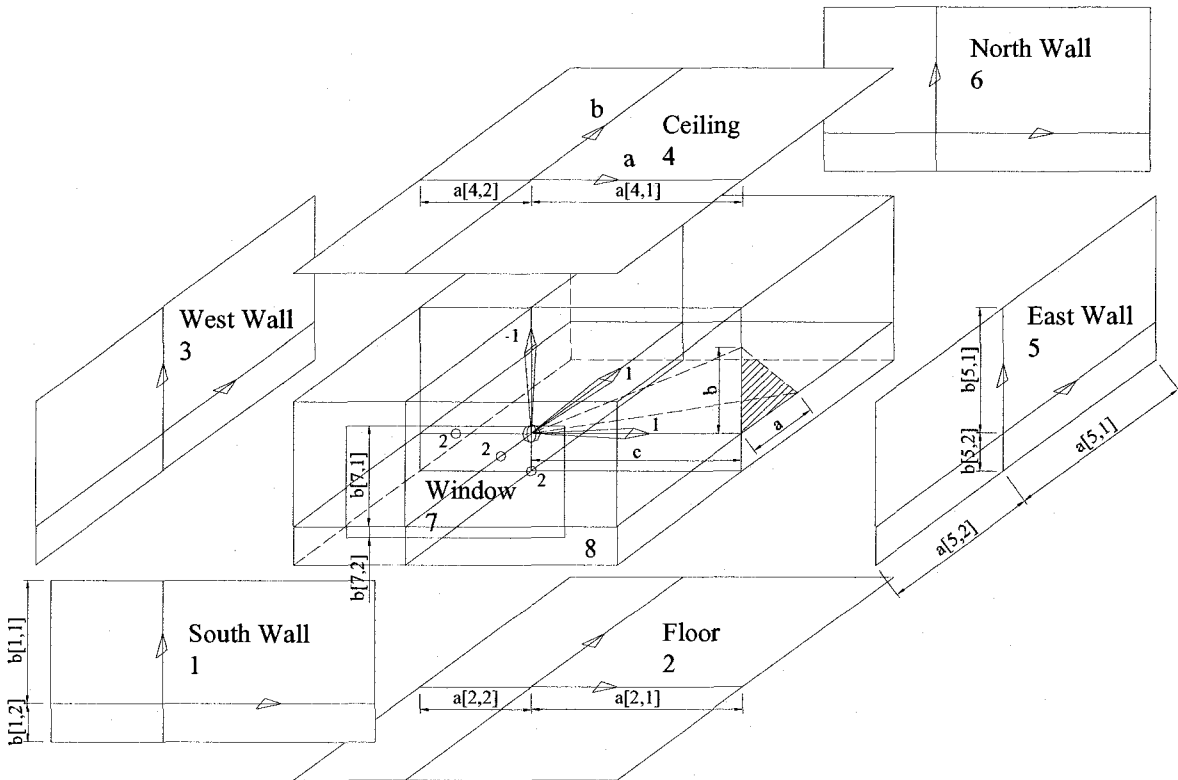
MR := 12      ...Number of divisions in room in Y direction (rows)

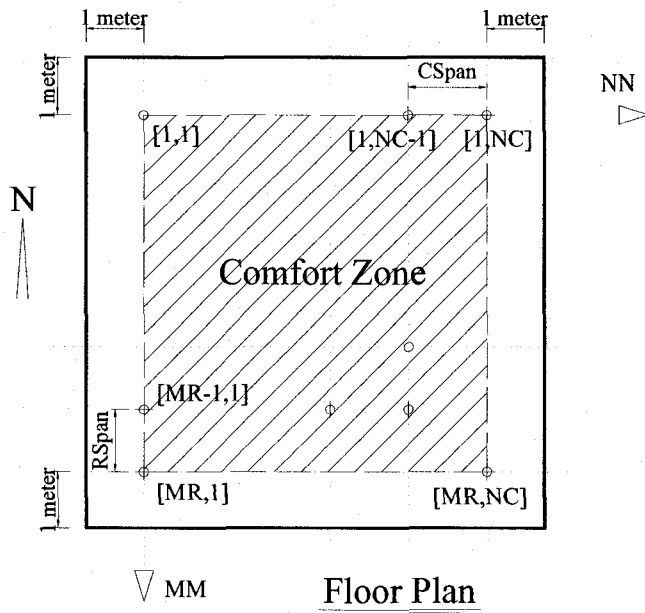
NC := 12      ...Number of divisions in room in X direction (columns)

SF := 1.. 8      ...indices of surfaces.

ORT = 1.. 3      ...indices of subject orientation. 1-facing south, 2-north, 3-partition.

- 1 south
- 2 floor
- 3 west
- 4 ceiling
- 5 east
- 6 north
- 7 window





$$RSpan := \frac{d_{rm} - 2 \cdot DSC}{MR - 1} \quad \dots \text{distance between rows} \qquad CSpan := \frac{w_{rm} - 2 \cdot DSC}{NC - 1} \quad \dots \text{distance between columns}$$

mm := 1, 2.. MR    nn := 1, 2.. NC    ...indices of locations starting from north-west corner of plan

$$aa(M, N) := \begin{bmatrix} w_{rm} - [DSC + (N - 1) \cdot CSpan] & DSC + (N - 1) \cdot CSpan \\ w_{rm} - [DSC + (N - 1) \cdot CSpan] & DSC + (N - 1) \cdot CSpan \\ DSC + (M - 1) \cdot RSpan & d_{rm} - [DSC + (M - 1) \cdot RSpan] \\ w_{rm} - [DSC + (N - 1) \cdot CSpan] & DSC + (N - 1) \cdot CSpan \\ DSC + (M - 1) \cdot RSpan & d_{rm} - [DSC + (M - 1) \cdot RSpan] \\ w_{rm} - [DSC + (N - 1) \cdot CSpan] & DSC + (N - 1) \cdot CSpan \\ |w_{rm} - dis_{win} - [DSC + (N - 1) \cdot CSpan]| & |[DSC + (N - 1) \cdot CSpan] - dis_{win}| \end{bmatrix} \quad a_{mm, nn} := aa(mm, nn)$$

$$bb(M, N) := \begin{bmatrix} h_{rm} - H_p & H_p \\ DSC + (M - 1) \cdot RSpan & d_{rm} - [DSC + (M - 1) \cdot RSpan] \\ h_{rm} - H_p & H_p \\ DSC + (M - 1) \cdot RSpan & d_{rm} - [DSC + (M - 1) \cdot RSpan] \\ h_{rm} - H_p & H_p \\ h_{rm} - H_p & H_p \\ |h_{rm} - d_{win} - H_p| & |H_p - e_{win}| \end{bmatrix} \quad b_{mm, nn} := bb(mm, nn)$$

$$cc(M, N) := \begin{bmatrix} d_{rm} - [DSC + (M - 1) \cdot RSpan] \\ H_p \\ [DSC + (N - 1) \cdot CSpan] \\ h_{rm} - H_p \\ w_{rm} - [DSC + (N - 1) \cdot CSpan] \\ DSC + (M - 1) \cdot RSpan \\ d_{rm} - [DSC + (M - 1) \cdot RSpan] \end{bmatrix} \quad c_{mm, nn} := cc(mm, nn)$$



a =

	1	2	3	4
1	[7,2]	[7,2]	[7,2]	[7,2]
2	[7,2]	[7,2]	[7,2]	[7,2]
3	[7,2]	[7,2]	[7,2]	[7,2]
4	[7,2]	[7,2]	[7,2]	[7,2]
5	[7,2]	[7,2]	[7,2]	[7,2]
6	[7,2]	[7,2]	[7,2]	[7,2]
7	[7,2]	[7,2]	[7,2]	[7,2]

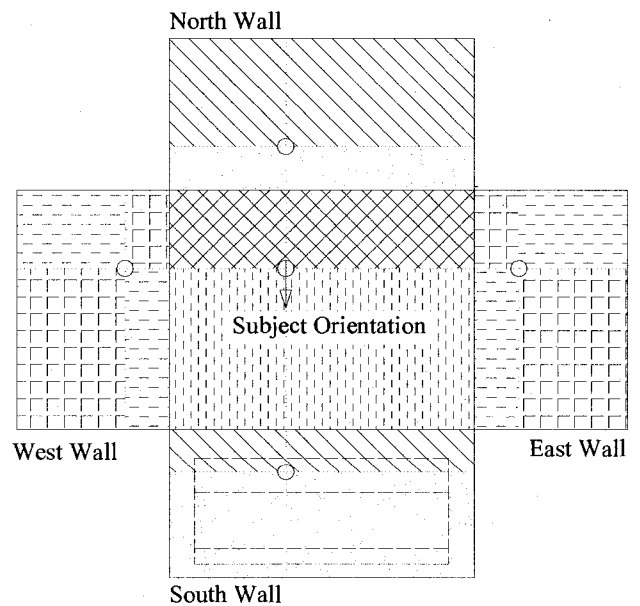
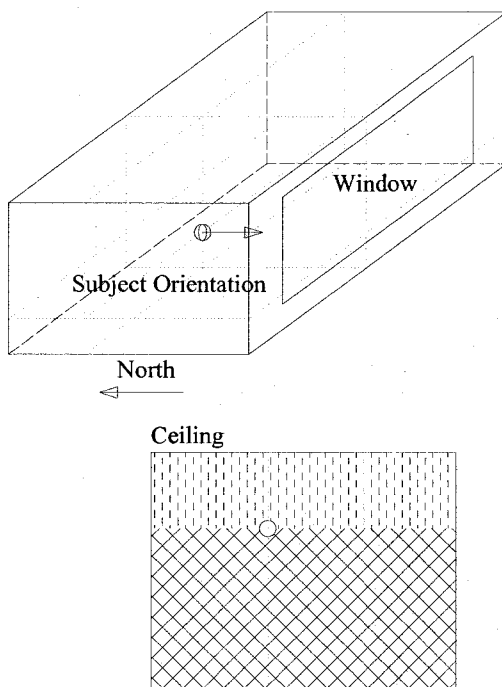
c =

	1	2	3	4
1	[7,1]	[7,1]	[7,1]	[7,1]
2	[7,1]	[7,1]	[7,1]	[7,1]
3	[7,1]	[7,1]	[7,1]	[7,1]
4	[7,1]	[7,1]	[7,1]	[7,1]
5	[7,1]	[7,1]	[7,1]	[7,1]

b =

	1	2	3
1	[7,2]	[7,2]	[7,2]
2	[7,2]	[7,2]	[7,2]
3	[7,2]	[7,2]	[7,2]
4	[7,2]	[7,2]	[7,2]
5	[7,2]	[7,2]	[7,2]

**For subjects facing south**  $F_{h1, SF}$  :



- [ ] SEK 1
- [ / ] SEK 2
- [ ] SEK 3
- [ - ] SEK 4
- [ X ] SEK 5
- [ ] SEK 6



North Wall

$$FF16(X, Y) := F\left[(a_{X,Y})_{6,1}, (b_{X,Y})_{6,2}, (c_{X,Y})_6\right]_1 + F\left[(a_{X,Y})_{6,2}, (b_{X,Y})_{6,2}, (c_{X,Y})_6\right]_1 \dots \\ + F\left[(a_{X,Y})_{6,1}, (b_{X,Y})_{6,1}, (c_{X,Y})_6\right]_2 + F\left[(a_{X,Y})_{6,2}, (b_{X,Y})_{6,1}, (c_{X,Y})_6\right]_2$$

$$F16_{mm,nn} := FF16(mm, nn)$$

$$Fh_{1,6} := F16$$

$Fh_{1,6} =$

	1	2	3	4	5
1	0.344	0.428	0.445	0.45	0.452
2	0.236	0.306	0.341	0.359	0.369
3	0.188	0.233	0.261	0.279	0.289
4	0.155	0.186	0.207	0.221	0.23
5	0.131	0.153	0.168	0.179	0.186
6	0.112	0.128	0.14	0.148	0.154
7	0.097	0.109	0.118	0.125	0.129

South Wall

$$FF11(X, Y) := F\left[(a_{X,Y})_{1,1}, (b_{X,Y})_{1,1}, (c_{X,Y})_1\right]_1 + F\left[(a_{X,Y})_{1,2}, (b_{X,Y})_{1,1}, (c_{X,Y})_1\right]_1 \dots \\ + F\left[(a_{X,Y})_{1,1}, (b_{X,Y})_{1,2}, (c_{X,Y})_1\right]_2 + F\left[(a_{X,Y})_{1,2}, (b_{X,Y})_{1,2}, (c_{X,Y})_1\right]_2$$

$$F11_{mm,nn} := FF11(mm, nn)$$

$$Fh_{1,1} := F11$$

$Fh_{1,1} =$

	1	2	3	4	5
1	0.06	0.065	0.069	0.072	0.074
2	0.067	0.073	0.078	0.081	0.083
3	0.075	0.082	0.088	0.092	0.095
4	0.085	0.094	0.1	0.105	0.109
5	0.096	0.107	0.116	0.122	0.126
6	0.109	0.124	0.134	0.142	0.147

East Wall

$$FF15(X, Y) := F\left[(a_{X,Y})_{5,1}, (b_{X,Y})_{5,2}, (c_{X,Y})_5\right]_3 + F\left[(a_{X,Y})_{5,2}, (b_{X,Y})_{5,1}, (c_{X,Y})_5\right]_3 \dots \\ + F\left[(a_{X,Y})_{5,1}, (b_{X,Y})_{5,1}, (c_{X,Y})_5\right]_4 + F\left[(a_{X,Y})_{5,2}, (b_{X,Y})_{5,2}, (c_{X,Y})_5\right]_4$$

$$F15_{mm,nn} := FF15(mm, nn)$$

$$Fh_{1,5} := F15$$

$$Fh_{1,5} =$$

	1	2	3	4	5
1	0.048	0.054	0.061	0.07	0.081
2	0.051	0.058	0.066	0.076	0.088
3	0.053	0.06	0.069	0.08	0.093
4	0.055	0.062	0.072	0.083	0.097
5	0.056	0.064	0.073	0.085	0.1
6	0.056	0.064	0.074	0.086	0.101
7	0.056	0.064	0.073	0.085	0.1

West Wall ...same as east wall, just switch sub-script 5 to 3

$$FF13(X, Y) := F[(a_{X,Y})_{3,1}, (b_{X,Y})_{3,2}, (c_{X,Y})_3]_3 + F[(a_{X,Y})_{3,2}, (b_{X,Y})_{3,1}, (c_{X,Y})_3]_3 \dots \\ + F[(a_{X,Y})_{3,1}, (b_{X,Y})_{3,1}, (c_{X,Y})_3]_4 + F[(a_{X,Y})_{3,2}, (b_{X,Y})_{3,2}, (c_{X,Y})_3]_4$$

$$F13_{mm,nn} := FF13(mm, nn) \quad Fh_{1,3} := F13$$

$$Fh_{1,3} =$$

	1	2	3	4	5
1	0.344	0.238	0.191	0.157	0.131
2	0.43	0.303	0.231	0.183	0.148
3	0.448	0.338	0.257	0.201	0.161
4	0.454	0.357	0.273	0.213	0.17
5	0.455	0.367	0.283	0.221	0.176
6	0.456	0.371	0.287	0.224	0.178
7	0.455	0.37	0.286	0.223	0.177

Ceiling

$$FF14(X, Y) := F[(a_{X,Y})_{4,1}, (b_{X,Y})_{4,2}, (c_{X,Y})_4]_5 + F[(a_{X,Y})_{4,2}, (b_{X,Y})_{4,2}, (c_{X,Y})_4]_5 \dots \\ + F[(a_{X,Y})_{4,1}, (b_{X,Y})_{4,1}, (c_{X,Y})_4]_6 + F[(a_{X,Y})_{4,2}, (b_{X,Y})_{4,1}, (c_{X,Y})_4]_6$$

$$F14_{mm,nn} := FF14(mm, nn) \quad Fh_{1,4} := F14$$

$$Fh_{1,4} =$$

	1	2	3	4	5
1	0.06	0.066	0.07	0.073	0.076
2	0.064	0.07	0.075	0.078	0.08
3	0.067	0.073	0.078	0.081	0.084
4	0.068	0.075	0.08	0.083	0.086
5	0.069	0.075	0.08	0.084	0.086
6	0.069	0.075	0.08	0.083	0.086
7	0.067	0.073	0.078	0.082	0.084

Floor

$$FF12(X, Y) := F\left[(a_X, Y)_{2,1}, (b_X, Y)_{2,1}, (c_X, Y)_2\right]^5 + F\left[(a_X, Y)_{2,2}, (b_X, Y)_{2,1}, (c_X, Y)_2\right]^5 \dots \\ + F\left[(a_X, Y)_{2,1}, (b_X, Y)_{2,2}, (c_X, Y)_2\right]^6 + F\left[(a_X, Y)_{2,2}, (b_X, Y)_{2,2}, (c_X, Y)_2\right]^6$$

$$F12_{mm,nn} := FF12(mm, nn)$$

$$Fh_{1,2} := F12$$

$Fh_{1,2} =$

	1	2	3	4	5
1	0.113	0.138	0.155	0.166	0.172
2	0.145	0.179	0.201	0.215	0.224
3	0.167	0.206	0.232	0.248	0.258
4	0.182	0.225	0.252	0.27	0.281
5	0.192	0.236	0.266	0.284	0.295
6	0.197	0.243	0.273	0.292	0.304
7	0.2	0.246	0.276	0.295	0.307

Window

For left and right

$$Sa1(X, Y) := \text{if}\left[w_{rm} - [DSC + (Y - 1) \cdot CSpan] \geq \text{dis}_{win, 1, -1}\right]$$

...to decide subtract or add from other parts of the window area (S for sign).

$$Sa2(X, Y) := \text{if}\left[DSC + (Y - 1) \cdot CSpan \geq \text{dis}_{win, 1, -1}\right]$$

$$Sb1(X, Y) := \text{if}\left(h_{rm} - d_{win} - H_p \geq 0, 1, -1\right)$$

$$Sb2(X, Y) := \text{if}\left(H_p \geq e_{win}, 1, -1\right)$$

For top and bottom

$$S1t(X, Y) := \text{if}\left(h_{rm} - d_{win} - H_p \geq 0, 1, 2\right)$$

...determine the SEK for top and bottom parts (S for SEK, 1 for subject facing south).

$$S1b(X, Y) := \text{if}\left(H_p \geq e_{win}, 2, 1\right)$$

$$FF17(X, Y) := Sa1(X, Y) \cdot Sb1(X, Y) \cdot F\left[(a_X, Y)_{7,1}, (b_X, Y)_{7,1}, (c_X, Y)_7\right] S1t(X, Y) \dots \\ + Sa2(X, Y) \cdot Sb1(X, Y) \cdot F\left[(a_X, Y)_{7,2}, (b_X, Y)_{7,1}, (c_X, Y)_7\right] S1t(X, Y) \dots \\ + Sa1(X, Y) \cdot Sb2(X, Y) \cdot F\left[(a_X, Y)_{7,1}, (b_X, Y)_{7,2}, (c_X, Y)_7\right] S1b(X, Y) \dots \\ + Sa2(X, Y) \cdot Sb2(X, Y) \cdot F\left[(a_X, Y)_{7,2}, (b_X, Y)_{7,2}, (c_X, Y)_7\right] S1b(X, Y)$$

$$F17_{mm,nn} := FF17(mm, nn)$$

$$Fh_{1,7} := F17$$

$$F_{h1,7} =$$

	1	2	3	4	5
1	0.043	0.047	0.05	0.052	0.053
2	0.048	0.052	0.056	0.058	0.06
3	0.054	0.059	0.063	0.066	0.068
4	0.06	0.067	0.071	0.075	0.077
5	0.068	0.076	0.082	0.086	0.089
6	0.077	0.087	0.094	0.1	0.103
7	0.087	0.1	0.11	0.116	0.121

$$F_{h1,8} := F_{h1,1} - F_{h1,7}$$

$$F_{h1,8} =$$

	1	2	3	4	5
1	0.017	0.018	0.019	0.02	0.021
2	0.019	0.021	0.022	0.023	0.023
3	0.022	0.024	0.025	0.026	0.027
4	0.025	0.027	0.029	0.03	0.031
5	0.028	0.031	0.034	0.036	0.037
6	0.033	0.037	0.04	0.042	0.044
7	0.039	0.044	0.048	0.051	0.053



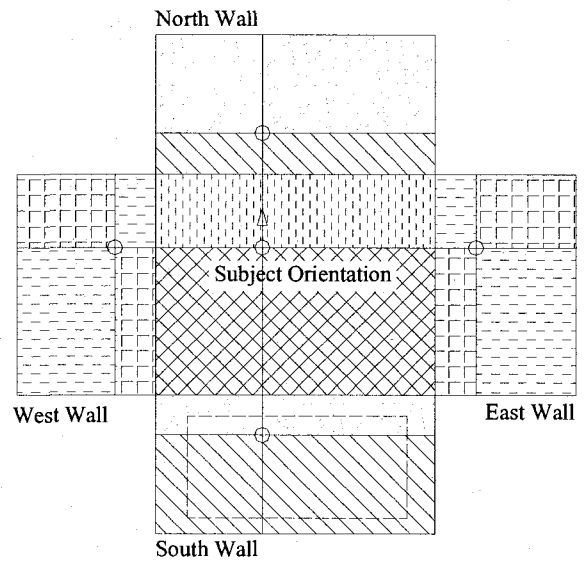
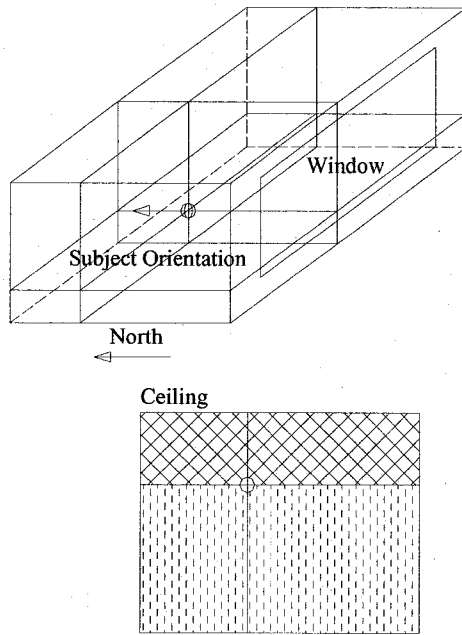
Sum up view factors to verify the accuracy:

$$SC := 2..8$$

$$\sum_{SC} F_{h1,SC} =$$

	1	2	3	4	5	6	7	8	9	10
1	0.97	0.99	0.991	0.988	0.985	0.983	0.983	0.985	0.988	0.991
2	0.993	0.988	0.99	0.992	0.992	0.993	0.993	0.992	0.992	0.99
3	0.999	0.993	0.985	0.982	0.981	0.98	0.98	0.981	0.982	0.985
4	0.999	0.998	0.984	0.976	0.973	0.971	0.971	0.973	0.976	0.984
5	0.999	1.002	0.986	0.975	0.969	0.967	0.967	0.969	0.975	0.986
6	0.999	1.005	0.987	0.975	0.969	0.966	0.966	0.969	0.975	0.987
7	1	1.006	0.989	0.977	0.971	0.969	0.969	0.971	0.977	0.989
8	1.002	1.007	0.991	0.981	0.976	0.974	0.974	0.976	0.981	0.991
9	1.004	1.006	0.993	0.987	0.984	0.983	0.983	0.984	0.987	0.993
10	1.004	1.002	0.996	0.994	0.995	0.995	0.995	0.995	0.994	0.996
11	0.997	0.995	0.999	1.003	1.004	1.005	1.005	1.004	1.003	0.999
12	0.967	0.989	0.993	0.992	0.99	0.989	0.989	0.99	0.992	0.993

For subjects facing north  $F_{h2, SF}$ .



- SEK 1
- SEK 2
- SEK 3
- SEK 4
- SEK 5
- SEK 6



North Wall

$$FF26(X, Y) := F\left[(a_{X,Y})_{6,1}, (b_{X,Y})_{6,1}, (c_{X,Y})_6\right]_1 + F\left[(a_{X,Y})_{6,2}, (b_{X,Y})_{6,1}, (c_{X,Y})_6\right]_1 \dots \\ + F\left[(a_{X,Y})_{6,1}, (b_{X,Y})_{6,2}, (c_{X,Y})_6\right]_2 + F\left[(a_{X,Y})_{6,2}, (b_{X,Y})_{6,2}, (c_{X,Y})_6\right]_2$$

$$F26_{mm,nn} := FF26(mm, nn)$$

$$Fh_{2,6} := F26$$

	1	2	3	4	5	6	7	8	9	10
1	0.341	0.425	0.442	0.447	0.45	0.45	0.45	0.45	0.447	0.442
2	0.243	0.316	0.352	0.371	0.381	0.385	0.385	0.381	0.371	0.352
3	0.201	0.25	0.28	0.299	0.31	0.315	0.315	0.31	0.299	0.28
4	0.17	0.204	0.227	0.243	0.253	0.257	0.257	0.253	0.243	0.227
5	0.146	0.17	0.188	0.2	0.208	0.212	0.212	0.208	0.2	0.188
6	0.126	0.144	0.158	0.168	0.174	0.177	0.177	0.174	0.168	0.158
7	0.109	0.124	0.134	0.142	0.147	0.149	0.149	0.147	0.142	0.134
8	0.096	0.107	0.116	0.122	0.126	0.128	0.128	0.126	0.122	0.116
9	0.085	0.094	0.1	0.105	0.109	0.11	0.11	0.109	0.105	0.1
10	0.075	0.082	0.088	0.092	0.095	0.096	0.096	0.095	0.092	0.088
11	0.067	0.073	0.078	0.081	0.083	0.084	0.084	0.083	0.081	0.078
12	0.06	0.065	0.069	0.072	0.074	0.075	0.075	0.074	0.072	0.069

Fh<sub>2,6</sub> =

South Wall

$$FF21(X, Y) := F\left[(a_{X,Y})_{1,1}, (b_{X,Y})_{1,2}, (c_{X,Y})_1\right]_1 + F\left[(a_{X,Y})_{1,2}, (b_{X,Y})_{1,2}, (c_{X,Y})_1\right]_1 \dots \\ + F\left[(a_{X,Y})_{1,1}, (b_{X,Y})_{1,1}, (c_{X,Y})_1\right]_2 + F\left[(a_{X,Y})_{1,2}, (b_{X,Y})_{1,1}, (c_{X,Y})_1\right]_2$$

$$F21_{mm,nn} := FF21(mm, nn)$$

$$Fh_{2,1} := F21$$

	1	2	3	4	5	6	7	8	9	10
1	0.053	0.057	0.06	0.062	0.064	0.065	0.065	0.064	0.062	0.06
2	0.059	0.064	0.067	0.07	0.072	0.073	0.073	0.072	0.07	0.067
3	0.066	0.072	0.077	0.08	0.082	0.083	0.083	0.082	0.08	0.077
4	0.074	0.082	0.087	0.092	0.094	0.096	0.096	0.094	0.092	0.087
5	0.084	0.094	0.101	0.106	0.11	0.111	0.111	0.11	0.106	0.101
6	0.097	0.109	0.118	0.125	0.129	0.131	0.131	0.129	0.125	0.118
7	0.112	0.128	0.14	0.148	0.154	0.156	0.156	0.154	0.148	0.14
8	0.131	0.153	0.168	0.179	0.186	0.189	0.189	0.186	0.179	0.168
9	0.155	0.186	0.207	0.221	0.23	0.234	0.234	0.23	0.221	0.207
10	0.188	0.233	0.261	0.279	0.289	0.294	0.294	0.289	0.279	0.261
11	0.236	0.306	0.341	0.359	0.369	0.373	0.373	0.369	0.359	0.341
12	0.344	0.428	0.445	0.45	0.452	0.453	0.453	0.452	0.45	0.445

Fh<sub>2,1</sub> =

East Wall

$$FF25(X, Y) := F[(a_{X,Y})_{5,1}, (b_{X,Y})_{5,1}, (c_{X,Y})_5]_3 + F[(a_{X,Y})_{5,2}, (b_{X,Y})_{5,2}, (c_{X,Y})_5]_3 \dots \\ + F[(a_{X,Y})_{5,1}, (b_{X,Y})_{5,2}, (c_{X,Y})_5]_4 + F[(a_{X,Y})_{5,2}, (b_{X,Y})_{5,1}, (c_{X,Y})_5]_4$$

$$F25_{mm,nn} := FF25(mm, nn)$$

$$Fh_{2,5} := F25$$

	1	2	3	4	5	6	7	8	9	10
1	0.046	0.051	0.058	0.066	0.076	0.088	0.103	0.123	0.147	0.18
2	0.049	0.055	0.063	0.072	0.084	0.099	0.117	0.142	0.175	0.222
3	0.052	0.059	0.067	0.077	0.09	0.107	0.128	0.156	0.195	0.25
4	0.054	0.061	0.07	0.081	0.095	0.113	0.136	0.166	0.209	0.268
5	0.055	0.063	0.072	0.084	0.098	0.117	0.141	0.173	0.218	0.28
6	0.056	0.064	0.073	0.085	0.1	0.119	0.144	0.177	0.223	0.286
7	0.056	0.064	0.074	0.086	0.101	0.12	0.145	0.178	0.224	0.287
8	0.056	0.064	0.073	0.085	0.1	0.118	0.143	0.176	0.221	0.283
9	0.055	0.062	0.072	0.083	0.097	0.115	0.139	0.17	0.213	0.273
10	0.053	0.06	0.069	0.08	0.093	0.11	0.132	0.161	0.201	0.257
11	0.051	0.058	0.066	0.076	0.088	0.103	0.123	0.148	0.183	0.231
12	0.048	0.054	0.061	0.07	0.081	0.094	0.11	0.131	0.157	0.191

West Wall

...same as east wall, just switch sub-script 5 to 3

$$FF23(X, Y) := F[(a_{X,Y})_{3,1}, (b_{X,Y})_{3,1}, (c_{X,Y})_3]_3 + F[(a_{X,Y})_{3,2}, (b_{X,Y})_{3,2}, (c_{X,Y})_3]_3 \dots \\ + F[(a_{X,Y})_{3,1}, (b_{X,Y})_{3,2}, (c_{X,Y})_3]_4 + F[(a_{X,Y})_{3,2}, (b_{X,Y})_{3,1}, (c_{X,Y})_3]_4$$

$$F23_{mm,nn} := FF23(mm, nn)$$

$$Fh_{2,3} := F23$$

	1	2	3	4	5	6	7	8	9	10
1	0.337	0.228	0.18	0.147	0.123	0.103	0.088	0.076	0.066	0.058
2	0.424	0.294	0.222	0.175	0.142	0.117	0.099	0.084	0.072	0.063
3	0.443	0.331	0.25	0.195	0.156	0.128	0.107	0.09	0.077	0.067
4	0.45	0.352	0.268	0.209	0.166	0.136	0.113	0.095	0.081	0.07
5	0.453	0.364	0.28	0.218	0.173	0.141	0.117	0.098	0.084	0.072
6	0.455	0.37	0.286	0.223	0.177	0.144	0.119	0.1	0.085	0.073
7	0.456	0.371	0.287	0.224	0.178	0.145	0.12	0.101	0.086	0.074
8	0.455	0.367	0.283	0.221	0.176	0.143	0.118	0.1	0.085	0.073
9	0.454	0.357	0.273	0.213	0.17	0.139	0.115	0.097	0.083	0.072
10	0.448	0.338	0.257	0.201	0.161	0.132	0.11	0.093	0.08	0.069
11	0.43	0.303	0.231	0.183	0.148	0.123	0.103	0.088	0.076	0.066
12	0.344	0.238	0.191	0.157	0.131	0.11	0.094	0.081	0.07	0.061

Ceiling

$$FF24(X, Y) := F\left[\left(a_{X,Y}\right)_{4,1}, \left(b_{X,Y}\right)_{4,1}, \left(c_{X,Y}\right)_4\right]_5 + F\left[\left(a_{X,Y}\right)_{4,2}, \left(b_{X,Y}\right)_{4,1}, \left(c_{X,Y}\right)_4\right]_5 \dots \\ + F\left[\left(a_{X,Y}\right)_{4,1}, \left(b_{X,Y}\right)_{4,2}, \left(c_{X,Y}\right)_4\right]_6 + F\left[\left(a_{X,Y}\right)_{4,2}, \left(b_{X,Y}\right)_{4,2}, \left(c_{X,Y}\right)_4\right]_6$$

$$F24_{mm,nn} := FF24(mm, nn)$$

$$Fh_{2,4} := F24$$

	1	2	3	4	5	6	7	8	9	10
1	0.046	0.05	0.053	0.055	0.057	0.057	0.057	0.057	0.055	0.053
2	0.052	0.057	0.06	0.063	0.065	0.066	0.066	0.065	0.063	0.06
3	0.058	0.063	0.067	0.07	0.072	0.073	0.073	0.072	0.07	0.067
4	0.062	0.067	0.072	0.075	0.077	0.078	0.078	0.077	0.075	0.072
5	0.065	0.071	0.076	0.079	0.081	0.082	0.082	0.081	0.079	0.076
6	0.067	0.073	0.078	0.082	0.084	0.085	0.085	0.084	0.082	0.078
7	0.069	0.075	0.08	0.083	0.086	0.087	0.087	0.086	0.083	0.08
8	0.069	0.075	0.08	0.084	0.086	0.088	0.088	0.086	0.084	0.08
9	0.068	0.075	0.08	0.083	0.086	0.087	0.087	0.086	0.083	0.08
10	0.067	0.073	0.078	0.081	0.084	0.085	0.085	0.084	0.081	0.078
11	0.064	0.07	0.075	0.078	0.08	0.082	0.082	0.08	0.078	0.075
12	0.06	0.066	0.07	0.073	0.076	0.077	0.077	0.076	0.073	0.07

Floor

$$FF22(X, Y) := F\left[\left(a_{X,Y}\right)_{2,1}, \left(b_{X,Y}\right)_{2,2}, \left(c_{X,Y}\right)_2\right]_5 + F\left[\left(a_{X,Y}\right)_{2,2}, \left(b_{X,Y}\right)_{2,2}, \left(c_{X,Y}\right)_2\right]_5 \dots \\ + F\left[\left(a_{X,Y}\right)_{2,1}, \left(b_{X,Y}\right)_{2,1}, \left(c_{X,Y}\right)_2\right]_6 + F\left[\left(a_{X,Y}\right)_{2,2}, \left(b_{X,Y}\right)_{2,1}, \left(c_{X,Y}\right)_2\right]_6$$

$$F22_{mm,nn} := FF22(mm, nn)$$

$$Fh_{2,2} := F22$$

	1	2	3	4	5	6	7	8	9	10
1	0.145	0.178	0.199	0.213	0.221	0.225	0.225	0.221	0.213	0.199
2	0.169	0.209	0.235	0.251	0.261	0.265	0.265	0.261	0.251	0.235
3	0.185	0.228	0.256	0.274	0.285	0.29	0.29	0.285	0.274	0.256
4	0.194	0.239	0.268	0.287	0.298	0.304	0.304	0.298	0.287	0.268
5	0.199	0.245	0.275	0.294	0.305	0.311	0.311	0.305	0.294	0.275
6	0.2	0.246	0.276	0.295	0.307	0.312	0.312	0.307	0.295	0.276
7	0.197	0.243	0.273	0.292	0.304	0.309	0.309	0.304	0.292	0.273
8	0.192	0.236	0.266	0.284	0.295	0.301	0.301	0.295	0.284	0.266
9	0.182	0.225	0.252	0.27	0.281	0.286	0.286	0.281	0.27	0.252
10	0.167	0.206	0.232	0.248	0.258	0.263	0.263	0.258	0.248	0.232
11	0.145	0.179	0.201	0.215	0.224	0.228	0.228	0.224	0.215	0.201
12	0.113	0.138	0.155	0.166	0.172	0.175	0.175	0.172	0.166	0.155

Window

Top and bottom

$$S2t(X, Y) := \text{if}(h_{\text{rm}} - d_{\text{win}} - H_p \geq 0, 2, 1)$$

$$S2b(X, Y) := \text{if}(H_p \geq e_{\text{win}}, 1, 2)$$

determine the SEK for top and bottom parts (S for SEK, 2 for subject facing north).

$$\begin{aligned} FF27(X, Y) := & Sa1(X, Y) \cdot Sb1(X, Y) \cdot F\left[\begin{matrix} (a_x, y)_{7,1}, (b_x, y)_{7,2}, (c_x, y)_7 \end{matrix}\right] S2t(X, Y) \dots \\ & + Sa2(X, Y) \cdot Sb1(X, Y) \cdot F\left[\begin{matrix} (a_x, y)_{7,2}, (b_x, y)_{7,2}, (c_x, y)_7 \end{matrix}\right] S2t(X, Y) \dots \\ & + Sa1(X, Y) \cdot Sb2(X, Y) \cdot F\left[\begin{matrix} (a_x, y)_{7,1}, (b_x, y)_{7,1}, (c_x, y)_7 \end{matrix}\right] S2b(X, Y) \dots \\ & + Sa2(X, Y) \cdot Sb2(X, Y) \cdot F\left[\begin{matrix} (a_x, y)_{7,2}, (b_x, y)_{7,1}, (c_x, y)_7 \end{matrix}\right] S2b(X, Y) \end{aligned}$$

$$F27_{\text{mm,nn}} := FF27(\text{mm}, \text{nn})$$

$$Fh_{2,7} := F27$$

$Fh_{2,7} =$

	1	2	3	4	5	6	7	8	9	10
1	0.043	0.047	0.05	0.052	0.053	0.054	0.054	0.053	0.052	0.05
2	0.048	0.052	0.056	0.058	0.06	0.061	0.061	0.06	0.058	0.056
3	0.054	0.059	0.063	0.066	0.068	0.069	0.069	0.068	0.066	0.063
4	0.06	0.067	0.071	0.075	0.077	0.078	0.078	0.077	0.075	0.071
5	0.068	0.076	0.082	0.086	0.089	0.09	0.09	0.089	0.086	0.082
6	0.077	0.087	0.094	0.1	0.103	0.105	0.105	0.103	0.1	0.094
7	0.087	0.1	0.11	0.116	0.121	0.123	0.123	0.121	0.116	0.11
8	0.1	0.116	0.129	0.137	0.142	0.145	0.145	0.142	0.137	0.129
9	0.114	0.137	0.152	0.163	0.169	0.172	0.172	0.169	0.163	0.152
10	0.131	0.162	0.182	0.194	0.2	0.204	0.204	0.2	0.194	0.182
11	0.152	0.196	0.218	0.229	0.235	0.237	0.237	0.235	0.229	0.218
12	0.202	0.248	0.257	0.259	0.26	0.261	0.261	0.26	0.259	0.257

$$Fh_{2,8} := Fh_{2,1} - Fh_{2,7}$$

$Fh_{2,8} =$

	1	2	3	4	5	6	7	8	9	10
1	$5 \cdot 10^{-3}$	$5 \cdot 10^{-3}$	0.01	0.011	0.011	0.011	0.011	0.011	0.011	0.01
2	0.011	0.011	0.012	0.012	0.012	0.013	0.013	0.012	0.012	0.012
3	0.012	0.013	0.014	0.014	0.014	0.015	0.015	0.014	0.014	0.014
4	0.014	0.015	0.016	0.017	0.017	0.017	0.017	0.017	0.017	0.016
5	0.017	0.018	0.019	0.02	0.021	0.021	0.021	0.021	0.02	0.019
6	0.02	0.022	0.024	0.025	0.026	0.026	0.026	0.026	0.025	0.024
7	0.025	0.028	0.03	0.032	0.033	0.034	0.034	0.033	0.032	0.03
8	0.031	0.036	0.04	0.042	0.044	0.045	0.045	0.044	0.042	0.04
9	0.041	0.049	0.055	0.058	0.061	0.062	0.062	0.061	0.058	0.055
10	0.057	0.071	0.08	0.085	0.089	0.09	0.09	0.089	0.085	0.08
11	0.084	0.109	0.123	0.13	0.134	0.136	0.136	0.134	0.13	0.123
12	0.142	0.18	0.188	0.191	0.192	0.192	0.192	0.192	0.191	0.188



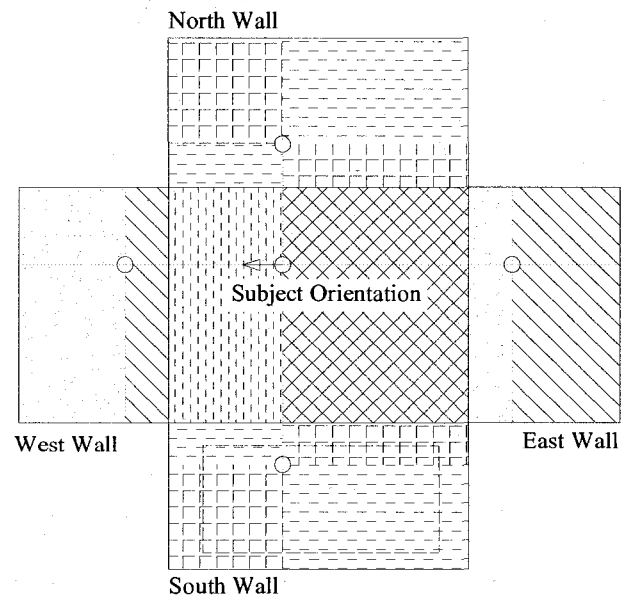
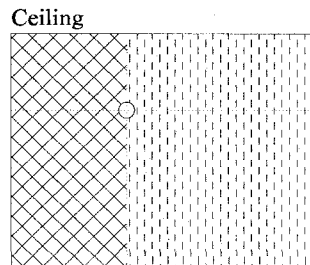
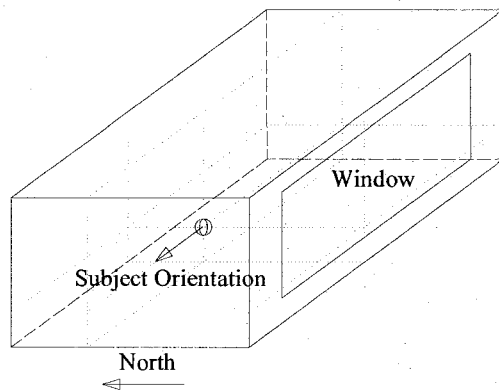
Sum up view factors to verify the accuracy:

SC := 2.. 8

$$\sum_{SC} F_{h2,SC} =$$

	1	2	3	4	5	6	7	8	9	10
1	0.967	0.989	0.993	0.992	0.99	0.989	0.989	0.99	0.992	0.993
2	0.997	0.995	0.999	1.003	1.004	1.005	1.005	1.004	1.003	0.999
3	1.004	1.002	0.996	0.994	0.995	0.995	0.995	0.995	0.994	0.996
4	1.004	1.006	0.993	0.987	0.984	0.983	0.983	0.984	0.987	0.993
5	1.002	1.007	0.991	0.981	0.976	0.974	0.974	0.976	0.981	0.991
6	1	1.006	0.989	0.977	0.971	0.969	0.969	0.971	0.977	0.989
7	0.999	1.005	0.987	0.975	0.969	0.966	0.966	0.969	0.975	0.987
8	0.999	1.002	0.986	0.975	0.969	0.967	0.967	0.969	0.975	0.986
9	0.999	0.998	0.984	0.976	0.973	0.971	0.971	0.973	0.976	0.984
10	0.999	0.993	0.985	0.982	0.981	0.98	0.98	0.981	0.982	0.985
11	0.993	0.988	0.99	0.992	0.992	0.993	0.993	0.992	0.992	0.99
12	0.97	0.99	0.991	0.988	0.985	0.983	0.983	0.985	0.988	0.991

For subjects facing west /east  $F_{h3,SF}$ :



- SEK 1
- SEK 2
- SEK 3
- SEK 4
- SEK 5
- SEK 6

North Wall

$$FF36(X, Y) := F\left[(a_{X,Y})_{6,2}, (b_{X,Y})_{6,1}, (c_{X,Y})_6\right]_3 + F\left[(a_{X,Y})_{6,1}, (b_{X,Y})_{6,2}, (c_{X,Y})_6\right]_3 \dots \\ + F\left[(a_{X,Y})_{6,1}, (b_{X,Y})_{6,1}, (c_{X,Y})_6\right]_4 + F\left[(a_{X,Y})_{6,2}, (b_{X,Y})_{6,2}, (c_{X,Y})_6\right]_4$$

$$F36_{mm,nn} := FF36(mm, nn)$$

$$Fh_{3,6} := F36$$

$Fh_{3,6} =$

	1	2	3	4	5	6	7	8	9	10
1	0.336	0.425	0.444	0.45	0.453	0.454	0.455	0.455	0.454	0.449
2	0.232	0.304	0.342	0.363	0.374	0.38	0.381	0.377	0.367	0.349
3	0.186	0.233	0.263	0.283	0.295	0.301	0.302	0.298	0.288	0.271
4	0.155	0.186	0.209	0.225	0.235	0.24	0.241	0.238	0.23	0.216
5	0.13	0.153	0.17	0.182	0.19	0.194	0.195	0.192	0.186	0.176
6	0.111	0.128	0.141	0.15	0.156	0.16	0.161	0.159	0.154	0.146
7	0.096	0.109	0.118	0.126	0.131	0.133	0.134	0.133	0.129	0.123
8	0.084	0.093	0.101	0.107	0.111	0.113	0.114	0.112	0.109	0.105
9	0.073	0.081	0.087	0.092	0.095	0.097	0.097	0.096	0.094	0.09
10	0.065	0.071	0.076	0.08	0.082	0.084	0.084	0.084	0.082	0.079
11	0.058	0.063	0.067	0.07	0.072	0.073	0.074	0.073	0.072	0.069
12	0.052	0.056	0.059	0.062	0.064	0.065	0.065	0.064	0.063	0.061

South Wall

$$FF31(X, Y) := F\left[(a_{X,Y})_{1,1}, (b_{X,Y})_{1,2}, (c_{X,Y})_1\right]_3 + F\left[(a_{X,Y})_{1,2}, (b_{X,Y})_{1,1}, (c_{X,Y})_1\right]_3 \dots \\ + F\left[(a_{X,Y})_{1,1}, (b_{X,Y})_{1,1}, (c_{X,Y})_1\right]_4 + F\left[(a_{X,Y})_{1,2}, (b_{X,Y})_{1,2}, (c_{X,Y})_1\right]_4$$

$$F31_{mm,nn} := FF31(mm, nn)$$

$$Fh_{3,1} := F31$$

$Fh_{3,1} =$

	1	2	3	4	5	6	7	8	9	10
1	0.052	0.056	0.059	0.062	0.064	0.065	0.065	0.064	0.063	0.061
2	0.058	0.063	0.067	0.07	0.072	0.073	0.074	0.073	0.072	0.069
3	0.065	0.071	0.076	0.08	0.082	0.084	0.084	0.084	0.082	0.079
4	0.073	0.081	0.087	0.092	0.095	0.097	0.097	0.096	0.094	0.09
5	0.084	0.093	0.101	0.107	0.111	0.113	0.114	0.112	0.109	0.105
6	0.096	0.109	0.118	0.126	0.131	0.133	0.134	0.133	0.129	0.123
7	0.111	0.128	0.141	0.15	0.156	0.16	0.161	0.159	0.154	0.146
8	0.13	0.153	0.17	0.182	0.19	0.194	0.195	0.192	0.186	0.176
9	0.155	0.186	0.209	0.225	0.235	0.24	0.241	0.238	0.23	0.216
10	0.186	0.233	0.263	0.283	0.295	0.301	0.302	0.298	0.288	0.271
11	0.232	0.304	0.342	0.363	0.374	0.38	0.381	0.377	0.367	0.349
12	0.336	0.425	0.444	0.45	0.453	0.454	0.455	0.455	0.454	0.449

East Wall

$$FF35(X, Y) := F[(a_{X,Y})_{5,1}, (b_{X,Y})_{5,2}, (c_{X,Y})_5]_1 + F[(a_{X,Y})_{5,2}, (b_{X,Y})_{5,2}, (c_{X,Y})_5]_1 \dots \\ + F[(a_{X,Y})_{5,1}, (b_{X,Y})_{5,1}, (c_{X,Y})_5]_2 + F[(a_{X,Y})_{5,2}, (b_{X,Y})_{5,1}, (c_{X,Y})_5]_2$$

$$F35_{mm,nn} := FF35(mm, nn)$$

$$Fh_{3,5} := F35$$

Fh<sub>3,5</sub> =

	1	2	3	4	5	6	7	8	9	10
1	0.047	0.052	0.059	0.067	0.077	0.089	0.104	0.123	0.148	0.181
2	0.05	0.056	0.064	0.073	0.084	0.099	0.117	0.141	0.174	0.221
3	0.053	0.059	0.068	0.078	0.09	0.106	0.127	0.155	0.193	0.247
4	0.054	0.062	0.07	0.081	0.095	0.112	0.134	0.164	0.205	0.264
5	0.056	0.063	0.072	0.083	0.097	0.115	0.139	0.17	0.213	0.274
6	0.056	0.064	0.073	0.085	0.099	0.117	0.141	0.173	0.217	0.279
7	0.056	0.064	0.073	0.085	0.099	0.117	0.141	0.173	0.217	0.279
8	0.056	0.063	0.072	0.083	0.097	0.115	0.139	0.17	0.213	0.274
9	0.054	0.062	0.07	0.081	0.095	0.112	0.134	0.164	0.205	0.264
10	0.053	0.059	0.068	0.078	0.09	0.106	0.127	0.155	0.193	0.247
11	0.05	0.056	0.064	0.073	0.084	0.099	0.117	0.141	0.174	0.221
12	0.047	0.052	0.059	0.067	0.077	0.089	0.104	0.123	0.148	0.181

West Wall

$$FF33(X, Y) := F[(a_{X,Y})_{3,1}, (b_{X,Y})_{3,1}, (c_{X,Y})_3]_1 + F[(a_{X,Y})_{3,2}, (b_{X,Y})_{3,1}, (c_{X,Y})_3]_1 \dots \\ + F[(a_{X,Y})_{3,1}, (b_{X,Y})_{3,2}, (c_{X,Y})_3]_2 + F[(a_{X,Y})_{3,2}, (b_{X,Y})_{3,2}, (c_{X,Y})_3]_2$$

$$F33_{mm,nn} := FF33(mm, nn)$$

$$Fh_{3,3} := F33$$

Fh<sub>3,3</sub> =

	1	2	3	4	5	6	7	8	9	10
1	0.342	0.239	0.195	0.163	0.137	0.117	0.101	0.088	0.077	0.068
2	0.424	0.306	0.238	0.192	0.158	0.133	0.113	0.097	0.084	0.073
3	0.442	0.342	0.266	0.213	0.174	0.144	0.121	0.104	0.089	0.078
4	0.447	0.361	0.284	0.227	0.184	0.152	0.128	0.109	0.093	0.081
5	0.45	0.372	0.295	0.236	0.191	0.158	0.132	0.112	0.096	0.083
6	0.451	0.376	0.3	0.24	0.195	0.16	0.134	0.114	0.097	0.084
7	0.451	0.376	0.3	0.24	0.195	0.16	0.134	0.114	0.097	0.084
8	0.45	0.372	0.295	0.236	0.191	0.158	0.132	0.112	0.096	0.083
9	0.447	0.361	0.284	0.227	0.184	0.152	0.128	0.109	0.093	0.081
10	0.442	0.342	0.266	0.213	0.174	0.144	0.121	0.104	0.089	0.078
11	0.424	0.306	0.238	0.192	0.158	0.133	0.113	0.097	0.084	0.073
12	0.342	0.239	0.195	0.163	0.137	0.117	0.101	0.088	0.077	0.068

Ceiling

$$FF34(X, Y) := F\left[(a_X, Y)_{4,2}, (b_X, Y)_{4,1}, (c_X, Y)_4\right]_5 + F\left[(a_X, Y)_{4,2}, (b_X, Y)_{4,2}, (c_X, Y)_4\right]_5 \dots \\ + F\left[(a_X, Y)_{4,1}, (b_X, Y)_{4,1}, (c_X, Y)_4\right]_6 + F\left[(a_X, Y)_{4,1}, (b_X, Y)_{4,2}, (c_X, Y)_4\right]_6$$

$$F34_{mm,nn} := FF34(mm, nn)$$

$$Fh_{3,4} := F34$$

$Fh_{3,4} =$

	1	2	3	4	5	6	7	8	9	10
1	0.046	0.053	0.058	0.062	0.065	0.066	0.068	0.068	0.067	0.066
2	0.051	0.058	0.064	0.068	0.071	0.073	0.074	0.074	0.073	0.072
3	0.055	0.062	0.068	0.073	0.076	0.078	0.079	0.079	0.078	0.076
4	0.058	0.065	0.071	0.076	0.08	0.082	0.083	0.083	0.082	0.08
5	0.06	0.067	0.074	0.078	0.082	0.084	0.086	0.086	0.084	0.082
6	0.061	0.068	0.075	0.08	0.083	0.086	0.087	0.087	0.086	0.083
7	0.061	0.068	0.075	0.08	0.083	0.086	0.087	0.087	0.086	0.083
8	0.06	0.067	0.074	0.078	0.082	0.084	0.086	0.086	0.084	0.082
9	0.058	0.065	0.071	0.076	0.08	0.082	0.083	0.083	0.082	0.08
10	0.055	0.062	0.068	0.073	0.076	0.078	0.079	0.079	0.078	0.076
11	0.051	0.058	0.064	0.068	0.071	0.073	0.074	0.074	0.073	0.072
12	0.046	0.053	0.058	0.062	0.065	0.066	0.068	0.068	0.067	0.066

Floor

$$FF32(X, Y) := F\left[(a_X, Y)_{2,1}, (b_X, Y)_{2,1}, (c_X, Y)_2\right]_5 + F\left[(a_X, Y)_{2,1}, (b_X, Y)_{2,2}, (c_X, Y)_2\right]_5 \dots \\ + F\left[(a_X, Y)_{2,2}, (b_X, Y)_{2,1}, (c_X, Y)_2\right]_6 + F\left[(a_X, Y)_{2,2}, (b_X, Y)_{2,2}, (c_X, Y)_2\right]_6$$

$$F32_{mm,nn} := FF32(mm, nn)$$

$$Fh_{3,2} := F32$$

$Fh_{3,2} =$

	1	2	3	4	5	6	7	8	9	10
1	0.142	0.166	0.182	0.192	0.198	0.2	0.2	0.195	0.187	0.173
2	0.172	0.202	0.223	0.236	0.244	0.247	0.246	0.241	0.23	0.213
3	0.192	0.226	0.249	0.264	0.273	0.277	0.276	0.27	0.258	0.239
4	0.206	0.242	0.266	0.282	0.291	0.295	0.294	0.288	0.276	0.255
5	0.214	0.251	0.276	0.292	0.302	0.306	0.305	0.299	0.286	0.264
6	0.218	0.255	0.281	0.297	0.307	0.311	0.31	0.304	0.29	0.268
7	0.218	0.255	0.281	0.297	0.307	0.311	0.31	0.304	0.29	0.268
8	0.214	0.251	0.276	0.292	0.302	0.306	0.305	0.299	0.286	0.264
9	0.206	0.242	0.266	0.282	0.291	0.295	0.294	0.288	0.276	0.255
10	0.192	0.226	0.249	0.264	0.273	0.277	0.276	0.27	0.258	0.239
11	0.172	0.202	0.223	0.236	0.244	0.247	0.246	0.241	0.23	0.213
12	0.142	0.166	0.182	0.192	0.198	0.2	0.2	0.195	0.187	0.173

Window

$$S3\_11(X, Y) := \text{if} \left[ (h_{\text{rm}} - d_{\text{win}} - H_p) \cdot [w_{\text{rm}} - [\text{DSC} + (Y - 1) \cdot \text{CSpan}] - \text{dis}_{\text{win}}] \geq 0, 4, 3 \right]$$

$$S3\_12(X, Y) := \text{if} \left[ (h_{\text{rm}} - d_{\text{win}} - H_p) \cdot [w_{\text{rm}} - [\text{DSC} + (Y - 1) \cdot \text{CSpan}] - \text{dis}_{\text{win}}] \geq 0, 3, 4 \right]$$

$$S3\_21(X, Y) := \text{if} \left[ (h_{\text{rm}} - d_{\text{win}} - H_p) \cdot [\text{DSC} + (Y - 1) \cdot \text{CSpan}] - \text{dis}_{\text{win}} \geq 0, 3, 4 \right]$$

$$S3\_22(X, Y) := \text{if} \left[ (h_{\text{rm}} - d_{\text{win}} - H_p) \cdot [\text{DSC} + (Y - 1) \cdot \text{CSpan}] - \text{dis}_{\text{win}} \geq 0, 4, 3 \right]$$

$$\begin{aligned} \text{FF37}(X, Y) := & \text{Sa1}(X, Y) \cdot \text{Sb1}(X, Y) \cdot F \left[ (a_x, y)_{7,1}, (b_x, y)_{7,1}, (c_x, y)_7 \right] S3\_11(X, Y) \dots \\ & + \text{Sa2}(X, Y) \cdot \text{Sb1}(X, Y) \cdot F \left[ (a_x, y)_{7,1}, (b_x, y)_{7,2}, (c_x, y)_7 \right] S3\_12(X, Y) \dots \\ & + \text{Sa1}(X, Y) \cdot \text{Sb2}(X, Y) \cdot F \left[ (a_x, y)_{7,2}, (b_x, y)_{7,1}, (c_x, y)_7 \right] S3\_21(X, Y) \dots \\ & + \text{Sa2}(X, Y) \cdot \text{Sb2}(X, Y) \cdot F \left[ (a_x, y)_{7,2}, (b_x, y)_{7,2}, (c_x, y)_7 \right] S3\_22(X, Y) \end{aligned}$$

$$F37_{\text{mm,nn}} := \text{FF37}(\text{mm}, \text{nn})$$

$$Fh_{3,7} := F37$$

Fh<sub>3,7</sub> =

	1	2	3	4	5	6	7	8	9	10
1	0.034	0.037	0.04	0.042	0.043	0.044	0.044	0.044	0.044	0.042
2	0.038	0.042	0.045	0.047	0.049	0.05	0.05	0.05	0.049	0.048
3	0.043	0.047	0.051	0.053	0.055	0.057	0.057	0.057	0.056	0.054
4	0.048	0.053	0.057	0.061	0.063	0.065	0.065	0.065	0.064	0.062
5	0.054	0.06	0.066	0.07	0.073	0.075	0.076	0.075	0.074	0.071
6	0.061	0.069	0.076	0.081	0.085	0.087	0.088	0.088	0.086	0.082
7	0.069	0.08	0.089	0.095	0.1	0.103	0.104	0.104	0.101	0.097
8	0.079	0.094	0.105	0.113	0.119	0.123	0.124	0.123	0.12	0.115
9	0.09	0.11	0.125	0.136	0.143	0.147	0.149	0.148	0.144	0.137
10	0.104	0.132	0.151	0.164	0.172	0.177	0.179	0.178	0.173	0.165
11	0.121	0.163	0.186	0.199	0.206	0.21	0.211	0.21	0.206	0.197
12	0.166	0.218	0.228	0.232	0.233	0.233	0.233	0.233	0.232	0.23

$$Fh_{3,8} := Fh_{3,1} - Fh_{3,7}$$

Fh<sub>3,8</sub> =

	1	2	3	4	5	6	7	8	9	10
1	0.017	0.018	0.019	0.02	0.02	0.021	0.021	0.02	0.02	0.019
2	0.019	0.021	0.022	0.023	0.023	0.024	0.024	0.023	0.022	0.021
3	0.022	0.024	0.026	0.027	0.027	0.027	0.027	0.027	0.026	0.025
4	0.026	0.028	0.03	0.031	0.032	0.032	0.032	0.031	0.03	0.029
5	0.03	0.033	0.035	0.037	0.038	0.038	0.038	0.037	0.036	0.034
6	0.035	0.039	0.042	0.044	0.046	0.046	0.046	0.045	0.043	0.04
7	0.042	0.048	0.052	0.055	0.056	0.057	0.056	0.055	0.053	0.049
8	0.051	0.059	0.065	0.069	0.071	0.071	0.071	0.069	0.066	0.061
9	0.064	0.076	0.084	0.089	0.092	0.093	0.092	0.09	0.085	0.079
10	0.082	0.101	0.112	0.119	0.123	0.124	0.123	0.12	0.115	0.106
11	0.11	0.141	0.156	0.164	0.168	0.17	0.169	0.167	0.161	0.151
12	0.17	0.207	0.215	0.218	0.22	0.221	0.222	0.223	0.222	0.219



Sum up view factors to verify the accuracy:

SC := 2.. 8

	1	2	3	4	5	6	7	8	9	10
1	0.967	0.989	0.993	0.992	0.99	0.989	0.989	0.99	0.992	0.993
2	0.997	0.995	0.999	1.003	1.004	1.005	1.005	1.004	1.003	0.999
3	1.004	1.002	0.996	0.994	0.995	0.995	0.995	0.995	0.994	0.996
4	1.004	1.006	0.993	0.987	0.984	0.983	0.983	0.984	0.987	0.993
5	1.002	1.007	0.991	0.981	0.976	0.974	0.974	0.976	0.981	0.991
6	1	1.006	0.989	0.977	0.971	0.969	0.969	0.971	0.977	0.989
7	0.999	1.005	0.987	0.975	0.969	0.966	0.966	0.969	0.975	0.987
8	0.999	1.002	0.986	0.975	0.969	0.967	0.967	0.969	0.975	0.986
9	0.999	0.998	0.984	0.976	0.973	0.971	0.971	0.973	0.976	0.984
10	0.999	0.993	0.985	0.982	0.981	0.98	0.98	0.981	0.982	0.985
11	0.993	0.988	0.99	0.992	0.992	0.993	0.993	0.992	0.992	0.99
12	0.97	0.99	0.991	0.988	0.985	0.983	0.983	0.985	0.988	0.991

$$\sum_{SC} F_{h2,SC} =$$

$$F_h = \left( \begin{array}{cccccccc} \{12,12\} & \{12,12\} & \{12,12\} & \{12,12\} & \{12,12\} & \{12,12\} & \{12,12\} & \{12,12\} \\ \{12,12\} & \{12,12\} & \{12,12\} & \{12,12\} & \{12,12\} & \{12,12\} & \{12,12\} & \{12,12\} \\ \{12,12\} & \{12,12\} & \{12,12\} & \{12,12\} & \{12,12\} & \{12,12\} & \{12,12\} & \{12,12\} \end{array} \right)$$

$$F_h = \left( \begin{array}{cccccccc} \{12,12\} & \{12,12\} & \{12,12\} & \{12,12\} & \{12,12\} & \{12,12\} & \{12,12\} & \{12,12\} \\ \{12,12\} & \{12,12\} & \{12,12\} & \{12,12\} & \{12,12\} & \{12,12\} & \{12,12\} & \{12,12\} \\ \{12,12\} & \{12,12\} & \{12,12\} & \{12,12\} & \{12,12\} & \{12,12\} & \{12,12\} & \{12,12\} \end{array} \right)$$

$$\sum_{SC} (F_{h3,SC})_{2,4} = 1.001$$

...sum of view factors for given orientation at a given position (x,y)

### Correction Factor for View Factors

The algorithm to calculate view factors between a person and surrounding surfaces does not generate results for the sum of view factors that add up to exactly 1.00. For example, some values add up to 0.975 which is considered accurate for most purposes. However, when calculating the MRT, absolute temperature is used - this means it is a weighted average of view factors and temperatures to the fourth power. These small differences in view factor summation will therefore be amplified when calculating MRT. Therefore, a correction factor is needed in order to force the view factors to add up to exactly 1.00:

X := 1, 2.. MR

Y := 1, 2.. NC

index := 1, 2.. 3

$$\text{CORR}(\text{index}, X, Y) := \left[ \frac{1}{\sum_{SC=2}^8 (F_{h_{\text{index}, SC}})_{X, Y}} \right]$$

ADJ(index, SC, X, Y) := CORR(index, X, Y) · (F<sub>h<sub>index, SC</sub></sub>)<sub>X, Y</sub> ...adjustment of view factors to add to 1.00

$$\sum_{SC=2}^8 \text{ADJ}(3, SC, X, Y) =$$

	1
1	1
2	1
3	1
4	1
5	1
6	1

### Definition of Orientation and Surface Temperatures

ORT := 3 ...indices of subject orientation. 1-facing south, 2-north, 3-partition.

$$T_p := \begin{pmatrix} T_{\text{exin}_p} \\ T_{\text{floorin}_p} \\ T_{\text{wallsin}_p} \\ T_{\text{ceilingin}_p} \\ T_{\text{wallsin}_p} \\ T_{\text{wallsin}_p} \\ \left| \begin{array}{l} T_{\text{sh}_p} \text{ if shade} = 1 \\ T_{\text{gin}_p} \text{ otherwise} \end{array} \right. \\ T_{\text{exin}_p} \end{pmatrix} \quad \begin{array}{l} 1 = \text{south (window + wall)} \\ 2 = \text{floor} \\ 3 = \text{west} \\ 4 = \text{ceiling} \\ 5 = \text{east} \\ 6 = \text{north} \\ 7 = \text{window} \\ 8 = \text{south wall (spandrel)} \end{array}$$

$$\text{MRT}(X, Y, p) := \sqrt[4]{\sum_{i=2}^8 \left[ (\text{ADJ}(\text{ORT}, i, X, Y)) \cdot [(T_p + 273)_i]^4 \right]} - 273$$

$$\text{MRT}\left(2, 8, 62 \frac{\text{hr}}{\text{dt}}\right) = 24.187$$

## Mean projected Area Factor for seated people (fp)

The mean projected area factor (fp) takes into account the position and orientation of the person relative to the sun's position (azimuth and altitude). A new parameter, the "person-solar azimuth angle" is used to define the azimuth angle between the sun and the front of the person (analogous to the surface-solar azimuth angle for tilted surfaces).

### Person-solar azimuth angle:

$$\text{Person's orientation: } \theta_{\text{per}} := \begin{cases} (0\text{deg}) & \text{if } \text{ORT} = 1 \\ (180\text{deg}) & \text{if } \text{ORT} = 2 \\ (90\text{deg}) & \text{if } \text{ORT} = 3 \end{cases} \quad \begin{matrix} \text{(facing facade = 0, with facade to} \\ \text{left, } \psi = +90\text{deg)} \end{matrix}$$

$$\gamma_{\text{per}_p} := \gamma_{s_p} + \theta_{\text{per}} \quad \dots \text{person-solar azimuth}$$

$$f_p(n, t) = \sum_{i=0}^4 Af_{i,j}(\alpha_s(n, t)) \gamma_{\text{per}}^i \quad \dots \text{a function of solar altitude, } \alpha, \text{ and person-solar azimuth angle, } \gamma_{\text{per}}$$

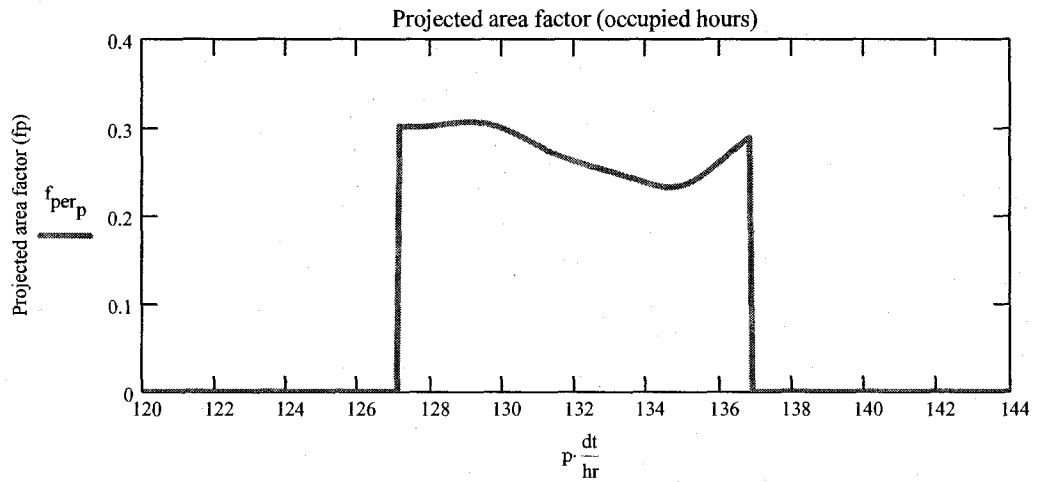
$$Af_{i,j}(n, t) = \sum_{j=0}^3 K_{\text{coeff}_{i,j}} \cdot \alpha_s(n, t)^j$$

$$K_{\text{coeff}} := \begin{pmatrix} 2.884 \cdot 10^{-1} & 2.225 \cdot 10^{-3} & -5.47 \cdot 10^{-5} & 1.802 \cdot 10^{-7} \\ 2.225 \cdot 10^{-3} & -7.653 \cdot 10^{-5} & 7.286 \cdot 10^{-7} & -1.457 \cdot 10^{-9} \\ -9.292 \cdot 10^{-5} & 4.021 \cdot 10^{-6} & -6.215 \cdot 10^{-8} & 3.152 \cdot 10^{-10} \\ 9.027 \cdot 10^{-7} & -4.632 \cdot 10^{-8} & 7.69 \cdot 10^{-10} & -4.015 \cdot 10^{-12} \\ -2.517 \cdot 10^{-9} & 1.38 \cdot 10^{-10} & -2.341 \cdot 10^{-12} & 1.231 \cdot 10^{-14} \end{pmatrix} \quad \dots \text{coeff. of the polynomial algorithm}$$

i := 1, 2.. 5

$$Af_{p,i} := \left[ \sum_{j=1}^4 \left[ K_{\text{coeff}_{i,j}} \left[ \alpha_{s_p} \cdot \left( \frac{180}{\pi} \right) \right]^{(j-1)} \right] \right]$$

$$f_{\text{per}_p} := \begin{cases} \left[ \left[ \sum_{i=1}^5 \left[ Af_{p,i} \left[ \gamma_{\text{per}_p} \cdot \left( \frac{180}{\pi} \right) \right]^{(i-1)} \right] \right] \right] & \text{if } 12\text{hr} - t_{\text{ss}}(n) \leq \text{mod}(p \cdot dt, 24 \cdot 3600\text{sec}) \leq 12\text{hr} + t_{\text{ss}}(n) \\ 0 & \text{otherwise} \end{cases}$$



## CALCULATION OF MEAN RADIANT TEMPERATURE

### MRT due to interior surface temperatures only:

$$MRT(X, Y, p) := \sqrt[4]{\sum_{i=2}^8 \left[ (ADJ(ORT, i, X, Y)) \cdot [(T_p + 273)]_i^4 \right]} - 273$$

### MRT due to solar radiation and interior surface temperatures

$\epsilon_s := 0.9$  ...emissivity of person

$\alpha_{b\_per} := 0.8$  ...beam absorptance of person

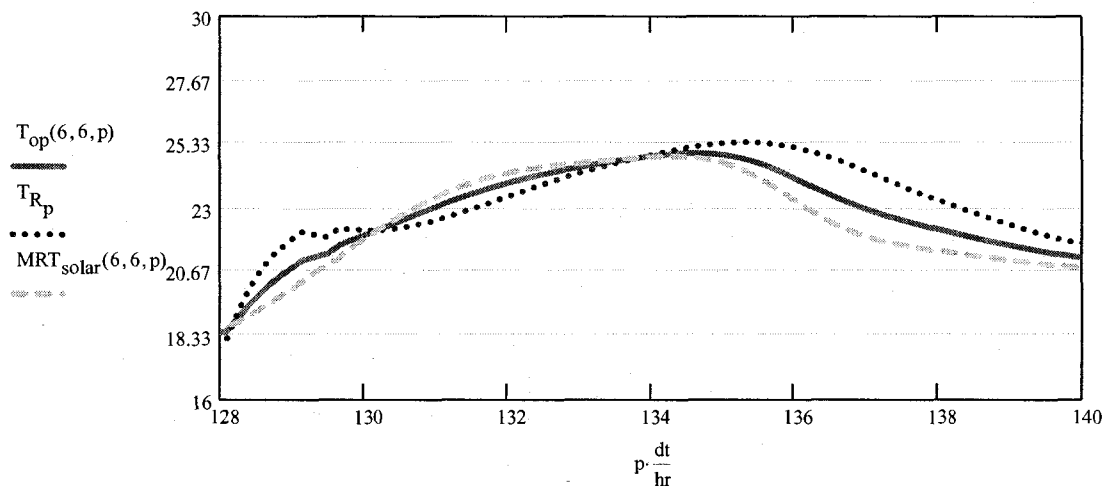
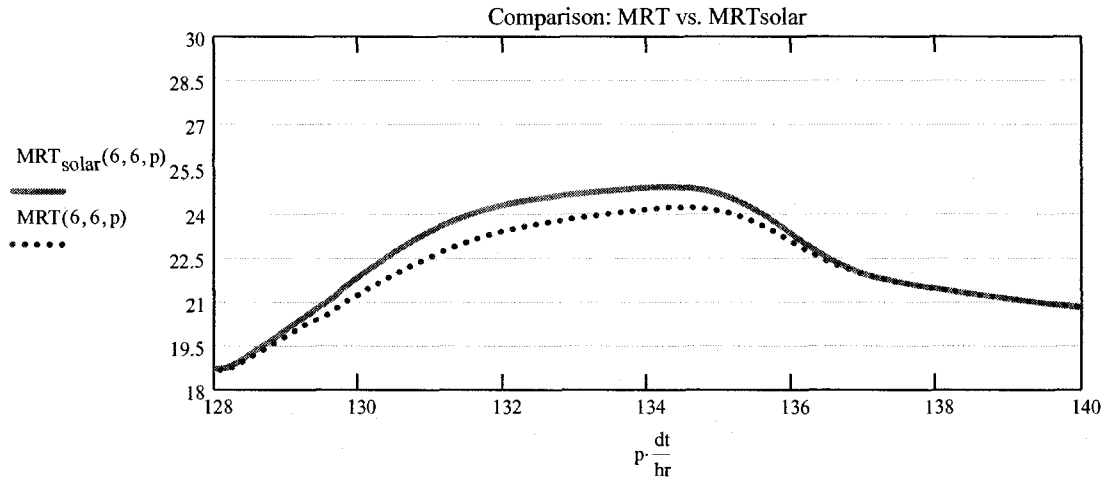
$\alpha_{d\_per} := 0.5$  ... diffuse absorptance of person

$\tau_{facade,p} := \begin{cases} \tau_e \cdot \tau_{sh} & \text{if shade} = 1 \\ \tau_e & \text{otherwise} \end{cases}$  ...solar transmittance of facade system with and without shading device

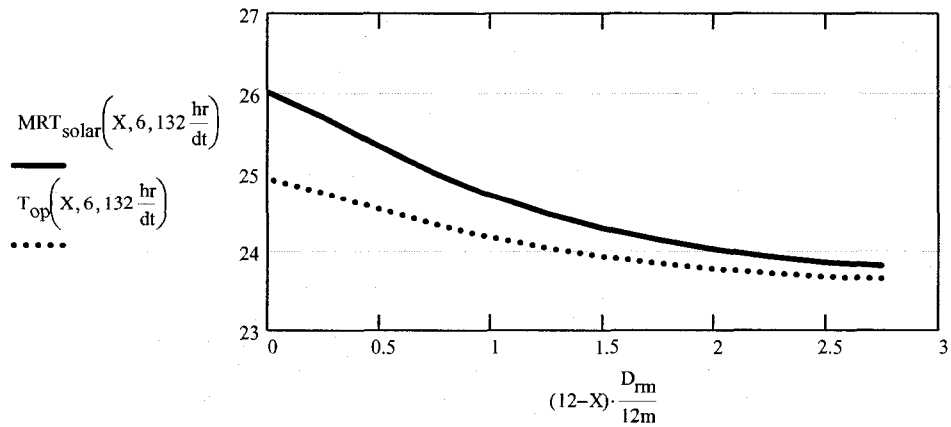
$$MRT_{solar}(X, Y, p) := \sqrt[4]{\sum_{i=2}^8 \left[ (ADJ(ORT, i, X, Y)) \cdot [(T_p + 273)]_i^4 \right]} + \frac{1}{\epsilon_s \cdot \frac{\text{watt}}{\text{m}^2 \cdot \text{K}^4}} \left[ \alpha_{d\_per} \cdot ADJ(ORT, 7, X, Y) \cdot \frac{I_{d,p} \cdot \tau_{de} \cdot \text{if}(\text{shade} = 1, \tau_{sh}, 1)}{\frac{\text{watt}}{\text{m}^2}} + \alpha_{b\_per} \cdot f_{per,p} \cdot \frac{I_{b,p} \cdot \tau_e \cdot \text{if}(\text{shade} = 1, \tau_{sh}, 1)}{\frac{\text{watt}}{\text{m}^2}} \right] - 273$$

## Operative Temperature:

$$T_{op}(X, Y, p) := \frac{3.1 T_{R_p} + 4.3 MRT_{solar}(X, Y, p)}{4.3 + 3.1}$$



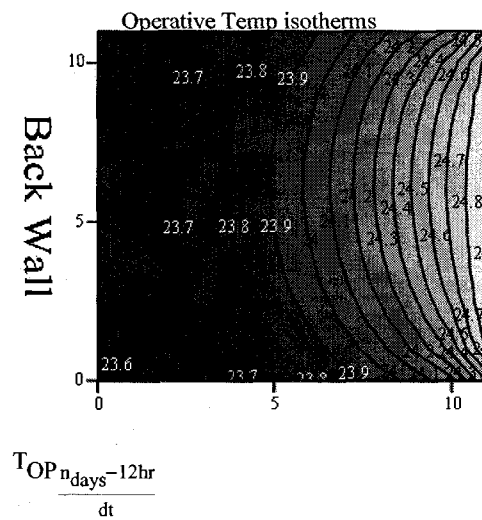
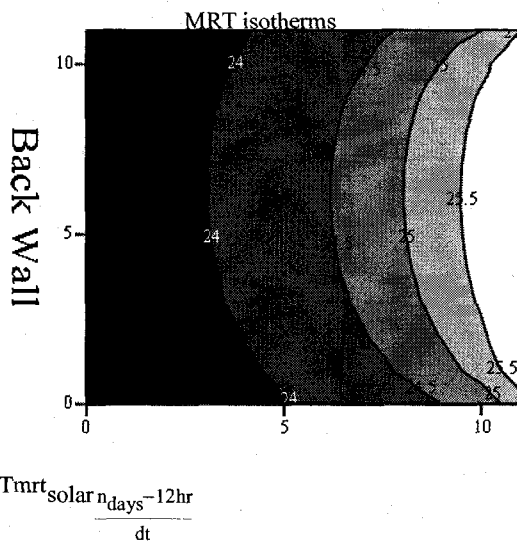
### MRT and Operative temperature as a function of distance from facade:



## Isotherms of MRT and Operative temperature (Plan View):

$$T_{mrt\_solar} := \begin{cases} \text{for } pc \in \left[ \frac{n_{days} - 1 \text{ day}}{dt}, \left( \frac{n_{days} - 1 \text{ day}}{dt} + 12 \right) .. \left( \frac{n_{days}}{dt} \right) \right] \\ \quad \begin{cases} \text{for } l \in 1..MR \\ \quad \text{for } k \in 1..NC \\ \quad \quad MRT_{p_{k,l}} \leftarrow MRT_{solar}(k,l,pc) \\ \quad \quad T_{mrt\_solar}_{pc} \leftarrow MRT_{p_{k,l}} \end{cases} \\ \quad T_{mrt\_solar} \end{cases}$$

$$T_{OP} := \begin{cases} \text{for } pc \in \left[ \frac{n_{days} - 1 \text{ day}}{dt}, \left( \frac{n_{days} - 1 \text{ day}}{dt} + 12 \right) .. \left( \frac{n_{days}}{dt} \right) \right] \\ \quad \begin{cases} \text{for } l \in 1..MR \\ \quad \text{for } k \in 1..NC \\ \quad \quad T_{op_{k,l}} \leftarrow T_{op}(k,l,pc) \\ \quad \quad T_{OP}_{pc} \leftarrow T_{op} \end{cases} \\ \quad T_{OP} \end{cases}$$



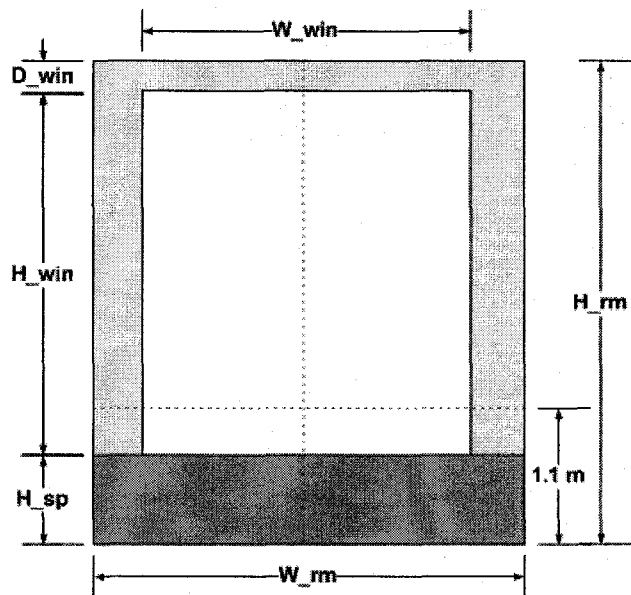
## RADIANT TEMPERATURE ASYMMETRY

The radiant temperature asymmetry (RTA) is the difference between plane radiant temperature in opposite directions. For this case, plane radiant temperature is calculated in the direction of the window and in the direction of the opposing wall. Therefore, RTA can be computed due to the effect of a hot/cold window surface.

### Vertical Surfaces

$$df := 0.0001, 0.5 \dots \frac{D_{rm}}{m} \quad \dots \text{distance from facade (m)}$$

#### Facade Wall



$$T_{op\_df}(X) := T_{op}\left(X, 6, 156 \frac{hr}{dt}\right)$$

#### TOP

$$a := h_{rm} - 1.1 \quad b := \frac{w_{rm}}{2} \quad c(df) := df \quad x(df) := \frac{a}{c(df)} \quad y(df) := \frac{b}{c(df)}$$

$$F_{pr\_south\_top}(df) := 2 \cdot \frac{1}{2 \cdot \pi} \left[ \frac{x(df)}{\sqrt{1 + (x(df))^2}} \cdot \text{atan} \left[ \frac{y(df)}{\sqrt{1 + (x(df))^2}} \right] + \frac{y(df)}{\sqrt{1 + (y(df))^2}} \cdot \text{atan} \left[ \frac{x(df)}{\sqrt{1 + (y(df))^2}} \right] \right]$$

#### TOP, GLAZING part

$$a := h_{rm} - 1.1 - d_{win} \quad b := \frac{w_{win}}{2} \quad x(df) := \frac{a}{c(df)} \quad y(df) := \frac{b}{c(df)}$$

$$F_{pr\_glazing\_top}(df) := 2 \cdot \frac{1}{2 \cdot \pi} \left[ \frac{x(df)}{\sqrt{1 + (x(df))^2}} \cdot \operatorname{atan} \left[ \frac{y(df)}{\sqrt{1 + (x(df))^2}} \right] + \frac{y(df)}{\sqrt{1 + (y(df))^2}} \cdot \operatorname{atan} \left[ \frac{x(df)}{\sqrt{1 + (y(df))^2}} \right] \right]$$

### TOP, WALL part

$$F_{pr\_southwall\_top}(df) := F_{pr\_south\_top}(df) - F_{pr\_glazing\_top}(df)$$

### BOTTOM (entire)

$$a := 1.1 \quad b := \frac{w_{rm}}{2} \quad x(df) := \frac{a}{c(df)} \quad y(df) := \frac{b}{c(df)}$$

$$F_{pr\_south\_bottom}(df) := 2 \cdot \frac{1}{2 \cdot \pi} \left[ \frac{x(df)}{\sqrt{1 + (x(df))^2}} \cdot \operatorname{atan} \left[ \frac{y(df)}{\sqrt{1 + (x(df))^2}} \right] + \frac{y(df)}{\sqrt{1 + (y(df))^2}} \cdot \operatorname{atan} \left[ \frac{x(df)}{\sqrt{1 + (y(df))^2}} \right] \right]$$

### BOTTOM, GLAZING part

$$a := 1.1 - e_{win} \quad b := \frac{w_{win}}{2} \quad x(df) := \frac{a}{c(df)} \quad y(df) := \frac{b}{c(df)}$$

$$F_{pr\_glazing\_bottom}(df) := 2 \cdot \frac{1}{2 \cdot \pi} \left[ \frac{x(df)}{\sqrt{1 + (x(df))^2}} \cdot \operatorname{atan} \left[ \frac{y(df)}{\sqrt{1 + (x(df))^2}} \right] + \frac{y(df)}{\sqrt{1 + (y(df))^2}} \cdot \operatorname{atan} \left[ \frac{x(df)}{\sqrt{1 + (y(df))^2}} \right] \right]$$

### BOTTOM, GLAZING + WALL (edges beside window)

$$b := \frac{w_{rm}}{2} \quad y(df) := \frac{b}{c(df)}$$

$$F_{pr\_glazing\_wall}(df) := 2 \cdot \frac{1}{2 \cdot \pi} \left[ \frac{x(df)}{\sqrt{1 + (x(df))^2}} \cdot \operatorname{atan} \left[ \frac{y(df)}{\sqrt{1 + (x(df))^2}} \right] + \frac{y(df)}{\sqrt{1 + (y(df))^2}} \cdot \operatorname{atan} \left[ \frac{x(df)}{\sqrt{1 + (y(df))^2}} \right] \right]$$

### BOTTOM, WALL

$$F_{pr\_southwall\_bottom}(df) := F_{pr\_glazing\_wall}(df) - F_{pr\_glazing\_bottom}(df)$$

### BOTTOM, SPANDREL

$$F_{pr\_spandrel}(df) := F_{pr\_south\_bottom}(df) - F_{pr\_glazing\_wall}(df)$$

## TOTAL GLAZING

$$F_{pr\_glazing}(df) := F_{pr\_glazing\_top}(df) + F_{pr\_glazing\_bottom}(df)$$

## TOTAL SOUTH WALL (facade excluding glazing)

$$F_{pr\_south\_wall}(df) := F_{pr\_southwall\_top}(df) + F_{pr\_southwall\_bottom}(df) + F_{pr\_spandrel}(df)$$

## Back Wall

### TOP

$$a := h_{rm} - 1.1 \quad b := \frac{w_{rm}}{2} \quad c(df) := d_{rm} - df \quad x(df) := \frac{a}{c(df)} \quad y(df) := \frac{b}{c(df)}$$

$$F_{pr\_north\_top}(df) := 2 \cdot \frac{1}{2 \cdot \pi} \left[ \frac{x(df)}{\sqrt{1 + (x(df))^2}} \cdot \operatorname{atan} \left[ \frac{y(df)}{\sqrt{1 + (x(df))^2}} \right] + \frac{y(df)}{\sqrt{1 + (y(df))^2}} \cdot \operatorname{atan} \left[ \frac{x(df)}{\sqrt{1 + (y(df))^2}} \right] \right]$$

### BOTTOM

$$a := 1.1 \quad x(df) := \frac{a}{c(df)}$$

$$F_{pr\_north\_bottom}(df) := 2 \cdot \frac{1}{2 \cdot \pi} \left[ \frac{x(df)}{\sqrt{1 + (x(df))^2}} \cdot \operatorname{atan} \left[ \frac{y(df)}{\sqrt{1 + (x(df))^2}} \right] + \frac{y(df)}{\sqrt{1 + (y(df))^2}} \cdot \operatorname{atan} \left[ \frac{x(df)}{\sqrt{1 + (y(df))^2}} \right] \right]$$

## TOTAL NORTH WALL

$$F_{pr\_north}(df) := F_{pr\_north\_top}(df) + F_{pr\_north\_bottom}(df)$$

## Side Walls

### TOP, FORWARD

$$a(df) := df \quad b := h_{rm} - 1.1 \quad c := \frac{w_{rm}}{2}$$

$$x(df) := \frac{a(df)}{b} \quad y := \frac{c}{b}$$

$$Fpr_{top\_forward}(df) := 2 \cdot \frac{1}{2 \cdot \pi} \left( \operatorname{atan}\left(\frac{1}{y}\right) - \frac{y}{\sqrt{x(df)^2 + y^2}} \cdot \operatorname{atan}\left(\frac{1}{\sqrt{x(df)^2 + y^2}}\right) \right)$$

### TOP, BEHIND

$$a(df) := d_{rm} - df \quad b := h_{rm} - 1.1 \quad c := \frac{w_{rm}}{2}$$

$$x(df) := \frac{a(df)}{b} \quad y := \frac{c}{b}$$

$$Fpr_{top\_behind}(df) := 2 \cdot \frac{1}{2 \cdot \pi} \left( \operatorname{atan}\left(\frac{1}{y}\right) - \frac{y}{\sqrt{x(df)^2 + y^2}} \cdot \operatorname{atan}\left(\frac{1}{\sqrt{x(df)^2 + y^2}}\right) \right)$$

### BOTTOM, FOWARD

$$a(df) := df \quad b := 1.1 \quad c := \frac{w_{rm}}{2}$$

$$x(df) := \frac{a(df)}{b} \quad y := \frac{c}{b}$$

$$Fpr_{bottom\_forward}(df) := 2 \cdot \frac{1}{2 \cdot \pi} \left( \operatorname{atan}\left(\frac{1}{y}\right) - \frac{y}{\sqrt{x(df)^2 + y^2}} \cdot \operatorname{atan}\left(\frac{1}{\sqrt{x(df)^2 + y^2}}\right) \right)$$

### BOTTOM, BEHIND

$$a(df) := d_{rm} - df \quad b := 1.1 \quad c := \frac{w_{rm}}{2}$$

$$x(df) := \frac{a(df)}{b} \quad y := \frac{c}{b}$$

$$Fpr_{bottom\_behind}(df) := 2 \cdot \frac{1}{2 \cdot \pi} \left( \operatorname{atan}\left(\frac{1}{y}\right) - \frac{y}{\sqrt{x(df)^2 + y^2}} \cdot \operatorname{atan}\left(\frac{1}{\sqrt{x(df)^2 + y^2}}\right) \right)$$

### TOTAL WALLS FORWARD

$$Fpr_{walls\_forward}(df) := Fpr_{top\_forward}(df) + Fpr_{bottom\_forward}(df)$$

### TOTAL WALLS BEHIND

$$Fpr_{walls\_behind}(df) := Fpr_{top\_behind}(df) + Fpr_{bottom\_behind}(df)$$

## Ceiling

### FORWARD

$$a(df) := df \quad b := \frac{w_{rm}}{2} \quad c := h_{rm} - 1.1$$

$$x(df) := \frac{a(df)}{b} \quad y := \frac{c}{b}$$

$$Fpr_{ceiling\_forward}(df) := 2 \cdot \left[ \frac{1}{2 \cdot \pi} \left( \operatorname{atan}\left(\frac{1}{y}\right) - \frac{y}{\sqrt{x(df)^2 + y^2}} \cdot \operatorname{atan}\left(\frac{1}{\sqrt{x(df)^2 + y^2}}\right) \right) \right]$$

### BEHIND

$$a(df) := d_{rm} - df \quad b := \frac{w_{rm}}{2} \quad c := h_{rm} - 1.1$$

$$x(df) := \frac{a(df)}{b} \quad y := \frac{c}{b}$$

$$Fpr_{ceiling\_behind}(df) := 2 \cdot \left[ \frac{1}{2 \cdot \pi} \left( \operatorname{atan}\left(\frac{1}{y}\right) - \frac{y}{\sqrt{x(df)^2 + y^2}} \cdot \operatorname{atan}\left(\frac{1}{\sqrt{x(df)^2 + y^2}}\right) \right) \right]$$

## Floor

### FORWARD

$$a(df) := df \quad b := \frac{w_{rm}}{2} \quad c := 1.1$$

$$x(df) := \frac{a(df)}{b} \quad y := \frac{c}{b}$$

$$Fpr_{floor\_forward}(df) := 2 \cdot \left[ \frac{1}{2 \cdot \pi} \left( \operatorname{atan}\left(\frac{1}{y}\right) - \frac{y}{\sqrt{x(df)^2 + y^2}} \cdot \operatorname{atan}\left(\frac{1}{\sqrt{x(df)^2 + y^2}}\right) \right) \right]$$

### BEHIND

$$a(df) := d_{rm} - df \quad b := \frac{w_{rm}}{2} \quad c := 1.1$$

$$x(df) := \frac{a(df)}{b} \quad y := \frac{c}{b}$$

$$F_{pr\_floor\_behind}(df) := 2 \cdot \left[ \frac{1}{2 \cdot \pi} \left( \operatorname{atan}\left(\frac{1}{y}\right) - \frac{y}{\sqrt{x(df)^2 + y^2}} \cdot \operatorname{atan}\left(\frac{1}{\sqrt{x(df)^2 + y^2}}\right) \right) \right]$$

**Check for unity:**

$$F_{pr\_glazing}(df) + F_{pr\_south\_wall}(df) + F_{pr\_walls\_forward}(df) + F_{pr\_ceiling\_forward}(df) + F_{pr\_floor\_forward}(df) =$$

$$\begin{pmatrix} 1 \\ 1 \\ 1 \\ 1 \\ 1 \\ 1 \\ 1 \end{pmatrix}$$

## FORWARD PLANE

$$T_{pr1}(df, p) := \sqrt[4]{ \left[ Fpr_{glazing}(df) \cdot \left[ \begin{array}{l} (T_{sh_p} + 273)^4 \text{ if shade} = 1 \quad \dots \\ (T_{gin_p} + 273)^4 \text{ otherwise} \end{array} \right] \dots - 273 \right] } + \left[ \begin{array}{l} \frac{1}{\sigma} \cdot Fpr_{glazing}(df) \cdot \frac{\tau_{de} \cdot I_{d_p} \cdot \text{if}(\text{shade} = 1, \tau_{sh}, 1)}{\text{watt} / \text{m}^2} \dots \\ \frac{\epsilon_s \cdot \text{watt} / \text{m}^2 \cdot \text{K}^4}{\text{m}^2} \\ \tau_{e_p} \cdot I_{b_p} \cdot \text{if}(\text{shade} = 1, \tau_{sh}, 1) \\ \frac{\text{watt}}{\text{m}^2} \end{array} \right] + \left[ Fpr_{south\_wall}(df) \cdot (T_{exin_p} + 273)^4 + Fpr_{walls\_forward}(df) \cdot (T_{wallsin_p} + 273)^4 \right] \dots + Fpr_{floor\_forward}(df) \cdot (T_{floorin_p} + 273)^4 + Fpr_{ceiling\_forward}(df) \cdot (T_{ceilingin_p} + 273)^4$$

$$T_{pr1}(1.5, 720) = 27.522$$

## BACKWARD PLANE

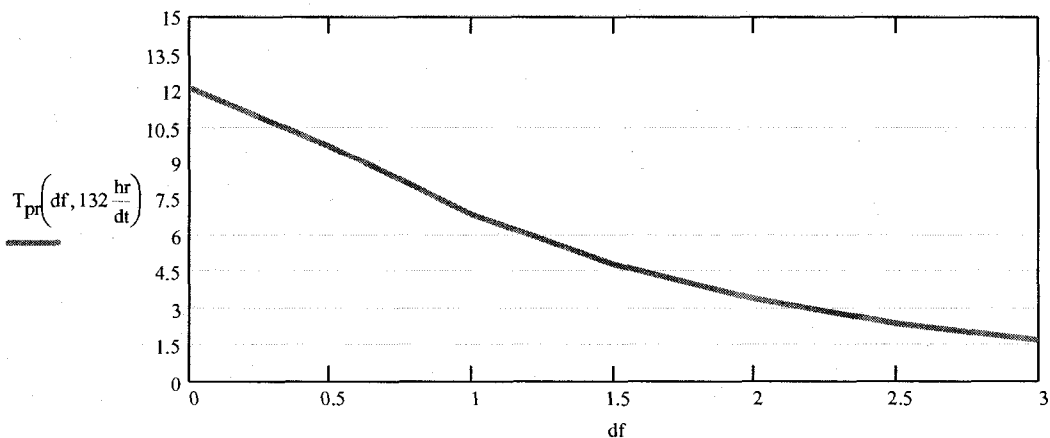
$$T_{pr2}(df, p) := \sqrt[4]{ \left[ \left( Fpr_{walls\_behind}(df) \cdot (T_{wallsin_p} + 273)^4 + Fpr_{north}(df) \cdot (T_{wallsin_p} + 273)^4 \right) \dots - 273 \right] + Fpr_{floor\_behind}(df) \cdot (T_{floorin_p} + 273)^4 + Fpr_{ceiling\_behind}(df) \cdot (T_{ceilingin_p} + 273)^4$$

$$T_{pr2}(1.5, 725) = 22.986$$

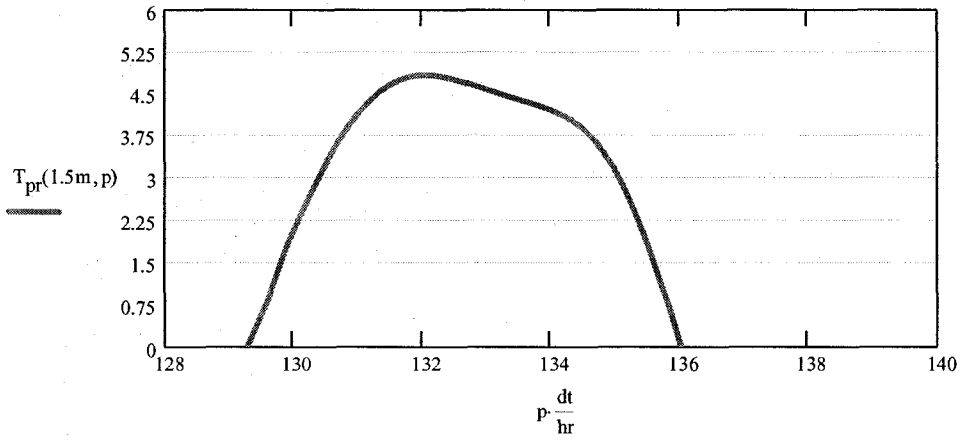
## RADIANT TEMPERATURE ASYMMETRY

$$T_{pr}(df, p) := T_{pr1}(df, p) - T_{pr2}(df, p)$$

**RTA as function of distance from facade:**



**RTA as function of time (center of room):**



$$n\_p := \left[ \frac{n\_days - 2day}{dt}, \left( \frac{n\_days - 2day}{dt} + 1 \right) .. \left( \frac{n\_days - 1day}{dt} \right) \right]$$

MRT(6, 6, n\_p) =

	1
1	19.427
2	19.398
3	19.368
4	19.338
5	19.308
6	19.279
7	19.25
8	19.221
9	19.199
10	19.182

MRT<sub>solar</sub>(6, 6, n\_p) =

	1
1	19.428
2	19.398
3	19.369
4	19.339
5	19.31
6	19.28
7	19.251
8	19.222
9	19.2
10	19.183

T<sub>op</sub>(6, 6, n\_p) =

	1
1	18.922
2	18.882
3	18.842
4	18.803
5	18.763
6	18.725
7	18.686
8	18.67
9	18.66
10	18.654

T<sub>pr</sub>( $\frac{D_{rm}}{2m}$ , n\_p) =

	1
1	-2.93
2	-2.93
3	-2.931
4	-2.932
5	-2.933
6	-2.934
7	-2.936
8	-2.937
9	-2.937
10	-2.935

T<sub>pr</sub>(df, 720) =

11.978
9.611
6.806
4.793
3.393
2.428
1.774

# THERMAL COMFORT MODEL

This file is used for analysis of thermal comfort based on the principles of human thermoregulation using a transient two-node model. The environmental variables calculated in the building thermal simulation model (room air temperature, mean radiant temperature) are used as inputs into this model. For this model, several assumptions need to be made for several parameters, such as: clothing insulation, body mass, surface area, metabolic rate, etc. Details regarding the thermoregulation model can be found in the literature (ASJHRAE Handbook, 2005; Parsons, Human Thermal Environments, 2003)

$$\text{kPa} = 1000\text{Pa} \quad \text{K} = 1$$

$$X := 6 \quad Y := 6 \quad \dots \text{position in room (X = distance from window, Y = distance from wall)}$$

$$M := 1.2 \cdot \left( 58.15 \cdot \frac{\text{watt}}{\text{m}^2} \right) \quad \dots \text{metabolic rate} \quad Wk := 0 \frac{\text{watt}}{\text{m}^2} \quad \dots \text{external work}$$

$$A_D := 1.8\text{m}^2 \quad \dots \text{DuBois surface area} \quad m_b := 80\text{kg} \quad \dots \text{body mass} \quad RH := 0.5 \quad \dots \text{relative humidity}$$

$$v_{\text{air}} := 0.1 \quad \dots \text{air velocity (m/s)} \quad \text{clo} := \begin{pmatrix} 0.5 & \text{if season} = 1 \\ 0.9 & \text{if season} = 2 \end{pmatrix} \quad \dots \text{clothing insulation}$$

$$C_{pB} := 3490 \frac{\text{J}}{\text{kg} \cdot \text{degC}} \quad \dots \text{specific heat of the body}$$

$$C_{pb} := 4187 \frac{\text{J}}{\text{kg} \cdot \text{degC}} \quad \dots \text{specific heat of blood}$$

$$k_{\text{crsk}} := 5.28 \frac{\text{watt}}{\text{m}^2 \cdot \text{degC}} \quad \dots \text{thermal conductance between core and skin}$$

$$T_{\text{cr}_n} := 36.8\text{degC} \quad \dots \text{neutral core temp.}$$

$$T_{\text{sk}_n} := 33.7\text{degC} \quad \dots \text{neutral skin temp.}$$

$$T_{B_n} := 36.49\text{degC} \quad \dots \text{neutral body temp.}$$

$$A_1 := -5.8002206 \cdot 10^3$$

$$A_2 := 1.3914993$$

$$A_3 := -48.640239 \cdot 10^{-3}$$

...coefficients used for calculating partial pressure at skin

$$A_4 := 41.764768 \cdot 10^{-6}$$

$$A_5 := -14.452093 \cdot 10^{-9}$$

$$A_7 := 6.5459673$$

$$h_{c\_cl\_air} := \text{if}(v_{\text{air}} < 0.2, 3.1, 8.3 \cdot v_{\text{air}}^{0.6}) \frac{\text{watt}}{\text{m}^2 \cdot \text{degC}}$$

...convective heat transfer coefficient between clothing and room air

$$f_{cl} := 1 + 0.3 \cdot \text{clo} \quad \dots \text{fractional increase in body surface attributed to clothing}$$

$$E_{\text{res}} = 0.0173 \cdot M \cdot \left( 5.87 - \frac{P_{\text{air}}}{\text{kPa}} \right) \quad \dots \text{latent evaporative heat loss by respiration}$$

$$R_{e\_cl} := 0.033 \frac{\text{m}^2 \text{kPa}}{\text{watt}} \quad \dots \text{evaporative resistance of clothing (Human Thermal Environments, Ch. 7)}$$

$$i_m := 0.4 \quad \dots \text{moisture permeability (ASHRAE)}$$

$$h_e := 16.5 \frac{\text{K}}{\text{kPa}} \cdot i_m \cdot h_{c\_cl\_air} \quad \dots \text{evaporative heat transfer coefficient}$$

$$h_e = 20.46 \frac{\text{watt}}{\text{m}^2 \text{kPa}}$$

$$E_{\text{max}} = h_e \cdot (P_{\text{sk\_pp}} - p_{\text{w\_pp}}) \quad \dots \text{max. evaporative heat loss}$$

### TIME STEP:

The environmental variables (MRT, room air temperature, etc.) calculated in the building thermal simulation model must be converted to the new time step that is to be used in the thermal comfort model. Two-node thermal comfort models are usually performed with a time step of between 20 - 60 seconds. For this simulation, a time step of 60 seconds is selected.

### Fourier transform:

$$nn := 1, 2.. 100 \quad j := \sqrt{-1}$$

$$\omega_{nn} := \frac{2 \cdot \pi \cdot (nn - 1)}{n_{\text{days}}}$$

$$\text{MRT1}_p := \text{MRT}(X, Y, p)$$

$$\text{MRT1}_{\text{solar}_p} := \text{MRT}_{\text{solar}}(X, Y, p)$$

$$T_{\text{opl}_p} := T_{\text{op}}(X, Y, p)$$

$$\frac{n_{\text{days}}}{dt} = 2.016 \times 10^3$$

$$\text{paux} := 1, 2.. \frac{n_{\text{days}}}{dt}$$

$$TT_{R_{nn}} := \sum_{\text{paux}} T_{R_{\text{paux}}} \cdot \frac{\exp(-j \cdot \omega_{nn} \cdot \text{paux} \cdot dt)}{n_{\text{days}}} \cdot dt$$

$$\text{MRTT}_{\text{solar}_{nn}} := \sum_{\text{paux}} \text{MRT1}_{\text{solar}_{\text{paux}}} \cdot \frac{\exp(-j \cdot \omega_{nn} \cdot \text{paux} \cdot dt)}{n_{\text{days}}} \cdot dt$$

$$\text{MRTT}_{nn} := \sum_{\text{paux}} \text{MRT1}_{\text{paux}} \cdot \frac{\exp(-j \cdot \omega_{nn} \cdot \text{paux} \cdot dt)}{n_{\text{days}}} \cdot dt$$

$$\text{TT}_{\text{op}_{nn}} := \sum_{\text{paux}} \text{T}_{\text{op1}_{\text{paux}}} \cdot \frac{\exp(-j \cdot \omega_{nn} \cdot \text{paux} \cdot dt)}{n_{\text{days}}} \cdot dt$$

$$\text{dt}_{\text{comf}} := 60\text{sec} \quad \dots \text{simulation time step for thermal comfort model} \quad \frac{n_{\text{days}}}{\text{dt}_{\text{comf}}} = 1.008 \times 10^4$$

$$\text{pp} := 1, 2, \dots, \frac{n_{\text{days}}}{\text{dt}_{\text{comf}}} \quad \dots \text{number of timesteps} \quad \text{tt}_{\text{pp}} := \text{pp} \cdot \text{dt}_{\text{comf}} \quad \dots \text{times at which simulation will be performed}$$

**Generation of data for each time step (back in time domain):**

$$n1 := 2, 3, \dots, 100$$

$$\text{T}_{\text{R}_{\text{pp}}} := \text{TT}_{\text{R}_1} + 2 \left( \sum_{n1} \text{Re} \left( \text{TT}_{\text{R}_{n1}} \cdot \exp(j \cdot \omega_{n1} \cdot \text{tt}_{\text{pp}}) \right) \right)$$

$$\text{MRT}_{\text{solar}_{\text{pp}}} := \text{MRTT}_{\text{solar}_1} + 2 \left( \sum_{n1} \text{Re} \left( \text{MRTT}_{\text{solar}_{n1}} \cdot \exp(j \cdot \omega_{n1} \cdot \text{tt}_{\text{pp}}) \right) \right)$$

$$\text{MRT}_{\text{pp}} := \text{MRTT}_1 + 2 \left( \sum_{n1} \text{Re} \left( \text{MRTT}_{n1} \cdot \exp(j \cdot \omega_{n1} \cdot \text{tt}_{\text{pp}}) \right) \right)$$

$$\text{T}_{\text{op}_{\text{pp}}} := \text{TT}_{\text{op}_1} + 2 \cdot \left( \sum_{n1} \text{Re} \left( \text{TT}_{\text{op}_{n1}} \cdot \exp(j \cdot \omega_{n1} \cdot \text{tt}_{\text{pp}}) \right) \right)$$

**Initial Conditions:**

$T_{sk_1} := T_{sk\_n}$  ...initial skin temperature = neutral skin temperature

$T_{cr_1} := T_{cr\_n}$  ...initial core temperature = neutral core temperature

$\left( \begin{array}{l} \text{WSIG}_{cr_1} \\ \text{CSIG}_{cr_1} \\ \text{WSIG}_{sk_1} \\ \text{CSIG}_{sk_1} \\ \text{WSIG}_{B_1} \\ \text{SKBF}_1 \\ h_{r\_cl\_air_1} \\ \alpha_{mass_1} \\ T_{B_1} \\ E_{rsw_1} \\ T_{abs_1} \\ P_{sk_1} \\ w_1 \end{array} \right)$	$:=$	$\left( \begin{array}{l} 0 \\ 0 \\ 0 \\ 0 \\ 0 \frac{\text{kg}}{\text{sec} \cdot \text{m}^2} \\ 3.7 \frac{\text{watt}}{\text{m}^2 \text{degC}} \\ 0.1 \\ 36 \text{degC} \\ 0 \frac{\text{watt}}{\text{m}^2} \\ 313 \text{K} \\ 5 \text{kPa} \\ 0 \end{array} \right)$	$\left( \begin{array}{l} w_1 \\ E_{sk_1} \\ T_{cl_1} \\ CS_1 \\ Q_{crsk_1} \\ C_{res_1} \\ RS_1 \\ S_{cr_1} \\ S_{sk_1} \\ Q_{bl_1} \\ P_{sat_1} \\ P_{w_1} \\ E_{max_1} \\ E_{res_1} \end{array} \right)$	$:=$	$\left( \begin{array}{l} 0 \\ 0 \frac{\text{watt}}{\text{m}^2} \\ 30 \text{degC} \\ 0 \frac{\text{watt}}{\text{m}^2} \\ 40 \frac{\text{L}}{\text{hr} \cdot \text{m}^2} \\ 2 \text{kPa} \\ 1 \text{kPa} \\ 100 \frac{\text{watt}}{\text{m}^2} \\ 20 \frac{\text{watt}}{\text{m}^2} \end{array} \right)$
---	------	---	--	------	--

$$0 \text{ if } T_{cr\_pp} \leq T_{cr\_n}$$

$$T_{cr\_pp} - T_{cr\_n} \text{ otherwise}$$

$$0 \text{ if } T_{cr\_pp} \geq T_{cr\_n}$$

$$T_{cr\_n} - T_{cr\_pp} \text{ otherwise}$$

$$0 \text{ if } T_{sk\_pp} \leq T_{sk\_n}$$

$$T_{sk\_pp} - T_{sk\_n} \text{ otherwise}$$

$$0 \text{ if } T_{sk\_pp} \geq T_{sk\_n}$$

$$T_{sk\_n} - T_{sk\_pp} \text{ otherwise}$$

$$0 \text{ if } T_{B\_pp} \leq T_{B\_n}$$

$$T_{B\_pp} - T_{B\_n} \text{ otherwise}$$

$$6.3 + 200 \cdot \text{WSIG}_{cr\_pp} \frac{\text{kg}}{\text{m} \cdot \text{sec}}$$

$$3600 \cdot \left( 1 + 0.5 \cdot \text{CSIG}_{sk\_pp} \right)^2$$

WSIG<sub>cr\_pp+1</sub>  
CSIG<sub>cr\_pp+1</sub>

WSIG <sub>sk</sub> <sub>pp+1</sub>	$\left( \frac{T_{cl\_pp} + MRT_{solar\_per\_pp}}{2} \right)^3$
CSIG <sub>sk</sub> <sub>pp+1</sub>	$4 \cdot 0.95 \cdot \sigma \cdot 0.7 \cdot 273.2 + \frac{0.00028}{2}$
WSIG <sub>B</sub> <sub>pp+1</sub>	$0.1 + \frac{0.00028}{SKBF_{pp} \left( \frac{m^2 \cdot sec \cdot degC}{kg} \right) + 0.0011}$
SKBF <sub>pp+1</sub>	$\left[ \alpha_{mass} \cdot T_{sk\_pp} + (1 - \alpha_{mass}) \cdot T_{cr\_pp} \right] \cdot degC$
h <sub>l\_cl\_air</sub> <sub>pp+1</sub>	$114.2 \cdot WSIG_B \cdot exp \left( \frac{WSIG_{sk\_pp} \cdot watt}{10.7} \right) \frac{watt}{m^2}$
α <sub>mass</sub> <sub>pp+1</sub>	$\left[ \frac{A_1}{T_{sk\_pp} + 273.15} + A_2 + A_3 \cdot (T_{sk\_pp} + 273.15)^2 + A_4 \cdot (T_{sk\_pp} + 273.15)^3 + A_5 \cdot (T_{sk\_pp} + 273.15)^4 + A_6 \cdot \ln(T_{sk\_pp} + 273.15) \right] \cdot Pa$
T <sub>B</sub> <sub>pp+1</sub>	$\left[ \frac{0.94 \cdot E_{rsw\_pp}}{0.06 + \frac{E_{max\_pp}}{w_{pp+1}}} \right]$
E <sub>rsw</sub> <sub>pp+1</sub>	$w_{pp} \cdot h_e \cdot (P_{sk\_pp} - P_{w\_pp})$
P <sub>sk</sub> <sub>pp+1</sub>	$\frac{T_{sk\_pp}}{0.155 \cdot clo} + f_{cl} \left[ h_{c\_cl\_air} \left( \frac{m^2}{watt} \right) \cdot T_{R\_per} + h_{l\_cl\_air} \left( \frac{m^2}{watt} \right) \cdot MRT_{solar\_per\_pp} \right]$
E <sub>sk</sub> <sub>pp+1</sub>	$\frac{1}{0.155 \cdot clo} + f_{cl} \left[ h_{c\_cl\_air} \left( \frac{m^2}{watt} \right) + h_{l\_cl\_air} \left( \frac{m^2}{watt} \right) \right]$
T <sub>cl</sub> <sub>pp+1</sub>	$h_{c\_cl\_air} \cdot f_{cl} \cdot (T_{cl\_pp} - T_{R\_per})$
CS <sub>pp+1</sub>	$(k_{crsk} + C_{pb} \cdot SKBF_{pp}) \cdot (T_{cr\_pp} - T_{sk\_pp})$
Q <sub>crsk</sub> <sub>pp+1</sub>	$0.0014 \cdot M \cdot (34 \cdot degC - T_{R\_per\_})$
C <sub>res</sub> <sub>pp+1</sub>	$0.0014 \cdot M \cdot (34 \cdot degC - T_{R\_per\_})$
RS <sub>pp+1</sub>	$0.0014 \cdot M \cdot (34 \cdot degC - T_{R\_per\_})$
S <sub>cr</sub> <sub>pp+1</sub>	$0.0014 \cdot M \cdot (34 \cdot degC - T_{R\_per\_})$
S <sub>sk</sub> <sub>pp+1</sub>	$0.0014 \cdot M \cdot (34 \cdot degC - T_{R\_per\_})$

$T_{R\_per\_pp+1}$   
 $MRT_{solar\_per\_pp+1}$   
 $T_{cr\_pp+1}$   
 $T_{sk\_pp+1}$   
 $T_{op\_per\_pp+1}$   
 $Q_{bl\_pp+1}$   
 $P_{sat\_pp+1}$   
 $P_w_{pp+1}$   
 $E_{max\_pp+1}$   
 $E_{res\_pp+1}$

$$h_{r\_cl\_air\_pp} \cdot f_{cl} \left( T_{cl\_pp} - MRT_{solar\_per\_pp} \right)$$

$$M - Wk - \left( C_{res\_pp} + E_{res\_pp} \right) - Q_{crsk\_pp}$$

$$Q_{crsk\_pp} - \left( CS_{pp} + RS_{pp} + E_{sk\_pp} \right)$$

$$T_{R\_pp} \quad \text{if } 8 \cdot 3600 \cdot \text{sec} \leq \text{mod}(pp \cdot dt_{comf}, 24 \cdot 3600 \cdot \text{sec}) \leq 20 \cdot 3600 \cdot \text{sec}$$

if(season = 1, 24.0.degC, 21.degC) otherwise

$$MRT_{solar\_pp} \quad \text{if } 8 \cdot 3600 \cdot \text{sec} \leq \text{mod}(pp \cdot dt_{comf}, 24 \cdot 3600 \cdot \text{sec}) \leq 20 \cdot 3600 \cdot \text{sec}$$

if(season = 1, 24.0.degC, 21.degC) otherwise

$$T_{cr\_pp} + \left[ \frac{S_{cr\_AD}}{(1 - \alpha_{mass\_pp}) \cdot m_b \cdot C_{pB\_pp}} \right] \cdot dt_{comf}$$

$$T_{sk\_pp} + \left[ \frac{S_{sk\_AD}}{\alpha_{mass\_pp} \cdot m_b \cdot C_{pB\_pp}} \right] \cdot dt_{comf}$$

$$\frac{h_{r\_cl\_air\_pp} \cdot MRT_{solar\_per\_pp} + h_{c\_cl\_air\_pp} \cdot T_{R\_per\_pp}}$$

$$h_{r\_cl\_air\_pp} + h_{c\_cl\_air\_pp}$$

$$\left[ \frac{6.3 + 50 \cdot \left( \text{if}(T_{cr\_pp} - 37 \cdot \text{degC} > 0, T_{cr\_pp} - 37 \cdot \text{degC}, 0) \right)}{1 + 0.5 \cdot \left( \text{if}(34 \cdot \text{degC} - T_{sk\_pp} > 0, 34 \cdot \text{degC} - T_{sk\_pp}, 0) \right)} \right] \left( \frac{L}{\text{hr} \cdot \text{m}^2} \right)$$

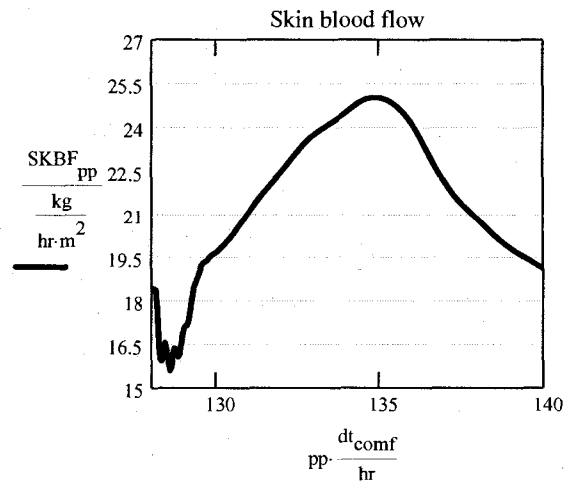
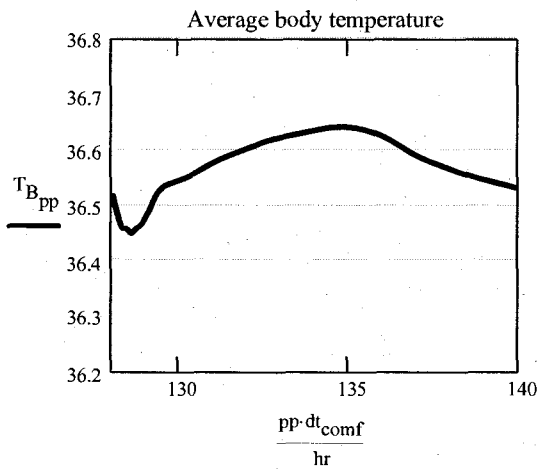
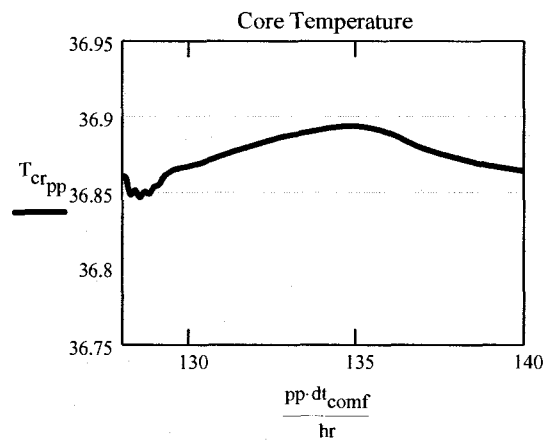
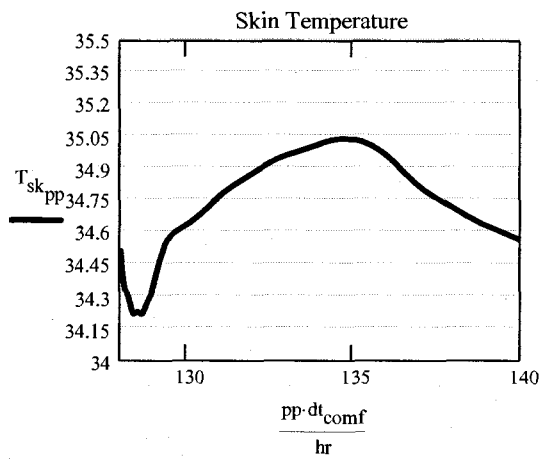
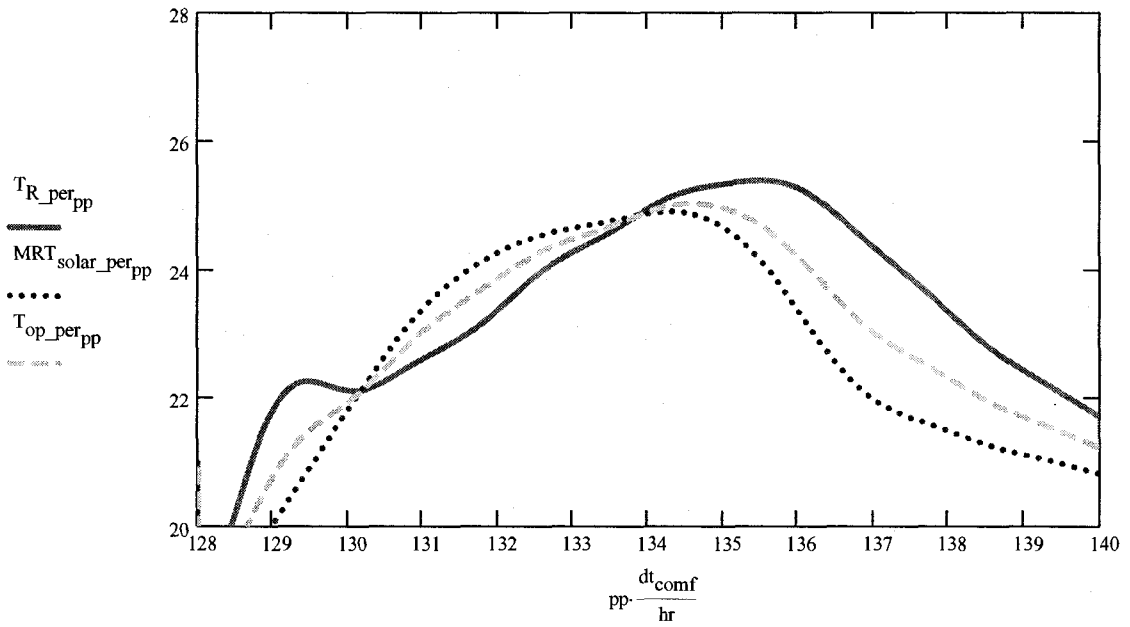
$$\left[ \frac{A_1}{T_{R\_pp} + 273.15} + A_2 + A_3 \cdot (T_{R\_pp} + 273.15)^2 + A_4 \cdot (T_{R\_pp} + 273.15)^3 + A_5 \cdot (T_{R\_pp} + 273.15)^3 + A_7 \cdot \ln(T_{R\_pp} + 273.15) \right] \cdot Pa$$

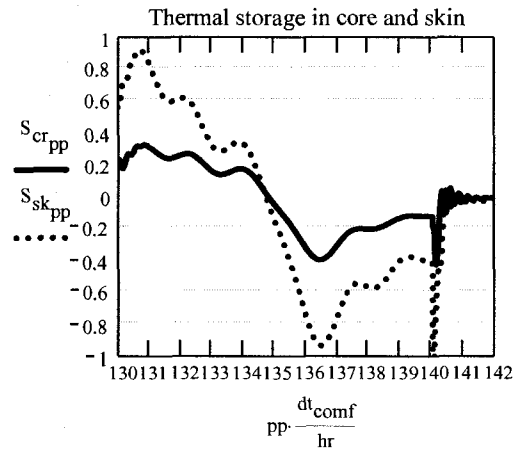
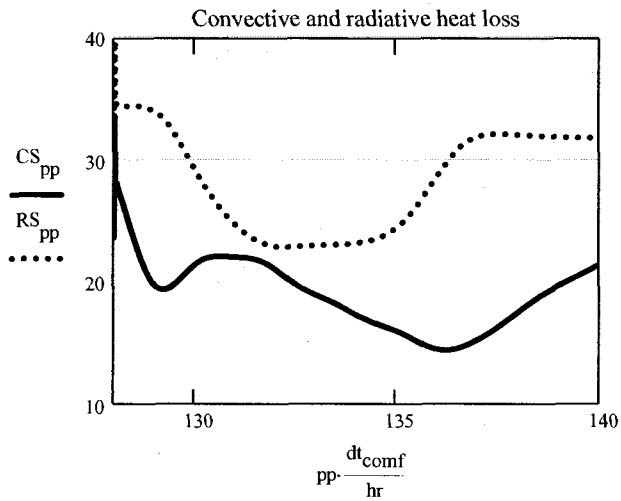
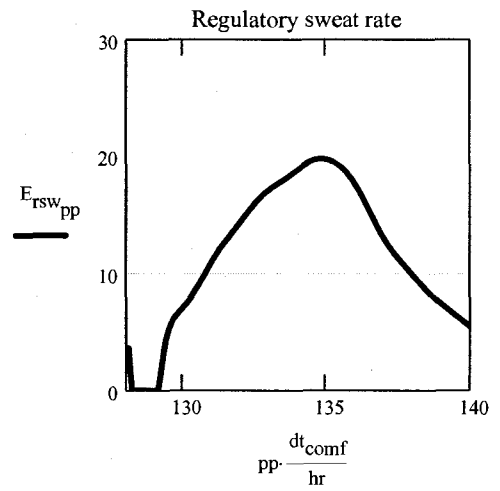
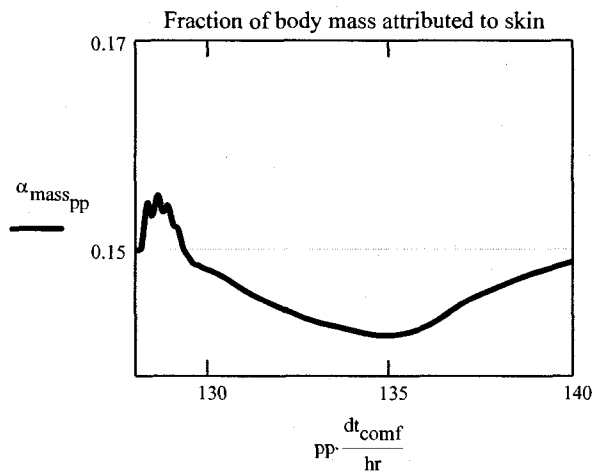
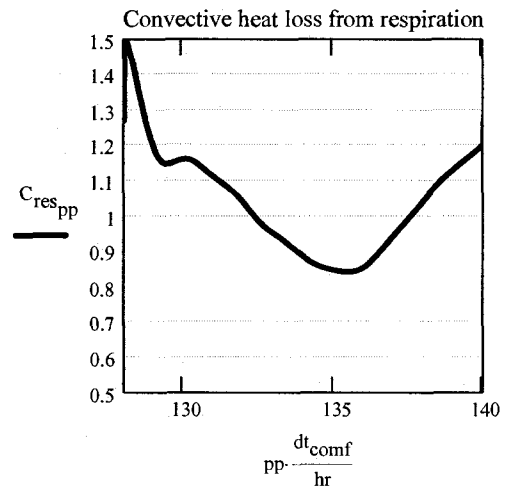
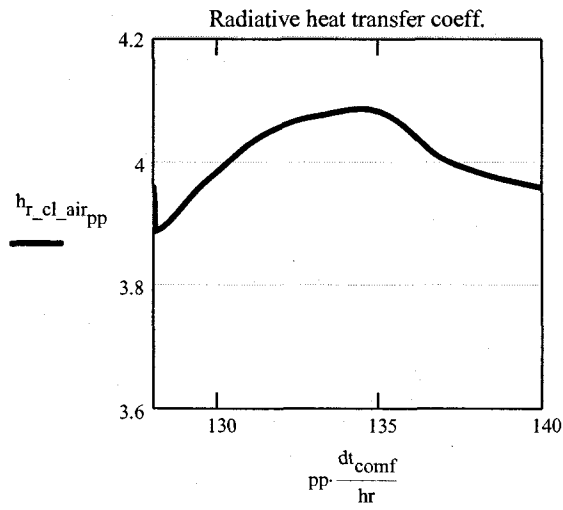
$$RH_{P_{sat\_pp}}$$

$$h_c \cdot (P_{sk\_pp} - P_w_{pp})$$

$$0.0173 \cdot M \cdot \left( 5.87 - \frac{P_w_{pp}}{kPa} \right)$$

**RESULTS:**





$$T_{B\_C} := \left[ \left( \frac{0.194}{58.15 \frac{\text{watt}}{\text{m}^2}} \right) \cdot (M - Wk) + 36.301 \right] \quad \dots \text{cold set-point for evaporative regulation zone}$$

$$T_{B\_H} := \left[ \left( \frac{0.347}{58.15 \frac{\text{watt}}{\text{m}^2}} \right) \cdot (M - Wk) + 36.669 \right] \quad \dots \text{hot set-point for evaporative regulation zone}$$

$$E_{\text{rsw\_req}} := 0.42 \cdot \left( M - Wk - 58.15 \frac{\text{watt}}{\text{m}^2} \right) \quad E_{\text{diff\_pp}} := \left( 1 - \frac{E_{\text{rsw\_pp}}}{E_{\text{max\_pp}}} \right) \cdot 0.06 \cdot E_{\text{max\_pp}}$$

$$T_{\text{SENS\_pp}} := \left[ \begin{array}{l} 0.4685 \cdot (T_{B\_pp} - T_{B\_C}) \quad \text{if } T_{B\_pp} < T_{B\_C} \\ \frac{3.995 \cdot (T_{B\_pp} - T_{B\_C})}{(T_{B\_H} - T_{B\_C})} \quad \text{if } T_{B\_C} \leq T_{B\_pp} \leq T_{B\_H} \\ 3.995 + 0.4685 \cdot (T_{B\_pp} - T_{B\_H}) \quad \text{if } T_{B\_H} < T_{B\_pp} \end{array} \right] \quad \dots \text{index of thermal sensation}$$

$$DISC_{\text{pp}} := \left[ \begin{array}{l} 0.4685 \cdot (T_{B\_pp} - T_{B\_C}) \quad \text{if } T_{B\_pp} < T_{B\_C} \\ \frac{4.7 \cdot (E_{\text{rsw\_pp}} - E_{\text{rsw\_req}})}{(E_{\text{max\_pp}} - E_{\text{rsw\_req}} - E_{\text{diff\_pp}})} \quad \text{otherwise} \end{array} \right] \quad \dots \text{index of thermal discomfort}$$

$$T_{\text{UL}} := \begin{cases} 26.5 & \text{if season} = 1 \\ 24 & \text{if season} = 2 \end{cases} \quad \dots \text{upper limit of T.op. for comfort zone} \quad T_{\text{LL}} := \begin{cases} 23 & \text{if season} = 1 \\ 20.5 & \text{if season} = 2 \end{cases} \quad \dots \text{lower limit of T.op. comfort zone}$$

